Development of Nickel-Catalyzed Methods for Deoxygenation Processes

by

David P. Todd

A dissertation submitted in partial fulfillment
of the requirements for the degree of
Doctor of Philosophy
(Chemistry)
in the University of Michigan
2017

Doctoral Committee:

Professor John Montgomery, Chair
Professor Rudy Richardson
Professor Melanie Sanford
Professor John Wolfe

Dedication

I dedicate this dissertation to my family, Paul, Rose and Laura, and to Jessica.

Acknowledgements

I would like to thank my advisor John Montgomery for his guidance and mentorship. Under his supervision, I have learned to be a more creative thinker and a dedicated researcher. I would also like to thank my dissertation committee for all of their helpful comments and advice.

I would also like to thank the members of the Montgomery Lab past and present who have helped me during my time in the group. Through my interactions and discussions with them, I have as a chemist, and they have helped make graduate school a more enjoyable experience. Eric Wiensch is acknowledged for his collaborative work in the developments described in Chapter 3 of my thesis.

Lastly, I would like to thank my family, friends, and my girlfriend Jessica for their support throughout my graduate career.

Table of Contents

List of Schemes

List of Tables

Abbreviations

Ac	acetyl
acac	acetylacetone
Ar	1,3-Bis(1-adamantyl)imidazole-2-ylidene
I(2-Ad)	aryl
BINAP	(±)-2,2′-Bis(diphenylphosphino)-1,1′-binaphthalene
^{t}Bu	tert-butyl
°C	degrees Celsius
COD	cyclooctadiene
Cy	cyclohexyl
Cp	cyclopentadienly
DMF	dimethylformamide
IPr^{Me}	4,5-dimethyl-1,3-bis(2,4,6-triisopropylphenyl)-4,5-dihydro-imidazolium
ee	enantiomeric excess
equiv	equivalent
Et	ethyl
^{n}hex	hexyl
hr	hour(s)
IMes	1,3-bis-(1,3,5-trimethylphenyl)imidazol-2-ylidene
IPr	1,3-bis-(2,6-diisopropylphenyl)imidazol-2-ylidene
IPr*OMe	N,N'-Bis(2,6-bis(diphenylmethyl)-4-methoxyphenyl)imidazol-2-ylidene

IPrBAC N^1,N^1,N^2,N^2-tetraisopropylcycloprop-1-ene-1,2-diamine

ITol   1,3-bis-(4-methylphenyl)imidazol-2-ylidene

Me   methyl

MMA   methyl methacrylate

Mes   mesityl

min   minute(s)

MS   molecular sieves

NHC   N-heterocyclic carbene

^{n}Oct   octyl

PG   protecting-group

Ph   phenyl

Pin   pinacol

Piv   pivalate

^{i}Pr   isopropyl

^{n}Pr   pentyl

rt   room temperature

SIPr   1,3-bis(2,6-diisopropylphenyl)-4,5-dihydro-imidazolium

TBS   tert-butyldimethylsilyl

TMDSO   1,1,3,3-tetramethyldisilyloxane

TBDPS   tert-butyldiphenylsilyl

TES   triethylsilyl

TESH   triethylsilane

Tf   triflate

THF	tetrahydrofuran
ᵗAm	tert-amyl
TBAF	tetra-n-butylammonium fluoride
PhMe	toluene
TIPS	triisopropylsilyl
TIPSH	triisopropylsilane
TMS	trimethylsilyl

Abstract

A new method for the reductive coupling of enals or enones and alkynes has been developed. The method results in a unique net four-electron reduction of the starting materials, leading to the formation of a deoxygenated 1,4-diene product. During the optimization of the reaction, a discrete nickel catalyst was synthesized, resulting in much higher levels of reactivity. The proposed reaction mechanism highlights the dual functionality of the titanium additive, as both a reductant and Lewis acid. This unique characteristic was then applied to the development of other novel organic reactions. The method also offers an improved substrate scope over analogous methods to synthesize 1,4-dienes.

Silyl protecting groups represent a powerful synthetic tool in organic chemistry. Despite their widespread use in synthesis, little work has been done in the activation of the C-O bond of silyl ethers. Utilizing mechanistic information obtained from previous work, the functionalization of silyl aryl ethers were explored using nickel catalysis. Through extensive optimization, the nickel-catalyzed reduction, silylation, and amination of silyl aryl ethers is reported. The methodology offers improved reaction conditions and substrate scopes compared to analogous carbon-oxygen bond functionalization reactions.

Chapter 1

Introduction to Nickel-Catalyzed Carbon(sp^2)-Oxygen Bond Activation

1.1   Introduction to Carbon(sp^2)-Oxygen Bond Cleavage

Scheme 1.1 Metal-Catalyzed Cross-Coupling Reactions
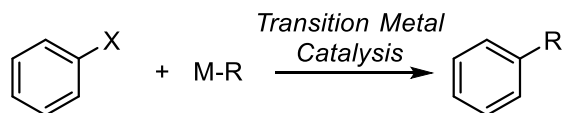
Metal-catalyzed cross-coupling reactions have become indispensable tools in a chemist's synthetic arsenal (Scheme 1.1).[1] The broad range of the utility of the reaction has allowed for their widespread use in both pharmaceutical and academic laboratories. Despite the synthetic importance of these transformations, the vast majority employ organic halides as the coupling partner and result in the production of toxic halogenated waste. As a result of these limitations, chemists have explored the use of other cross-coupling analogues that exhibit improved flexibility, and practicality. One type of cross-coupling analogue that is quite appealing are phenol derivatives, as they are naturally abundant, and relatively nontoxic.[2] Currently, there are approximately 50,000 phenols commercially available. Additionally, their inclusion into cross-coupling chemistry could allow for the design of orthogonal cross-coupling strategies (Scheme 1.2).

Scheme 1.2 Orthogonal Reactivity

X = I, Br, or Cl
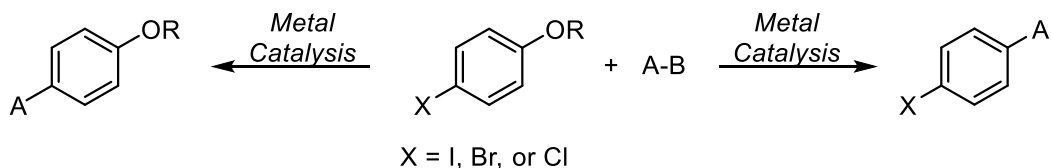
One of the first examples of carbon(sp^2)-oxygen bond cross-coupling reactions was reported in 1951 by the Hill group.[3] They showed that 1-aryl-substituted vinyl ethers reacted with Grignard reagents to yield 1,1-diaryl -substituted olefins in good yields (Scheme 1.3).

Scheme 1.3 Initial C-O Cleavage

2.4 equivs PhMgBr

Et$_2$O, reflux

88%
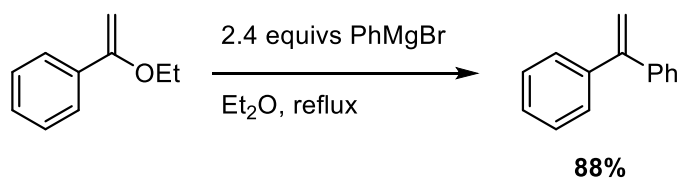
Several years later, the Meyer group described analogous reactivity for aryl methyl ethers bearing an oxazoline directing group at the *ortho*-position (Scheme 1.4).[4] The substrates could be reacted with Grignard reagents to efficiently yield the desired product. It was observed that only methyl ethers *ortho* to the oxazoline directing group would react with the Grignard reagent. It was proposed that a Mg^{2+} ion could coordinate to the oxazoline nitrogen atom and the ethereal oxygen atom. The formation of this adduct would then explain the increased activity of *ortho* activation over *para*.

Scheme 1.4 Meyer Activation of Aryl Methyl Ethers

1 equiv.EtMgBr

THF, -45 °C to rt

50%
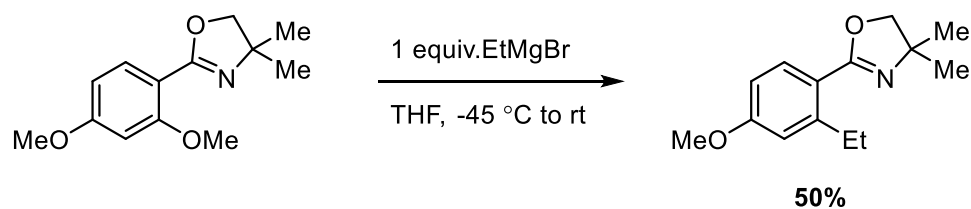
As scientists began to expand the scope and breadth of carbon(sp^2)-O bond activation reactions, more work went into the design and implementation of a variety of protecting groups.[5] In general, the protecting groups for phenols in cross-coupling reactions can be divided into three distinct classes (Scheme 1.5).[6] The first class of protecting groups is considered particularly active, possessing rather weak carbon-oxygen bonds such as aryl tosylates, triflates, mesylates, and nonaflates (**A**). While incredibly active in cross-coupling reactions, the protecting groups are plagued by high cost of starting materials and moisture instability. Despite these limitations, the vast majority of carbon-oxygen bond functionalization reactions utilize one of these groups. The second class of protecting groups include esters, carbamates, and sulfonates (**B**). This class of protecting group is less reactive than those in depicted in **A**, but offer improved bench-top stability. Additionally, the groups can be readily appended to the desired phenol under somewhat mild conditions, utilizing reagents cheaper than in class **A**. Despite these benefits, the protecting groups suffer from issues in selectively activating the desired carbon-oxygen bond as the presence of a carbon(acyl)-oxygen bond is also capable of competing with carbon-oxygen bond cleavage. Furthermore, despite the improved stability compared to those protecting groups in class **A**, they suffer from hydrolysis under somewhat harsh reaction conditions. The final class of protecting groups include aryl alkyl ethers (**C**). In particular, the aryl methyl ether motif is the most common of this type of protecting group. Aryl methyl ethers are highly inert, even under harsh reaction conditions, and so are not susceptible to the same bench-top instabilities inherent in classes **A** and **B**. Additionally, aryl methyl ethers are abundant in a variety of natural products, including many that are available for commercial purchase. Despite these benefits, aryl methyl ethers are much more inert than protecting groups in classes **A** and **B**. Activating the desired carbon-oxygen bond

usually requires very forcing reaction conditions and relatively low conversions to the desired

products.

Scheme 1.5 Commonly Employed Protecting Groups

R = CF$_3$, Me, p-MeC$_6$H$_4$ | R = alkyl, aryl, NMe$_2$
Moisure Instability | **C-O Selectivity** | **Highly Inert**
High Cost (OTf, OMs) | **Hydrolysis** | **Low Cost**
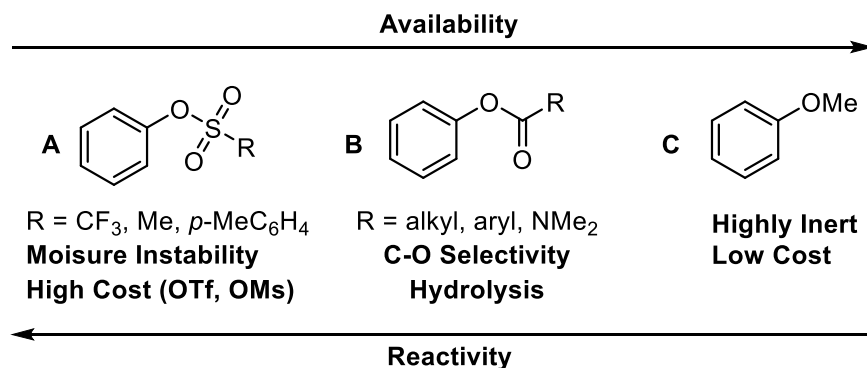
1.2   Advantages of Nickel Catalysts toward Carbon(sp^2)-Oxygen Bond Cleavage

For a considerable length of time, most of the work in employing phenol derivatives for

cross-coupling reactions utilized palladium catalysts. The reasoning for this is due to the discovery

that aryl triflates were capable cross-coupling reagents for a variety of famous cross-coupling

reactions that normally employ an aryl halide as the cross-coupling reagent (Scheme 1.6).[7-9]

Scheme 1.6 Triflates Used in Palladium Cross-Coupling Reactions
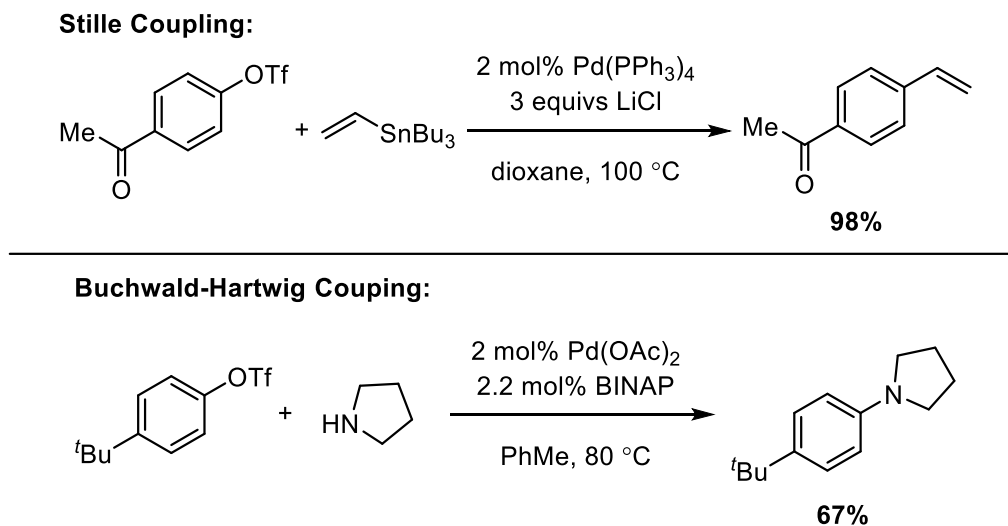
Despite the extensive employment of aryl triflates in palladium cross-coupling reactions, chemists began to explore the use of carbon(sp^2)-oxygen bond functionalization reactions using different transition metal catalysts for several reasons. Specifically, much of the work was centered on developing nickel-catalyzed methodologies. One of the main drawbacks to palladium catalyzed carbon(sp^2)-oxygen functionalization reactions are the limitations in protecting groups capable of yielding the desired products (Scheme 1.7). While aryl triflates, tosylates, and mesylates are all highly reactive reagents under palladium catalysis, many other commonly employed phenol protecting groups are inert when subjected to similar reactions conditions. As described above (Scheme 1.5), protecting groups such as aryl triflates suffer from poor bench-top stability and require the use of expensive organic reagents for their installation. Implementing new protecting groups that do not suffer from these limitations would then require a different transition metal catalysts to deliver the desired reactivity.

Scheme 1.7 Limitations using Palladium

Reactive under palladium catalysis:

R = CF$_3$, Me, p-MeC$_6$H$_4$

triflates, tosylates, mesylates

Inert (or much less reactive) under palladium catalysis but reactive under nickel catalysis:

sulfamates   esters   carbamates   ethers
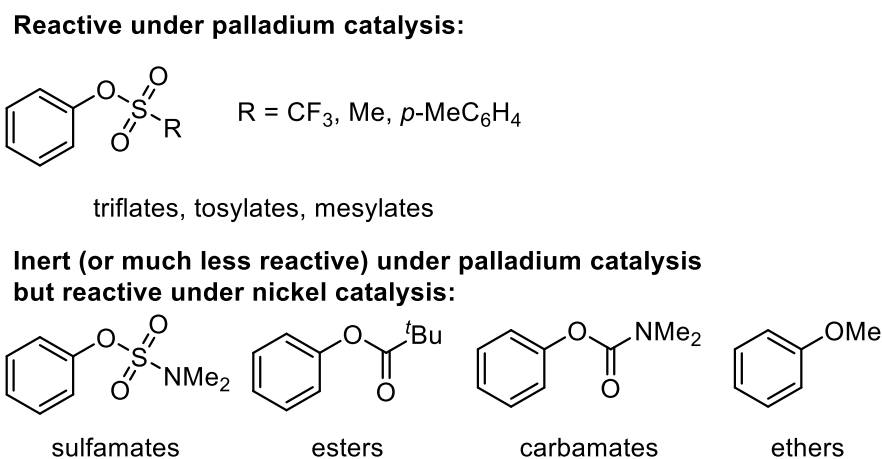
Nickel catalysis has been shown to activate a variety of phenol protecting groups that are unreactive using palladium catalysis. The enhanced reactivity is proposed to arise from the smaller size of nickel compared to palladium, enhancing its nucleophilicity towards the activation of carbon(sp^2)-oxygen bonds. Computational studies comparing the carbon(sp^2)-X bond activation

between nickel and palladium catalysts provide support for this theory (Table 1.1).[10] Both palladium and nickel were shown to have very similar transition state barriers comparing the activation of a carbon(sp^2)-bromide bond (entry 1). Yet, comparing the activation barrier for carbon(sp^2)-triflates indicated that the barrier for palladium catalysis was 21.4 kcal/mol higher in energy than compared to nickel (entry 2). Despite this large difference, palladium catalysts are still capable of activating the carbon(sp^2)-triflate bonds, as evidenced by all the reports in the literature. The activation barrier for carbon(sp^2)-acetate was reported to be 26.4 kcal/mol for nickel and 34.0 kcal/mol for palladium (entry 3). While the barriers for activation are both considerable higher compared to the activation of the C-Br bond, the much higher barrier for palladium catalysis inhibits productive C-O bond activation. Finally, the activation of aryl methyl ethers was calculated to be 29.5 kcal/mol for nickel and 42 kcal/mol for palladium (entry 4). The barrier for activations are both considerably higher than activations of other C-X bonds. Yet, the palladium barrier is too large to allow for the desired bond activation based on the dearth of examples reported in the literature, whereas multiple reports have shown the ability of nickel catalysts to activate aryl methyl ethers. Additionally, the increase in the barrier of activation between triflates, acetates, and methyl ethers supports the trend in decreasing reactivity described above (Scheme 1.5).

Table 1.1 Nickel and Palladium Bond Activations
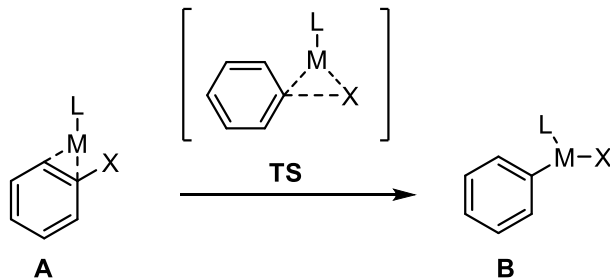
Entry	Ph-X	TS Barrier using Ni(0)PMe$_3$	TS Barrier using Pd(0)PMe$_3$
1	Ph-Br	3.3 kcals	3.4 kcals
2	Ph-OTf	4.5 kcals	25.9 kcals
3	Ph-OAc	26.4 kcals	34.0 kcals
4	Ph-OMe	29.5 kcals	42.0 kcals

Another benefit to using nickel catalysis to activate carbon(sp^2)-oxygen bonds involves the cost of the catalyst used in the transformation. Commercially available palladium catalysts are much more expensive than their nickel counterparts.[11]

1.3 Nickel-Catalyzed Carbon(sp^2)-Oxygen Bond Cleavage Background

One of the first examples of nickel-catalyzed carbon(sp^2)-oxygen bond cleavage was reported in 1979 by the Wenkert group.[12] They showed that aryl methyl ethers could be applied for their use in Kumada-Tamou-Corriu reactions (Scheme 1.8). The reaction employed a NiCl$_2$(PPh$_3$)$_2$ catalyst and only worked with naphthyl methyl ethers. Anisole derivatives proved to be unreactive.

Scheme 1.8 Wenkert Discovery

77%
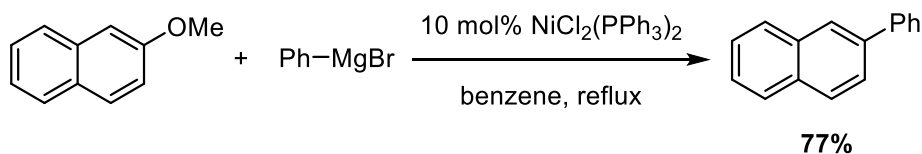
Twenty-five years passed before any additional work was reported in this area. The gap in time is proposed to be a result of the success of palladium catalyzed cross-coupling reactions. There was little incentive to develop nickel-catalyzed variants of transformations readily performed using palladium. Yet in 2004, the Dankwardt group showed they could expand the scope of this transformation to tolerate anisole derivatives (Scheme 1.9).[13] The enhanced reactivity could be attributed to the use of the electron rich ligand, PCy_3. Additionally, the reaction proceeded with very high yields and employed relatively mild reaction conditions.

Scheme 1.9 Dankwardt's Modified System
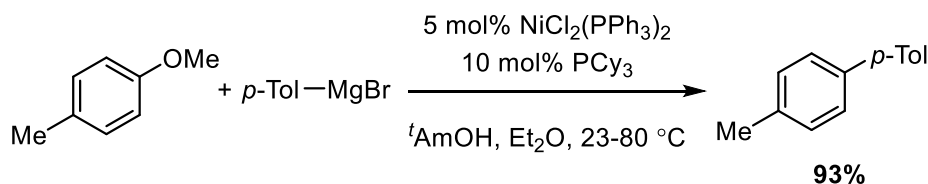
While the work from the Dankwardt expanded the scope of aryl methyl ethers for Kumada-Tamou-Corriu reactions, this proved rather trivial compared to the over-arching impact of the publication. Dankwardt showed that phenol derivatives were finally shown to be competent cross-coupling reagents usually reserved for aryl halides. Since, the seminal publication in 2004, there has been an explosion of publications in the field of nickel-catalyzed carbon(sp^2)-oxygen bond functionalization reactions. Phenol derivatives are now capable of serving as cross-coupling partners in a multitude of synthetic transformations (Scheme 1.10).[14-16]

Scheme 1.10 Scope of Transformations
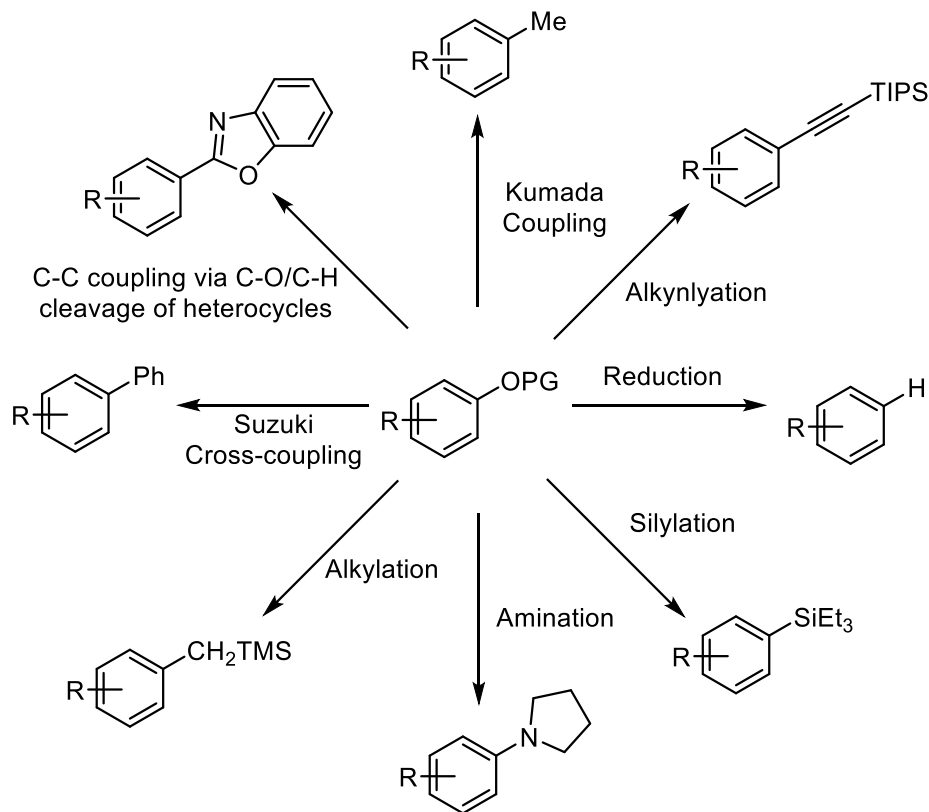
1.4 Statement of Thesis Content and Scope

This dissertation describes the development of nickel-catalyzed methods towards the deoxygenation of simple organic molecules. The first iteration of the methodology involves the serendipitous discovery of the reductive coupling of enones or enals and alkynes to yield 1,4-dienes. The reaction employed a small NHC ligand, typically not used in reductive coupling methodology. The development of a discrete nickel catalyst provided an increase in reactivity, highlighting the benefits of rational catalyst design. Mechanistic inquiries into this transformation revealed a mechanism that could be used toward the development of additional carbon(sp^2)-oxygen bond activations. With this knowledge, the nickel-catalyzed functionalization of silyl aryl ethers was explored. It was realized that these substrates could undergo reduction, silylation,

amination, or Suzuki cross-coupling transformations. The approach to the activation of carbon(sp^2)-silyloxy bonds avoids some of the limitations commonly encountered in other carbon-oxygen bond functionalization reactions.

Chapter 2

Deoxygenative C-C Bond-Forming Processes via a Net Four-Electron Reductive Coupling

2.1　Synthesis of 1,4-Dienes

Scheme 2.1 Natural Products Containing a 1,4-Diene

Phorbasin C

Ripostatin A

Arachidonic Acid

Madangamine A
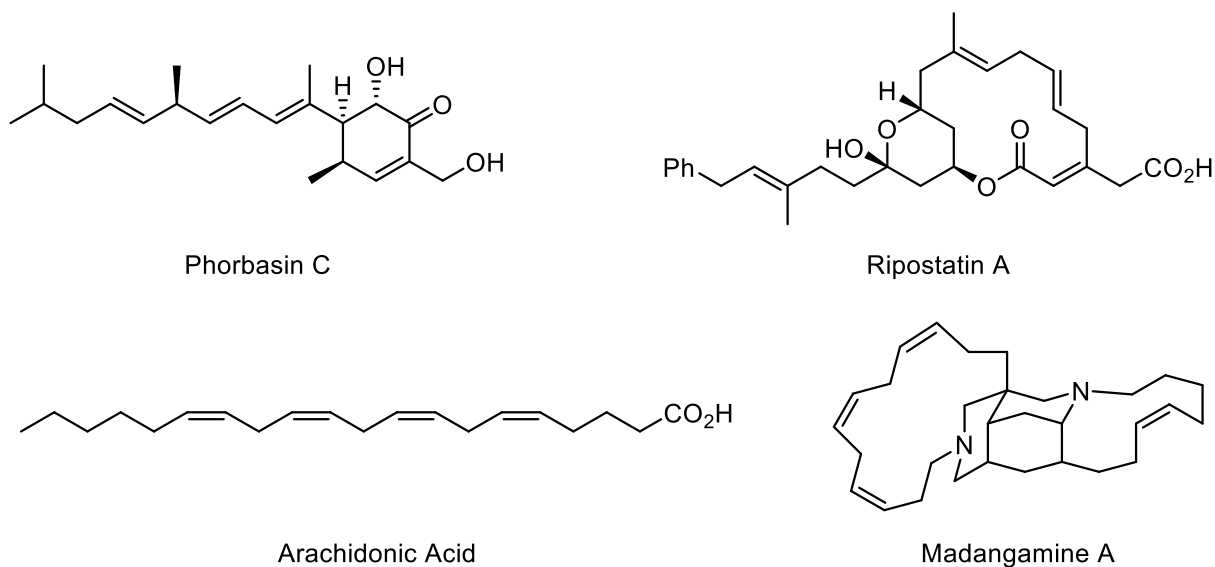
The 1,4-skipped diene is an important structural motif in organic chemistry, and is present in a multitude of natural products and other molecules with interesting biological activity (Scheme 2.1).[17] There are a multitude of synthetic methods available to synthesize 1,4-dienes, but many of the methods suffer from the inability to achieve high levels of *E*/*Z* selectivity. One of the earliest methods for the synthesis of 1,4-dienes came about from the synthesis of analogues of arachidonic

acid. The strategy employs the use of a silyl group adjacent to a cyclopropyl ring, that upon elimination of the silyl group can open to form a 1,4-diene product (Scheme 2.2).[18] The resulting stereoselectivity of the olefins is dictated by the stereochemistry of the cyclopropyl ring, and as such allows for control of the stereoselectivity of only one of the olefins.

Scheme 2.2 Wilson 1,4-Diene Synthesis
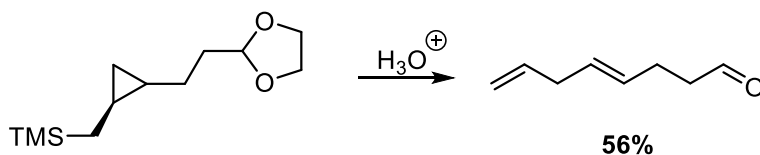
An additional method for the formation of 1,4-dienes was developed in the Trost group during their synthesis of alternaric acid. The method employs the coupling of an alkyne and an alkene via formation of a metallacycle (Scheme 2.3).[19] The regioselectivity of the olefin is believed to be dictated by the steric hindrance of the alkyne. Subsequent β-hydride elimination from the metallacycle forms the *E*-olefin, followed by reductive elimination to afford the 1,4-diene product. It was determined that the branched product was favored over the linear due to the steric interactions of the ester group on the alkyne and the ruthenium complex.

Scheme 2.3 Trost 1,4-Diene Synthesis
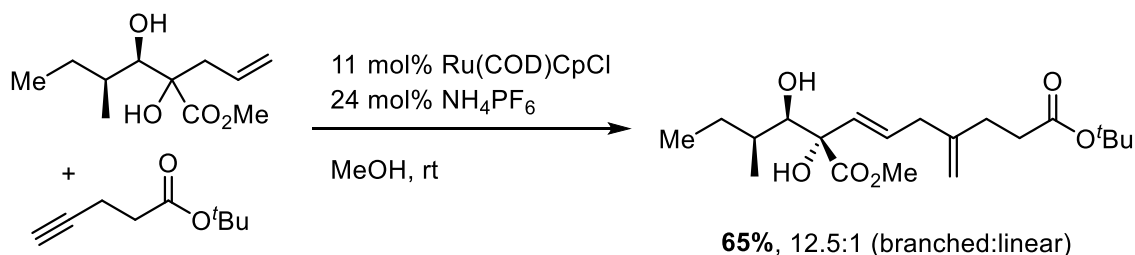
Work in the Micalizio group has shown that 1,4-dienes can be accessed from the stereoselective cross-coupling of allylic alcohols and alkynes (Scheme 2.4).[20] Allylic alcohols bearing 1,1-disubstitution were shown to be able to afford superior selectivity, while simple, unsubstituted allylic alcohols proceed with poor stereoselection. These results are consistent with

12

an empirical model where carbon-carbon bond formation occurs via a boat-like geometry of a transient mixed titanate ester. The reaction was shown to proceed efficiently with both cyclic and acyclic allylic alcohols, along with symmetric and asymmetric alkynes in good yields and middling diastereoselectivity.

Scheme 2.4 Micalizio 1,4-Diene Synthesis

59%, >20:1 (*E:Z*)
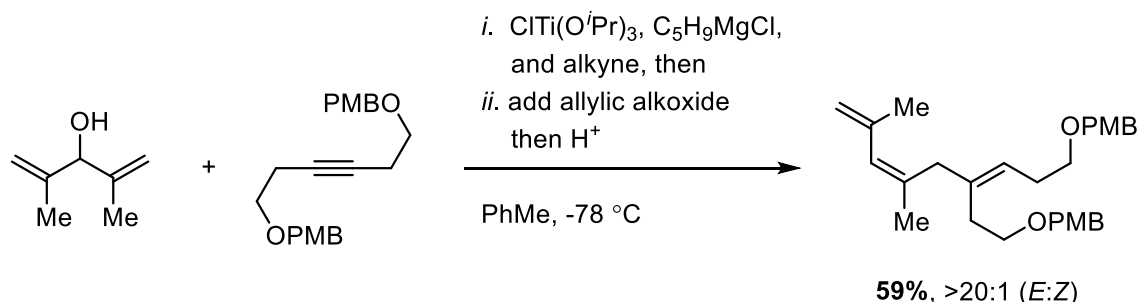
Finally, 1,4-dienes can be readily synthesized from 1,3-diene precursors, through the coupling with terminal olefins (Scheme 2.5).[21] The coupling of the 1,3-diene and olefin is catalyzed by an iron catalyst bearing an iminopyridine ligand (**1**). The transformation occurs via an oxidative cyclization minimizing the steric repulsion between the two coupling partners. A subsequent *syn* β-hydride elimination followed by reductive elimination results in the transfer of a hydride from the terminal alkene to the diene. The reaction provides linear 1,4-dienes in good yields and high levels of regioselectivity.

Scheme 2.5 Coupling of Dienes and Terminal Olefins

94%   **1**
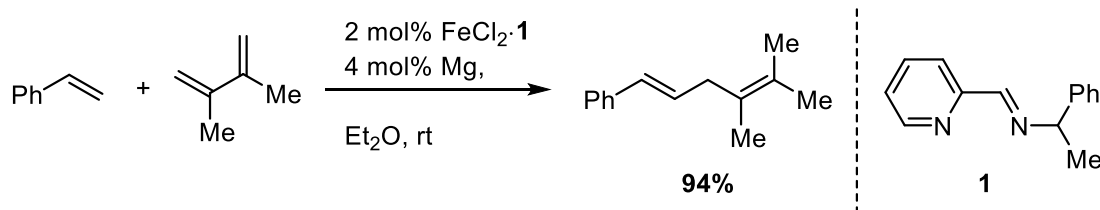
While there are several other methods to form 1,4-dienes, few methods exist allowing for the formation of linear 1,4-dienes with a large substrate scope as well as the synthesis of dienes

13

bearing substitution at the methylene between the two olefins. Additionally, many of the methods are plagued with poor E/Z selectivity for the newly formed olefins. A method addressing these limitations would improve the ease of synthesizing a wide range of skipped-diene products.

2.2   Net Four-Electron Reductive Couplings

A vast array of research has gone into the development of the union of two π-components via carbon-carbon bond formation. Most these methods involve the redistribution of atoms without a net change in oxidation state of the components. These reactions are referred to as net-neutral, as they are completely atom economical, without a net formal change in oxidation state of the reactants. Several examples of these transformations include the coupling of an alkyne and alkene to form a diene (**A**), the hydroacylation of an alkene or alkyne with an aldehydes (**B**), and the hydrovinylation of alkenes (**C**) (Scheme 2.6).[22-24] Additionally, substrates lacking a π-bond are capable of participating in net-neutral reactions via sequential hydrogen transfer/ carbon-carbon coupling events. An example of this transformation is the coupling of an alcohol and an allene to produce a homoallylic alcohol (**D**).[25]

Scheme 2.6 Net Neutral Couplings

14
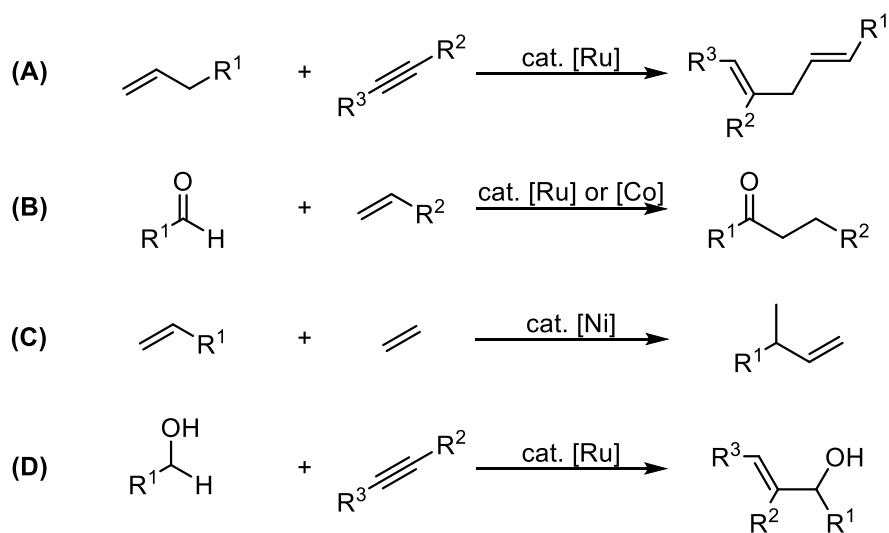
A second group of catalytic transformations involving the coupling of two π-components involves the use of a reductant. During these transformations, a two-electron reduction of the starting materials occurs during the coupling event. Several examples of these types of transformations include the coupling of aldehydes and alkynes to furnish allylic alcohols (**A**), the coupling of enones and alkynes to produce γ, δ-unsaturated ketones (**B**), and the coupling of allylic alcohols and alkynes to produce skipped dienes (**C**) (Scheme 2.7).[26-28] The processes described all involve a net two-electron reduction of the starting materials during the carbon-carbon coupling event.

Scheme 2.7 Two-Electron Reductive Couplings
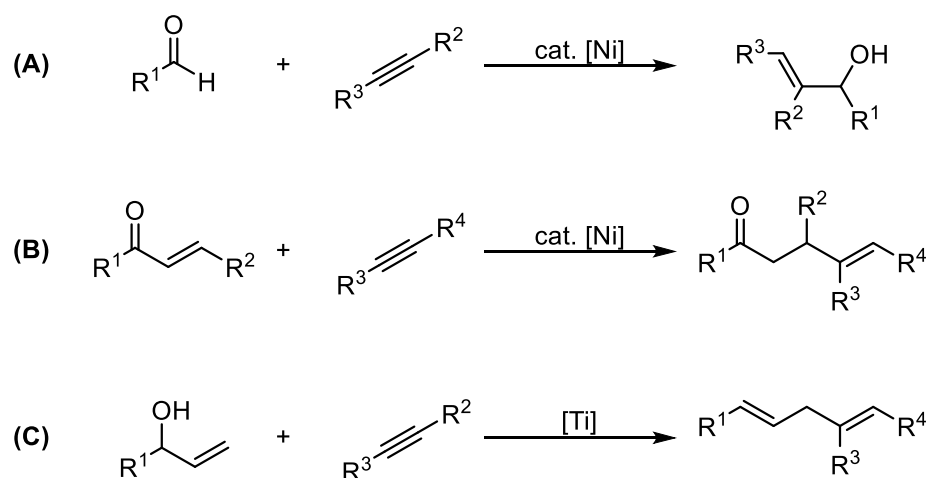
Despite the prevalence of both net-neutral (**A**) and two-electron reduction processes (**B**) involving the coupling of two π-components, reactions that involve a net four-electron reduction are much rarer (**C**) (Scheme 2.8).

15

Scheme 2.8 Net Four-Electron Reductive Couplings
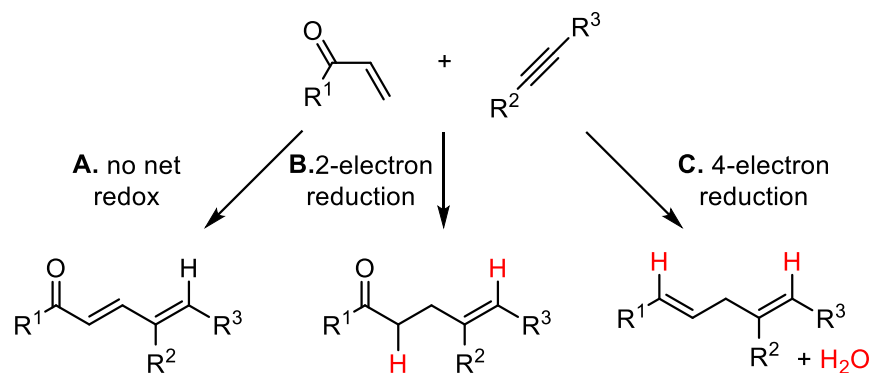
2.3   Optimization of Reaction Conditions

Scheme 2.9 Formation of Z-Enol Silanes from Enals and Alkynes
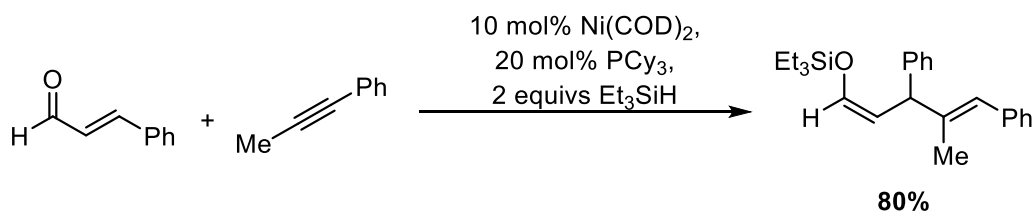
Prior work in the Montgomery Lab showed that the coupling of enals and alkynes with a nickel catalyst and trialkyl silane reductant can afford Z-enol silanes in good yields and high levels of selectivity (Scheme 2.9).[29] During efforts to expand this methodology to enones instead of enals, it was discovered that using an unhindered NHC ligand, along with triethyl silane and a titanium(IV) isopropoxide additive led to the unexpected production of a 1,4-diene product in 37% isolated yield (Scheme 2.10).[30]

Scheme 2.10 Initial Findings for 1,4-Diene Formation
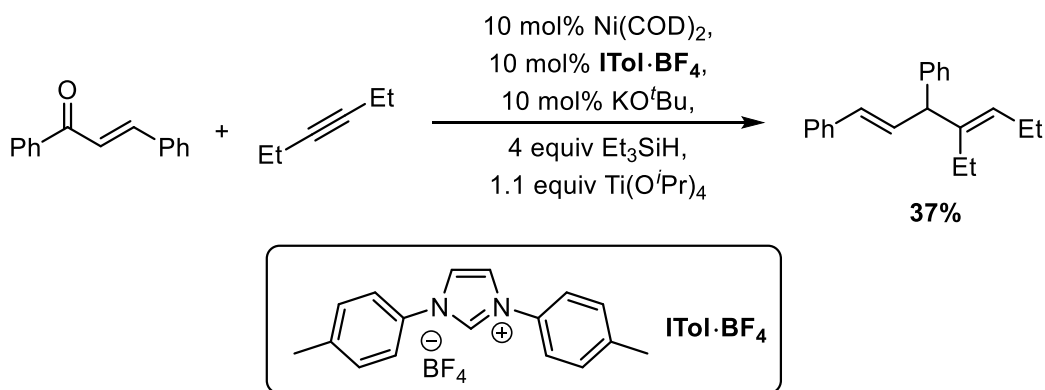
*Initial Discovery done by Dr. Ben Thompson

Changing the ligand to other common NHC ligands such as IMes or IPr (entry 2 and 3) failed to yield any of the desired product (Table 2.1). Other commonly employed ligands in reductive coupling reactions, such as PCy_3 or PPh_3 (entry 4 and 5) also failed to yield the desired product.

Table 2.1 Ligand Screen

Entry	Ligand	Yield
1	ITol·HBF_4	37%
2	IMes·HCl	NP
3	IPr·HCl	NP
4	PCy_3	NP
5	PPh_3	NP

Despite extensive optimization of reaction conditions, yields could not be raised beyond those obtained during the initial ligand screen. Additionally, the reaction was plagued with

17

inconsistent results. The lack of reactivity and inconsistent results were attributed to the nature of

the ITol ligand. Ligands such as ITol that lack *ortho*-substituents on the *N*-aryl group typically

lead to low-yielding and inconsistent reactions compared to other NHCs bearing *ortho*-alkyl

substituents, like IMes or IPr. It is theorized the poor reactivity could be attributed to difficulty in

forming the active catalyst in appreciable amounts via the *in situ* method. Given this limitation,

along with the unique nature of the ITol ligand to catalyze this reaction, efforts were undertaken

to examine the preparation of stable nickel(0) precatalysts.

Scheme 2.11 Synthesis of the Discrete ITol Catalyst

Crystal Strucutre:

18
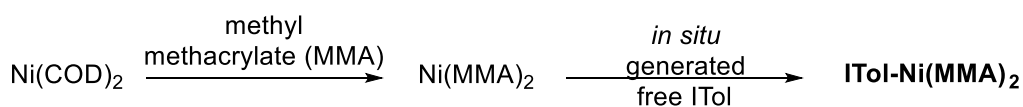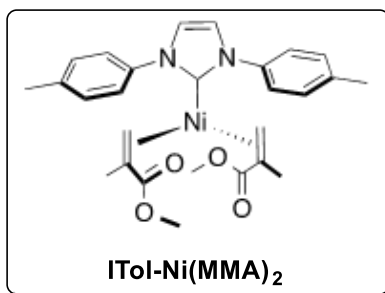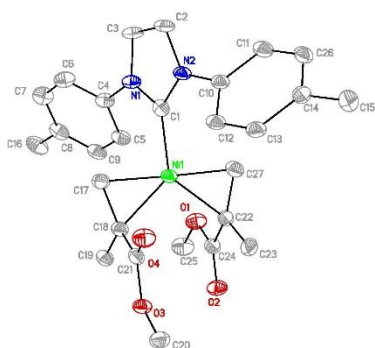
While several well-defined catalyst classes were examined, nickel(0) complex ITol-Ni(MMA)$_2$, derived from methyl methacrylate, ITol·HBF$_4$, and Nickel(COD)$_2$, was chosen due to the ease of synthesis (Scheme 2.11). A crystal structure of ITol-Ni(MMA)$_2$ was obtained, confirming the presence of two methyl methacrylate ancillary ligands coordinated to the nickel center. Upon subjection to reaction conditions, the pre-defined catalyst provided very high levels of reactivity, yielding the desired 1,4-diene product in a 94% isolated yield (Table 2.2, entry 2).

Table 2.2 Evaluation of Discrete Catalyst

Entry	Catalyst	Yield
1	10 mol% Ni(COD)$_2$, ITol·HBF$_4$, and KO^{t}Bu	37%
2	10 mol% ITol-Ni(MMA)$_2$	94%

Additional controls and optimization of the reaction system utilizing the discrete nickel catalyst were conducted (Table 2.3). Catalyst loadings could be lowered to 5 mol% but resulted in a large drop in yield (entry 2). The catalyst exhibited moderate air stability, as product formation could be observed even after exposure of the discrete catalyst to air for one hour (entry 3). Additional optimization in the choice of ancillary ligands used to stabilize the defined catalyst could potentially allow for improved air stability. Reactions conducted at room temperature failed to yield any of the desired product, indicating that the discrete catalyst may require mild heating to displace the methyl methacrylate ligands, eventually leading to productive catalysis (entry 4). Adding exogenous isopropanol with catalytic titanium(IV) isopropoxide provided much lower conversion to the desired product as well, indicating that a stoichiometric amount of Lewis acid is

required for optimal reaction conditions (entry 5). Aluminum alkoxides also resulted in product formation, albeit in lower conversions (entry 6).

Table 2.3 Optimization using Discrete Catalyst

Entry	Deivations From Standard Conditions	Yield
1	None	94%
2	5 mol% ITol-Ni(MMA)$_2$	26%
3	Catalyst exposed to air for 1 hour	73%
4	Reaction done at RT	NP
5	10 mol% Ti(O^{i}Pr)$_4$ + 4 equivs isopropanol	trace
6	1.1 equiv. Al(O^{i}Pr)$_3$	38%

2.4 Mechanistic Considerations

Scheme 2.12 Formation of *Z*-Enol Silanes from Enals and Alkynes

80%
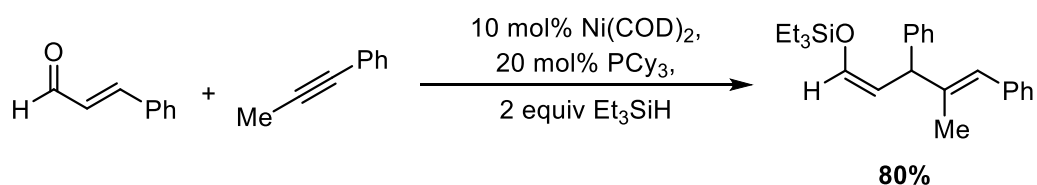
Due to the unique nature of the four-electron reductive coupling, a series of experiments were conducted to better understand the mechanism of this process. Initially, multiple potential mechanisms were proposed for this reaction. Considering the precedent for two-electron reductive couplings to generate enol silane products (Scheme 2.12), it was proposed that enol silane product formation followed by reductive cleavage of the C-OSiEt$_3$ was the operative mechanistic pathway (Scheme 2.13).[29] The reaction pathway would involve the oxidative cyclization of the substrates to form a seven-member metallacycle (**1**) that can perform α-bond metathesis with the silane,

forming an enol silane and a nickel hydride (**2**), which could undergo reductive elimination to give

the enol silane product (**3**). Oxidative addition of the nickel catalyst into the C-OSiEt$_3$ bond (**4**),

followed by displacement of the silyloxy group with a 'hydride source' and subsequent reductive

elimination would yield the desired product (**5**).

Scheme 2.13 C-O Reduction Mechanism
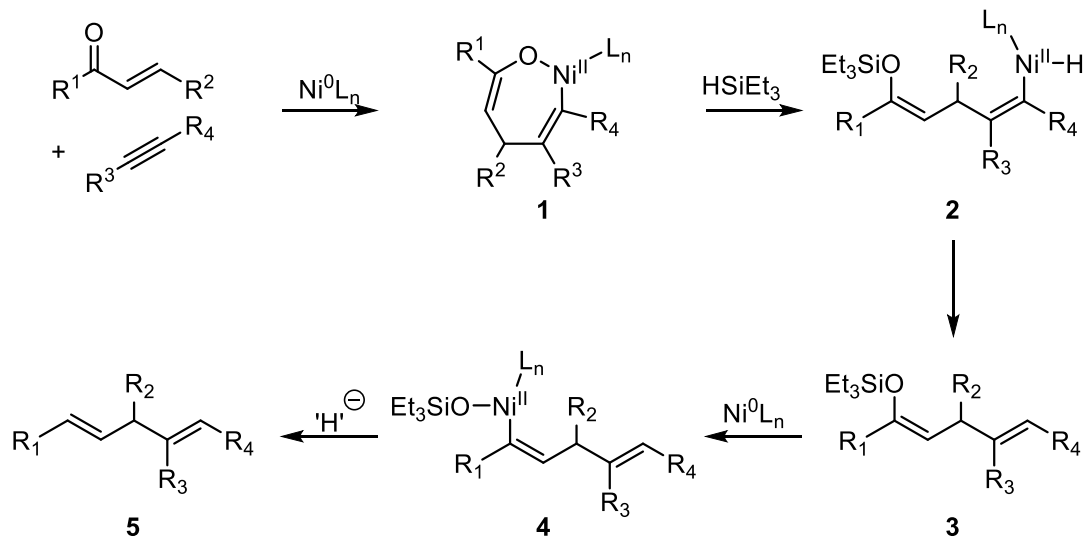
Scheme 2.14 Chatani Reduction of Aryl Pivalates

The oxidative addition of a nickel catalyst into a carbon-oxygen bond followed by α-bond

metathesis with a silane to yield a nickel-hydride that reductively eliminates to provide the reduced

product has been previously reported from the Chatani group (Scheme 2.14).[31] If this pathway

were operative, one would expect that subjection of an enol silane to reaction conditions would

yield the reduced 1,4-diene product. To test this proposed mechanism, a *Z*-enol silane was

synthesized following a previous report in the Montgomery lab, and subjected to the standard

reaction conditions (Scheme 2.15). However, attempts to reduce the Z-enol silane under standard reaction conditions failed to yield the desired product. Based on this experimental evidence, it seems unlikely that the probable mechanism involves the formation and subsequent reduction of an enol silane.

Scheme 2.15 Evaluation of Enol Silane for Productive 1,4-Diene Formation
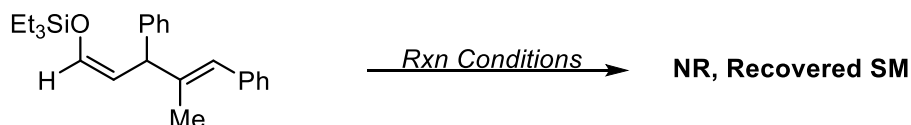
Another potential mechanism involves the initial 1,2-reduction of the enone or enal to the silyl-protected allylic alcohol (**2**), which then undergoes oxidative cyclization with the alkyne and nickel catalyst to form a 5-membered metallacycle (**3**) (Scheme 2.16).[32] The nickel catalyst could then undergo a α-bond metathesis with the proximal carbon-oxygen bond, forming the alkene and delivering a silyloxy group to the nickel center (**4**). From this intermediate, a nickel-hydride could potentially be formed via α-bond metathesis with another equivalent of silane, extruding a bis-silyl ether, or alkoxide exchange with the titanium alkoxide additive, followed by β-hydride elimination releasing an equivalent of acetone. Subsequent reductive elimination would furnish the 1,4-diene (**5**).

Scheme 2.16 Mechanism Involving Formation of an Allylic Alcohol
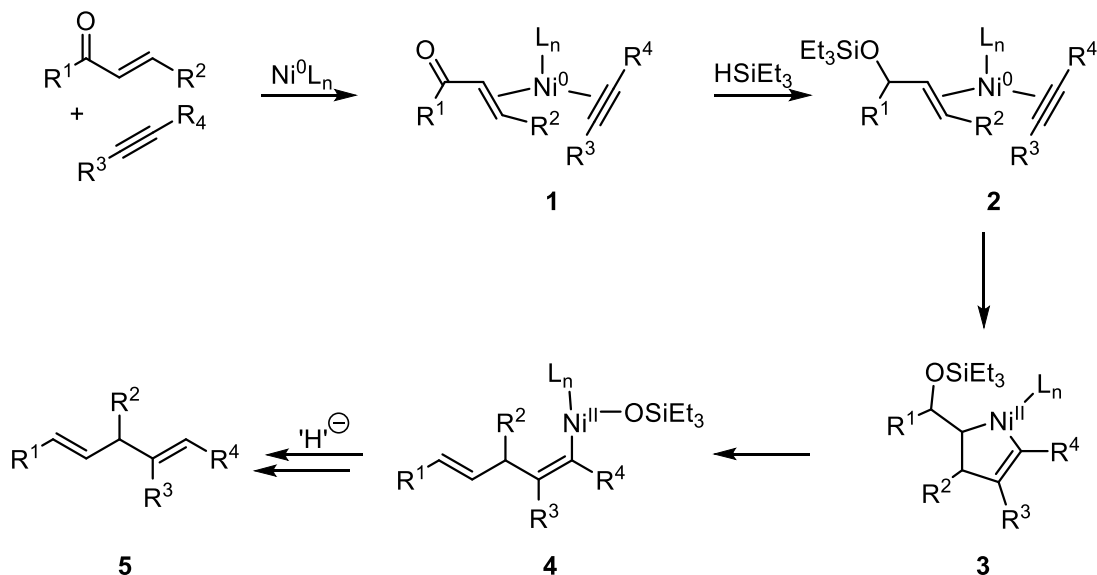
The proposed mechanism was evaluated by independently synthesizing a silyl-protected allylic alcohol and subjecting it to standard reaction conditions (Scheme 2.17). However, the reaction failed to yield the desired 1,4-diene and only starting material was observed. Based on this experiment, it seems unlikely that formation of a silyl-protected allylic alcohol would proceed to yield the desired product.

Scheme 2.17 Evaluation of Allylic Alcohol in Proposed Mechanism
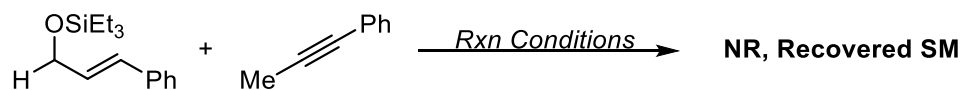
To gain additional insight into the probable reaction mechanism, several deuterium labelling studies were conducted. Following a previously published procedure for the synthesis of Z-enol silanes, a reaction was carried out using Et_3SiD as the reductant (Scheme 2.18). As expected, the deuterium label is exclusively introduced on the alkyne-derived terminus of the product (**A**). However, in the skipped diene production, using Et_3SiD as the reductant, deuteration of the enal-derived terminal methylene group exclusively cis to the central carbon was observed,

23

while no label incorporation in the alkyne-derived terminus was detected (**B**). To determine the source of the second hydride, Ti(O^{i}Pr)$_4$-d$_{28}$ was synthesized and used in the standard reaction conditions. Deuterium incorporation (91%) in the alkyne-derived terminus was observed in the product, while no label incorporation at the enal-derived terminus was observed (**C**).

Scheme 2.18 Deuterium Labeling Studies
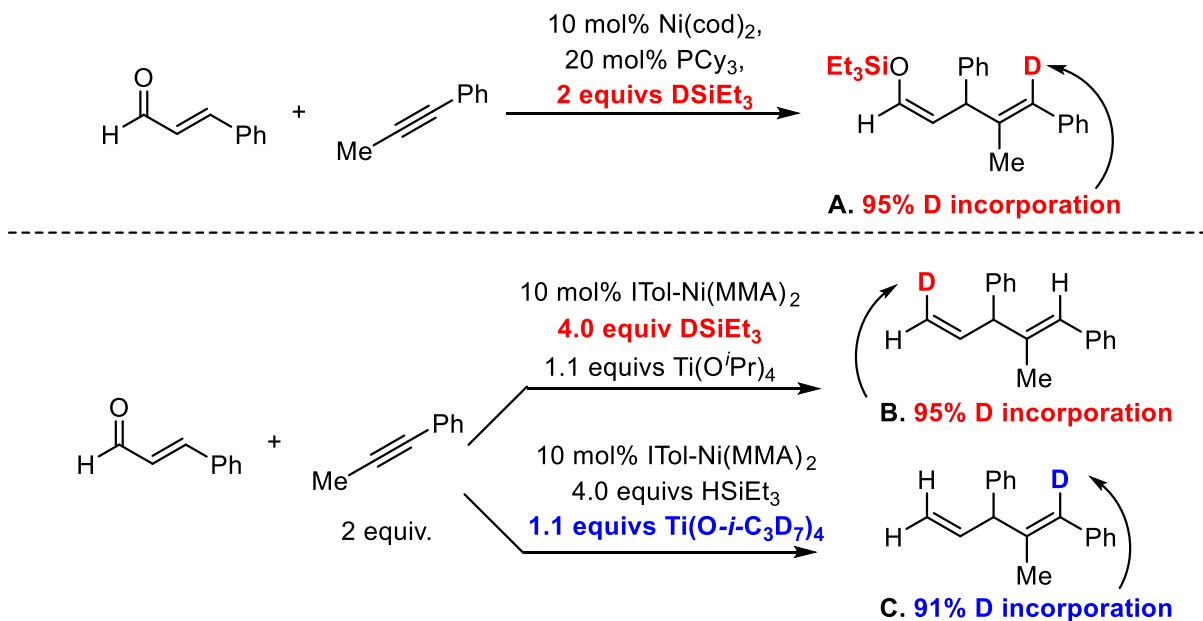
Based on these experiments, a mechanism explaining the surprising results of the labeling experiments can be postulated (Scheme 2.19). Oxidative cyclization of the enal or enone and alkyne with nickel(0) provides a seven membered metallacycle with an η^1 nickel-O enolate motif (**1**), and α-bond metathesis of the silane with the Ni-O bond provides a nickel hydride intermediate bearing an enol silane functionality (**2**). This intermediate can then lead to either a two-electron or four-electron reductive coupling product depending on the ligand employed in the reaction. With PCy$_3$ as the ligand, reductive elimination occurs, resulting in the formation of the Z-enol silane product as previously reported (**3**). However, the unique reactivity illustrated by the unhindered NHC ligand ITol likely suppresses the efficiency of reductive elimination. Instead, coordination

of the enol silane functionality allows for insertion of the nickel-hydride to provide intermediate

4. Rotation of the bond produces rotamer **5** allowing for a selective trans-β-silyloxy elimination

promoted by the Lewis acid Ti(O^{i}Pr)$_4$ (**6**). Isopropoxy transfer from Ti to Ni provides intermediate

7, and subsequent β-hydride elimination extrudes acetone, forming a nickel-hydride intermediate

8. Subsequent reductive elimination provides the desired 1,4-diene product (**9**).

Scheme 2.19 Proposed Reaction Mechanism
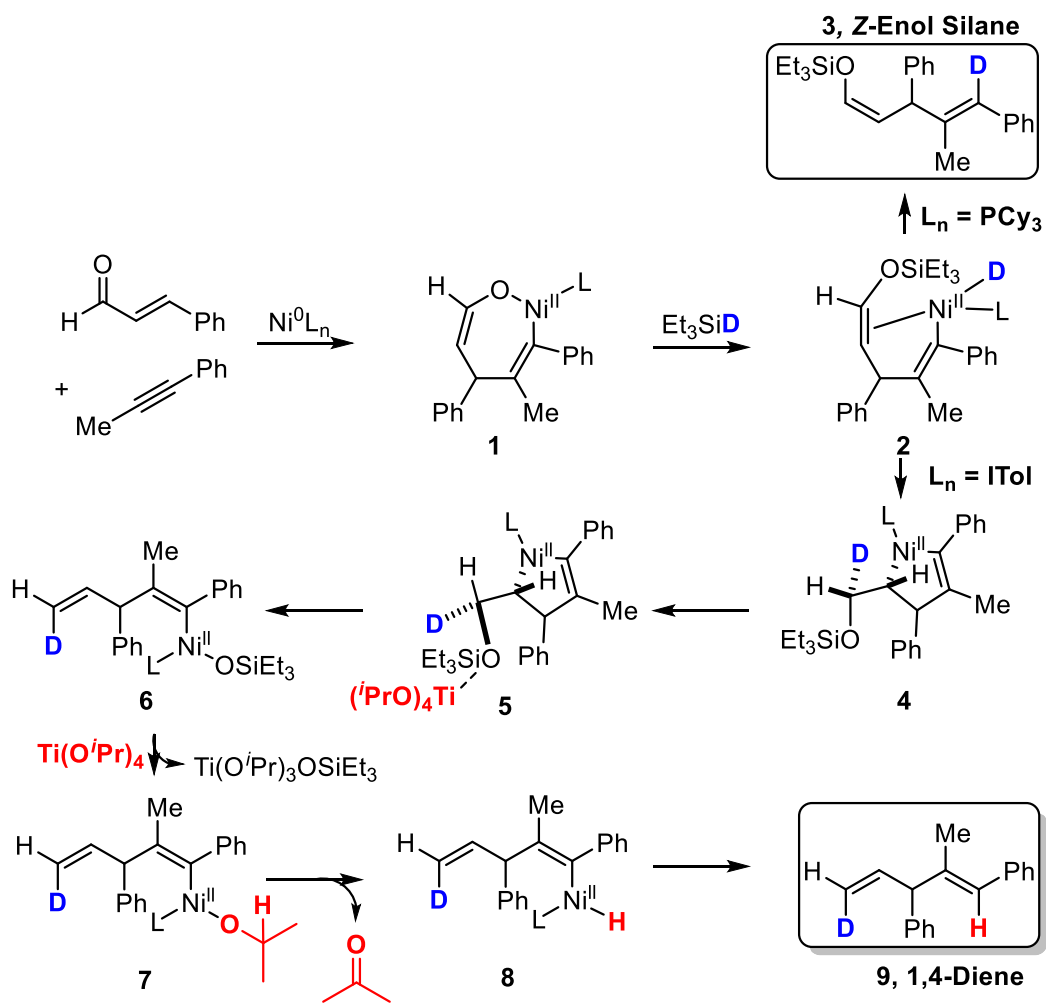
Several experimental observations support the above-postulated mechanistic pathway. The

η^1 nickel-O enolate proposed as intermediate **2** is supported by the observed Z-enol silane

stereochemistry observed in previous reports.[31] It is also consistent with prior crystallographic

analysis of the analogous tmeda and bypyridine metallacycles.[33,34] Additionally, while the stereoselective formation of the 1,2-*trans*-alkene generated from an enone could potentially be biased by the thermodynamic stability of the trans-alkene, the stereochemical outcome of enal coupling using Et_3SiD removes this bias. Starting from the known stereochemistry, *syn* addition to *Z*-enol silane (**2**) followed by trans-β-silyloxy elimination to generate (**6**) explains the observed stereochemical outcome. The inability of cyclic enones to undergo productive formation of the 1,4-diene also supports this postulated mechanism. The intermediate formed from this substrate cannot undergo the bond rotation necessary to adopt the necessary *syn* conformation to undergo the trans-β-silyloxy elimination. The labelling studies (Scheme 2.18), comparing products **B** and **C**, are fully consistent with the proposed mechanistic pathway.

2.5   Substrate Scope

Utilizing the optimized reaction conditions, the production of skipped diene products from a range of alkynes with enals or enones was examined (Scheme 2.20). From a range of enone substrates, products were obtained in good yields with >95:5 regioselectivity. The enone substrates included phenyl and methyl ketones with aromatic or aliphatic substituents at the β-position. It should be noted that decreasing the size of the substituent at the β-position of the enone resulted in diminished yields, and enones lacking a β-substituent altogether failed to yield any desired product. Cyclic enones (such as cyclohexenone) were generally ineffective substrates in this transformation as well. The alkyne could be varied to include symmetrical or unsymmetrical alkynes, including aromatic alkynes, terminal alkynes, and alkynes bearing a phthalimido or silyloxy functionality. Enal substrates possessing aromatic or aliphatic β-substituents were obtained in good yields and >95:5 regioselectivity. Unlike enone substrates, enals lacking a β-substituent proved to be efficient substrates. The difference in reactivity could be a result of enones

coordinating to the nickel catalyst more strongly than enals. As the enone size decreases, the increased stability of the enone-nickel complex inhibits coordination of an alkyne, and shuts down productive catalysis.

Scheme 2.20 Substrate Scope
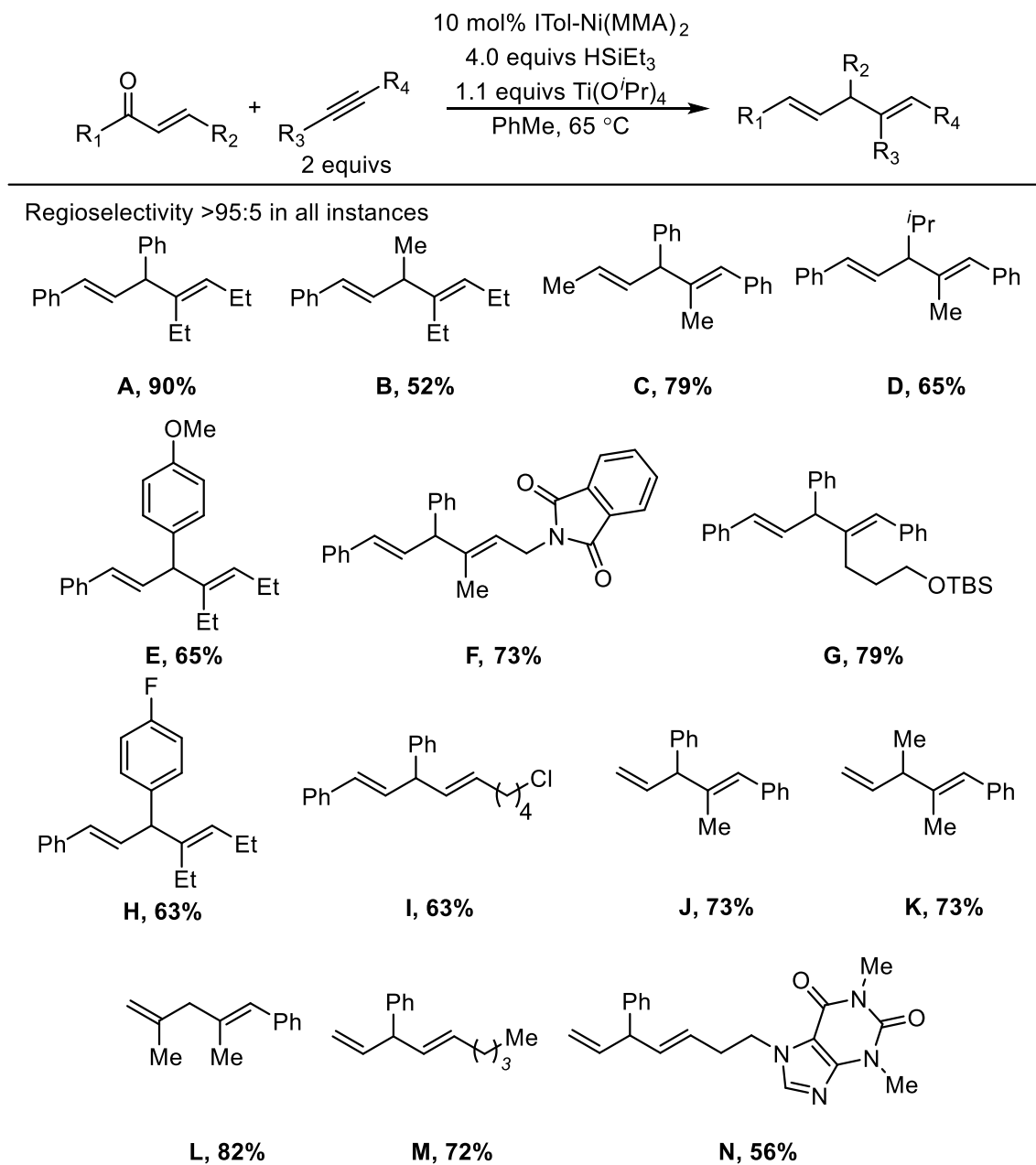
2.6   Future Directions

Scheme 2.21 New Reductive Couplings
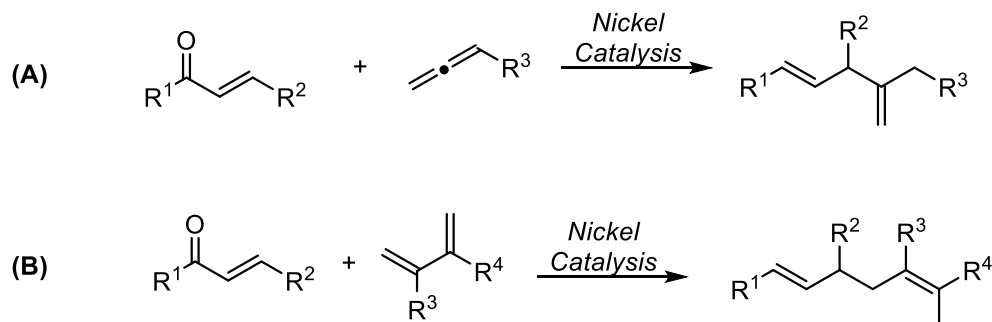
Future work should expand the coupling of the transformation to other simple π-components such as allenes (**A**) or 1,3-dienes (**B**) (Scheme 2.21).[35] These transformations could potentially allow for a wide array of skipped-diene products traditionally difficult to access. Additionally, previous transformations that yielded poor results using ITol should be re-examined utilizing the discrete catalyst. The relatively unhindered ITol ligand has previously shown promising regioselectivites in the reductive coupling of aldehydes and alkynes, but poor reactivity made it an unsuitable ligand for the transformation (Scheme 2.22).[36] The use of the discrete catalyst could overcome the poor reactivity while still affording products with promising regioselective outcomes. Additionally, new transformations utilizing the proposed mechanistic pathway and the ability of titanium(IV) isopropoxide to act as both a Lewis acid and reductant should be explored.

Table 2.4 Poor Reactivity of ITol

Entry	Ligand	Yield, (1:2)
1	ITol·HCl	18%, (87:13)
2	IPr·HCl	84%, (20:80)

2.7   Summary of Net Four-Electron Reductive Coupling

In conclusion, a new method for the synthesis of 1,4-dienes has been disclosed. The reactions proceed via a unique four net-electron reductive coupling between an enone or enal and alkyne. The reaction capitalizes on the inherent reactivity of unsaturated carbonyl substrates while yielding a product lacking the carbonyl moiety. The reaction proceeds with high levels of regioselectivity and modest to excellent yields. The relatively unhindered ITol ligand was shown to be an effective ligand for the transformation, while more commonly employed NHC ligands resulted in no product formation. Due to the instability of the ITol ligand in its use for catalytic transformations, a defined pre-catalyst was synthesized that provided superior reactivity compared to the *in-situ* catalyst formation. Deuterium labelling studies shed light on the probable mechanism, indicating the unusual outcome in which both triethyl silane and titanium(IV) isopropoxide serve as reductants in this transformation.

Chapter 3

Nickel-Catalyzed Functionalization of Silyl Aryl Ethers

3.1   Introduction to Silyl-Protecting Groups

Scheme 3.1 Installation and Removal of a Silyl Protecting Group
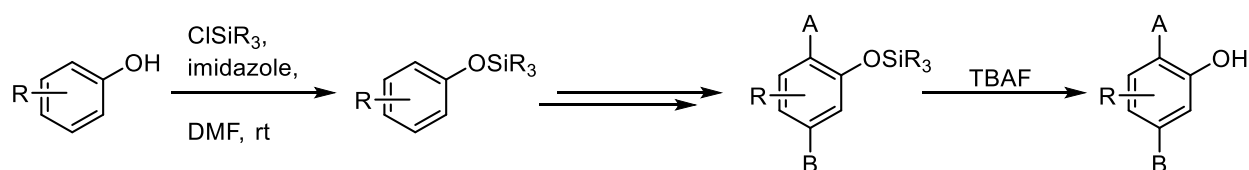
Silyl-protecting groups represent an important class of protecting groups used by chemists.[37] They are often employed to protect a variety of alcohols during an organic synthesis. Their wide use in synthetic chemistry can be attributed to the ease of their installation and their subsequent removal under mild reactions conditions (Scheme 3.1).[38] Additionally, one can install a silyl protecting group early in a synthesis and carry it through several subsequent steps without deprotection occurring. At the end of these steps, one can then remove the protecting group under mild conditions so it does not react with other functional groups present in the molecule. The stability of the silyl-protecting group can also be tailored by varying the bulk of substituents attached to silicon. Several of the most common silyl-protecting groups along with their relative resistance to hydrolysis in both acidic and basic media are shown below (Scheme 3.2).[37]

Scheme 3.2 Relative Stability of Silyl Protecting Groups

Relative Stability in acidic media:

R−OSiMe$_3$ (1) < R−OSiEt$_3$ < R−OSi^{t}BuMe$_2$ (20,000) < R−OSi^{i}Pr$_3$ (700,000) < R-OSi^{t}BuPh$_2$ (5,000,000)
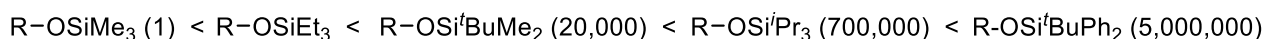
Relative Stability in basic media:

R−OSiMe$_3$ (1) < R−OSiEt$_3$ (10-100) < R−OSi^{t}BuMe$_2$/^{t}BuPh$_2$ (20,000) < R-OSi^{i}Pr$_3$(100,000)

3.1.1 Nickel-Catalyzed Functionalization of Silyl Aryl Ethers

Scheme 3.3 Silyl Aryl Ethers as Cross-Coupling Partners
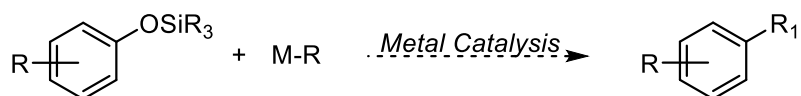
Despite the importance of silyl protecting groups in organic synthesis, very little work has gone into using silyl protected alcohols, specifically silyl aryl ethers, as electrophilic cross-coupling partners in transition-metal catalyzed reactions (Scheme 3.3). Currently, known C(sp^2)-O activation of silyl aryl ethers are limited to nickel-catalyzed Kumada cross-coupling reactions. Seminal work from the Kumada group showed that TMS-protected vinyl ethers are capable of coupling with a Grignard reagent and nickel catalyst, under mild reaction conditions, to afford the desired product in good yields (**A**) (Scheme 3.4).[39] The Shi group expanded the scope of this transformation, illustrating the coupling of a variety of silyl naphthyl ethers with both alkyl and phenyl Grignard reagents using a nickel catalyst (**B**).[40]

Scheme 3.4 Kumada Couplings Utilizing Silyl Aryl Ethers
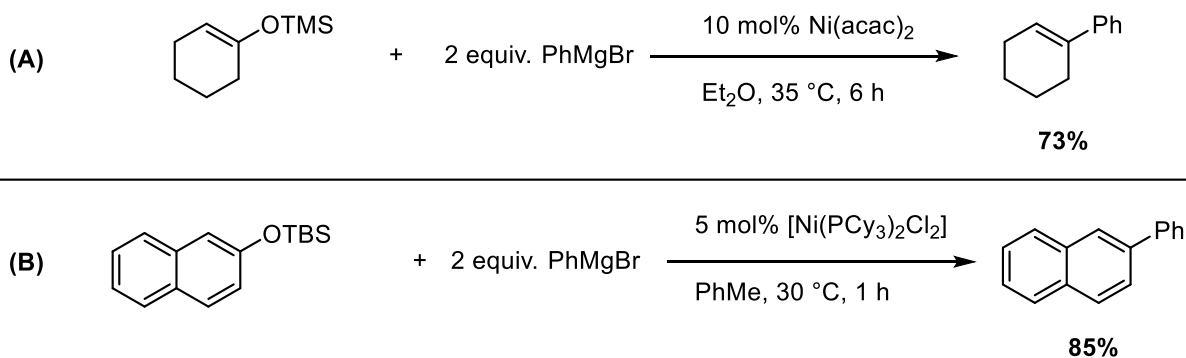
3.2   Introduction to Nickel-Catalyzed Reduction of Carbon(sp²)-Oxygen Bonds

Scheme 3.5 *Ortho*-metalation of Phenol Derivatives
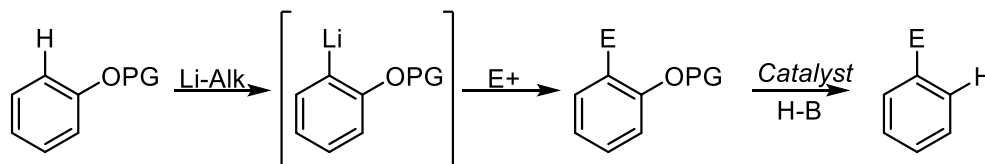
The reduction of carbon(sp²)-oxygen bonds represents an important transformation in synthetic chemistry. For instance, aryl ethers can act as a directing group, maximizing the reactivity and selectivity of a wide range of transformations such as *ortho*-metalation (Scheme 3.5).[41,42] Despite this utility, their selective cleavage represents a tremendous challenge. The ability to selectively replace the carbon-oxygen bond with a hydrogen would be highly desirable, allowing for an alternative method towards arene functionalization, as electronically unbiased arenes lead to unselective transformations.

Another important application for the selective reduction of carbon(sp²)-oxygen bonds involves the conversion of oxygen-rich lignocellulosic plant biomass to deoxygenated fuels and commercial chemicals (Scheme 3.6).[43-45] Lignin is one of the most abundant organic polymers on Earth, so being able to selectively break-down the structure in smaller molecules could be very beneficial as a feedstock towards commodity chemicals.

Scheme 3.6 Reduction of Lignin Models

Model for the α-O-5 lignin linkage:
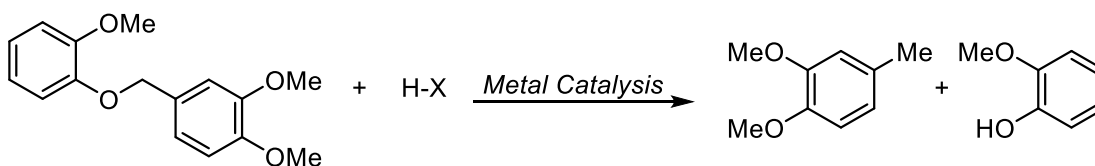
Model for the β-O-4 lignin linkage:
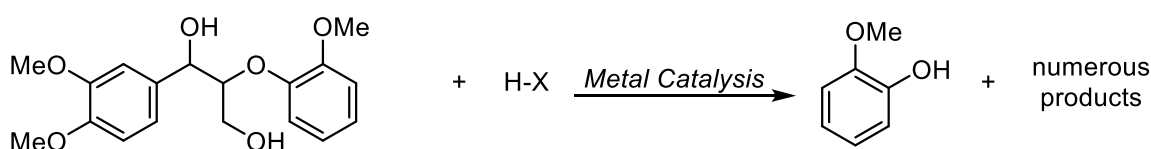
3.2.1   Existing Methods for the Nickel-Catalyzed Reduction of Carbon(sp^2)-Oxygen Bonds

Scheme 3.7 Martin Reduction Method

10 mol% Ni(COD)$_2$
20 mol% PCy$_3$
1 equiv TMDSO

PhMe, 110 °C, 14 h

73%
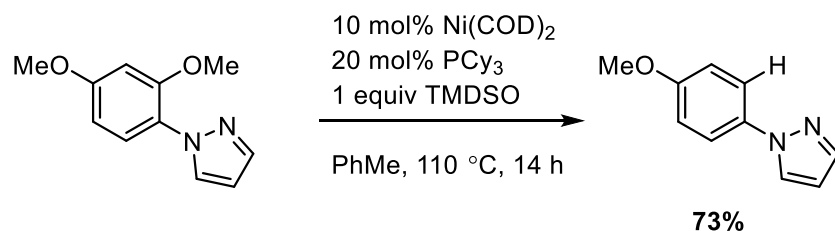
Due to the reasons highlighted above regarding the importance of the reduction of carbon(sp^2)-oxygen bonds, much work has gone into the development of methods capable of carrying out this transformation with high levels of selectivity and conversion. Work from the Martin group showed that aryl methyl ethers could be reduced in the presence of catalytic Ni(COD)$_2$ and PCy$_3$, along with tetramethyldisiloxane (TMDSO) as the reductant (Scheme 7).[46] The substrate scope was limited to naphthyl methyl ethers or aryl methyl ethers containing an *ortho*-directing group. Changing the protecting group from a methyl to an ethyl group or other commonly employed protecting group, such as a triflate or pivalate yielded very poor conversion

33

to product. The mechanism of the transformation was later revealed to proceed through a nickel(I) silyl intermediate.[47] It should also be noted that work from the Chatani group published a transformation similar to the Martin reduction shortly thereafter.[48] The substrate scope and conditions were almost identical, except dimethoxy methyl silane was used as the silane reductant.

Scheme 3.8 Hartwig Reduction Method

65%
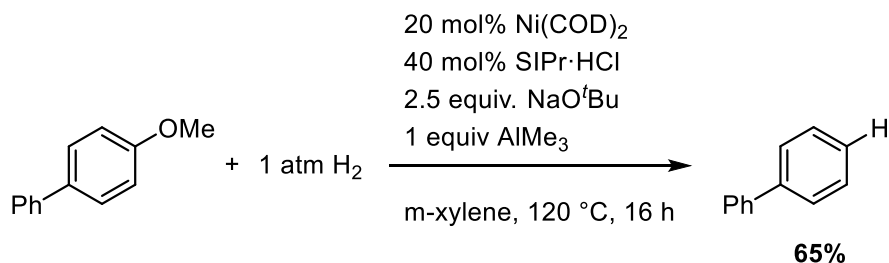
An additional method to reduce $C(sp^2)$-O bonds comes from work in the Hartwig group.[49] They showed that using nickel catalysis, both diaryl ethers and alkyl phenyl ethers could be reduced using hydrogen gas as the reductant (Scheme 3.8). The method required relatively high catalyst and ligand loadings (20 mol% $Ni(COD)_2$ and 40 mol% SIPr), along with high reaction temperatures (> 120 °C) and long reaction times (24-48 hours). Alkyl phenyl ethers were much less reactive than diaryl ethers and required the addition of a Lewis acid ($AlMe_3$) to achieve satisfactory conversions to the reduced arene.

Scheme 3.9 Chatani Reduction

51%
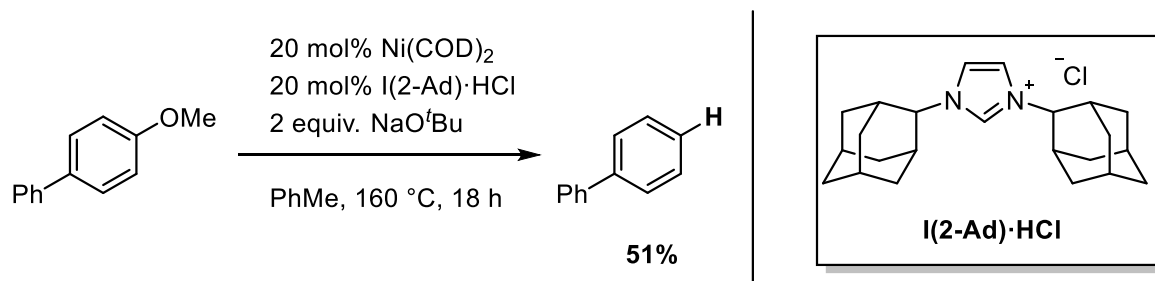
Work in the Chatani group presented the nickel catalyzed reduction of alkyl methyl ethers without an external reductant (Scheme 3.9).[50] Deuterium labeling studies indicated that the

hydrogen in the reduced arene originated from the alkyl protecting group. This process potentially could occur via oxidative addition into the carbon(sp^2)-oxygen bond, followed by β-hydrogen elimination to extrude formaldehyde. Subsequent reductive elimination would yield the reduced arene. Work in the Agapie group has also shown a similar type of reduction mechanism via stoichiometric nickel studies.[51] The substrate scope could accommodate both aryl and naphthyl alkyl ethers. While the naphthyl substrates provide the reduced arenes in high yields, simple aryl systems required much more forcing reaction conditions and resulted in much lower conversion to products.

Despite the multitude of methods towards the reduction of alkyl aryl ethers using nickel catalysis, there is room for improvement in the methodology. All the methods utilize $Ni(COD)_2$, requiring the use of a glove box to perform the reaction. Additionally, the methods typically require high catalyst loadings, temperatures, and reaction times. These issues are only exacerbated when employing simply aryl ethers as the substrates. Several of the methods fail to yield any product with these substrates, while those that do accommodate them are plagued by poor conversions to product. A method for the reduction of simple phenol substrates utilizing bench-top stable catalysts, along with low catalyst loadings, reactions times, and temperatures would greatly enhance the field.

3.2.2   Optimizations of Reaction Conditions

Scheme 3.10 Role of Titanium Lewis Acid in Synthesis of 1,4-Dienes
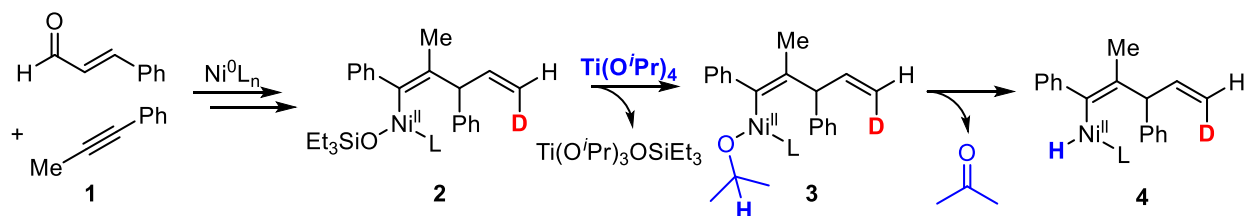
As discussed previously (Chapter 2), it was shown that enones or enals and alkynes could be reductively coupled with a nickel catalyst to afford 1,4-dienes.[52] During the study, deuterium labelling experiments indicated that titanium(IV) isopropoxide served as a reductant during the transformation. It was hypothesized that alkoxide exchange with the nickel silyloxy intermediate (**2**), furnished intermediate (**3**) (Scheme 3.10). Subsequent β-hydride elimination would extrude acetone (**4**), followed by reductive elimination to furnish the desired skipped diene product. Considering the proposed mechanism, it was theorized that if one could access intermediate (**2**) from other starting materials, the titanium additive would be able to intercept the intermediate to furnish the reduced product. If a nickel catalyst could undergo oxidative addition to the carbon-oxygen bond present in silyl aryl ethers (**A**), titanium(IV) isopropoxide should then be capable of intercepting the intermediate, producing the reduced arene (**B**) (Scheme 3.11).

Scheme 3.11 Proposed Reduction of Silyl Enol Ethers
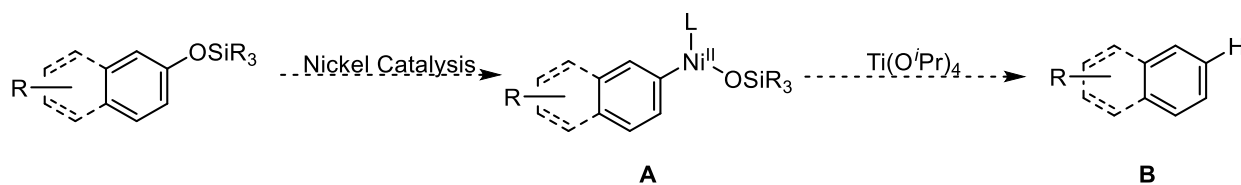
To test this hypothesis, a naphthyl silyl ether was subjected to reaction conditions similar to the Hartwig method for reduction of alkyl aryl ethers (Scheme 3.8), except titanium(IV) isopropoxide and triisopropyl silane were used rather than hydrogen gas (Scheme 3.12). Both the silane and titanium additive were included, as it was theorized that either one could serve as the reductant during the transformation. Upon running the reaction, it was determined that the major product detected via GC-MS was that of the reduced arene (**A**), with a substantial amount of hydrolysis byproduct (**B**).

Scheme 3.12 Initial Reduction Findings
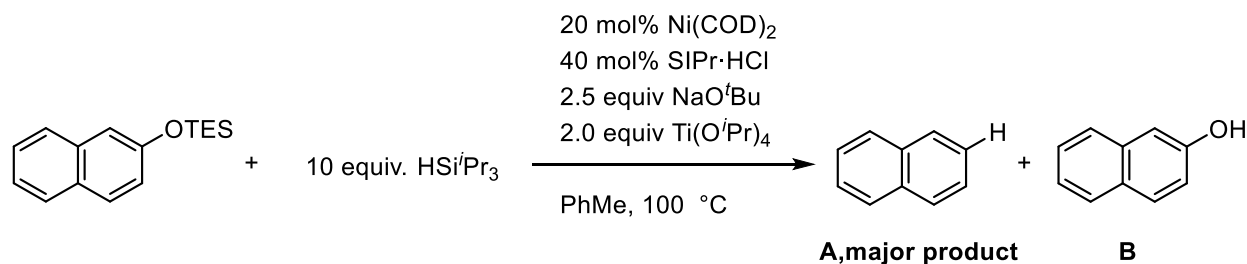
After the initial data point, extensive optimization was undertaken to efficiently reduce

silyl enol ethers via nickel catalysis (Note: All work described hereafter was done in conjunction

with Eric Wiensch). The optimal conditions for the reduction of the model substrate are shown

below (Scheme 3.13). The model substrate, TBS protected 4-phenylphenol could be reduced to

the arene in very high yields and relatively low catalyst loadings. Additional details regarding how

the optimization results were determined will be discussed below.

Scheme 3.13 Optimized Reduction Reaction Conditions
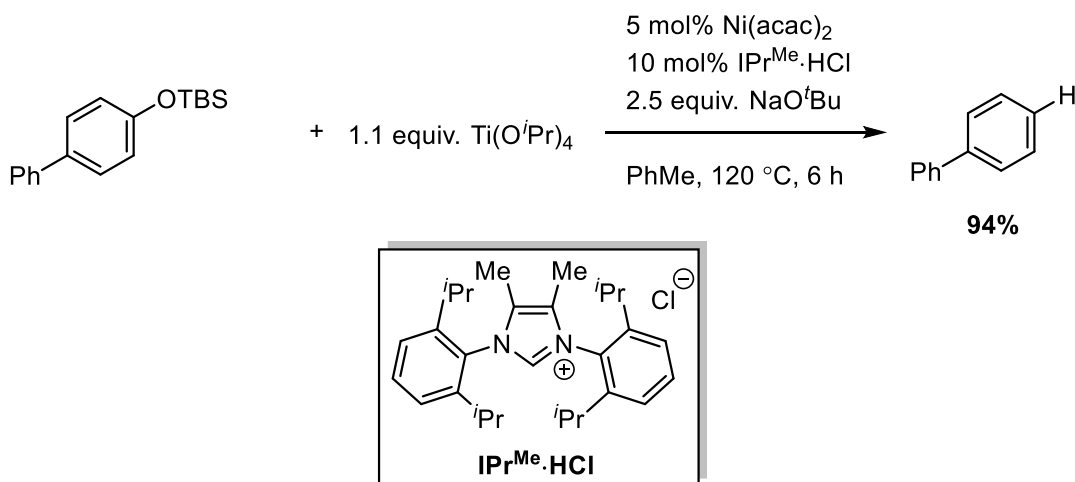
Both the nature of the nickel catalyst and length of time of the reaction were varied to

obtain optimal results (Table 3.1). Using 5 mol% Ni(acac)$_2$ along with reaction temperature of 120

°C for 6 hours resulted in a 94% yield of the desired product (entry 1). Changing the nickel source

to Ni(COD)$_2$ resulted in a 13 % decrease in yield of the desired product (entry 2). The reaction

time could be halved to 3 hours using 10 mol% of $Ni(acac)_2$, with only a very slight decrease in yield of the product (entry 3). Finally, running the reaction at temperatures lower than 120 °C resulted in only modest conversion to the desired product (entry 4).

Table 3.1 Optimization of Catalyst and Reaction Time

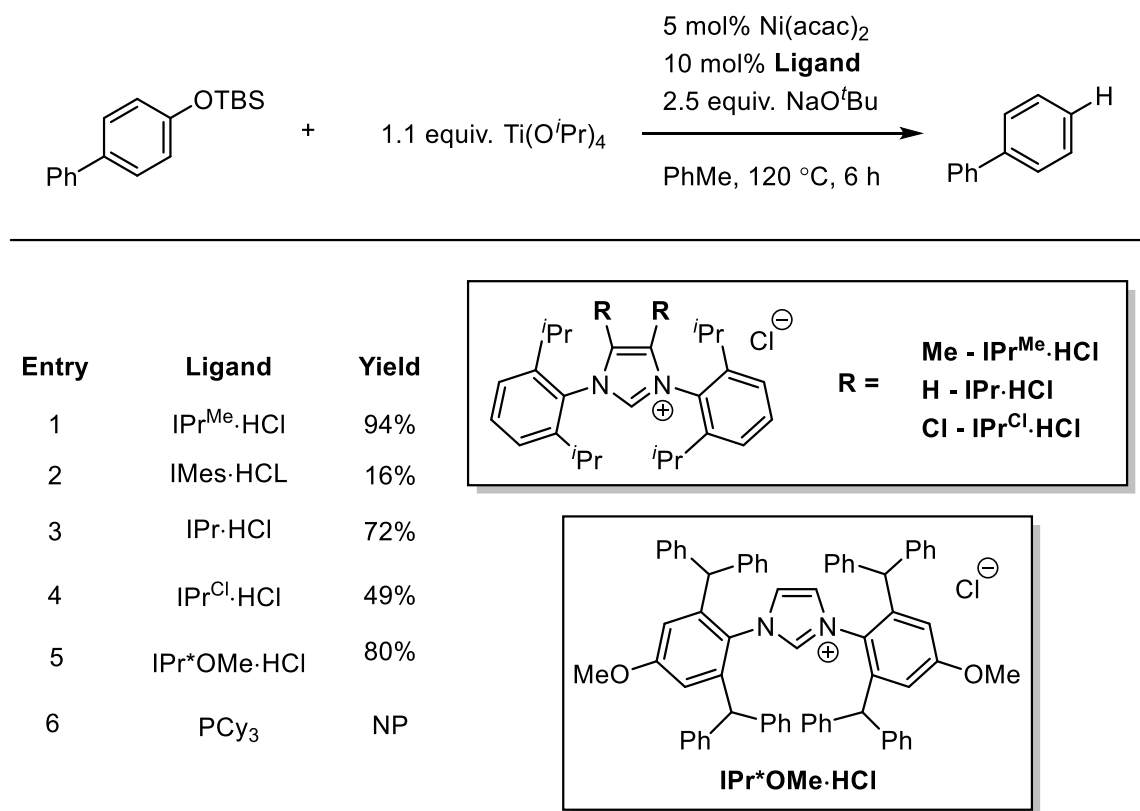| Entry	Deviations from Standard Conditions	Yield
1	None	94%
2	$Ni(COD)_2$ for $Ni(acac)_2$	81%
3	10 mol% $Ni(acac)_2$, 3 h	91%
4	100 °C, 16 h	67%

The nature of the ligand employed in the reaction was also varied to obtain optimal reaction conditions (Table 3.2). Using IPr^{Me}·HCl gave a 94% conversion to the desired product (entry 1). A smaller ligand, such as IMes·HCl gave very poor conversion to desired product (entry 2). Both IPr·HCl and IPr^{Cl}·HCl both gave modest yields as well (entry 3 and 4). The extremely bulky IPr*OMe·HCl ligand gave the next best result with an 80% conversion to the desired product (entry 5). Simple monodentate phosphine ligands, such as PCy_3, resulted in no product formation (entry 6). From the ligand screen, one can theorize that bulky NHC ligands result in the best conversion to desired product (entries 1 and 5). Additionally, the methyl groups on the backbone of the imidazole ring in IPr^{Me}·HCl clearly lead to superior conversion to product, as replacing those groups with a hydrogen or chlorine hinders reactivity (entries 1,3, and 4). The methyl groups could be increasing the electron donating ability of the ligand, resulting in a stronger ligand to nickel bond.

Table 3.2 Optimization of the Ligand for Reduction

Entry	Ligand	Yield
1	IPr^{Me}·HCl	94%
2	IMes·HCL	16%
3	IPr·HCl	72%
4	IPr^{Cl}·HCl	49%
5	IPr*OMe·HCl	80%
6	PCy$_3$	NP

The protecting group employed during the reaction was also optimized (Table 3.3). A variety of silyl protecting groups were explored (entries 1-4). The TBS protecting group provided the highest yield of the desired product at 94%. Other bulky silyl groups gave comparable yields or slightly worse (entries 2 and 3). Silyl groups more susceptible to hydrolysis resulted in greatly diminished yields (entry 4). Other commonly employed protecting groups in carbon(sp^2)-oxygen bond activation chemistry were also explored. Aryl methyl ethers resulted in only a 16% yield of the desired product (entry 5). Both pivalates and triflates gave either trace or no product formation (entries 7 and 8). A phenyl protecting group gave slightly diminished yields, with only a 78% yield of the desired product.

Table 3.3 Optimization of Reduction Protecting Group
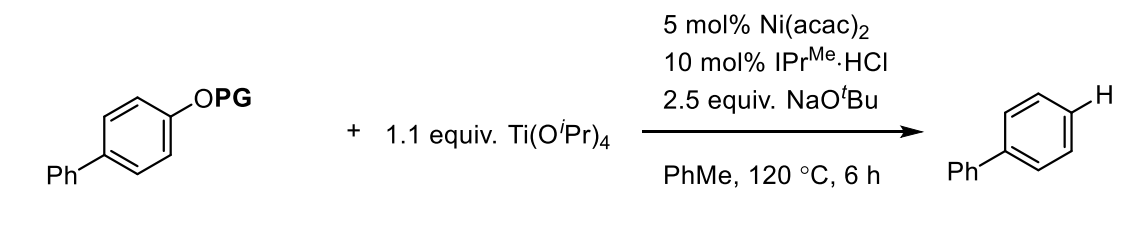
Entry	Protecting Group (PG)	Yield
1	TBS	94%
2	TIPS	90%
3	TBDP	76%
4	TES	49%
5	Me	16%
6	Piv	trace
7	Tf	2%
8	Ph	78%

The type of base employed and the stoichiometry were also varied (Table 3.4). Using 2.5 equivalents of NaO^{t}Bu resulted in a 94% yield of the desired product (entry 1). Changing the base to either LiO^{t}Bu or KO^{t}Bu resulted in greatly diminished yield of product, indicating that changing the counter ion of the base greatly affects reactivity of the system (entries 2 and 3). Other sodium alkoxide bases resulted in either very little to no product formation (entries 4 and 5). Finally, using only 1.5 equivalents of base resulted in diminished yields (entry 6), while using 0.1 equivalents of base resulted in no product formation (entry 7).

Table 3.4 Optimization of Base Screen
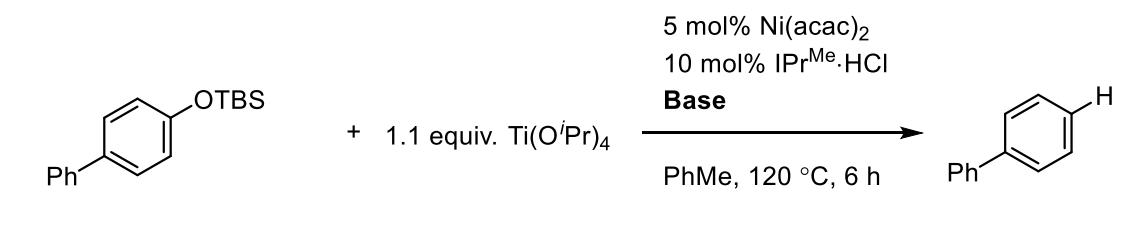
Entry	Base	Yield
1	2.5 equiv NaO^{t}Bu	94%
2	2.5 equiv LiO^{t}Bu	42%
3	2.5 equiv KO^{t}Bu	5%
4	NaOPh	8%
5	NaO^{i}Pr	NP
6	1.5 equiv NaO^{t}Bu	72%
7	0.1 equiv NaO^{t}Bu	NP

The Lewis acid employed during the reaction was also varied to obtain optimal reaction conditions (Table 3.5). Using 1.1 equivalent of titanium(IV) isopropoxide resulted in a 94% yield of the desired product (entry 1). Lowering the equivalents of Lewis acid to 0.5 equivalents resulted in a diminished yield of the desired product (entry 2). Using other titanium alkoxide or aluminum alkoxide Lewis acids resulted in greatly diminished yields of the desired product (entries 3 and 4). To determine whether the titanium Lewis acid was simply serving as a source of isopropoxide anions, the titanium additive was replaced with four equivalents of NaO^{i}Pr, resulting in no product formation (entry 5).

Table 3.5 Lewis Acid Screening for Reduction
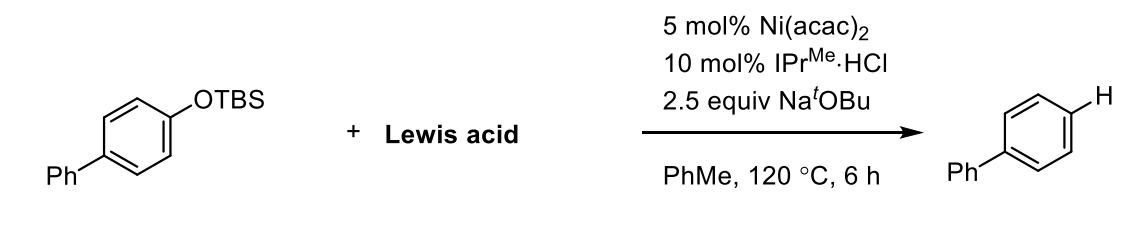
Entry	Lewis acid	Yield
1	1.1 equiv Ti(O^{i}Pr)$_4$	94%
2	0.5 equiv Ti(O^{i}Pr)$_4$	73%
3	1.1 equiv Ti(OMe)4	4%
4	1.1 equiv Al(O^{i}Pr)4	55%
5	4 equiv. of NaO^{i}Pr	NP

3.2.3 Mechanistic Investigations

Scheme 3.14 Deuterium Labeling Study
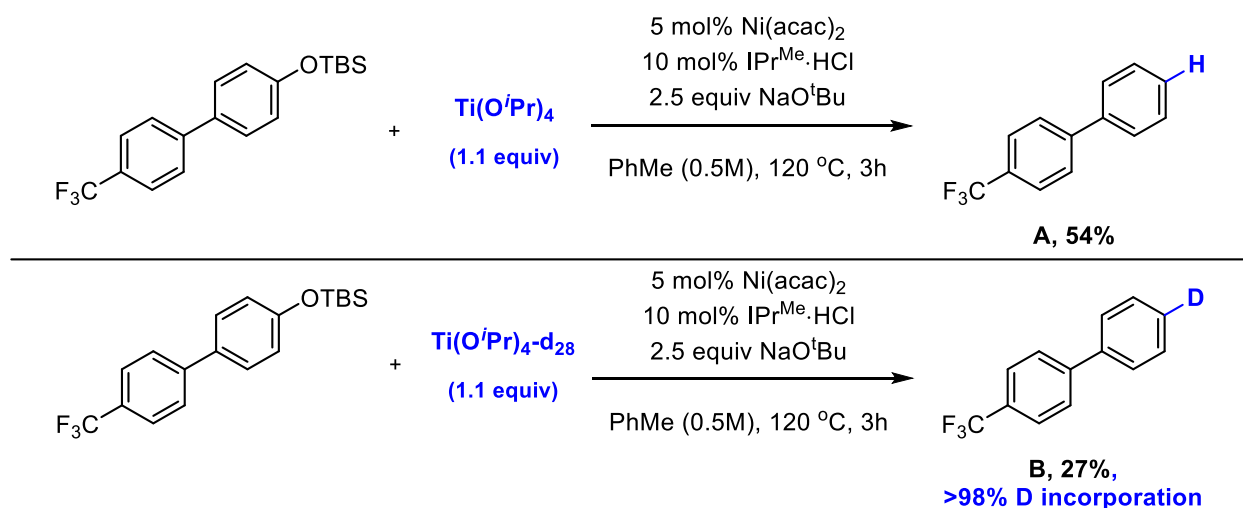
A deuterium labelling study was conducted to determine the source of the hydrogen introduced into the arene during the transformation (Scheme 3.14). The model reaction was conducted using standard titanium(IV) isopropoxide to obtain the standard spectra (**A**). Using deuterated titanium(IV) isopropoxide, it was determined that the hydrogen did indeed originate

from the Lewis acid, with greater than 98% deuterium incorporation observed (**B**). This result is consistent with the labeling study observed regarding the synthesis of skipped dienes (Chapter 2).

In terms of an operative mechanism, one can be theorized using the available reaction trends and computational studies conducted on similar systems (Scheme 3.15). It is proposed that the nickel species forms a bisligated species (**A**), that then has a t-butoxide anion coordinated to the nickel center resulting in a monoligated nickelate species (**B**). Oxidative addition into the carbon-silyloxy bond provides intermediate (**C**). Dissociation of the silyloxy group from the nickel center yields a nickel(II) intermediate with an aryl group and t-butoxide bound to the metal center (**D**). Alkoxide exchange with titanium (IV) isopropoxide provides intermediate (**E**). β-hydride elimination extrudes acetone leading to a nickel-hydride bond that can subsequently reductively elimination to provide the reduced arene (**F**). Displacement of the product from the nickel center by another equivalent of sodium t-butoxide would complete the catalytic cycle (**B**).

Scheme 3.15 Proposed Reaction Mechanism
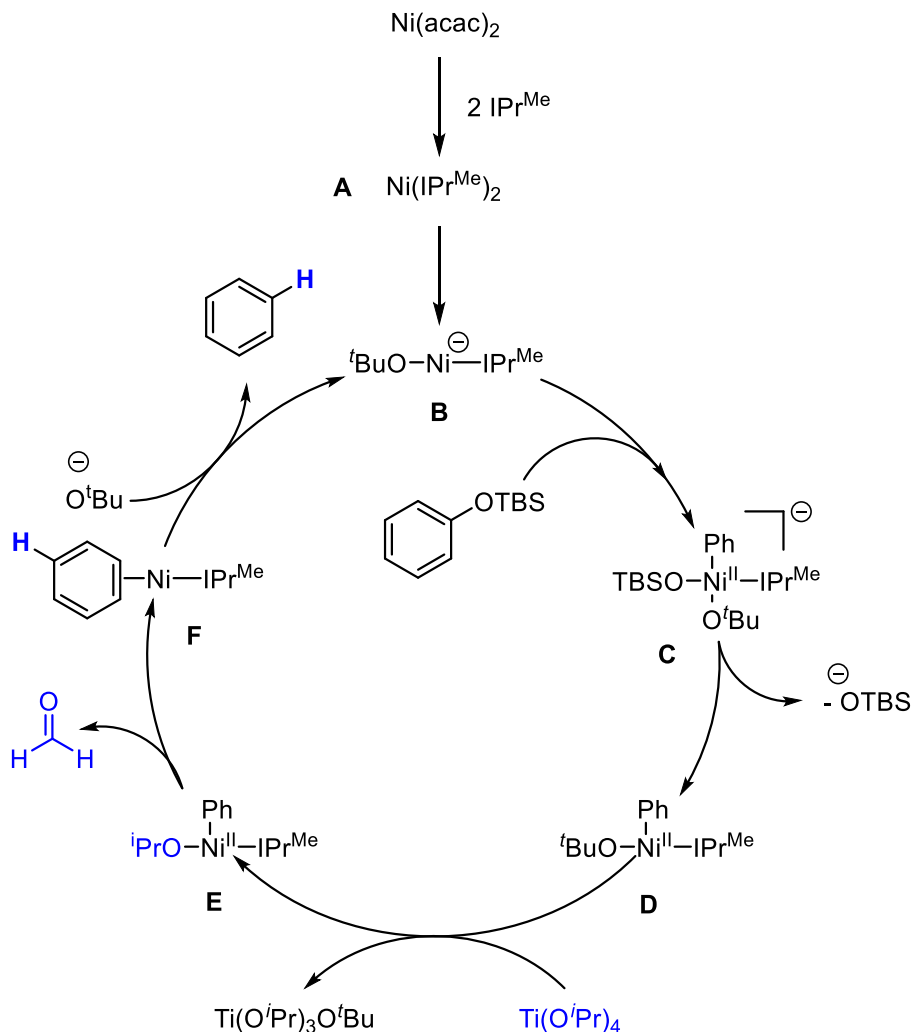
Both the data obtained during the optimization of the transformation, along with computational studies conducted by the Wu group provide reasonable evidence of this operative mechanism. Work in the Wu group studied the Hartwig method for reduction of phenyl ethers using hydrogen gas and nickel catalysis, providing energy values and proposed intermediates of the carbon-oxygen bond activation (Scheme 3.16).[53] Due to the similar nature of the transformation along with the conditions employed, it seems reasonable that a similar transformation could be occurring during the reduction of silyl enol ethers. The study indicated that the nickelate species (**B**) to be over 12 kcal downhill in energy from Ni(COD)$_2$. From here, they computed the oxidative

44

addition into the carbon-oxygen bond from the nickelate species and that of a nickel center without base bound. It was determined that the nickelate species (**B**) favored oxidative addition into the carbon-oxygen bond by more than 4 kcal/mol compared to the nickel(0) complex only ligated with ligand. The subsequent nickelate(II) intermediate (**C**) was found to be -16.5 kcal/mol in energy downhill. From here, dissociation of the phenoxide group to generate the nickel(II) complex bound to the aryl and t-butoxide group was another 9 kcal/mol downhill (**D**). At this point, the reaction diverges as the Hartwig method used hydrogen gas as the reductant.

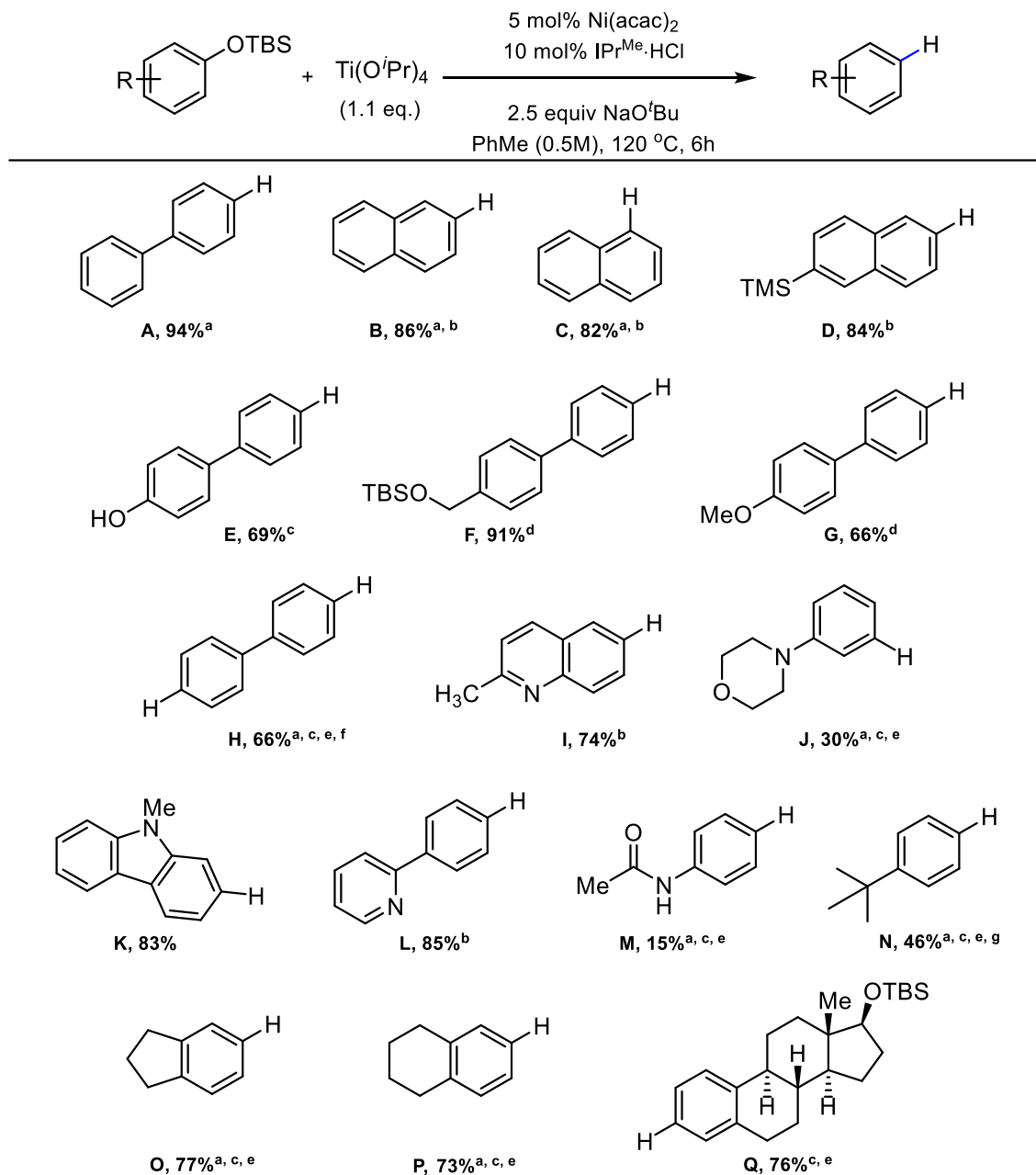**Scheme 3.16** Wu Computational Study of the Reduction of Phenyl Ethers
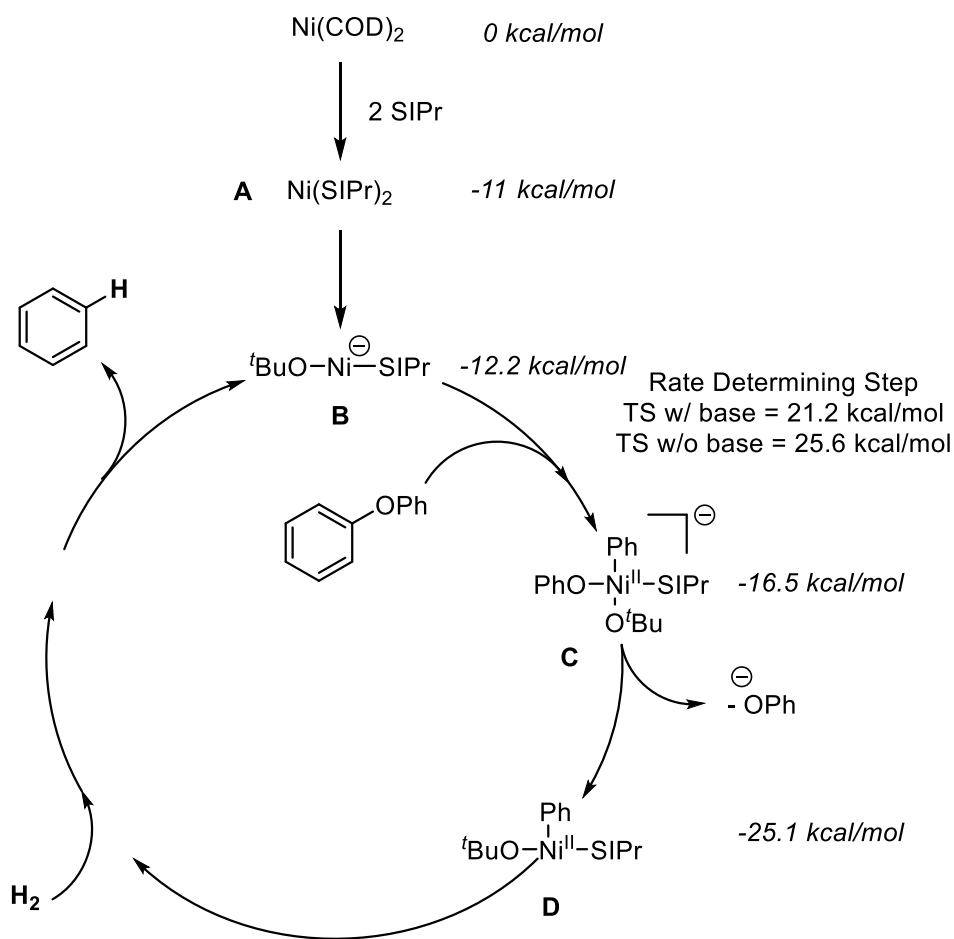
This data provides support regarding the experimental work obtained during the optimization of the reduction of silyl aryl ethers. The study confirms the necessity of super

stoichiometric base which was noted during the optimization of the reaction. The labeling study also confirms the role of the titanium Lewis acid as the reductant during the transformation. While this work does shed considerable light into the relative energy profile of the mechanism, there are still aspects of the mechanism that remain unclear. While the role of the base seems rational, the computational study does not explain the effect of the counter ion of the base on the transformation. Additionally, the nature of the NHC and how it affects reactivity is not entirely clear. Sterically encumbered and electron-donating NHC ligands provided the best reactivity, but understanding how these effects specifically influence the reaction mechanism remain unclear.

3.2.4 Substrate Scope

The reduction of silyl aryl ethers was carried out under various reaction conditions, resulting in moderate to high yields (Scheme 3.17). Notable functional group tolerance includes the ability of the reaction system to tolerate free alcohols (entry E). Surprisingly, the reaction can selectively reduce the carbon-silyloxy bond in the presence of an aryl methyl ether (entry G). This provides a complementary reaction pathway to methods capable of selectively activating the aryl methyl ether as described above (Scheme 3.7). Benzyl silyloxy groups were also not activated during the reaction, illustrating the reduction's preference to activate $C(sp^2)$-O bonds (entry F). Simple electron-rich aryl systems were also able to yield the desired product, albeit with modified reactions conditions that required higher catalyst loadings (entries N-Q). It should be noted that the yields surpass those obtained with other carbon(sp^2)-oxygen reduction methods. Several other functional tolerant of the reaction system include the trimethyl silyl group, pyridines, morpholines, and amides (entries D, J, L, M).

Scheme 3.17 Substrate Scope for Reduction of Silyl Aryl Ethers

A, 94%[a]

B, 86%[a, b]

C, 82%[a, b]

D, 84%[b]

E, 69%[c]

F, 91%[d]

G, 66%[d]

H, 66%[a, c, e, f]

I, 74%[b]

J, 30%[a, c, e]

K, 83%

L, 85%[b]

M, 15%[a, c, e]

N, 46%[a, c, e, g]

O, 77%[a, c, e]

P, 73%[a, c, e]

Q, 76%[c, e]

(a) Yield determined by GCFID with tridecane as internal standard. (b) Reaction run for 3 hours. (c) Reaction run using 10 mol% Ni(acac)$_2$, 20 mol% IPr^{Me}·HCl, 4 eq. NaOBu for 16 hours. (d) Reaction run for 16 hours. (e) Reaction run at 130 °C. (f) Reaction run using 2.2 eq. Ti(O^{i}Pr)$_4$. (g) Reaction run using Ni(COD)$_2$.
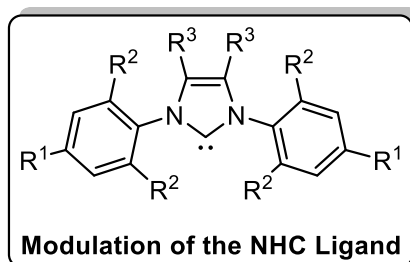
3.2.5 Future Work

Scheme 3.18 Proposed Reduction of Silyl Enol Ethers
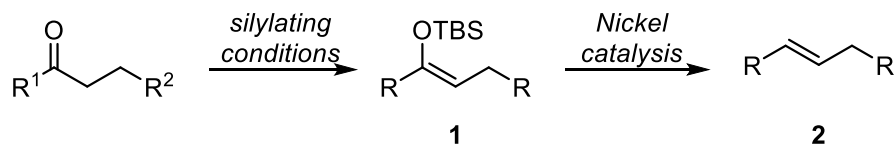
While the method currently tolerates a variety of silyl aryl ethers, there are still certain

aspects of the methodology that could be expanded and improved upon. To start, the reaction

conditions should be adapted to accommodate silyl enol ethers. One could feasibly take any ketone

or aldehyde and convert the product to the silyl enol ether (**1**) and yield an olefin product upon

subjection to the standard reduction reaction conditions (**2**) (Scheme 3.18). Initial findings in this

area resulted in poor conversion to the desired reduced product, likely due to the increased strength

of the carbon-oxygen bond. One could potentially overcome the poor reactivity through rational

ligand design. As described above, increasing the electron donating ability of the NHC ligand,

along with increased steric encumbrance resulted in greatly improved reactivity and yields of the

reduced arene (Scheme 3.19).[54] Additional work into the synthesis of novel NHC ligands bearing

more EDG's on the R^3 position of the NHC, along with bulky steric groups in the *ortho* position

of the *N*-aryl groups (R^2) could lead to an increase in reactivity for the reduction of silyl enol
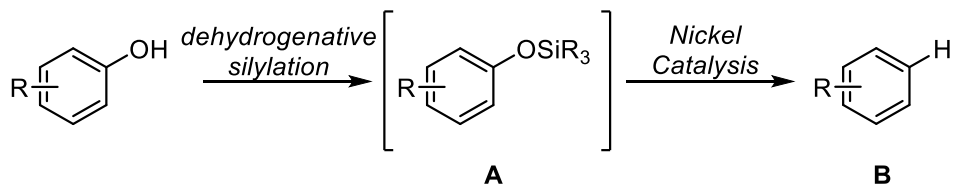
ethers.

Scheme 3.19 Modulation of the NHC Ligand

Another area of future work could explore the dehydrogenative silylation of phenol

substrates (**A**), followed by reduction of the newly formed carbon-silyloxy bond using nickel

catalysis (**B**) (Scheme 3.20). This could potentially allow for the one-pot reduction of any phenol without the need of an additional step to install the protecting group. Several boron Lewis acids have been shown to catalyze the dehydrogenative silylation of phenols indicating the transformation may be feasible with extensive optimization of reaction conditions.[55]

**Scheme 3.20** One Pot Reduction of Phenols

3.2.6   Summary of Reduction of Silyl Aryl Ethers

In summary, a variety of silyl aryl ethers were selectively reduced to the arene via nickel catalysis. The commonly employed TBS protecting group was determined to be the optimal protecting group. The reaction employs a very cheap nickel(II) source allowing for the reactions to be set-up without the benefit of a glove box. The reactions can also be run with relatively low catalyst loadings (5 mol%) and short reaction times (6 hours). Additionally, it was determined that super-stoichiometric sodium t-butoxide was required to obtain efficient conversion to products. Labeling studies confirmed that the hydrogen of the C-H bond formed during the reaction originates from titanium(IV) isopropoxide. The reduction was also shown to selectively reduce carbon-silyloxy bonds in the presence of aryl methyl ethers. Since aryl methyl ethers have been used in a variety of $C(sp^2)$-O bond activation reactions, this method offers orthogonal depending on the protecting group employed in the reaction. Additionally, the reaction can reduce simple aryl rings with modest to great yields. Previous reduction methods were either unable or yielded very poor conversion to these aryl scaffolds.

3.3   Introduction to Metal-Catalyzed Silylation of Carbon(sp²)-O Bonds

Scheme 3.21 Hiyama-Denmark Cross-Coupling
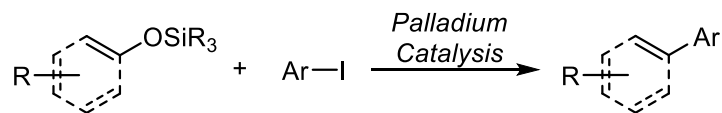
The silylation of carbon(sp^2)-oxygen bonds represents an important transformation in synthetic chemistry. Aryl silanes are valuable synthetic intermediates of considerable interest in both medicinal and material science.[56-58] Additionally, aryl silanes can be used as electrophiles in cross-coupling reactions. The most famous of this type of transformation are either the Hiyama cross-coupling reaction or Hiyama-Denmark cross-coupling reaction (Scheme 3.21).[59,60] The reaction employs a vinyl or aryl silane along with an aryl iodide and palladium catalyst. The silyl protecting group is very important in terms of reactivity and is what differentiates the two transformations. The Hiyama-Denmark cross-coupling reaction employs a silanol protecting group to obtain the desired product. The Hiyama cross-coupling reaction on the other hand, commonly employs protecting groups such as dimethylbenzylsilane, phenyl dimethyl silane, trifluorosilane, methyl cyclobutylsilane, or alkoxy silanes. Both reactions allow for the synthesis of new carbon-carbon bonds and represent an important synthetic transformation in organic chemistry.

3.3.1 Existing Methods for the Metal-Catalyzed Silylation of Carbon(sp^2)-O Bonds

**Scheme 3.22** Martin Silylation of Aryl Pivalates
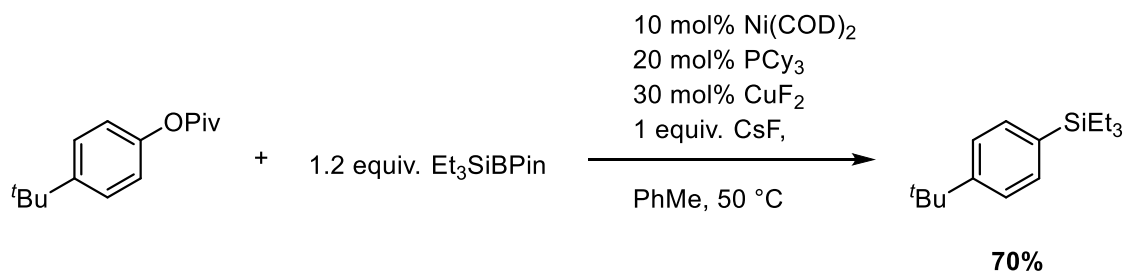
While there exist a few methods for the metal-catalyzed silylation of carbon(sp^2)-X bonds, there are even less for those originating from phenol derivatives. Work in the Martin lab has

demonstrated that aryl pivalates can be converted to aryl silanes using dual nickel and copper catalysts, along with silylboranes as the silylating reagent (Scheme 3.22).[61] The work represents the only published example of the *c*-silylation of a phenol derivative. It is proposed that the combination of CuF_2, CsF, and the silylborane result in the formation of a copper(I) silyl species. Upon oxidative of the nickel catalyst into the carbon-oxygen bond, transmetallation with the copper-silyl species yields a nickel(II) intermediate bonded to an aryl and silyl group. Reductive elimination then leads to the desired product. The substrate scope for the reaction works well with both naphthyl and phenyl pivalates, and the reaction temperatures are quite mild. Yet, the methodology is limited to the use of silylboranes as the silylating reagents. These reagents are air and moisture sensitive, with only a few that are commercially available. The work only presents the incorporation two different silyl groups into the final products (triethyl silyl and dimethyl phenyl silyl). Methodology capable of silylating phenol derivatives, allowing for the incorporation of a broader variety of silyl groups would greatly enhance work in this area.

3.3.2 Optimization of Reaction Conditions

**Scheme 3.23** Initial Discovery of Silylation
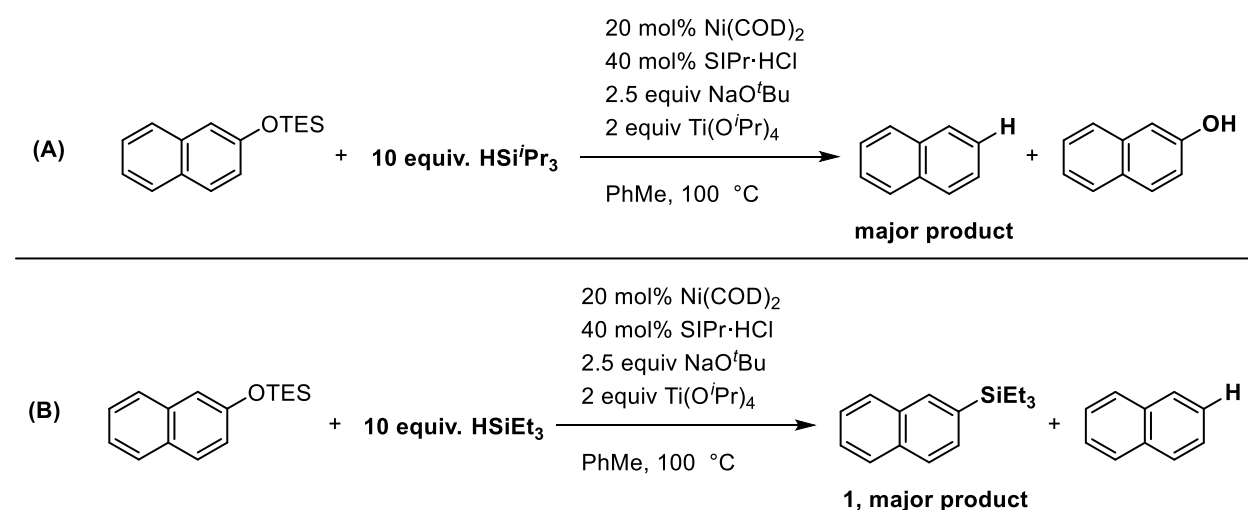
As described above (Scheme 3.12), initial work into the exploration of the reduction of silyl aryl ethers employed reaction conditions with silane additives (**A**) (Scheme 3.23). During this exploration, the silane additive was altered to optimize the reaction. Surprisingly, when triethyl silane replaced triisopropyl silane in the reaction, the formation of aryl silane (**1**) was observed as the major product (**B**).

Scheme 3.24 Silanes as Reductants
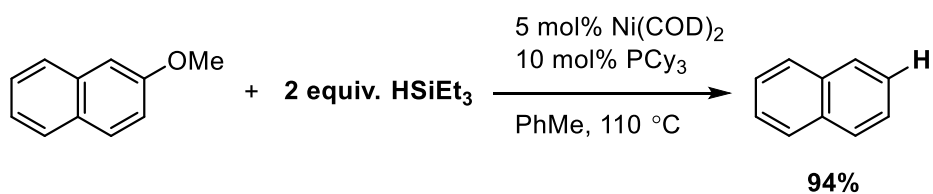
The reaction was quite surprising considering work published in the Martin group. As described above (Scheme 3.7), silanes have been shown to be used as reductants in the nickel-catalyzed reduction of aryl methyl ethers (Scheme 3.24). Yet, the reverse was observed in the attempted reduction of aryl silyl ethers in the presence of silane, as the aryl silane was the major product detected. This indicates that depending on the reactions conditions, one can potentially utilize a silane as either a reductant or silylating reagent.

Scheme 3.25 Optimized Reactions Conditions
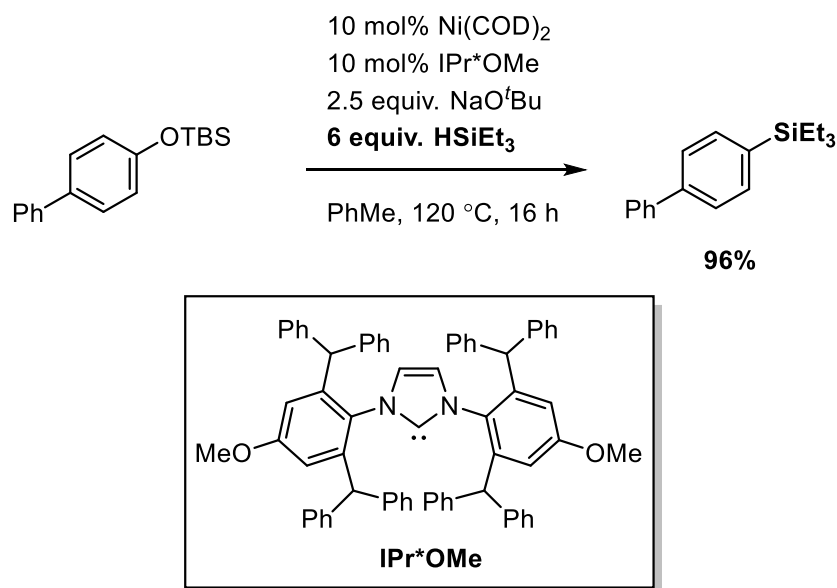
After the initial data point, extensive optimization was undertaken to efficiently silylate silyl enol ethers via nickel catalysis. The optimal conditions for the reduction of the model substrate are shown (Scheme 3.25). The model substrate, TBS protected 4-phenylphenol could be silylated to the aryl silane in very high yields (96%) with relatively low catalyst loadings. Additional details regarding how the optimization results were determined will be discussed below.
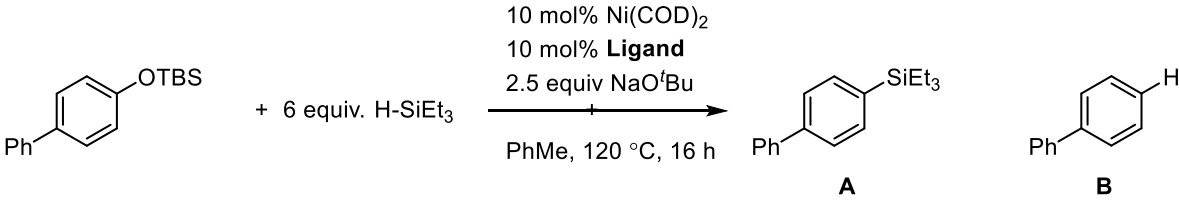
Table 3.6 Catalyst Optimization
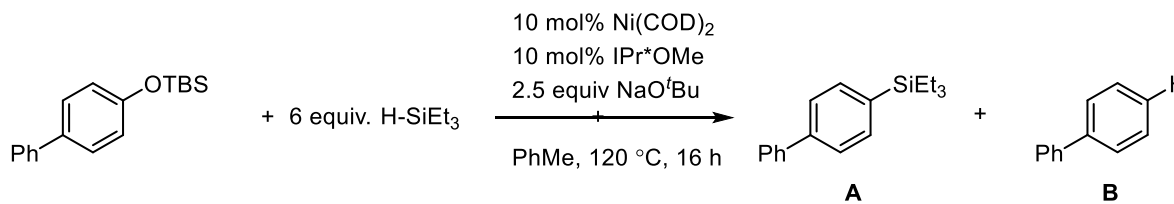
Entry	Deviations from Standard Conditions	Yield (A,B)
1	None	96%, 1%
2	$Ni(acac)_2$ for $Ni(COD)_2$	34%, 4%
3	5 mol% $Ni(COD)_2$	35%, 3%

The nature of the nickel catalyst was optimized (Table 3.6). Using 10 mol% Ni(COD)$_2$ resulted in a 96% yield of the desired product (entry 1). Changing the nickel source to Ni(acac)$_2$ resulted in a substantial decrease in yield of the desired product (entry 2). This is probably due to issues in reducing the catalyst from nickel(II) to nickel(0). The catalyst loading could be lowered to 5 mol% Ni(COD)$_2$, but only 35% of the desired product was obtained (entry 3).

Table 3.7 Optimization of the Ligand

Entry	Ligand	Yield (A,B)
1	IPr*OMe	96%, 1%
2	IMes	10%, 14%
3	IPr	20%, 2%
4	IPr^{Me}	18%, 5%
5	PCy3	NP

The nature of the ligand employed in the reaction were also varied to obtain optimal reaction conditions (Table 3.7). Using IPr*OMe gave a 96% conversion to the desired product (entry 1). Small NHC ligands, such as IMes gave very poor conversion to desired product, while favoring the formation of the reduced arene (entry 2). Both IPr and IPr^{Me} both gave greatly diminished yields as well (entries 3 and 4). Simple monodentate phosphine ligands, such as PCy$_3$, resulted in no product formation, including no observed reduced arene byproduct (entry 6). From the ligand screen, one can theorize that only very bulky NHC ligands result in the best conversion to desired product (entries 1). No other ligand screened gave high conversion to the aryl silane product, highlighting the unique nature of the IPr*OMe ligand. Additionally, it seems that as the

54

ligand size decreases, the amount of reduce arene byproduct increases, potentially shedding light on the mechanism (entries 2 and 3).
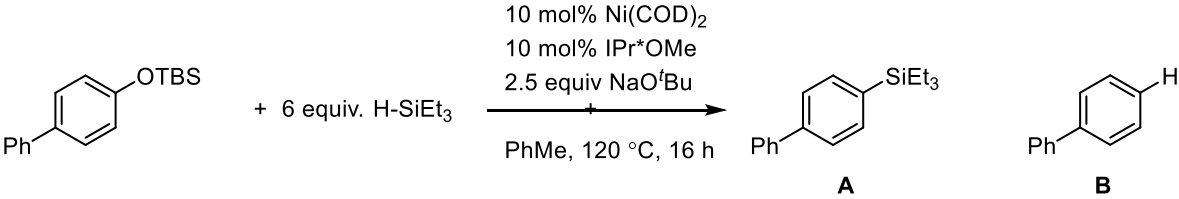
Table 3.8 Optimization of Bases

Entry	Base	Yield (A,B)
1	2.5 equiv NaO^{t}Bu	96%, 1%
2	2.5 equiv LiO^{t}Bu	NP
3	2.5 equiv KO^{t}Bu	0%, 8%
4	1.5 equiv NaO^{t}Bu	47%, 1%
5	NaOPh	trace
6	No Base	NP

The type of base employed, along with varying the stoichiometry was also studied (Table 3.8). Using 2.5 equivalents of NaO^{t}Bu resulted in a 96% yield of the desired product (entry 1). Changing the base to either LiO^{t}Bu or KO^{t}Bu resulted in no aryl silane product formation, indicating that changing the counter ion of the base greatly affects the reactivity of the system (entries 2 and 3). Using only 1.5 equivalents of base resulted in diminished yields to the desired product, indicating the necessity of multiple equivalents of base (entry 4). The use of sodium phenoxide as the base resulted no product formation (5). Finally, the lack of base entirely resulted in no product formation as well (entry 6).

Table 3.9 Optimization of the Protecting Group

| Entry	Protecting Group (PG)	Yield A,B
1	TBS	96%, 1%
2	TIPS	32%, 2%
3	TBDPS	34%, 1%
4	TES	90%, 1%
5	Me	1%, 37%
6	Piv	3%, 4%
7	Tf	25%, 25%
8	Ph	42%, 8%

The protecting group employed during the reaction was also optimized (Table 3.8). A variety of silyl protecting groups were explored (entries 1-4). The TBS protecting group provided the highest yield of the desired product at 94%. Other bulky silyl groups resulted in much poor conversion to the aryl silane product potentially due to the increased difficulty of nickel to activate the carbon-oxygen bond (entries 2 and 3). Silyl groups similar in size to TBS gave very comparable yields (entry 4). Other commonly employed protecting groups in carbon(sp^2)-oxygen bond activation chemistry were also explored. Aryl methyl ethers resulted in only trace amounts of aryl silane product with 37% of the reduced arene byproduct (entry 5). It is unclear why aryl methyl ethers are not capable of producing the aryl silane product, as they are readily used in other carbon-oxygen bond activation reactions. Pivalates gave trace amounts of product formation (entries 6), while triflates yielded the desired product in greatly diminished yields, along with an equal amount of reduced arene byproduct (entry 7). A phenyl protecting group gave greatly diminished yields, with only a 42% yield of the desired product (entry 8).

3.3.3   Mechanistic Considerations

While no mechanistic experiments have been performed regarding the mechanism of this transformation, several experimental observations do provide some understanding of how the transformation may occur. It has been noted that only very bulky NHC ligands provide the aryl silane in good yields. While the size of the NHC ligand decreases, the amount of product also decreases, along with the ratio of silylation to reduced product. This may indicate that there is a competing mechanism for silylation and reduction, and that as ligand size increases, the reduction pathway becomes inoperable. Additionally, as the size of the silane increases, the ratio of silylation to reduction products decreases until the size of the silane becomes large enough that only reduction product is observed.

In terms of an operative mechanism, one can be theorized using the available reaction trends and computational studies conducted on similar systems (Scheme 3.26). It is purposed that Ni(COD)$_2$ forms a ligated species (**A**), that then has a t-butoxide anion coordinate to nickel center resulting in a monoligated nickelate species (**B**). From this intermediate, the silly aryl ether can coordinate to the nickel catalyst (**C**). A subsequent S$_N$Ar-like mechanism can then occur which results in the carbon-silyloxy bond activation, forming a new carbon-nickel bond and extruding a silyloxy anion (**D**). The nickel(II) intermediate can then be approached by an equivalent of silane setting it up to undergo a α-bond metathesis with the nickel-carbon bond (**E**). This would extrude the aryl silane product, forming a nickel(II) hydride alkoxy intermediate (**F**). Deprotonation of the nickel-hydride with a t-butoxide anion would then complete the catalytic cycle (**B**).

Scheme 3.26 Proposed Silylation Mechanism
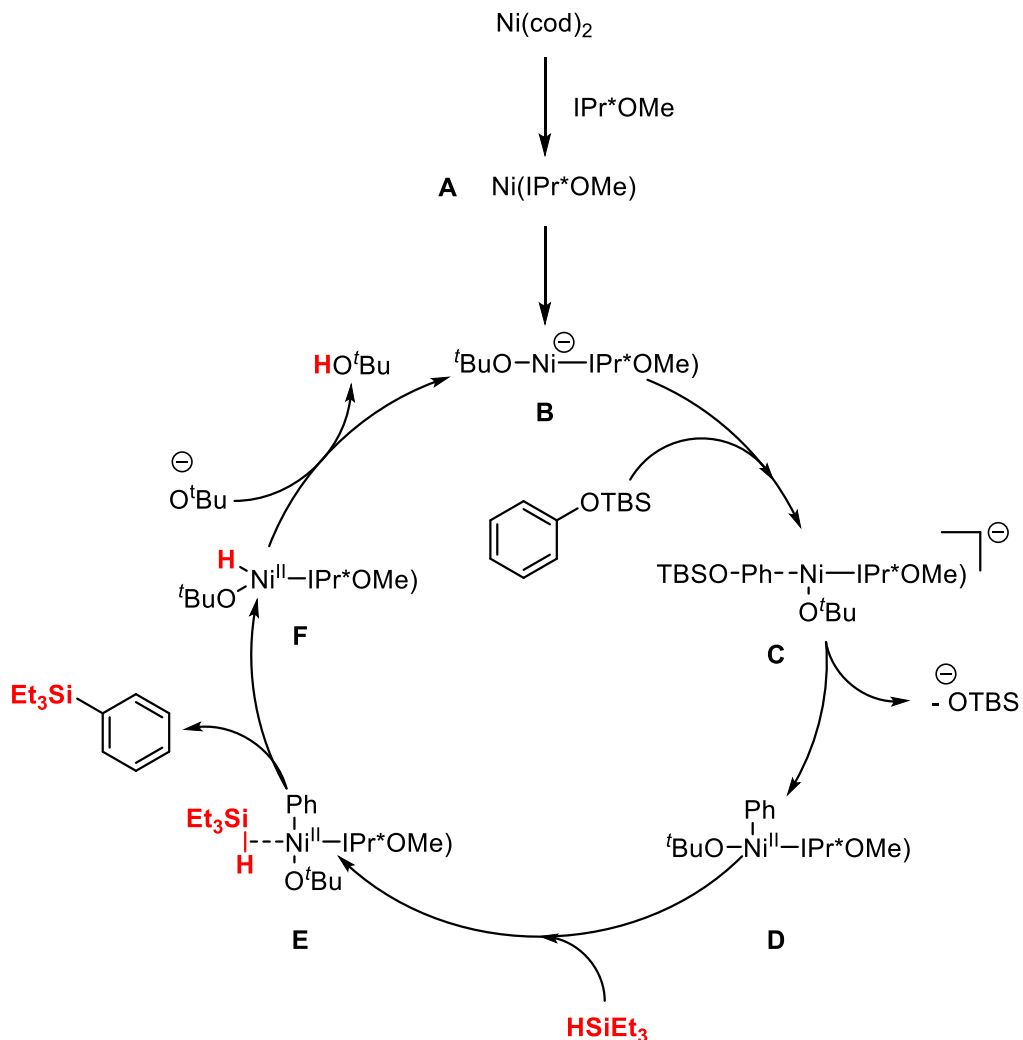
Both the experimental data trends, along with computational studies conducted by the Wu group provide reasonable evidence of this operative mechanism. Work in the Wu group studied the Hartwig method for reduction of phenyl ethers using hydrogen gas and nickel catalysis.[53] More information regarding this transformation can be found above (Scheme 3.8). While the Hartwig methodology led to the reduction in bisaryl ethers, the similar reactions conditions could provide some insight into the probable reaction mechanism of the silylation of silyl aryl ethers. The study indicated that the nickelate species (**B**) to be over 12 kcal downhill in energy starting from

Ni(COD)$_2$. From here, the carbon-phenoxide bond can be cleaved by two separately proposed mechanism. The first, involves the direct oxidative addition into the C(sp2)-O bond described above (Scheme 3.16). It is believed that this pathway predominates during the reduction of silyl aryl ethers. The other proposed mechanism involves coordination of the phenyl ether to the nickel center (**C**) (Scheme 3.27). A subsequent S$_N$Ar-like mechanism will result in the cleavage of the carbon-oxygen bond, releasing the phenoxide anion and forming a carbon-nickel bond (**D**). The computational study indicated that the oxidative addition mechanism is 1.4 kcal/mol lower in energy than the S$_N$Ar-like mechanism using SIPr as the ligand. Yet, the study indicated that both electron rich arene systems, along with a bulkier NHC ligand would alter the energetics of this transformation, and begin to favor the S$_N$Ar-like pathway. This would likely be the case with the silylation transformation, as electron rich arenes react much more efficiently than those with electron-withdrawing groups and a very bulky NHC is needed to obtain high levels of reactivity.

Scheme 3.27 Computational Insight into the Probable Reaction Mechanism
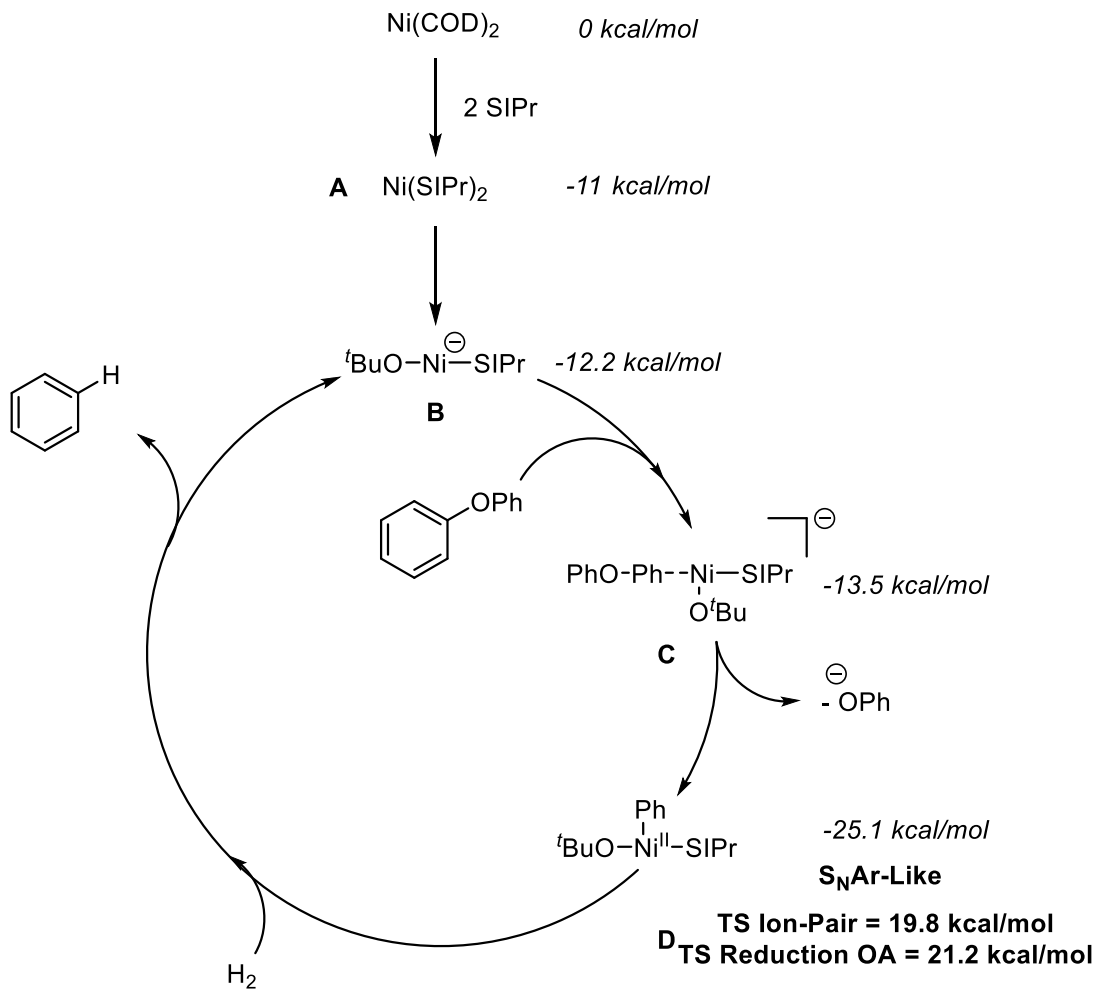
The subsequent α-bond metathesis step with the silane fits the observed trends of the experimental data (Scheme 3.26, E to F). The very bulky NHC ligand employed in the reaction would sterically repel the more hindered region of the silane prior to the α-bond metathesis (**1**) (Scheme 3.28). This confirmation would then favor the formation of the aryl silane product (**A**). As the size of the NHC ligand decreased however, the steric interactions of the ligand with the silane would begin to favor the extrusion of the reduced arene (**B**). Additionally, as the size of the silane increases, it becomes more difficult to adopt the necessary confirmation to allow for the α-

bond metathesis favoring formation of the aryl silane. This would then begin to favor production

of the arene to minimize the steric interaction between the silane and substrate (**2**).

Scheme 3.28 Proposed Mechanism of the α-Bond Metathesis of the Silane
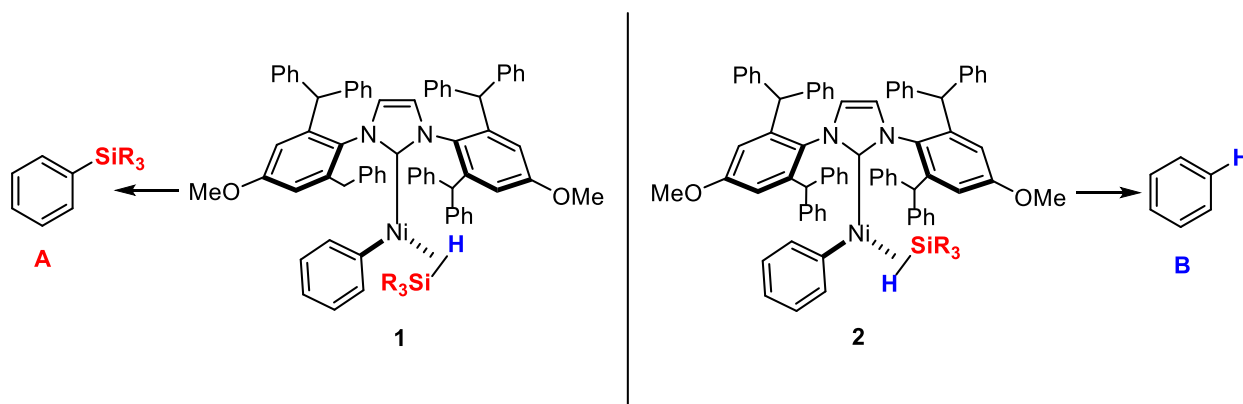
While additional mechanistic inquiries should be conducted to provide more support for

the proposed mechanism, the combination of computational studies and experimental data trends

do allow for a reasonable mechanism to be proposed.

3.3.4 Substrate Scope

A range of silyl aryl ethers were subjected to the silylation reaction conditions, resulting in

moderate to excellent yields (Scheme 3.29). Notable substrates include the ability of the reaction

system to tolerate free alcohols (entry E). Surprisingly, the reaction can selectively silylate the

carbon-silyloxy bond in the presence of an aryl methyl ether (entry G). This provides a

complementary reaction pathway to methods capable of selectively activating the aryl methyl ether

as described above (Scheme 3.7). Benzyl silyloxy groups were also not activated during the

reaction, illustrating the reduction's preference to activate $C(sp^2)$-O bonds (entry F). Simple

electron-rich aryl systems were also able to yield the desired products in excellent yields (entries

N-Q). It should be noted that the yields of electron rich substrates are much higher than those

obtained when subjected to the reduction reaction conditions, indicating that the silylation and

reduction transformations may involve divergent mechanistic pathways. Several other functional groups tolerant of the reaction system include the trimethyl silyl group, pyridines, morpholines, and amides (entries D, J, L, M).

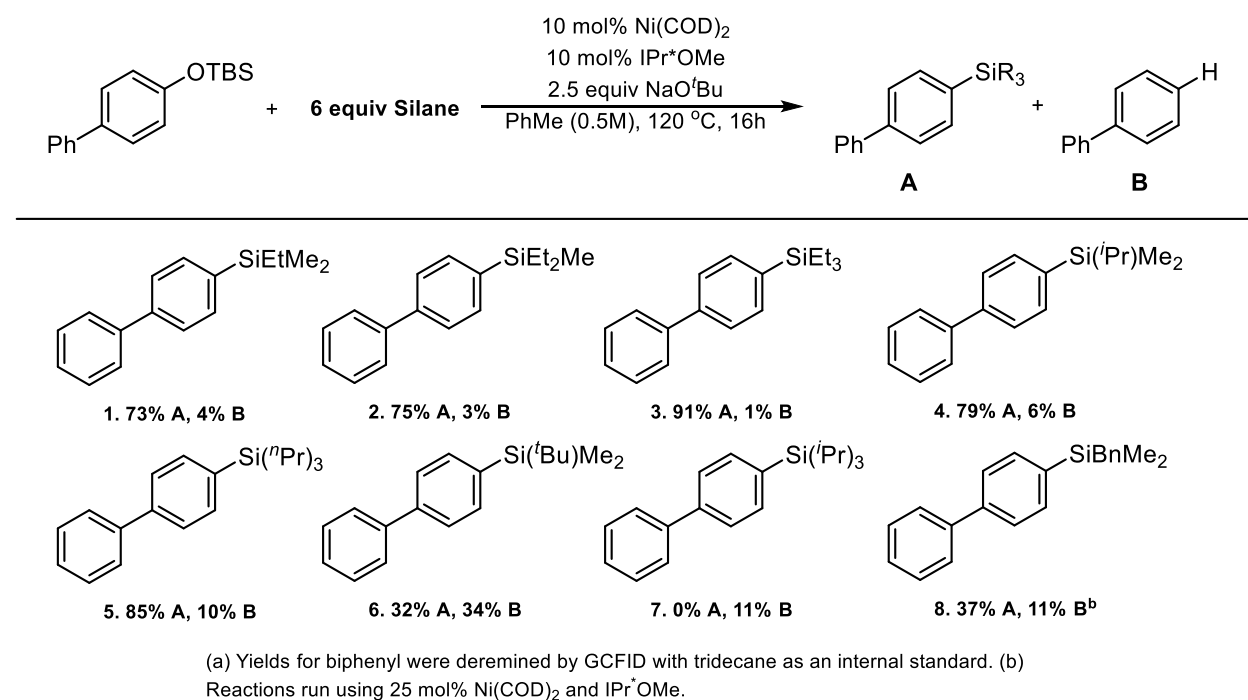**Scheme 3.29** Silylation Substrate Scope

The scope of silanes capable of producing the aryl silane product were also examined (Scheme 3.30). A variety of trialkyl silanes could be used as the silane to furnish a variety of aryl
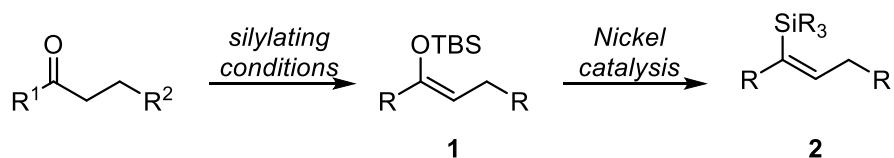
silanes. The most efficient silanes were those bearing small alkyl groups such as dimethyl ethyl

silane or ethyl dimethyl silane. As the size of the silane was increased however, more of the

reduced arene byproduct was formed. Increasing the size of the silane to even larger sizes, such as

triisopropyl silane yielded none of the desired aryl silane and only the reduced arene was observed.

Benzyl dimethyl silane can furnish the desired product in a 37% yield. While the yield is not great,

the aryl silane product can undergo a Hiyama cross-coupling transformation highlighting the

synthetic utility of the product. A variety of alkoxy silanes were also subjected to reaction

conditions but provided none of the desired aryl silane product.

Scheme 3.30 Scope of the Silanes in the Silylation Reaction

(a) Yields for biphenyl were deremined by GCFID with tridecane as an internal standard. (b) Reactions run using 25 mol% Ni(COD)$_2$ and IPr*OMe.

3.3.5   Future Work

Scheme 3.31 Formation of Vinyl Silyl Ethers

While the method currently tolerates a variety of silyl aryl ethers, there are still certain aspects of the methodology that could be expanded and improved upon. To start, the reaction conditions should be adapted to accommodate silyl enol ethers. One could feasibly take any ketone or aldehyde and convert the product to the silyl enol ether (**1**) and yield the vinyl silane product upon subjection to the standard reduction reaction conditions (**2**) (Scheme 3.31). Initial findings in this area produced very poor results to conversion to the desired reduced product likely due to the increased strength of the carbon-oxygen bond. Considering that only the IPr*OMe ligand yielded the desired aryl silane product in appreciable yields, one should consider only very bulky NHC ligands while attempting to achieve greater levels of reactivity through ligand design.

Another area of future work could explore the dehydrogenative silylation of phenol substrates (**A**), followed by reduction of the newly formed carbon-silyloxy bond using nickel catalysis (**B**) (Scheme 3.32). This could potentially allow for the one-pot silylation of any phenol without the need of an additional step to install the protecting group. Several boron Lewis acids have been shown to be capable of catalyzing the dehydrogenative silylation of phenols indicating the transformation may be feasible with extensive optimization of reaction conditions.[55] Additionally, excess silane initially used to form (**A**), could then in turn be used to provide product (**B**).

Scheme 3.32 One Pot Reduction of Phenols
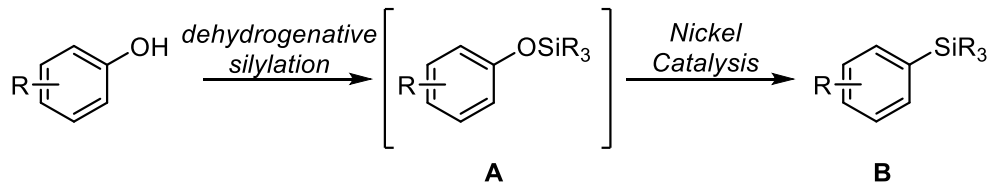
Finally, work should be invested in expanding the silane scope to those that provide aryl silanes capable of use in Hiyama cross-coupling reactions. While the use of triethyl silane does result in excellent yields of aryl silanes, the resulting products are not broadly useful in synthetic applications. Expanding the scope of this transformation to silanes that do provide interesting products, such as phenyldimethylsilane or the alkoxy-silanes would greatly increase the synthetic utility of the method.

3.3.6   Summary of Silylation of Silyl Aryl Ethers

In summary, a variety of silyl aryl ethers were selectively silylated to the arene via nickel catalysis. The commonly employed TBS protecting group was determined to be the optimal protecting group. The very bulky NHC ligand, IPr*OMe proved to be unique in proving high conversions to the desired product. The reactions could also be run with relatively low catalyst loadings (10 mol%). Additionally, it was determined that super-stoichiometric sodium t-butoxide was required to obtain efficient conversion to products. The silylation was also shown to selectively silylate carbon-silyloxy bonds in the presence of aryl methyl ethers. Since aryl methyl ethers have been used in a variety of $C(sp^2)$-O bond activation reactions, this method offers orthogonal reactivity by changing the protecting employed in the reaction. Additionally, the reaction can silylate simple aryl rings with modest to great yields. Previous carbon(sp^2)-oxygen activation methods often were unable to provide product or resulted in very poor conversions using these aryl scaffolds. Additionally, a variety of trialkyl silanes were shown to provide the desired

aryl silane in good yield. More synthetically interesting aryl silane products can also be accessed using benzyl dimethyl silane.

3.4 Introduction to Nickel-Catalyzed Amination of Carbon(sp^2)-Oxygen Bonds

The amination of carbon(sp^2)-oxygen bonds represents an important transformation in synthetic chemistry. A variety of natural products or medicinal drug targets contain an aryl amine motif.[25] The ability to selectively synthesize these compounds in good yield represents an important field of study in organic chemistry. For instance, the Buchwald-Hartwig amination method for the coupling of aryl halides and amines using palladium catalysis allows for the synthesis of a variety of important products (Scheme 3.33).[62-64] While this is a very powerful synthetic method for the synthesis of aryl amines, the reactions typically employ expensive palladium catalysts, along with super stoichiometric aryl halides. A method for the generation of aryl amines from cheaper catalyst sources and more environmentally friendly cross-coupling reagents would be synthetically attractive.

Scheme 3.33 Application of the Buchwald-Hartwig Method to Synthesis[65]

aminotetralin
(CNS-active)
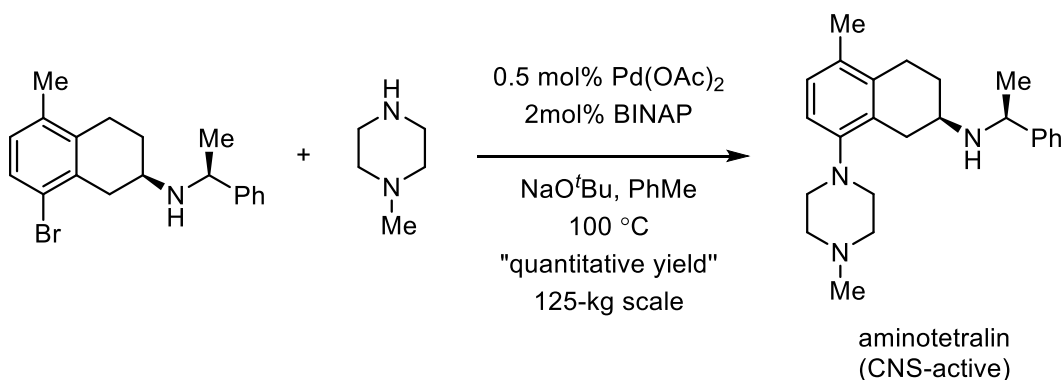
3.4.1 Existing Methods for the Nickel-Catalyzed Amination of Carbon(sp^2)-Oxygen Bonds

Currently, several methods exist for the cross-coupling of phenol derivatives with amines. Work in the Chatani group has demonstrated the amination of aryl methyl ethers using a nickel catalysis (Scheme 3.34).[66] The reaction employs Ni(COD)$_2$ and IPr as the optimal catalyst with

relatively high catalyst loadings. Super stoichiometric NaO*t*Bu was also found to be needed for efficient conversion to product. While naphthyl methyl ethers could provide the desired aryl amine in high yields, simple phenyl systems led to much lower conversions to product. Additionally, only secondary aliphatic amines were shown capable of undergoing the transformation.

Scheme 3.4 Amination of Aryl Methyl Ethers
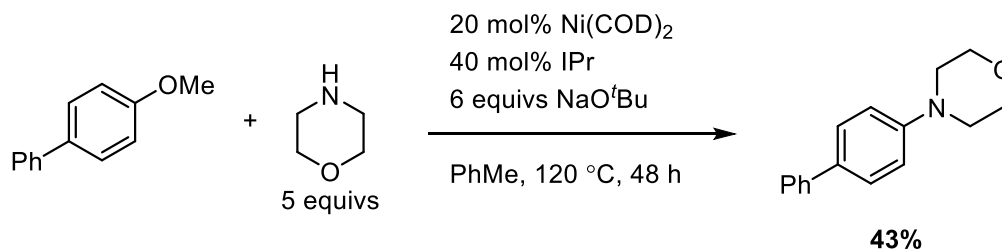
The Chatani group later expanded upon this methodology to include *N*-heteroaryl methyl ethers (Scheme 3.35).[67] The reaction conditions were very similar to the prior report, albeit with slightly lower reaction temperatures and shorter reactions times. Unlike the first publication, simple pyridine methyl ethers could provide the desired product in high yields, presumably due to the electron deficient nature of the aryl ring.

Scheme 3.35 Amination of *N*-heteroaryl Methyl Ethers
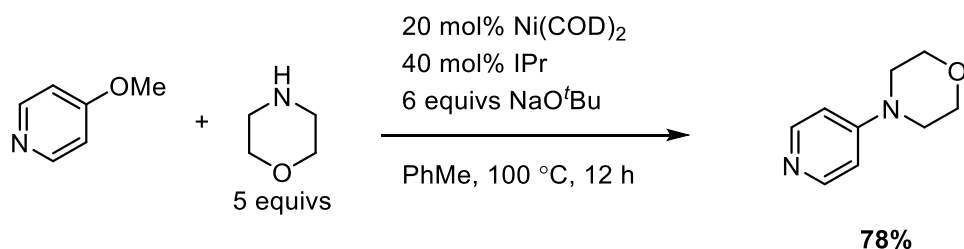
Despite the progress in this area, the development of amination methods using phenol derivatives that allowed for a wider range of both aryl cross-coupling partner and amine would greatly benefit synthetic chemistry.

3.4.2   Optimization of Reaction Conditions

Due to the success in the reduction of aryl silyl ethers, it was theorized that the reaction scope could potentially be expanded to using amines as the nucleophile. Replacing the titanium Lewis acid additive with an amine would hopefully provide the desired aryl amine product. Using similar reactions conditions to the reduction of silyl aryl ethers, the desired amination product could be obtained. Further optimization of the reaction conditions provided the desired aryl amine with in a 93% isolated yield (Scheme 3.36). The reaction conditions employed low catalyst loadings (5 mol%) and only 1.5 equivalents of amine.

Scheme 3.36 Optimized Reaction Conditions
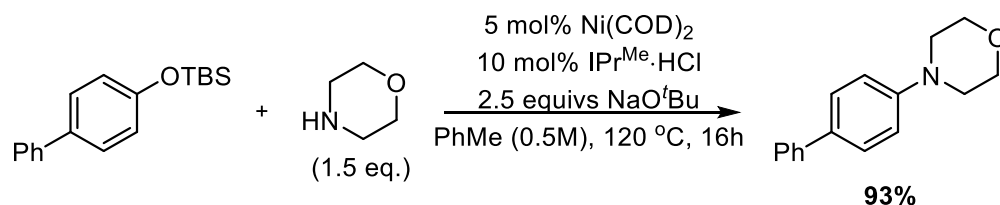
Relevant optimization data points are shown below (Table 3.). Under optimal reaction conditions the desired product could be obtained in a 93% isolated yield (entry 1). It was determined that IPr^{Me} was the most effective ligand for the transformation. Using IPr as the ligand gave substantially lower yields of the desired product (entry 2). The reaction temperature could be lowered to 100 °C to provide reasonable yields of the product (entry 3), but lowering the temperature further shut down productive product formation (entry 4). Finally, using only one equivalent of base provided 71% of the desired product as well (entry 5).

Table 3.10 Amination Optimization
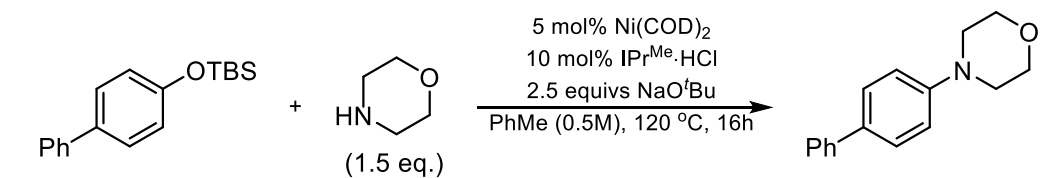
Entry	Deviations from Standard Conditions	Yield
1	None	93%
2	10 mol% IPr	58%
3	100 °C	71%
4	80 °C	trace
5	1 equiv NaO^{t}Bu	71%

3.4.3 Reaction Mechanism

Due to the similar experimental trends and reactions conditions also employed in the reduction of aryl silyl ethers, it is believed that the amination of silyl aryl ethers proceeds through a very similar mechanistic pathway. It is purposed that the nickel species forms a bisligated species (**A**), that then has a t-butoxide anion coordinate to nickel center resulting in a monoligated nickelate species (**B**). Oxidative addition into the carbon-silyloxy bond provides intermediate (**C**). Dissociation of the silyloxy group from the nickel center yields a nickel(II) intermediate with an aryl group and t-butoxide bound to the metal center (**D**). From this intermediate, it is unclear exactly how the carbon-nitrogen bond forms to regenerate the catalyst. (**B**). Additional work will need to be conducted to elucidate the remaining mechanism.

Scheme 3.37 Proposed Amination Mechanism
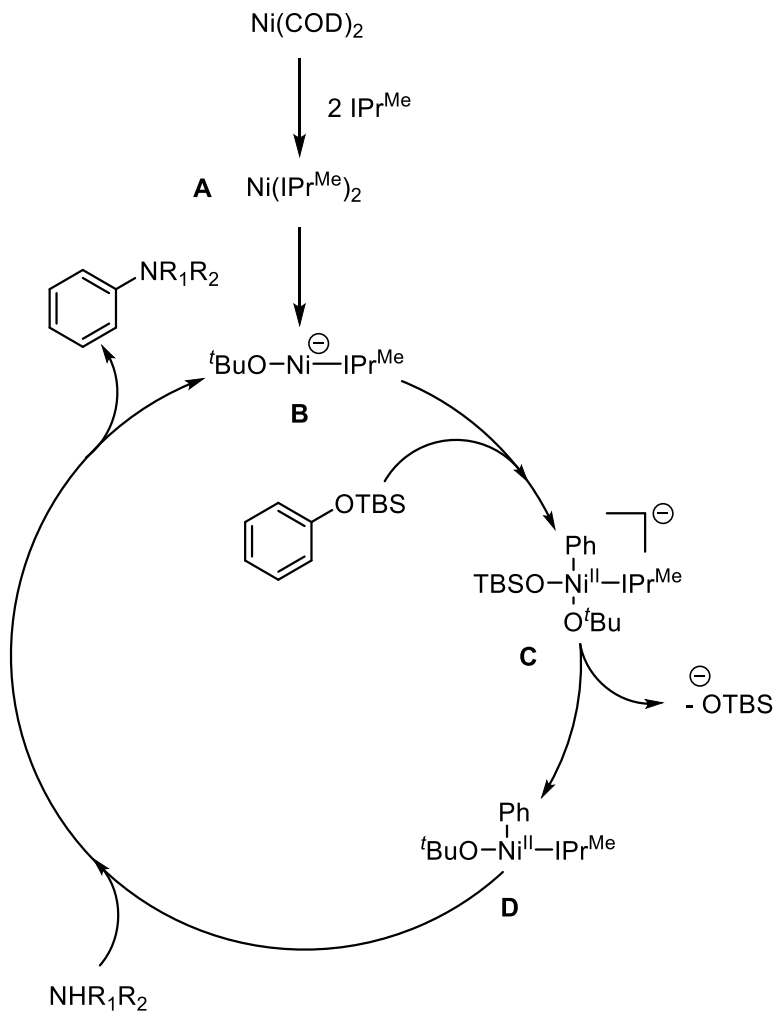
3.4.4   Substrate Scope

A variety of aryl and naphthyl silyl ethers and amines were subjected to the optimized amination conditions (Scheme 3.38). The reaction could tolerate both pyridine and quinoline derivatives (entries B and E). Like the reduction of aryl silyl ethers, the reaction selectively activated the carbon-silyloxy group in the presence of a carbon-methoxy functional group (entry D). A variety of amines could also be successfully subjected to reaction conditions. The reaction was able to tolerate a variety of secondary aliphatic amines (entries A, D, and E). Surprisingly, the reaction was also able to successfully couple aryl silyl ethers with primary amines (entries B and

F). Previous amination methodologies involving phenol derivatives were not shown to tolerate them. Methyl phenylaniline also proved to be an efficient amine in the transformation, resulting in the desired product in a 61% isolated yield (entry C). However, attempts to use primary aryl amines did not lead to the formation of any desired product.

Scheme 3.38 Amination Substrate Scope
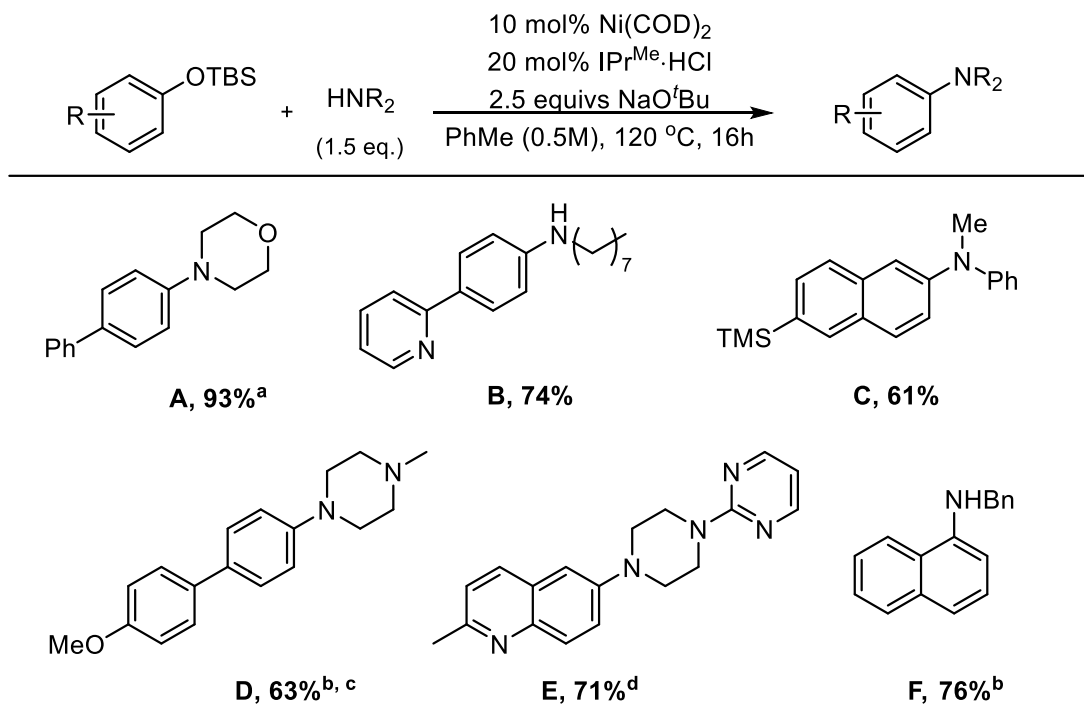
(a) Reaction used 5 mol% Ni(COD)$_2$ and 10 mol% IPr^{Me}·HCl. (b) Reaction used 4 eqiv of base. (c) Reaction used 15 mol% Ni(COD)$_2$, 30 mol% IPr^{Me}·HCl. (d) Reaction used 2.5 eqiv of amine. (e) Reaction at 130 °C.

3.4.5 Future Work

Additional work should expand the scope of the amine to include *N*-aryl amines. This would allow for the expansion of the substrate scope to produce a wide array of aryl amine motifs present in both natural products and medicinal drug targets. The poor reactivity of these amines could potentially be overcome through ligand optimization. Electron-donating NHC ligands gave the best conversion to products, so exploring ligands with even more electron-donating capability

may allow for the expansion of the substrate scope (Scheme 3.39). Altering the R^3 position to other alkyl or EDG's could lead to the desired increase in reactivity.

Scheme 3.39 Ligand Framework

Modulation of the NHC Ligand
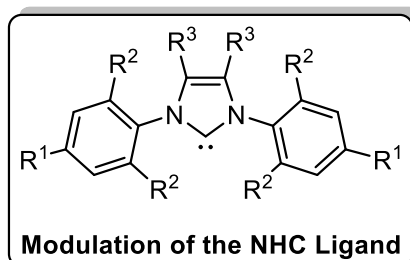
Additionally, future work should explore the expansion of nucleophiles tolerated in the functionalization of silyl aryl ethers. One class that should be explored would be using silyl aryl ethers in Suzuki-cross coupling reactions. Other phenol protecting groups have shown the capability to serve as the electrophile during this transformation.[68,69] Preliminary work has shown the capability of aryl silyl ethers to undergo Suzuki reactions using nickel catalysis (Scheme 3.40). The reaction conditions employ dual bases to achieve the desired reactivity and were shown to work best with aryl boronic acids. However, altering the electronic nature of the aryl boronic acid shut down the reaction, and only biphenyl or naphthyl systems could give appreciable amounts of product. Expanding the scope of this transformation would add another tool into the functionalization of silyl aryl ethers.

Scheme 3.40 Suzuki Reactions with Aryl Silyl Ethers
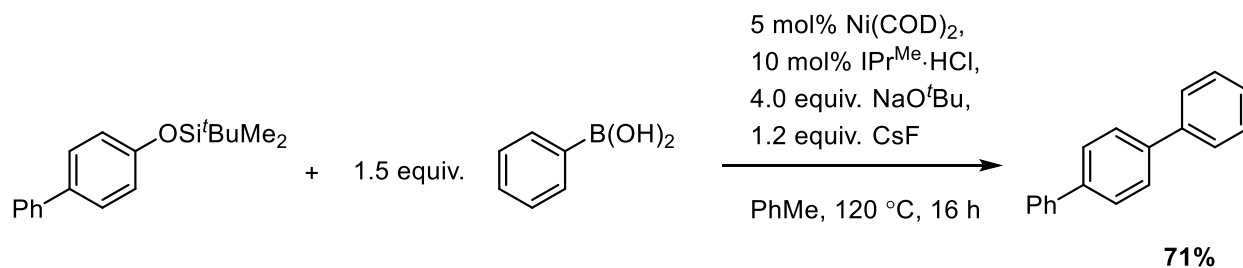
3.4.5 Summary

In summation, the expansion of the functionalization of silyl aryl ethers to allow for the formation of aryl amines has been described. The reaction works well with both aryl and naphthyl silyl ethers and low catalyst loadings (5 mol% Ni(COD)$_2$). Additionally, the reaction tolerates a variety of primary and secondary amines. Previous nickel-catalyzed aminations of phenolic derivatives were limited to only secondary amines.

Chapter 4

Conclusion

4.1 Conclusion to Methodologies Towards the Deoxygenation of Small Molecules

In summary, the introduction and background to carbon(sp^2)-oxygen bond reactions has been described. Despite publications citing the role of nickel in these activations over thirty years ago, only in the last decade have efforts gone into developing novel carbon(sp^2)-oxygen reactions using nickel catalysts (Scheme 4.1).

Scheme 4.1 Nickel-Catalyzed Functionalization of Phenol Derivatives
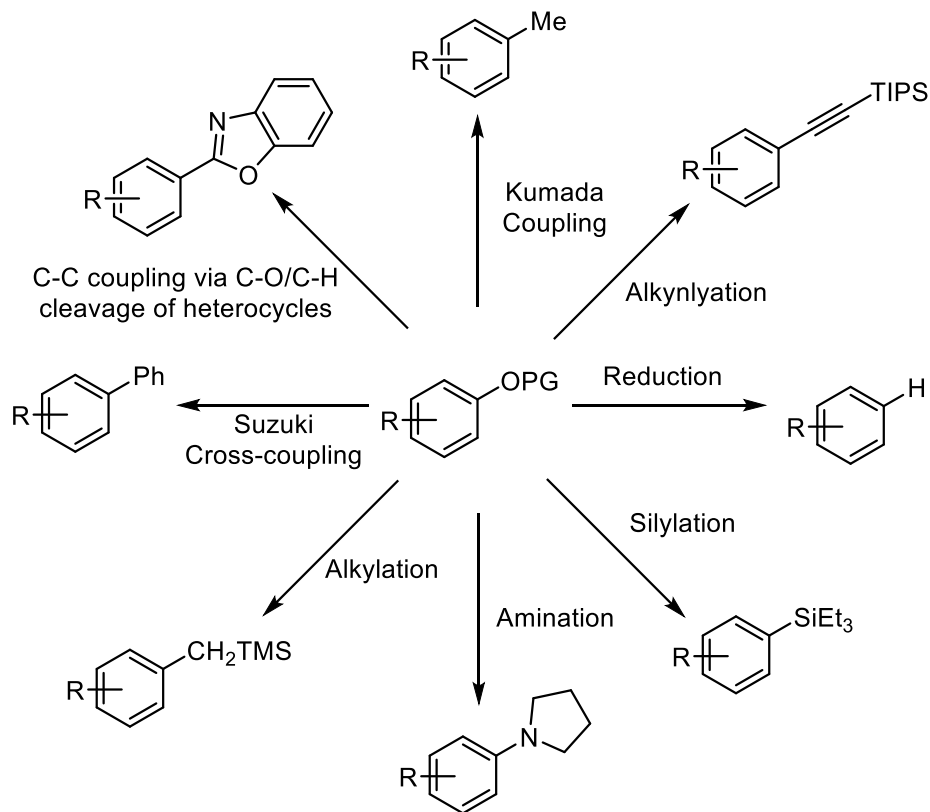
During previous studies in the Montgomery Lab, the serendipitous discovery of a net four-electron reductive coupling of an enone and alkyne to yield a 1,4-diene was realized (Scheme 4.2). It was found that a discrete nickel catalyst was needed to obtain optimal yields for this transformation due to the unique nature of the ligand employed. The reaction could accommodate a variety of enones or enals and both internal and terminal alkynes. Mechanistic inquiries were then conducted revealing a probable mechanism in which the titanium acid serves as both a Lewis acid and a reductant.

Scheme 4.2 Initial Net Four-Electron Discovery
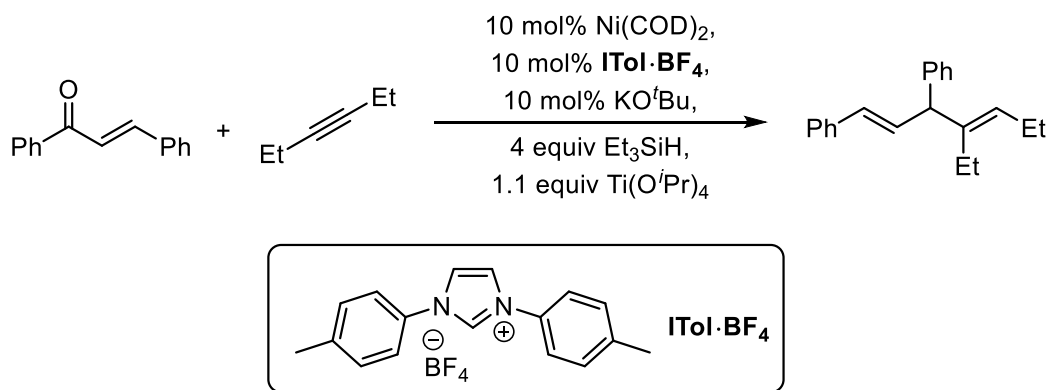
Using the mechanistic information obtained during the study of the formation of skipped

dienes, the nickel-catalyzed functionalization of aryl silyl ethers was explored. Previous reports of

the aryl silyl ethers were relatively scarce, but remain an attractive electrophilic partner due to the

ease of installation of the silyl protecting groups and its ability to withstand harsh reaction

conditions. Through extensive optimization, aryl silyl ethers were shown to be competent

surrogates for reduction, silylation, amination and Suzuki cross-coupling reactions (Scheme 5.3).

Scheme 4.3 Functionalization of Silyl Aryl Ethers
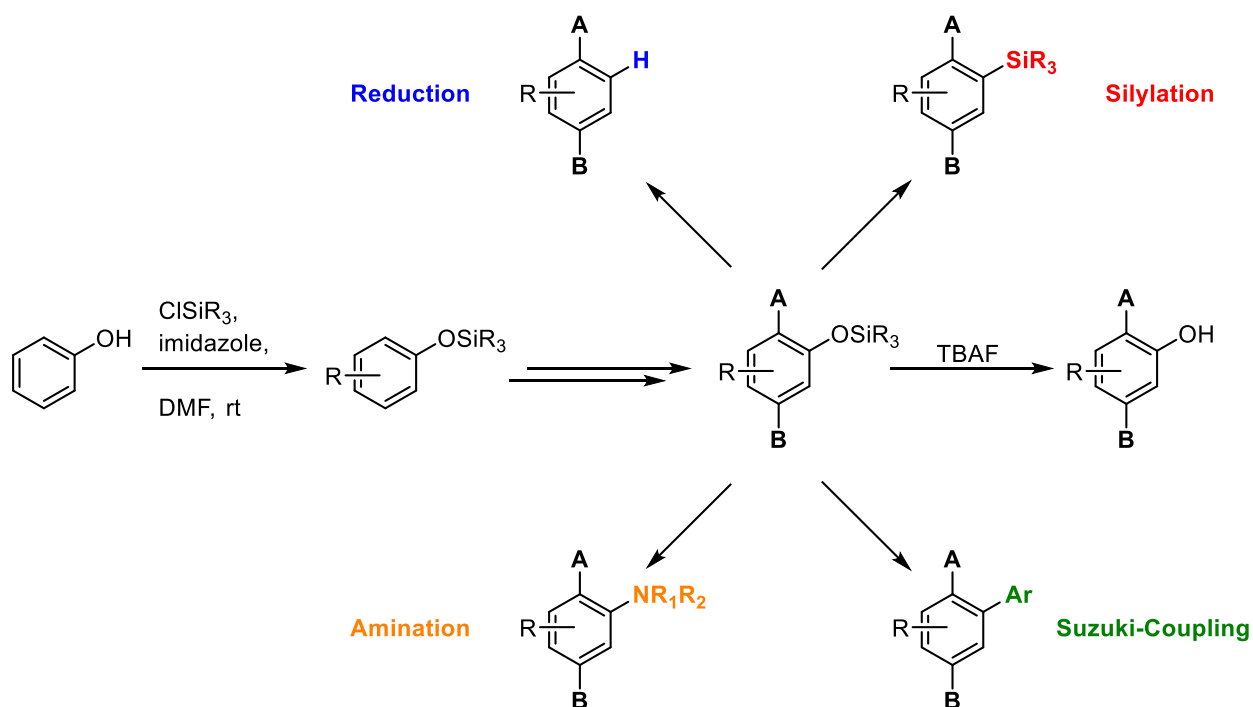
In conclusion, the background and importance of carbon-oxygen bond activation in synthesis, along with two new methods developed during my time in the Montgomery lab have been disclosed. While, more work will need to be conducted to fully realize the importance the of carbon-oxygen bond methodology reactions, hopefully these reactions do well to highlight some of its potential benefits and appeal in synthetic chemistry.

Chapter 5

Experimental

5.1 General Experimental Details

Unless otherwise noted, all reactions were conducted in flame-dried or oven dried (120 °C) glassware with magnetic stirring under an atmosphere of dry nitrogen. Toluene was purified under nitrogen using a solvent purification system (Innovative Technology, inc., Model # SPS-400-3). Benzylideneactecone (Acros), trans-chalcone (Sigma-Aldrich), (E)-1-phenylbut-2-en-1-one (AstraTech, Inc.), 1-phenyl-1-propyne (Sigma-Aldrich), 3-hexyne (Sigma-Aldrich), 1-octyne (Sigma-aldrich), and N-(2-butynyl)phthalimide (Sigma-Aldrich), 6-chloro-1-hexyne (Sigma-Aldrich) and cyclohex-2-en-1-one (Sigma-Aldrich) were used as received. (E)-5-methylhex-3-en-2-one (Sigma-Aldrich), trans-cinnamaldehyde (Sigma-Aldrich), crotonaldehyde (Acros), and methacrolein (Sigma-Aldrich) were distilled prior to use. (E)-3-(4-fluorophenyl)-1-phenylprop-2-en-1-one, (E)-3-(4-methoxyphenyl)-1-phenylprop-2-en-1-one, tert-butyldimethyl((5-phenylpent-4-yn-1-yl)oxy)silane, (cinnamyloxy)triethylsilane, triethyl(((1Z,4E)-4-methyl-3,5-diphenylpenta-1,4-dien-1-yl)oxy)silane, and 7-(but-3-yn-1-yl)-1,3-dimethyl-3,7-dihydro-1H-purine-2,6-dione were prepared as per the literature procedure. Triethylsilane (Sigma-Aldrich) was passed through basic alumina and stored under nitrogen in Schlenk glassware. Titanium(IV) isopropoxide (Sigma-Aldrich) was distilled and stored under

nitrogen in Schlenk glassware. Triethylsilyldeuteride (Sigma-Aldrich) and 2-propanol-d_8 (Sigma-Aldrich) were used without further purification. 1,3-Bis(4-methylphenyl)imidazolium chloride (ITol) was prepared as per the literature procedure. Et_3SiH and i-Pr_3SiH (Aldrich) were passed through basic alumina before use and stored under nitrogen and $tBuMe_2SiH$ (Oakwood Chemicals) was used without further purification. Anhydrous $Ni(acac)_2$ (Strem Chemicals), N-heterocyclic carbenes (Sigma Aldrich, Strem Chemicals), and tBuONa (Strem Chemicals) were stored and weighed in an inert atmosphere glovebox.

Analytical thin layer chromatography (TLC) was performed on Kieselgel 60 F254 (250 μm silica gel) glass plates and compounds were visualized with UV light and p-anisaldehyde or potassium permanganate stains. Flash column chromatography was performed using Kieselgel 60 (230-400 mesh) silica gel. Eluent mixtures are reported as v:v percentages of the minor constituent in the major constituent. All compounds purified by column chromatography were sufficiently pure for use in further experiments unless otherwise indicated.

.^{1}H NMR spectra were collected at 400 MHz on a Varian MR400, at 500 MHz on a Varian Inova 500 or Varian vnmrs 500, or at 700 MHz on a Varian vnmrs 700 instrument. The proton signal of the residual, nondeuterated solvent (δ 7.26 for $CHCl_3$ or 7.15 for C_6D_6) was used as the internal reference for ^{1}H NMR spectra. ^{13}C NMR spectra were completely heterodecoupled and measured at 125 MHz. Residual chloroform-d_3 (δ 77.0) or benzene-d_6 (δ 128.0) was used as an internal reference. High resolution mass spectra were recorded on a VG 70-250-s spectrometer manufactured by Micromass Corp. (Manchester UK) at the University of Michigan Mass Spectrometry Laboratory. GCFID analysis was carried out on a HP 6980N Series GC system with a HP-5 column (30 m x 0.32 mm x 0.25 μm).

5.2 Chapter 2 Experimental

5.2.1 General Procedure

Procedure for the preparation of ITol·BF₄:
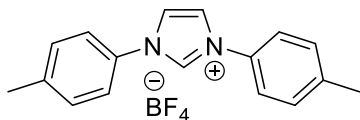
A solution of 1,3-Bis(4-methylphenyl)imidazolium chloride (5.82 g, 20.4 mmol) in 100.0 mL of water was allowed to stir. To this was added HBF₄ (40% in H₂O, 5.38 mL, 24.5 mmol) and the resulting mixture was stirred at room temperature for 12 hours. The solution was then filtered and the resulting precipitate was washed with water. The volatiles were then removed in vacuo. The resulting orange-brown solid was then recrystallized from CH₂Cl₂ and methanol to afford the desired product as a dark-brown solid (4.01 g, 0.12 mmol, 59% yield).

¹H-NMR (500 MHz, CDCl₃): δ 9.36 (s, 1H), 7.69 (s, 2H), 7.58 (d, J = 8.3 Hz, 4H), 7.35 (d, J = 8.1 Hz, 4H), 2.40 (s, 6H).

¹³C-NMR (125 MHz, CDCl₃): δ 141.3, 132.6, 131.8, 131.1, 122.17, 122.11, 21.1.

HRMS (ESI) *m/z*: [M-BF₄⁻] calc. for $C_{17}H_{17}N_2^+$, 249.1386, found, 249.1387.

Procedure for the preparation of Ni(ITol)(MMA)₂:
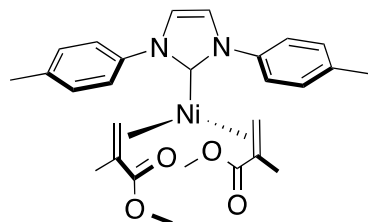
A solution of Ni(COD)₂ (550 mg, 2.00 mmol) and methyl methacrylate (0.84 mL, 8.0 mmol) was stirred in 8.0 mL of toluene for 30 min. In a separate vial, a slurry of ITol·HBF₄ (672 mg, 2.00 mmol) and KO-*t*-Bu (246 mg, 2.20 mmol) was stirred for 30 min in 10 mL of toluene.

The ligand slurry was added dropwise to the nickel solution, and the reaction mixture was stirred overnight at rt. The solution was filtered and the precipitate was washed with toluene. The volatiles were then removed in vacuo. The resulting dark yellow solid was washed with pentane yielding a pale yellow powder (537 mg, 1.06 mmol, 53 % yield). X-ray quality crystals were grown at -20 °C in a solution of toluene and diethyl ether.

^{1}H-NMR (700 MHz, C$_6$D$_6$): The ^{1}H NMR peaks reported correspond to the major isomer, although the spectrum also shows the presence of higher symmetry diastereomers. δ 7.59 (d, J = 7.7 Hz, 4H), 7.03 (d, J = 7.7 Hz, 4H), 6.71 (s, 2H), 3.54 (s, 6H), 3.46 (s, 2H), 2.34 (s, 2H), 2.01 (s, 6H), 1.60 (s, 6H).

^{13}C-NMR (175 MHz, C$_6$D$_6$): Major and minor isomers are reported together. δ 174.0, 138.5, 137.6 137.5, 137.4, 129.9, 129.8, 129.6, 124.5, 123.9, 123.6, 122.0, 121.7, 121.6, 50.6, 20.9, 20.8, 20.1, 18.8.

Anal calcd for C$_{27}$H$_{32}$N$_2$NiO$_4$: C (63.93 %), N (5.52 %), H (6.36 %); found: C (63.32 %), N (5.09 %), H (6.52 %).

ORTEP of Ni(ITol)(MMA)$_2$. The cif file is also provided as a separate supporting information file.
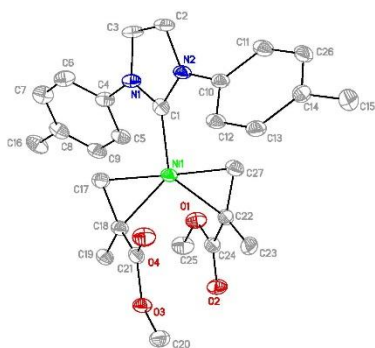
General Procedure for the Ni(ITol)(MMA)$_2$ promoted coupling of enones or enals and alkynes (A):

10 mol % of Ni(ITol)(MMA)$_2$ was dissolved in 1.0 mL toluene. Enone or enal (1.0 equiv) and alkyne (2.0 equiv) were added neat to the reaction mixture. Triethylsilane (4.0 equiv) was then added, followed by addition of Ti(O-iPr)$_4$ (1.1 equiv), and the reaction mixture was placed in

a heating mantle set to 65 °C and allowed to stir until starting materials were consumed (typically 8 h). The reaction mixture was then filtered through a plug of silica and was washed with a 1:1 mixture of EtOAc:hexanes. The solvent was then removed *in vacuo*, and the crude reaction mixture was purified via flash chromatography to afford the desired product.

General Safety Warning

It should be noted that according to previous work in the Buchwald lab, the combination of trialkoxysilanes and titanium isopropoxide has the potential to generate SiH_4. While our current conditions using trialkyl silanes will not facilitate that product formation, readers who wish to modify the general procedure should be aware of the hazard and not substitute trialkoxy silanes in the method.

5.2.2 Scheme 2.12 Substrate Scopes

((1*E*,4*E*)-4-Ethylhepta-1,4-diene-1,3-diyl)dibenzene.
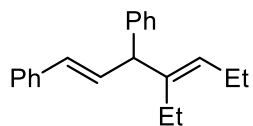
Scheme 2.12, Compound A: Following the general procedure (**A**), the reaction of Ni(ITol)(MMA)$_2$ (15.3 mg, 0.03 mmol), triethylsilane (139.2 mg, 1.2 mmol), titanium(IV) isopropoxide (93.7 mg, 0.33 mmol), *trans*-chalcone (62.4 mg, 0.3 mmol), and 3-hexyne (49.3 mg, 0.6 mmol) gave a crude residue, which was purified via flash chromatography (100% hexanes) to afford a single product (74.5 mg, 0.27 mmol, 90 % yield).

^{1}H-NMR (500 MHz, CDCl$_3$): δ 7.39 – 7.21 (m, 10H), 6.51 (dd, J = 15.8, 7.6 Hz, 1H), 6.28 (d, J = 15.8 Hz, 1H), 5.29 (t, J = 7.2 Hz, 1H), 4.21 (d, J = 7.5 Hz, 1H), 2.19 – 2.11 (m, 3H), 1.92 (dq, J = 14.6, 7.6 Hz, 1H), 1.02 (t, J = 7.5 Hz, 3H), 0.96 (t, J = 7.5 Hz, 3H).

¹³C-NMR (125 MHz, CDCl₃): δ 142.8, 142.2, 137.7, 132.9, 130.4, 128.9, 128.7, 128.5, 128.3,127.0, 126.3, 126.2, 54.6, 23.3, 21.1, 14.6, 13.7.

IR (film, cm⁻¹): 3024, 2959, 2869, 1599, 1491,1447.

HRMS (EI) *m/z*: [M+]⁺ calc. for C₂₁H₂₄, 276.1878, found, 276.1866.

((1*E*,4*E*)-4-Ethyl-3-methylhepta-1,4-dien-1-yl)benzene.
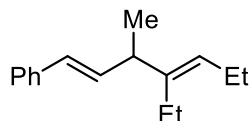
Scheme 2.12, Compound B: Following the general procedure (**A**), the reaction of Ni(ITol)(MMA)₂ (15.3 mg, 0.03 mmol), triethylsilane (139.2 mg, 1.2 mmol), titanium(IV) isopropoxide (93.7 mg, 0.33 mmol), (E)-1-phenylbut-2-en-1-one (43.8 mg, 0.3 mmol), and 3-hexyne (49.3 mg, 0.6 mmol) gave a crude residue, which was purified via flash chromatography (100% hexanes) to afford a single product (34.1 mg, 0.16 mmol, 53 % yield).

¹H-NMR (400 MHz, CDCl₃): δ 7.33 (d, *J* = 7.8 Hz, 2H), 7.25 (t, *J* = 7.4, 2H), 7.17 (t, *J* = 7.4 Hz, 1H), 6.33 (d, *J* = 15.8 Hz, 1 H), 6.13 (dd, *J* = 15.9, 7.2 Hz, 1H), 5.17 (t, *J* = 7.0 Hz, 1H), 2.93 (m, 1H), 2.01 (m, 4H), 1.18 (d, *J* = 7.0 Hz, 3H), 0.96 (dt, *J* = 2.5 7.3 Hz, 6 H).

¹³C-NMR (125 MHz, CDCl₃): δ 143.7, 137.9, 135.7, 128.5, 128.1, 126.8, 126.02, 126.00, 43.2, 22.5, 21.0, 19.3, 14.7, 14.1.

IR (film, cm⁻¹): 2963, 2870, 2164, 1497, 1458.

HRMS (EI) *m/z*: [M+]⁺ calc. for C₁₆H₂₂, 214.1722, found, 214.1723.

((1*E*,4*E*)-2-Methylhexa-1,4-diene-1,3-diyl)dibenzene.
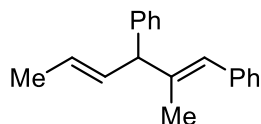
Scheme 2.12, Compound C: Following the general procedure (**A**), the reaction of Ni(ITol)(MMA)$_2$ (15.3 mg, 0.03 mmol), triethylsilane (139.2 mg, 1.2 mmol), titanium(IV) isopropoxide (93.7 mg, 0.33 mmol), benzylideneactecone (43.8 mg, 0.3 mmol), and 1-phenyl-1-propyne (70.2 mg, 0.6 mmol) gave a crude residue, which was purified via flash chromatography (100% hexanes) to afford a single regioisomer in a >95:5 isolated regioselectivity (>95:5 crude regioselectivity) (58.8 mg, 0.24 mmol, 79 % yield).

^{1}H-NMR (500 MHz, CDCl$_3$): δ 7.36 – 7.21(m, 10H), 6.46 (s, 1H), 5.85 (dd, J = 15.1, 7.5 Hz, 1H), 5.52 (dq, J = 15.1, 7.8 Hz), 4.11 (d, J = 7.8 Hz, 1 H), 1.79 (s, 3H), 1.78, (s, 3H).

^{13}C-NMR (125 MHz, CDCl$_3$): δ 142.9, 140.8, 138.4, 132.2, 129.0, 128.4, 128.3, 120.0, 127.0, 126.6, 126.3, 126.1, 57.8, 18.1, 17.3.

IR (film, cm^{-1}): 3023, 2913, 2854, 1492, 1447.

HRMS (EI) *m/z*: [M+]$^+$ calc. for C$_{19}$H$_{20}$, 248.1565, found, 248.1563.

((1*E*,4*E*)-3-Isopropyl-2-methylhexa-1,4-dien-1-yl)benzene.
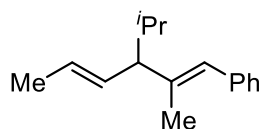
Scheme 2.12, Compound D: Following the general procedure (**A**), the reaction of Ni(ITol)(MMA)$_2$ (15.3 mg, 0.03 mmol), triethylsilane (139.2 mg, 1.2 mmol), titanium(IV) isopropoxide (93.7 mg, 0.33 mmol), (*E*)-5-methylhex-3-en-2-one (33.7 mg, 0.3 mmol), and 1-phenyl-1-propyne (70.2 mg, 0.6 mmol) gave a crude residue, which was purified via flash chromatography (100% hexanes) to afford a single regioisomer in a >95:5 isolated regioselectivity (>95:5 crude regioselectivity) (41.8 mg, 0.20 mmol, 65 % yield).

^{1}H-NMR (400 MHz, CDCl$_3$): δ 7.33 (t, J = 7.8 Hz, 2H), 7.29 (d, J = 5.4 Hz, 2H), 7.19 (t, J = 8.6 Hz, 1H), 6.3 (s, 1H), 5.55 - 5.49 (m, overlapping dd and dq, 2H), 2.36 (dd, J = 8.1, 2.9 Hz, 1H), 1.84 – 1.77 (m, 1H), 1.82 (s, 3H), 1.72 (d, J = 4.9 Hz, 3H), 0.93 (d, J = 6.6 Hz, 3H), 0.90 (d, J = 6.6 Hz, 3H).

¹³C-NMR (125 MHz, CDCl₃):

^{13}C-NMR (125 MHz, CDCl$_3$): δ 141.4, 138.6, 132.5, 128.9, 127.9, 125.8, 125.7, 125.3, 61.3, 29.6, 21.2, 20.8, 18.1, 15.3.

IR (film, cm^{-1}): 3021, 2950, 2864, 2356, 1494, 1441.

HRMS (EI) *m/z*: [M+]$^+$ calc. for C$_{16}$H$_{22}$, 214.1722, found, 214.1722.

1-((1*E*,4*E*)-4-Ethyl-1-phenylhepta-1,4-dien-3-yl)-4-methoxybenzene.
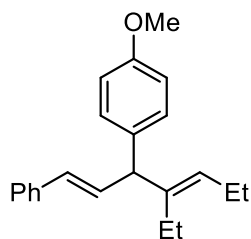
Scheme 2.12, Compound E: Following the general procedure (**A**), the reaction of Ni(ITol)(MMA)$_2$ (15.3 mg, 0.03 mmol), triethylsilane (139.2 mg, 1.2 mmol), titanium(IV) isopropoxide (93.7 mg, 0.33 mmol), (E)-3-(4-methoxyphenyl)-1-phenylprop-2-en-1-one (71.5 mg, 0.3 mmol), and 3-hexyne (49.3 mg, 0.6 mmol) gave a crude residue, which was purified via flash chromatography (hexanes: ethyl acetate = 99:1) to afford a single product (59.7 mg, 0.20 mmol, 65 % yield).

^{1}H-NMR (500 MHz, CDCl$_3$): δ 7.37 (d, *J* = 7.3 Hz, 2H), 7.30 (t, *J* = 7.6 Hz, 2H), 7.21 (t, *J* = 7.1 Hz, 1H), 7.17 (d, *J* = 8.5 Hz, 2H), 6.87 (d, *J* = 8.5 , 2H), 6.47 (dd, *J* = 15.9, 7.6 Hz, 1H), 6.23 (d, *J* = 15.8 Hz, 1 H), 5.26 (t, *J* = 7.3, 1H), 4.15 (d, *J* = 7.6 Hz, 1H), 3.82 (s, 3H), 2.16 – 2.10 (m, 3H), 1.93 – 1.89 (m, 1H), 1.01 (t, *J* = 7.3 Hz, 3H), 0.95 (t, *J* = 7.3 Hz, 3H).

^{13}C-NMR (125 MHz, CDCl$_3$): δ 158.1, 142.5, 137.7, 134.8, 133.2, 130.1, 129.6, 128.7, 128.4, 127.0, 126.2, 113.6, 55.2, 53.7, 23.2, 21.1, 14.6, 13.7.

IR (film, cm^{-1}): 2960, 2869, 2054, 1507, 1459.

HRMS (EI) *m/z*: [M+]$^+$ calc. for C$_{22}$H$_{26}$O, 306.1984, found, 306.1985.

2-((2*E*,5*E*)-3-Methyl-4,6-diphenylhexa-2,5-dien-1-yl)isoindoline-1,3-dione.
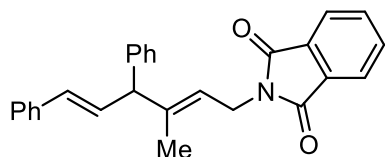
Scheme 2.12, Compound F: Following the general procedure (**A**), the reaction of Ni(ITol)(MMA)$_2$ (15.3 mg, 0.03 mmol), triethylsilane (139.2 mg, 1.2 mmol), titanium(IV) isopropoxide (93.7 mg, 0.33 mmol), trans-chalcone (62.4 mg, 0.3 mmol), and *N*-(2-butynyl)phthalimide (119.5 mg, 0.6 mmol) gave a crude residue, which was purified via flash chromatography (hexanes: ethyl acetate = 97:3) to afford a single regioisomer in a >95:5 isolated regioselectivity (>95:5 crude regioselectivity) (93.2 mg, 0.22 mmol, 73 % yield).

^{1}H-NMR (500 MHz, CDCl$_3$): δ 7.86 (dd, *J* = 5.3, 3.1 Hz, 2H), 7.21 (dd, *J* = 5.4, 3.2 Hz, 2H), 7.35 – 7.20 (m, 10H), 6.45 (dd, *J* = 15.8, 7.5 Hz, 1 H), 6.31 (d, *J* = 15.8 Hz, 1H), 5.48 (t, *J* = 6.8 Hz, 1H), 4.40 (d, *J* = 7.1 Hz, 2H), 4.15 (d, *J* = 7.6 Hz, 1H), 1.82 (s, 3H).

^{13}C-NMR (125 MHz, CDCl$_3$): δ 168.1, 141.8, 141.7, 137.3, 133.8, 132.3, 131.4, 130.9, 128.46, 128.45, 1128.40, 127.2, 126.5, 126.3, 123.2, 120.7, 57.1, 35.9, 15.9.

IR (film, cm^{-1}): 3024, 2165, 1771, 1711 1497.

HRMS (EI) *m/z*: [M+]$^+$ calc. for C$_{27}$H$_{23}$NO$_2$, 393.1729, found, 393.1735.

(((*E*)-4-((*E*)-Benzylidene)-5,7-diphenylhept-6-en-1-yl)oxy)(*tert*-butyl) dimethylsilane.
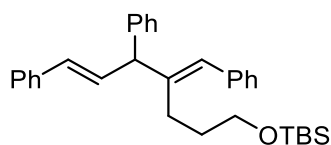
Scheme 2.12, Compound G: Following the general procedure (**A**), the reaction of Ni(ITol)(MMA)$_2$ (15.3 mg, 0.03 mmol), triethylsilane (139.2 mg, 1.2 mmol), titanium(IV) isopropoxide (93.7 mg, 0.33 mmol), trans-chalcone (62.4 mg, 0.3 mmol), and tert-butyldimethyl((5-phenylpent-4-yn-1-yl)oxy)silane (164.5 mg, 0.6 mmol) gave a crude residue,

which was purified via flash chromatography (hexanes: ethyl acetate = 99:1) to afford a single

regioisomer in a >95:5 isolated regioselectivity (>95:5 crude regioselectivity) (111.0 mg, 0.24

mmol, 79 % yield).

**^{1}H-NMR (500 MHz, CDCl$_3$):** δ 7.40-7.20 (m, 15H), 6.59 (dd, J = 15.9, 7.5 Hz, 1H), 6.43 (s, 1H), 6.34 (d, J = 16.0, 1H), 4.39 (d, J = 7.3 Hz, 1H), 3.56 (t, J = 6.4 Hz, 2H), 2.46 (ddd, J = 13.5, 9.4, 6.9 Hz, 1H), 2.15 (ddd, J = 13.5, 9.6, 6.7 Hz, 1H), 1.83 – 1.65 (m, 2H), 0.93 (s, 9H), 0.09 (s, 6H).

^{13}C-NMR (125 MHz, CDCl$_3$): δ 144.8, 142.2, 138.1, 137.4, 132.3, 131.2, 128.8, 128.7, 128.51, 128.48, 128.2, 127.9, 127.2, 126.6, 126.28, 126.27, 63.1, 55.0, 31.9, 27.6, 26.0, 18.3, -5.3.

IR (film, cm^{-1}): 2929, 2856, 1491, 1104, 832.

HRMS (EI) m/z: [M+]$^+$ calc. for C$_{32}$H$_{40}$OSi, 468.2848, found, 468.2854.

1-((1E,4E)-4-Ethyl-1-phenylhepta-1,4-dien-3-yl)-4-fluorobenzene.
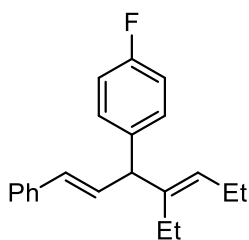
Scheme 2.12, Compound H: Following the general procedure (**A**), the reaction of

Ni(ITol)(MMA)$_2$ (15.3 mg, 0.03 mmol), triethylsilane (139.2 mg, 1.2 mmol), titanium(IV)

isopropoxide (93.7 mg, 0.33 mmol), (E)-3-(4-fluorophenyl)-1-phenylprop-2-en-1-one (67.9 mg,

0.3 mmol), and 3-hexyne (49.3 mg, 0.6 mmol) gave a crude residue, which was purified via flash

chromatography (hexanes: ethyl acetate = 99:1) to afford a single product (53.0 mg, 0.18 mmol,

60 % yield 58.6 mg, 0.18 mmol, 63 % yield).

^{1}H-NMR (500 MHz, CDCl$_3$): δ 7.36 (d, J = 7.3 Hz, 2H), 7.31 (t, J = 7.6 Hz, 2H), 7.20 (m, overlapping t and t, 3H), 7.01 (t, J = 8.8 Hz, 2H), 6.45, (dd, J = 15.8, 7.6 Hz, 1H), 6.22 (d, J = 15.8 Hz, 1H), 5.26 (t, J = 7.1 Hz, 1H), 4.18 (d, J = 7.3 Hz, 1H), 2.15-2.10 (m, 3H), 1.90 (m, 1H), 1.01 (t, J = 7.6 Hz, 3H), 0.95 (t, J = 7.8 Hz, 3H).

¹³C-NMR (125 MHz, CDCl₃): δ 161.5 (d, *J* = 244.1 Hz), 142.1, 138.3 (d, *J* = 2.8 Hz), 137.5, 132.6, 130.6, 130.1 (d, *J* = 7.6 Hz), 129.1, 128.5, 127.1, 126.2, 115.1 (d, *J* = 21 Hz), 53.7, 23.2, 21.1, 14.6, 13.7. A ¹³C spectrum was also acquired at 100 MHz (CDCl₃) in order to elucidate the fluorine coupling assignments. 143.8, 137.1, 133.5, 132.7, 130.6, 128.7, 128.51, 128.48, 128.1, 127.6, 126.8, 126.2, 46.5, 44.9, 32.0, 31.7, 26.5.

IR (film, cm⁻¹): 3022, 2960, 2869, 1505, 1448.

HRMS (EI) *m/z*: [M+]⁺ calc. for C₂₁H₂₃F, 294.1784, found, 294.1776. [M+]⁺ calc. for C₂₁H₂₃Cl, 310.1488, found, 310.1494.

((1E,4E)-6-chlorohexa-1,4-diene-1,3-diyl)dibenzene.
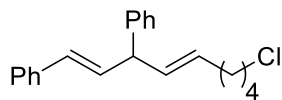
Scheme 2.12, Compound I: Following the general procedure (**A**), the reaction of Ni(ITol)(MMA)₂ (15.3 mg, 0.03 mmol), triethylsilane (139.2 mg, 1.2 mmol), titanium(IV) isopropoxide (93.7 mg, 0.33 mmol), trans-chalcone (62.4 mg, 0.3 mmol), and 6-chloro-1-hexyne (70.0 g, 0.6 mmol) gave a crude residue, which was purified via flash chromatography (hexanes: ethyl acetate = 99:1) to afford a single regioisomer in a >95:5 isolated regioselectivity (>95:5 crude regioselectivity) (58.6 mg, 0.18 mmol, 63 % yield).

¹H-NMR (500 MHz, CDCl₃): δ 7.27 – 7.14 (m, 10H), 6.50 (d, *J* = 11.4 Hz, 1H), 5.72 (t, *J* = 11.6 Hz, 1H), 5.70 (dd, *J* = 15.4, 3.1 Hz, 1 H), 5.48 (ddd, *J* = 15.3, 6.6, 1.3 Hz, 1H), 4.64 (dd, *J* = 10.2, 6.1 Hz, 1H), 3.54 (t, *J* = 6.7 Hz, 2H), 2.04 (q, *J* = 7.1 Hz, 2H), 1.73 – 1.68 (m, 2H), 1.50 – 1.44 (m, 2H).

¹³C-NMR (125 MHz, CDCl₃): δ 143.8, 137.1, 133.5, 132.7, 130.6, 128.7, 128.51, 128.48, 128.1, 127.6, 126.8, 126.2, 46.5, 44.9, 32.0, 31.7, 26.5.

IR (film, cm⁻¹): 3058, 2933, 1599, 1492, 1446.

HRMS (EI) *m/z*: [M+]⁺ calc. for C₂₁H₂₃Cl, 310.1488, found, 310.1494.

(*E*)-(2-Methylpenta-1,4-diene-1,3-diyl)dibenzene.
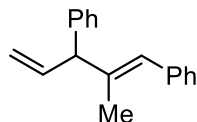
Scheme 2.12, Compound J: Following the general procedure (**A**), the reaction of Ni(ITol)(MMA)$_2$ (15.3 mg, 0.03 mmol), triethylsilane (139.2 mg, 1.2 mmol), titanium(IV) isopropoxide (93.7 mg, 0.33 mmol), trans-cinnamaldehyde (39.7 mg, 0.3 mmol), and 1-phenyl-1-propyne (70.2 mg, 0.6 mmol) gave a crude residue, which was purified via flash chromatography (100% hexanes) to afford a single regioisomer in a >95:5 isolated regioselectivity (>95:5 crude regioselectivity) (51.3 mg, 0.22 mmol, 73 % yield).

^{1}H-NMR (500 MHz, CDCl$_3$): δ 7.36 – 7.22 (m, 10H), 6.46 (s, 1H), 6.24 (ddd, *J* = 17.3, 10.2, 7.3 Hz, 1H), 5.24 (d, *J* = 10.2 Hz, 1H), 5.08 (d, *J* = 17.2 Hz, 1H), 4.17 (d, *J* = 7.3 Hz, 1H), 1.80 (s, 3H).

^{13}C-NMR (125 MHz, CDCl$_3$): δ 141.9, 140.0, 139.5, 138.3, 129.0, 128.5, 128.4, 128.08, 128.04, 127.8, 127.0, 126.4, 126.2, 116.4, 58.7, 17.4.

IR (film, cm^{-1}): 3023, 2193, 2049, 1494, 1332.

HRMS (EI) *m/z*: [M+]$^+$ calc. for C$_{18}$H$_{18}$, 234.1409, found, 234.1405.

(*E*)-(2,3-Dimethylpenta-1,4-dien-1-yl)benzene.
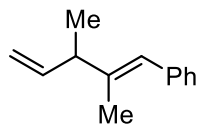
Scheme 2.12, Compound K: Following the general procedure (**A**), the reaction of Ni(ITol)(MMA)$_2$ (15.3 mg, 0.03 mmol), triethylsilane (139.2 mg, 1.2 mmol), titanium(IV) isopropoxide (93.7 mg, 0.33 mmol), crotonaldehyde (39.7 mg, 0.3 mmol), and 1-phenyl-1-propyne (70.2 mg, 0.6 mmol) gave a crude residue, which was purified via flash chromatography (100%

hexanes) to afford a single regioisomer in a >95:5 isolated regioselectivity (>95:5 crude regioselectivity) (37.7 mg, 0.22 mmol, 73 % yield).

¹H-NMR (500 MHz, CDCl₃): δ 7.34 (t, J = 7.6 Hz, 2H), 7.28 (d, J = 6.8 Hz, 2H), 7.21 (t, 7.3 Hz, 1H), 6.37 (s, 1H), 5.92 (ddd, J = 17.0, 10.3, 6.5 Hz, 1H), 5.13 – 5.07 (m, 2H), 3.09 – 2.88 (m, 1H), 1.84 (s, 3H), 1.26 (d, J = 7.1, 3H).

¹³C-NMR (125 MHz, CDCl₃): δ 142.2, 141.8, 138.5, 128.9, 128.0, 125.9, 124.5, 113.6, 46.8, 18.1, 15.7.

IR (film, cm⁻¹): 2962, 2175, 2016, 1278, 1027.

HRMS (EI) *m/z*: [M+]⁺ calc. for $C_{13}H_{16}$, 172.1252, found, 172.1246.

**(*E*)-(2,4-dimethylpenta-1,4-dien-1-yl)benzene.**
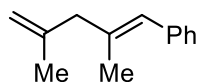
Scheme 2.12, Compound L: Following the general procedure (**A**), the reaction of Ni(ITol)(mma)₂ (15.3 mg, 0.03 mmol), triethylsilane (139.2 mg, 1.2 mmol), titanium(IV) isopropoxide (93.7 mg, 0.33 mmol), methacrolein (39.7 mg, 0.3 mmol), and 1-phenyl-1-propyne (70.2 mg, 0.6 mmol) gave a crude residue, which was purified via flash chromatography (100% hexanes) to afford a single regioisomer in a >95:5 isolated regioselectivity (>95:5 crude regioselectivity) (42.3 mg, 0.25 mmol, 82 % yield).

¹H-NMR (500 MHz, CDCl₃): δ 7.35 (t, J = 7.6 Hz, 2H), 7.30 (d, J = 7.6 Hz, 2H), 7.22 (t, J = 7.3 Hz, 1H), 6.36 (s, 1H), 4.88 (s, 1H), 4.84 (s, 1H), 2.90 (s, 2H), 1.85 (s, 3H), 1.76 (s, 3H).

¹³C-NMR (125 MHz, CDCl₃): δ 143.7, 138.5, 136.7, 128.8, 128.1, 126.8, 126.0, 112.3, 49.6, 21.9, 17.3.

IR (film, cm⁻¹): 3072, 2970, 2909, 2163, 1497.

HRMS (EI) *m/z*: [M+]⁺ calc. for $C_{13}H_{16}$, 172.1252, found, 172.1245.

(*E*)-Undeca-1,4-dien-3-ylbenzene.
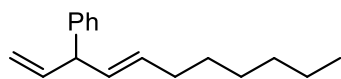
Scheme 2.12, Compound M: Following the general procedure (**A**), the reaction of Ni(ITol)(MMA)$_2$ (15.3 mg, 0.03 mmol), triethylsilane (139.2 mg, 1.2 mmol), titanium(IV) isopropoxide (93.7 mg, 0.33 mmol), trans-cinnamaldehyde (39.7 mg, 0.3 mmol), and 1-octyne (66.1 mg, 0.6 mmol) gave a crude residue, which was purified via flash chromatography (100% hexanes) to afford a single regioisomer in a >95:5 isolated regioselectivity (>95:5 crude regioselectivity) (49.3 mg, 0.22 mmol, 72 % yield). The spectral data matches that previously reported in the literature.[70]

¹H-NMR (500 MHz, CDCl₃): δ 7.31 (dt, *J* = 8.1 Hz, 1.7 Hz, 2H), 7.22 – 7.19 (m, 3H), 6.02 (ddd, *J* = 17.0, 10.2, 6.8 Hz, 1H), 5.61 (dd, *J* = 15.3, 7.0 Hz, 1H), 5.51 – 5.46 (ddt, 15.4, 6.7, 0.8 Hz, 1H), 5.10 (ddd, *J* = 10.2, 1.4, 1.4 Hz, 1H), 5.04 (ddd, *J* = 17.1,1.4, 1.4 Hz, 1H), 4.01 (dd, *J* = 7.0, 6.9 Hz, 1H), 2.04 (dt, *J* = 7.1, 7.0 Hz, 2H), 1.39 – 1.24 (m, 8H), 0.88 (t, 7.1 Hz, 3H).

¹³C-NMR (125 MHz, CDCl₃): δ 143.4, 140.9, 131.8, 131.4, 128.4, 127.9, 126.2, 114.8, 52.2, 32.6, 31.7, 29.3, 28.9, 22.6, 14.1.

IR (film, cm⁻¹): 3025, 2956, 2924, 2854,2036, 1495.

HRMS (EI) *m/z*: [M+]⁺ calc. for C₁₇H₂₄, 228.1878, found, 228.1884.

(E)-1,3-dimethyl-7-(5-phenylhepta-3,6-dien-1-yl)-3,7-dihydro-1H-purine-2,6-dione.
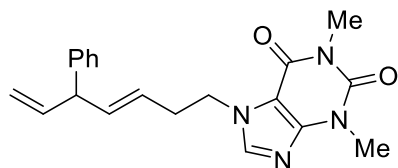
Scheme 2.12, Compound N: Following the general procedure (**A**), the reaction of Ni(ITol)(MMA)$_2$ (15.3 mg, 0.03 mmol), triethylsilane (139.2 mg, 1.2 mmol), titanium(IV) isopropoxide (93.7 mg, 0.33 mmol), trans-cinnamaldehyde (39.7 mg, 0.3 mmol), and 7-(but-3-yn-

1-yl)-1,3-dimethyl-3,7-dihydro-1H-purine-2,6-dione (130.8 mg, 0.6 mmol) gave a crude residue, which was purified via flash chromatography (hexanes: ethyl acetate = 70:30) to afford a single regioisomer in a >95:5 isolated regioselectivity (>95:5 crude regioselectivity) (58.8 mg, 0.17 mmol, 56 % yield).

^{1}H-NMR (500 MHz, CDCl$_3$): δ 7.46 (s, 1H), 7.27 (m, 2H), 7.20 (t, J = 7.4 Hz, 1H), 7.06 (d, J = 7.8 Hz, 2H), 5.92 (ddd, J = 17.1, 10.2, 6.8 Hz, 1H), 5.61 (dd, J = 15.3, 7.1 Hz, 1H), 5.41 – 5.39 (m, 1H), 5.08 (d, J = 10.2, 1H), 4.95 (d, J = 17.2, 1H), 4.39 – 4.28 (m, 2H), 3.95 (t, J = 7.0 Hz, 1H), 3.58 (s, 3H), 3.40 (s, 3H), 2.61 (q, J = 6.9 Hz, 2H).

^{13}C-NMR (125 MHz, CDCl$_3$): δ 155.0, 151.5, 148.7, 147.2, 140.7, 139.7, 136.0, 128.3, 127.6, 126.4, 125.5, 115.1, 106.7, 51.9, 46.6, 33.9, 29.6, 27.8.

IR (film, cm^{-1}): 3111, 2950, 1699, 1651,1546.

HRMS (EI) *m/z*: [M+H]$^+$ calc. for C$_{20}$H$_{23}$N$_4$O$_2^+$, 351.1816, found, 351.1813.

5.2.3 Scheme 2.18 Deuterium Labeling Studies

triethyl((((1Z,4E)-4-methyl-3,5-diphenylpenta-1,4-dien-1-yl-5-d)oxy)silane.
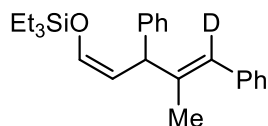
Scheme 2.18, Entry A: Following a previously published modified procedure utilizing triethyl(silane-d), a crude residue was obtained, which was purified via flash chromatography (100% hexanes) to afford a single regioisomer in a >98:2 isolated regioselectivity (>98:2 crude regioselectivity) with >95 % deuterium incorporation at the proton shown above (36.1 mg, 0.10 mmol, 33 % yield). The undeuterated standard was previously reported.[29]

^{1}H-NMR (400 MHz, CDCl$_3$): δ 7.34-7.18 (m, 10H), 6.40 (d, J = 5.6 Hz, 1H), 4.88 (dd, J = 5.6, 9.6 Hz, 1H), 4.75 (d, J = 9.6 Hz, 1H), 1.78 (d, J = 1.2 Hz, 3H), 0.99 (t, J = 8.0 Hz, 9H), 0.67 (q, J = 8.0 Hz, 6H).

((1E,4Z)-2-methylpenta-1,4-diene-1,3-diyl-5-d)dibenzene.
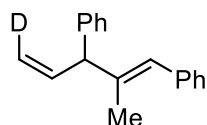
Scheme 2.18, Entry B: Following the general procedure (**A**), the reaction of Ni(ITol)(MMA)$_2$ (15.3 mg, 0.03 mmol), triethyl(silane-d) (140.2 mg, 1.2 mmol), titanium(IV) isopropoxide (93.7 mg, 0.33 mmol), trans-cinnamaldehyde (39.7 mg, 0.3 mmol), and 1-phenyl-1-propyne (70.2 mg, 0.6 mmol) gave a crude residue, which was purified via flash chromatography (100% hexanes) to afford a single regioisomer in a >98:2 isolated regioselectivity (>98:2 crude regioselectivity) with >95 % deuterium incorporation at the proton shown above (51.3 mg, 0.22 mmol, 63 % yield).

^{1}H-NMR (500 MHz, CDCl$_3$): δ 7.36 – 7.21 (m, 10H), 6.46 (s, 1H), 6.22 (m, 1H), 5.21 (d, $J =$ 10.2 Hz, 1H), 4.16 (d, $J =$ 7.1 Hz, 1H), 1.80 (s, 3H).

^{13}C-NMR (125 MHz, CDCl$_3$): δ 141.9, 140.0, 139.4, 138.3, 128.4, 128.5, 128.4, 128.0, 127.0, 126.4, 126.2, 116.1 (t, $J =$ 23.8 Hz), 58.6, 17.4.

tetrakis((propan-2-yl-d$_7$)oxy)titanium.
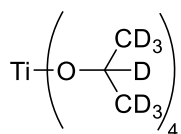
Scheme 2.18: Titanium(IV) isopropoxide (1.0 ml, 3.4 mmol) was added to a flame dried round bottom under a nitrogen atmosphere. To this was added 2-propanol-d$_8$ (99.5%) (2.0 ml, 26.1 mmol) and the mixture was allowed to stir for 2 h. The reaction mixture was then concentrated, and the addition of 2-propanol-d$_8$ (99.5%) (2.0 ml, 26.1 mmol) and subsequent concentration after stirring for two hours was repeated two more times to afford the desired product with 99% deuterium incorporation.

Standard Titanium(IV) isopropoxide, MS (EI) *m/z*: [M-CH$_3$]$^+$ calc. for C$_{12}$H$_{28}$O$_4$Ti, 269.12, found, 269.1.

Titanium(IV) isopropoxide-d$_{28}$ MS (EI) m/z: [M-CD$_3$]$^+$ calc. for C$_{12}$D$_{28}$O$_4$Ti, 294.28, found, 294.3. No d$_{21}$, d$_{14}$, or d$_7$ products detected. Characteristic peaks at m/z 290.3, 287.2, 283.2, 280.2, 276.2, and 273.1 indicate incomplete deuterium incorporation.

(E)-(2-methylpenta-1,4-diene-1,3-diyl-1-d)dibenzene.
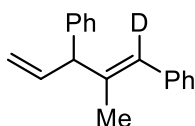
Scheme 2.18, Entry C: Following the general procedure (**A**), the reaction of Ni(ITol)(MMA)$_2$

(15.3 mg, 0.03 mmol), triethylsilane (140.2 mg, 1.2 mmol), titanium(IV) isopropoxide-d$_{28}$ (99%)

(93.7 mg, 0.33 mmol), trans-cinnamaldehyde (39.7 mg, 0.3 mmol), and 1-phenyl-1-propyne (70.2

mg, 0.6 mmol) gave a crude residue, which was purified via flash chromatography (100% hexanes)

to afford a single regioisomer in a >98:2 isolated regioselectivity (>98:2 crude regioselectivity)

with 91% deuterium incorporation at the proton shown above (35.6 mg, 0.15 mmol, 51 % yield).

^{1}H-NMR (500 MHz, CDCl$_3$): δ 7.36 – 7.22 (m, 10H), 6.46 (s, 0.09H), 6.24 (ddd, J = 17.3, 10.2, 7.3 Hz, 1H), 5.24 (d, J = 10.2 Hz, 1H), 5.08 (d, J = 17.2 Hz, 1H), 4.17 (d, J = 7.3 Hz, 1H), 1.80 (s, 3H).

^{13}C-NMR (125 MHz, CDCl$_3$): δ 141.9, 140.0, 139.5, 138.2, 128.9, 128.5, 128.4, 128.1, 128.0, 127.8, 127.0, 126.4, 126.2, 116.3, 58.7, 17.3.

5.3 Chapter 3 Experimental

5.3.1 General Procedures

General Procedure for the synthesis of aryl silyl ethers (A):

In a round bottom flask, aryl alcohol (1 equiv.) was dissolved in DMF or DCM (5.0 mL). The

solution was then charged with imidazole (2 equiv.) and *tert*-butyldimethylchlorosilane (1.5

equiv.) and stirred until full conversion. The reaction was diluted with 25 mL Et$_2$O, washed with

deionized H$_2$O (3 × 25 mL), dried over MgSO$_4$, filtered, concentrated under reduced pressure and purified by flash column chromatography on silica gel to afford the aryl silyl ether.

General Procedure for the Ni(acac)$_2$/IPr^{Me}·HCl promoted reduction of aryl silyl ethers using titanium(IV) isopropoxide (B):

A reaction tube containing a stir bar was charged with aryl silyl ether (1 equiv.), Ni(acac)$_2$ (5 mol%), IPr^{Me}·HCl (10 mol%), and NaO^{t}Bu (2.5 equiv.) in a nitrogen atmosphere glovebox. The sealed reaction tube was brought outside the glovebox then toluene (0.5 M) and titanium(IV) isopropoxide (1.1 equiv.) were added sequentially via syringe. The reaction tube was then placed in a heated block set to 120 °C and stirred for 6 hours, unless noted otherwise. The mixture was cooled to room temperature, internal standard was then added (tridecane, 1 equiv.), diluted with EtOAc (3 mL), and quenched with deionized water (5 mL). The mixture was then extracted with EtOAc (3 × 10 mL), dried over MgSO$_4$, filtered, concentrated under reduced pressure and purified by flash column chromatography on silica gel to afford the desired product.

General Procedure the for Ni(cod)$_2$/IPr*OMe promoted silylation of aryl silyl ethers using triethylsilane (C):

A reaction tube containing a stir bar was charged with aryl silyl ether (1 equiv.), Ni(cod)$_2$ (10 mol%), IPr*OMe (10 mol%), and NaO^{t}Bu (2.5 equiv.) in a nitrogen atmosphere glovebox. The sealed reaction tube was brought outside the glovebox then toluene (0.5 M) and triethylsilane (6 equiv.) were added sequentially via syringe. The reaction tube was then placed in a heated block set to 120 °C and stirred for 16 hours, unless noted otherwise. The mixture was cooled to room temperature, an internal standard was then added (tridecane, 1 equiv.), diluted with EtOAc (3 mL), and quenched with deionized water (5 mL). The mixture was then extracted with EtOAc (3 × 10 mL), dried over MgSO$_4$, filtered, concentrated under reduced pressure and purified by flash column chromatography on silica gel to afford the desired product.

General Procedure for the Ni(COD)₂/IPr^Me·HCl promoted amination of aryl silyl ethers using amines (D):

A reaction tube containing a stir bar was charged with aryl silyl ether (1 equiv.), Ni(COD)$_2$ (5 mol%), IPr^Me·HCl (10 mol%), and NaO^{t}Bu (2.5 equiv.) in a nitrogen atmosphere glovebox. The sealed reaction tube was brought outside the glovebox then toluene (0.5 M) and amine (1.5 equiv.) were added sequentially via syringe. The reaction tube was then placed in a heated block set to 120 °C and stirred for 6 hours, unless noted otherwise. The mixture was cooled to room temperature, quenched with dichloromethane (1 mL), and diluted with EtOAc (3 mL). The mixture was then run through a silica plug, concentrated under reduced pressure and purified by flash column chromatography on silica gel to afford the desired product.

Procedure for Generating a Calibration Curve Utilizing the GC-FID

Solutions containing a constant concentration of an internal standard (tridecane (0.164 M) and varying concentrations of the desired product (0.05, 0.10, 0.15 and 0.20 M) were prepared in ethyl acetate. Each was analyzed by GC-FID and the response factor F calculated by fitting the data to the following equation:

$$\frac{Area\ of\ Product\ Signal}{Concentration\ of\ Product} = F\left(\frac{Area\ of\ Internal\ Standard\ Signal}{Concentration\ of\ Internal\ Standard}\right)$$

Calibration Curve for biphenyl.
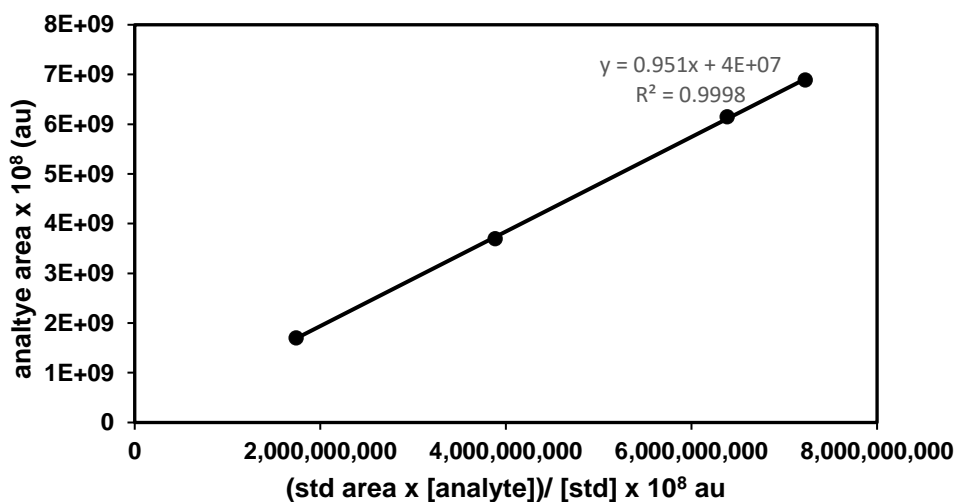
Plot of analyte area versus (std area x [**S1**]) / [std] fitted to y = mx + b where m = 0.951 and b = 4 x 10^7 with a R^2 of 0.9998.

concentration of biphenyl (**S1**)	area of **S1** (analyte)	area tridecane (std)	(std area x [**S1**]) / [std]
0.0509	17.07 x 10^8	56.48 x 10^8	17.42 x 10^8
0.0966	37.00 x 10^8	65.97 x 10^8	38.86 x 10^8
0.1582	61.49 x 10^8	66.22 x 10^8	63.88 x 10^8
0.1920	68.92 x 10^8	61.77 x 10^8	72.28 x 10^8

Calibration Curve for naphthalene.
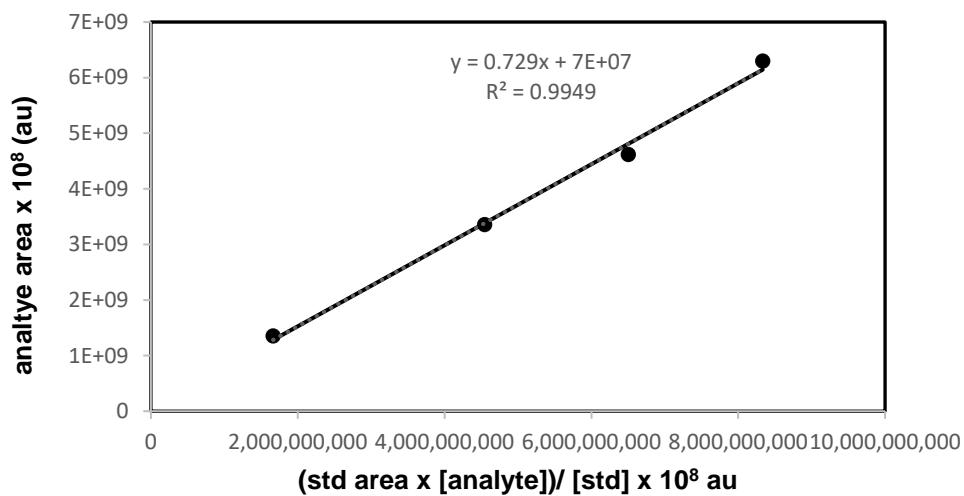
Plot of analyte area versus (std area x [**S2**]) / [std] fitted to $y = mx + b$ where $m = 0.729$ and $b = 7$ x 10^7 with a R^2 of 0.9949.

Concentration of naphthalene (**S2**)	Area of **S2** (analyte)	area tridecane (std)	(std area x [**S2**]) / [std]
0.0492	13.53 x 10^8	55.61 x 10^9	16.66 x 10^8
0.1038	33.53 x 10^8	71.85 x 10^9	45.45 x 10^8
0.1545	46.15 x 10^8	69.04 x 10^9	65.02 x 10^8
0.2013	62.96 x 10^8	67.90 x 10^9	83.33 x 10^8

Calibration Curve for [1,1'-biphenyl]-4-yltriethylsilane.
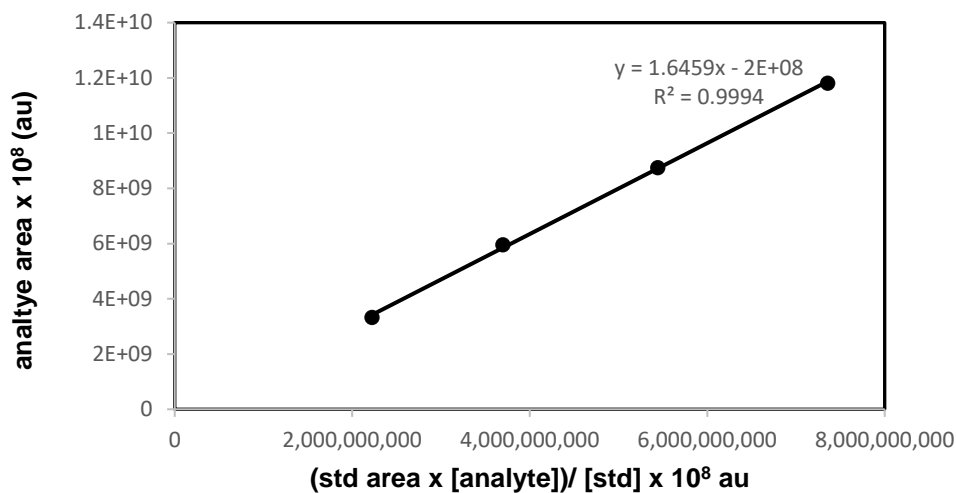
Plot of analyte area versus (std area x [**S3**]) / [std] fitted to y = $mx + b$ where $m = 1.6459$ and $b = -2$ x 10^8 with a R^2 of 0.9994.

Concentration of [1,1'-biphenyl]-4-yltriethylsilane (**S3**)	Area of **S3** (analyte)	area tridecane (std)	(std area x [**S3**]) / [std]
0.0484	33.29 x 10^8	75.35 x 10^9	22.25 x 10^8
0.0872	59.61 x 10^8	69.62 x 10^9	36.99 x 10^8
0.1430	87.51 x 10^8	62.43 x 10^9	54.43 x 10^8
0.1929	11.81 x 10^9	62.54 x 10^9	73.57 x 10^8

Calibration Curve for *tert*-butylbenzene.

y = 0.6932x - 2E+07
R² = 0.9981
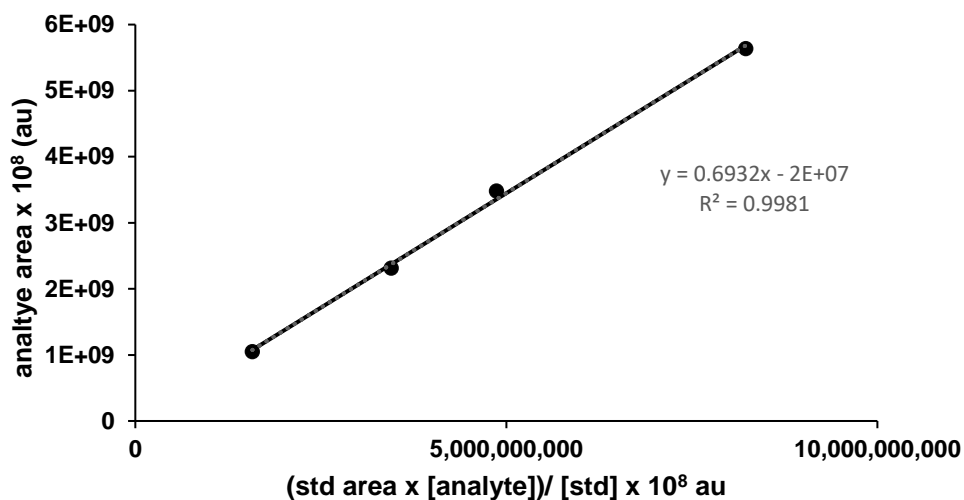
Plot of analyte area versus (std area x [**S4**]) / [std] fitted to y = mx + b where m = 0.6932 and b = -2 x 10^7 with a R^2 of 0.9981.

Concentration of *tert*-butylbenzene (**S4**)	area of **S4** (analyte)	area tridecane (std)	(std area x [**S4**]) / [std]
0.0425	10.52 x 10^8	60.91 x 10^8	15.77 x 10^8
0.0969	23.16 x 10^8	58.41 x 10^8	34.49 x 10^8
0.1378	34.82 x 10^8	57.91 x 10^8	48.66 x 10^8
0.2161	56.38 x 10^8	62.45 x 10^8	82.26 x 10^8

Calibration Curve for 2,3-dihydro-1H-indene.
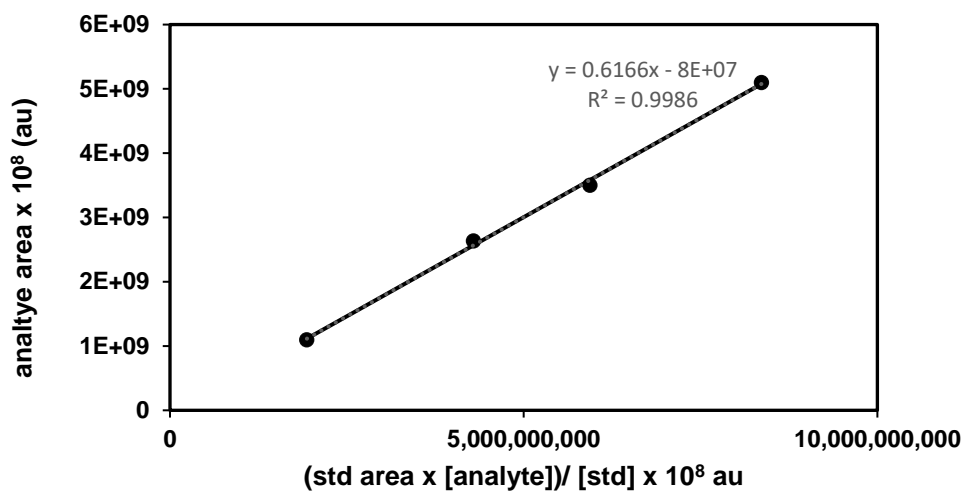
Plot of analyte area versus (std area x [**S6**]) / [std] fitted to y = *m*x + *b* where *m* = 0.6166 and *b* = -8 x 10^7 with a R^2 of 0.9986.

Concentration of 2,3-dihydro-1H-indene (**S6**)	area of **S6** (analyte)	area tridecane (std)	(std area x [**S6**]) / [std]
0.0550	10.99 x 10^8	57.69 x 10^8	19.34 x 10^8
0.1090	26.37 x 10^8	64.57 x 10^8	42.91 x 10^8
0.1506	35.03 x 10^8	64.65 x 10^8	59.36 x 10^8
0.2488	50.99 x 10^8	55.12 x 10^8	83.61 x 10^8

Calibration Curve for 1,2,3,4-tetrahydronaphthalene.
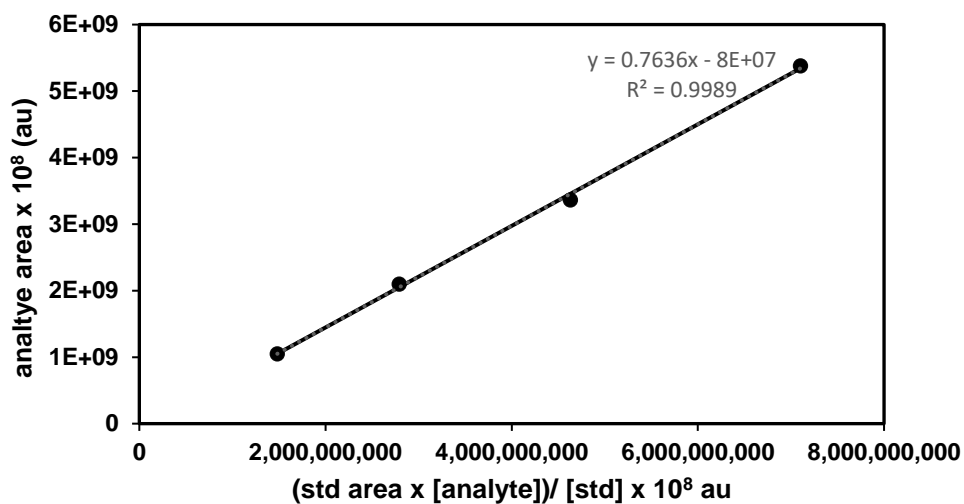
Plot of analyte area versus (std area x [**S7**]) / [std] fitted to $y = mx + b$ where $m = 0.7636$ and $b = -8$ x 10^7 with a R^2 of 0.9989.

Concentration of 1,2,3,4-tetrahydronaphthalene (**S7**)	area of **S7** (analyte)	area tridecane (std)	(std area x [**S7**]) / [std]
0.0431	10.52 x 10^8	56.40 x 10^8	14.82 x 10^8
0.0938	20.99 x 10^8	48.83 x 10^8	27.93 x 10^8
0.1354	33.67 x 10^8	56.08 x 10^8	46.29 x 10^8
0.2080	53.80 x 10^8	56.01 x 10^8	71.03 x 10^8

Calibration Curve for 4-phenylmorpholine.
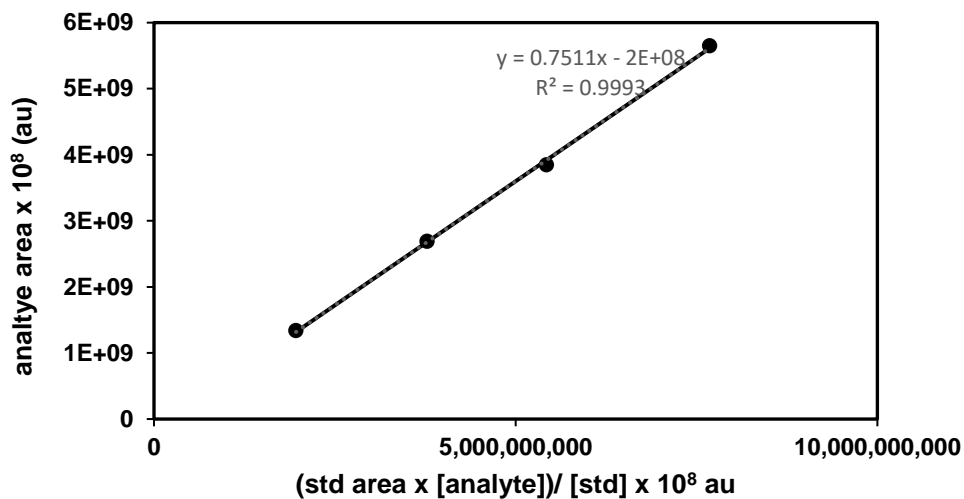
Plot of analyte area versus (std area x [**S5**]) / [std] fitted to y = mx + b where m = 0.7511 and b = -2 x 10^8 with a R^2 of 0.9993.

Concentration of 4-phenylmorpholine (**S5**)	area of **S5** (analyte)	area tridecane (std)	(std area x [**S5**]) / [std]
0.0545	13.38 x 10^8	59.08 x 10^8	19.63 x 10^9
0.1017	26.91 x 10^8	60.88 x 10^8	37.75 x 10^9
0.1482	38.17 x 10^8	60.03 x 10^8	54.24 x 10^9
0.2169	56.51 x 10^8	58.08 x 10^8	76.80 x 10^9

Calibration Curve for N-phenylacetamide.
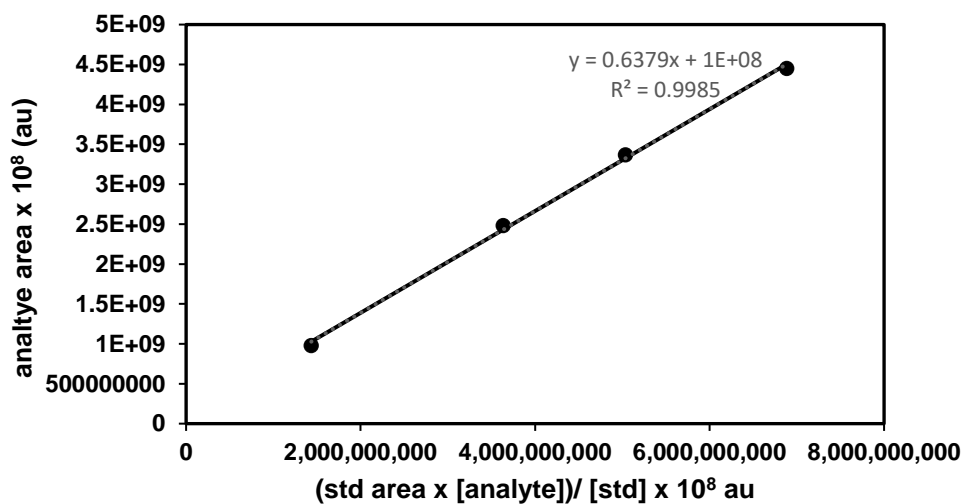
Plot of analyte area versus (std area x [**S5**]) / [std] fitted to y = *m*x + *b* where *m* = 0.6379 and *b* = 1 x 10^8 with a R^2 of 0.9985.

Concentration of trifluorotoluene (**S5**)	area of **S5** (analyte)	area tridecane (std)	(std area x [**S5**]) / [std]
0.0444	9.806 x 10^8	53.02 x 10^8	14.35 x 10^9
0.0888	24.84 x 10^8	67.18 x 10^8	36.36 x 10^9
0.1480	33.68 x 10^8	55.81 x 10^8	50.34 x 10^9
0.1850	44.52 x 10^8	61.05 x 10^8	68.83 x 10^9

Calibration Curve for 4-methoxy-1,1'-biphenyl.
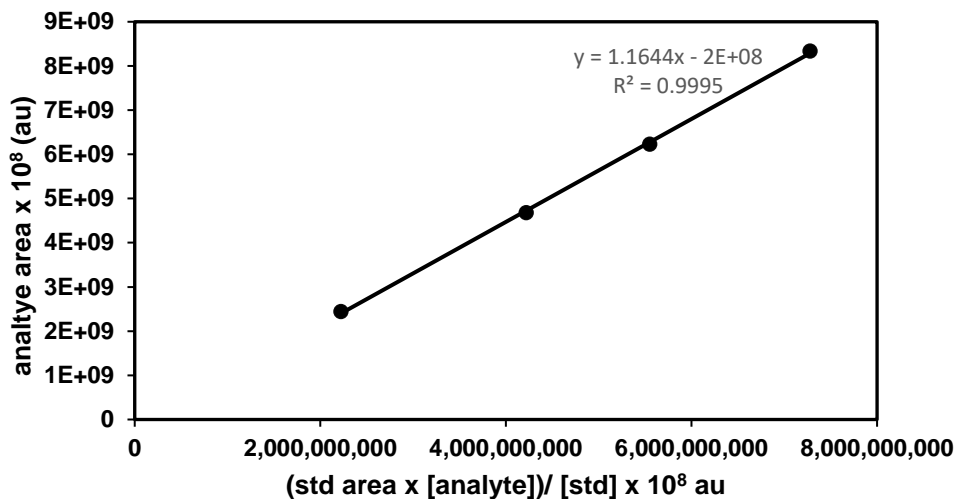
Plot of analyte area versus (std area x [**S5**]) / [std] fitted to y = mx + b where m = 1.1644 and b = -2 x 10^8 with a R^2 of 0.9995.

Concentration of trifluorotoluene (**S5**)	area of **S5** (analyte)	area tridecane (std)	(std area x [**S5**]) / [std]
0.0516	24.49 x 10^8	70.77 x 10^8	22.25 x 10^9
0.0934	46.81 x 10^8	74.70 x 10^8	42.22 x 10^9
0.1455	62.31 x 10^8	62.61 x 10^8	55.52 x 10^9
0.1922	83.41 x 10^8	62.15 x 10^8	72.81 x 10^9

5.3.2 Scheme 3.17 Substrate Scope for Reduction of Silyl Aryl Ethers

1,1'-biphenyl.
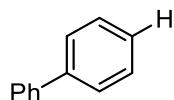
Scheme 3.17, Entry A: Following general procedure B, Ni(acac)$_2$ (1.9 mg, 0.0075 mmol), IPr^{Me}·HCl (6.8 mg, 0.015 mmol), NaO^{t}Bu (36.0 mg, 0.375 mmol), ([1,1'-biphenyl]-4-yloxy)(*tert*-butyl)dimethylsilane (42.0 mg, 0.148 mmol) and titanium(IV) isopropoxide (49 μL, 0.165 mmol) gave a crude residue. The yield was determined by GC-FID analysis using tridecane as an internal standard due to sublimability of the product (tridecane integration: 329116406, biphenyl integration: 265260257, 0.141 mmol, 93%). The spectral data matches that previously reported in the literature.[48] The reaction was performed in multiple iterations in concert with Eric Wiensch. The optimal yield from these reactions has been reported.

^{1}H-NMR (500 MHz, CDCl$_3$): δ 7.61 (d, *J* = 7.5 Hz, 4H), 7.45 (t, *J* = 7.5 Hz, 4H), 7.36 (t, *J* = 7.5 Hz, 2H).

Naphthalene.
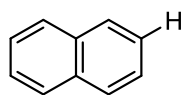
Scheme 3.17, Entry B: Following general procedure B, Ni(acac)$_2$ (1.9 mg, 0.0075 mmol), IPr^{Me}·HCl (6.8 mg, 0.015 mmol), NaO^{t}Bu (36.0 mg, 0.375 mmol), *tert*-butyldimethyl(naphthalen-2-yloxy)silane (39.0 mg, 0.151 mmol), and titanium(IV) isopropoxide (49 μL, 0.165 mmol) at 120 °C for 3 hours gave a crude residue. The yield was determined by GC-FID analysis using tridecane as an internal standard due to sublimability of the product (tridecane integration: 332901580, naphthalene integration: 191812112, 130 mmol, 86%). The spectral data matches that previously

reported in the literature.[48] The reaction was performed in multiple iterations in concert with Eric Wiensch. The optimal yield from these reactions has been reported.
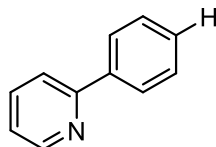
Naphthalene.
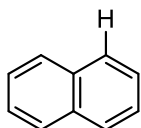
Scheme 3.17, Entry C: Following general procedure B, Ni(acac)$_2$ (1.9 mg, 0.0075 mmol), IPr^{Me}·HCl (6.8 mg, 0.015 mmol), NaO^{t}Bu (36.0 mg, 0.375 mmol), *tert*-butyldimethyl(naphthalen-1-yloxy)silane (39.4 mg, 0.152 mmol), and titanium(IV) isopropoxide (49 µL, 0.165 mmol) at 120 °C for 3 hours gave a crude residue. The yield was determined by GC-FID analysis using tridecane as an internal standard due to sublimability of the product (tridecane integration: 229475874, naphthalene integration: 127832132, 125 mmol, 82%). The spectral data matches that previously reported in the literature.[48] The reaction was performed in multiple iterations in concert with Eric Wiensch. The optimal yield from these reactions has been reported.

trimethyl(naphthalen-2-yl)silane.
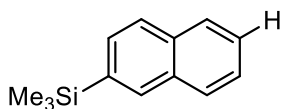
Scheme 3.17, Entry D: Following general procedure B, Ni(acac)$_2$ (1.9 mg, 0.0075 mmol), IPr^{Me}·HCl (6.8 mg, 0.015 mmol), NaO^{t}Bu (36.0 mg, 0.375 mmol), *tert*-butyldimethyl((6-(trimethylsilyl)naphthalen-2-yl)oxy)silane (50.0 mg, 0.151 mmol), and titanium(IV) isopropoxide (49 µL, 0.165 mmol) at 120 °C for 3 hours gave a crude residue which was purified by flash chromatography (100% hexanes) to afford the desired product (25.4 mg, 127 mmol, 84% yield). The spectral data matches that previously reported in the literature.[46] The reaction was performed

in multiple iterations in concert with Eric Wiensch. The optimal yield from these reactions has been reported.

¹H-NMR (500 MHz, CDCl₃): δ 8.01 (s, 1H), 7.84 (m, 3H), 7.61 (d, *J* = 8.0 Hz, 1H), 7.48 (m, 2H), 0.34 (s, 3H).

[1,1'-biphenyl]-4-ol.
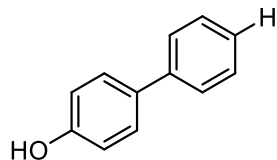
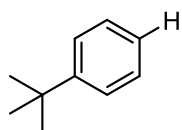**Scheme 3.17, Entry E:** Following general procedure B, Ni(acac)₂ (3.9 mg, 0.015 mmol), IPr^Me·HCl (13.6 mg, 0.030 mmol), NaO^tBu (57.7 mg, 0.6 mmol), 4'-((*tert*-butyldimethylsilyl)oxy)-[1,1'-biphenyl]-4-ol (45.1 mg, 0.15 mmol), and titanium(IV) isopropoxide (49 μL, 0.165 mmol) for 16 hours gave a crude residue which was purified by flash chromatography (hexanes: ethyl acetate 95:5) to afford the desired product (17.7 mg, 0.104 mmol, 69% yield). The spectral data matches that previously reported in the literature.[71] The reaction was performed in multiple iterations in concert with Eric Wiensch. The optimal yield from these reactions has been reported.

¹H-NMR (500 MHz, CDCl₃): δ 7.54 (m, 2H), 7.48 (m, 2H), 7.41 (t, *J* = 7.5 Hz, 2H), 7.32 (m, 1H), 6.91 (m, 2H), 4.70 (br, 1H).

([1,1'-biphenyl]-4-ylmethoxy)(*tert*-butyl)dimethylsilane.
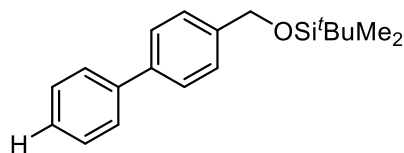
Scheme 3.17, Entry F: Following general procedure B, Ni(acac)₂ (1.9 mg, 0.0075 mmol), IPr^Me·HCl (6.8 mg, 0.015 mmol), NaO^tBu (36.0 mg, 0.375 mmol), *tert*-butyl((4'-((*tert*-

butyldimethylsilyl)oxy)-[1,1'-biphenyl]-4-yl)methoxy)dimethylsilane (68.5 mg, 0.15 mmol), and titanium(IV) isopropoxide (49 μL, 0.165 mmol) for 16 hours gave a crude residue which was purified by flash chromatography (100% hexanes) to afford the desired product (41.3 mg, 0.138 mmol, 91% yield). The spectral data matches that previously reported in the literature.[72] The reaction was performed in multiple iterations in concert with Eric Wiensch. The optimal yield from these reactions has been reported.

¹H-NMR (500 MHz, CDCl₃): δ 7.58 (m, 4H), 7.42 (m, 4H), 7.33 (t, J = 7.5 Hz, 1H), 4.79 (s, 2H), 0.96 (s, 9H), 0.13 (s, 6H).

4-methoxy-1,1'-biphenyl.
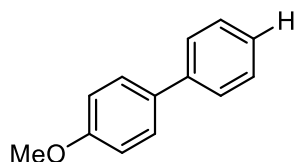
Scheme 3.17, Entry G: Following general procedure B, Ni(acac)₂ (1.9 mg, 0.0075 mmol), IPr^Me·HCl (6.8 mg, 0.015 mmol), NaOᵗBu (36.0 mg, 0.375 mmol), *tert*-butyl((4'-methoxy-[1,1'-biphenyl]-4-yl)oxy)dimethylsilane (48.1 mg, 0.153 mmol), and titanium(IV) isopropoxide (49 μL, 0.165 mmol) for 16 hours gave a crude residue which was purified by flash chromatography (hexanes: ethyl acetate 99:1) to afford the desired product (18.6 mg, 0.101 mmol, 66% yield). The spectral data matches that previously reported in the literature.[50] The reaction was performed in multiple iterations in concert with Eric Wiensch. The optimal yield from these reactions has been reported.

¹H-NMR (500 MHz, CDCl₃): δ 7.55 (m, 4H), 7.42 (t, J = 7.5 Hz, 2H), 7.31 (t, J = 7.5 Hz, 1H), 6.99 (m, 2H), 3.86 (s, 3H).

1,1'-biphenyl.
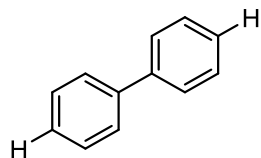
Scheme 3.17, Entry H: Following general procedure B, Ni(acac)$_2$ (3.9 mg, 0.015 mmol), IPr^{Me}·HCl (13.6 mg, 0.030 mmol), NaO^{t}Bu (57.7 mg, 0.6 mmol), 4,4'-bis((*tert*-butyldimethylsilyl)oxy)-1,1'-biphenyl (61.8 mg, 0.149 mmol) and titanium(IV) isopropoxide (49 µL, 0.165 mmol) at 130 °C for 16 hours gave a crude residue. The yield was determined by GC-FID analysis using tridecane as an internal standard due to sublimability of the product (tridecane integration: 254280859, biphenyl integration: 144283275, 0.099 mmol, 67%). The spectral data matches that previously reported in the literature.[48] The reaction was performed in multiple iterations in concert with Eric Wiensch. The optimal yield from these reactions has been reported.

2-methylquinoline.
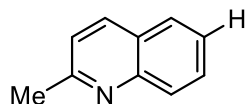
Scheme 3.17, Entry I: Following general procedure B, Ni(acac)$_2$ (1.9 mg, 0.0075 mmol), IPr^{Me}·HCl (6.8 mg, 0.015 mmol), NaO^{t}Bu (36.0 mg, 0.375 mmol), 6-((*tert*-butyldimethylsilyl)oxy)-2-methylquinoline (40.9 mg, 0.150 mmol), and titanium(IV) isopropoxide (49 µL, 0.165 mmol) at 120 °C for 3 hours gave a crude residue which was purified by flash chromatography (hexanes: ethyl acetate 90:10) to afford the desired product (15.8 mg, 110 mmol, 74% yield). The spectral data matches that previously reported in the literature.[46] The reaction was performed in multiple iterations in concert with Eric Wiensch. The optimal yield from these reactions has been reported.

^{1}H-NMR (500 MHz, CDCl$_3$): δ 8.04 (m, 2H), 7.77 (d, *J* = 7.0 Hz, 1H), 7.68 (t, *J* = 7.0 Hz, 1H), 7.48 (t, *J* = 7.5 Hz, 1H), 7.29 (d, *J* = 8.5 Hz, 1H), 2.75 (s, 3H).

4-phenylmorpholine.
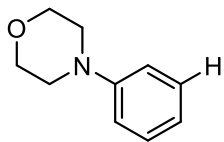
Scheme 3.17, Entry J: Following general procedure B, Ni(acac)$_2$ (3.9 mg, 0.015 mmol), IPr^{Me}·HCl (13.6 mg, 0.030 mmol), NaO^{t}Bu (57.7 mg, 0.60 mmol), 4-(3-((*tert*-butyldimethylsilyl)oxy)phenyl)morpholine (44.5 mg, 0.152 mmol), and titanium(IV) isopropoxide (49 μL, 0.165 mmol) gave a crude residue. The yield was determined by GC-FID analysis using tridecane as an internal standard due to sublimability of the product (tridecane integration: 289820445, 4-phenylmorpholine integration: 61169732, 0.048 mmol, 32%). The spectral data matches that previously reported in the literature.[73] The reaction was performed in multiple iterations in concert with Eric Wiensch. The optimal yield from these reactions has been reported.

9-methyl-9H-carbazole.
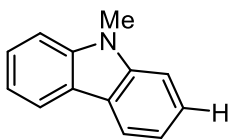
Scheme 3.17, Entry K: Following general procedure B, Ni(acac)$_2$ (1.9 mg, 0.0075 mmol), IPr^{Me}·HCl (6.8 mg, 0.015 mmol), NaO^{t}Bu (36.0 mg, 0.375 mmol), 2-((*tert*-butyldimethylsilyl)oxy)-9-methyl-9H-carbazole (47.2 mg, 0.152 mmol), and titanium(IV) isopropoxide (49 μL, 0.165 mmol) gave a crude residue which was purified by flash chromatography (hexanes: ethyl acetate 98:2) to afford the desired product (22.7 mg, 125 mmol, 83% yield). The spectral data matches that previously reported in the literature.[74] The reaction was

performed in multiple iterations in concert with Eric Wiensch. The optimal yield from these reactions has been reported.

^{1}H-NMR (500 MHz, CDCl$_3$): δ 8.11 (d, J = 7.5 Hz, 2H), 7.49 (t, J = 7.5 Hz, 2H), 7.41 (d, J = 8.0 Hz, 2H), 7.24 (t, J = 7.0 Hz, 2H), 3.87 (s, 3H).

2-phenylpyridine.

Scheme 3.17, Entry L: Following general procedure B, Ni(acac)$_2$ (1.9 mg, 0.0075 mmol), IPr^{Me}·HCl (6.8 mg, 0.015 mmol), NaO^{t}Bu (36.0 mg, 0.375 mmol), 2-(4-((*tert*-butyldimethylsilyl)oxy)phenyl)pyridine (42.9 mg, 0.150 mmol), and titanium(IV) isopropoxide (49 μL, 0.165 mmol) gave a crude residue which was purified by flash chromatography (hexanes: ethyl acetate 95:5) to afford the desired product (19.8 mg, 128 mmol, 85% yield). The spectral data matches that previously reported in the literature.[46] The reaction was performed in multiple iterations in concert with Eric Wiensch. The optimal yield from these reactions has been reported.

^{1}H-NMR (500 MHz, CDCl$_3$): δ 8.73 (d, J = 5.0 Hz, 1H), 8.02 (d, J = 8.0 Hz, 2H), 7.79 (m, 2H), 7.51 (t, J = 7.5 Hz, 2H), 7.44 (t, J = 7.5 Hz, 1H), 7.27 (m, 1H).

N-phenylacetamide.
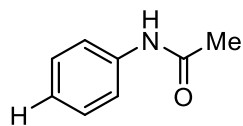
Scheme 3.17, Entry M: Following general procedure B, Ni(acac)$_2$ (3.9 mg, 0.015 mmol), IPr^{Me}·HCl (13.6 mg, 0.030 mmol), NaO^{t}Bu (57.7 mg, 0.60 mmol), N-(4-((*tert*-butyldimethylsilyl)oxy)phenyl)acetamide (39.0 mg, 0.147 mmol), and titanium(IV) isopropoxide (49 μL, 0.165 mmol) gave a crude residue. The yield was determined by GC-FID analysis using

tridecane as an internal standard due to sublimability of the product (tridecane integration: 258912979, N-phenylacetamide integration: 22126637, 0.022 mmol, 15%). The spectral data matches that previously reported in the literature.[75] The reaction was performed in multiple iterations in concert with Eric Wiensch. The optimal yield from these reactions has been reported.

tert-butylbenzene.

Scheme 3.17, Entry N: Following general procedure B, Ni(COD)$_2$ (4.1 mg, 0.015 mmol), IPr^{Me}·HCl (13.6 mg, 0.030 mmol), NaO^{t}Bu (57.7 mg, 0.60 mmol), *tert*-butyl(4-(*tert*-butyl)phenoxy)dimethylsilane (39.8 mg, 0.150 mmol), and titanium(IV) isopropoxide (89 μL, 0.3 mmol) at 130 °C for 16 hours gave a crude residue. The yield was determined by GC-FID analysis using tridecane as an internal standard due to volatility of the product (tridecane integration: 581498251, *tert*-butylbenzene integration: 170920319, 0.070 mmol, 46%). The spectral data matches that previously reported in the literature.[50] The reaction was performed in multiple iterations in concert with Eric Wiensch. The optimal yield from these reactions has been reported.

2,3-dihydro-1H-indene.
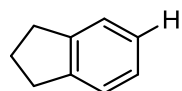
Scheme 3.17, Entry O: Following a modified general procedure B, Ni(acac)$_2$ (3.9 mg, 0.015 mmol), IPr^{Me}·HCl (13.6 mg, 0.030 mmol), NaO^{t}Bu (57.7 mg, 0.60 mmol), *tert*-butyl((2,3-dihydro-1H-inden-5-yl)oxy)dimethylsilane (37.0 mg, 0.149 mmol), and titanium(IV) isopropoxide (49 μL, 0.165 mmol) at 130 °C for 16 hours gave a crude residue. The yield was determined by GC-FID

analysis using tridecane as an internal standard due to volatility of the product (tridecane integration: 355781667, 2,3-dihydro-1H-indene integration: 153470439, 0.117 mmol, 79%). The spectral data matches that previously reported in the literature.[76] The reaction was performed in multiple iterations in concert with Eric Wiensch. The optimal yield from these reactions has been reported.

1,2,3,4-tetrahydronaphthalene.
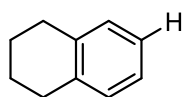
Scheme 3.17, Entry P: Following a modified general procedure B, Ni(acac)$_2$ (3.9 mg, 0.015 mmol), IPr^{Me}·HCl (13.6 mg, 0.030 mmol), NaO^{t}Bu (57.7 mg, 0.60 mmol), *tert*-butyldimethyl((5,6,7,8-tetrahydronaphthalen-2-yl)oxy)silane (39.5 mg, 0.150 mmol), triisopropylsilane (184 μL, 0.9 mmol), and titanium(IV) isopropoxide (89 μL, 0.3 mmol) at 130 °C for 16 hours gave a crude residue. The yield was determined by GC-FID analysis using tridecane as an internal standard due to volatility of the product (tridecane integration: 377773699, 1,2,3,4-tetrahydronaphthalene integration: 153470439, 0.109 mmol, 73%). The spectral data matches that previously reported in the literature.[77] The reaction was performed in multiple iterations in concert with Eric Wiensch. The optimal yield from these reactions has been reported.

***tert*-butyldimethyl(((8R,9S,13S,14S,17S)-13-methyl-7,8,9,11,12,13,14,15,16,17-decahydro-6H-cyclopenta[a]phenanthren-17-yl)oxy)silane.**
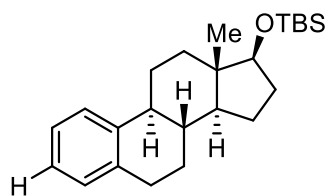
Scheme 3.17, Entry Q: Following general procedure B, Ni(acac)$_2$ (3.9 mg, 0.015 mmol), IPr^{Me}·HCl (13.6 mg, 0.030 mmol), NaO^{t}Bu (57.7 mg, 0.60 mmol), (((8R,9S,13S,14S,17S)-13-methyl-7,8,9,11,12,13,14,15,16,17-decahydro-6H-cyclopenta[a]phenanthrene-3,17-diyl)bis(oxy))bis(*tert*-butyldimethylsilane) (75.0 mg, 0.15 mmol), and titanium(IV) isopropoxide (49 μL, 0.165 mmol) at 130 °C for 16 hours gave a crude residue which was purified by flash chromatography (100% hexanes) to afford the desired product as a white solid (42.5 mg, 0.115 mmol, 76% yield). The reaction was performed in multiple iterations in concert with Eric Wiensch. The optimal yield from these reactions has been reported.

^{1}H-NMR (700 MHz, CDCl$_3$): δ 7.30 (d, J = 7.0 Hz, 1H), 7.14 (t, J = 7.0 Hz, 1H), 7.11 (t, J = 7.0 Hz, 1H), 7.08 (d, J = 7.0 Hz, 1H), 3.65 (t, J = 8.4 Hz, 1H), 2.86 (m, 2H), 2.32 (m, 1H), 2.23 (m, 1H), 1.89 (m, 3H), 1.66 (m, 1H), 1.50 (m, 4H), 1.33 (m, 2H), 1.18 (m, 3H), 0.90 (s, 9H), 0.75 (s, 3H), 0.03 (d, J = 9.1 Hz, 6H).

^{13}C-NMR (175 MHz, CDCl$_3$): δ 140.53, 136.79, 128.99, 125.54, 125.49, 125.34, 81.77, 49.84, 44.62, 43.58, 38.64, 37.20, 30.98, 29.58, 27.25, 26.28, 25.87, 23.29, 18.12, 11.35, 4.46, 4.78.

IR (film, cm^{-1}): 2923, 2852, 1469, 1247, 1097.

HRMS (EI) *m/z*: [M]$^+$ predicted for C$_{24}$H$_{38}$OSi, 370.2692; found, 370.2689.

5.3.3 Scheme 3.29 Silylation Substrate Scope

[1,1'-biphenyl]-4-yltriethylsilane.
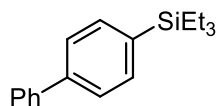
Scheme 3.29, Entry A: Following general procedure C, Ni(cod)$_2$ (4.1 mg, 0.015 mmol), IPr*OMe (14.2 mg, 0.015 mmol), NaO^{t}Bu (36.0 mg, 0.375 mmol), ([1,1'-biphenyl]-4-yloxy)(*tert*-butyl)dimethylsilane (42.6 mg, 0.15 mmol), and triethylsilane (144 μL, 0.9 mmol) gave a crude residue which was purified by flash chromatography (100% hexanes) to afford the desired product (36.6 mg, 0.137 mmol, 91% yield). The yield for biphenyl was determined by GC-FID analysis

using tridecane as an internal standard due to sublimability of the product (tridecane integration: 163648334, biphenyl integration: 776212, 0.0008 mmol, 1%). The reaction was performed in multiple iterations in concert with Eric Wiensch. The optimal yield from these reactions has been reported.

¹H-NMR (500 MHz, CDCl₃): δ 7.64 - 7.58 (m, 6H), 7.46 (dt, J = 7.3, 0.7 Hz, 2H), 7.36 (m, 1H), 1.02 (t, J = 8.0 Hz, 9H), 0.85 (q, J = 8.0, 6H).

¹³C-NMR (125 MHz, CDCl₃): δ 141.4, 141.2, 136.2, 134.7, 128.7, 127.3, 127.1, 126.4, 7.4, 3.4.

IR (film, cm⁻¹): 3026, 2951, 2873, 1597, 1484, 1236.

HRMS (EI) _m/z_: [M]⁺ predicted for $C_{18}H_{24}Si$, 268.1647; found, 268.1652.

triethyl(naphthalen-2-yl)silane.
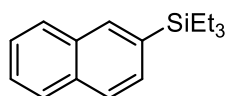
Scheme 3.29, Entry B: Following general procedure C, Ni(cod)₂ (4.1 mg, 0.015 mmol), IPr*OMe (14.2 mg, 0.015 mmol), NaO^{t}Bu (36.0 mg, 0.375 mmol), _tert_-butyldimethyl(naphthalen-2-yloxy)silane (39.1 mg, 0.151 mmol), and triethylsilane (144 μL, 0.9 mmol) gave a crude residue which was purified by flash chromatography (100% hexanes) to afford the desired product (27.2 mg, 0.112 mmol, 74% yield). The spectral data matches that previously reported in the literature.[61] The reaction was performed in multiple iterations in concert with Eric Wiensch. The optimal yield from these reactions has been reported.

¹H-NMR (500 MHz, CDCl₃): δ 8.0 (s, 1H), 7.83 (m, 3H), 7.58 (d, J = 8.0, 1H), 7.49 (dd, J = 6.3, 3.2 Hz, 2H), 1.02 (t, J = 7.5 Hz, 9H), 0.89 (q, J = 7.6 Hz, 6H).

triethyl(naphthalen-1-yl)silane.
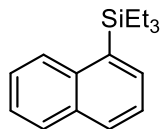
Scheme 3.29, Entry C: Following a modified general procedure C, Ni(cod)₂ (10.3 mg, 0.038 mmol), IPr*OMe (35.5 mg, 0.038 mmol), NaOᵗBu (36.0 mg, 0.375 mmol), *tert*-butyldimethyl(naphthalen-1-yloxy)silane (39.3 mg, 0.152 mmol), and triethylsilane (144 μL, 0.9 mmol) at 130 °C for 24 hours gave a crude residue which was purified by flash chromatography (100% hexanes) to afford the desired product (22.9 mg, 0.094 mmol, 62% yield). The spectral data matches that previously reported in the literature.[61] The reaction was performed in multiple iterations in concert with Eric Wiensch. The optimal yield from these reactions has been reported.

¹H-NMR (500 MHz, CDCl₃): δ 8.10 (d, J = 7.5 Hz, 1H), 7.86 (m, 2H), 7.8 (m, 1H), 7.47 (m, 3H), 0.99 (m, 15H).

triethyl(6-(trimethylsilyl)naphthalen-2-yl)silane.
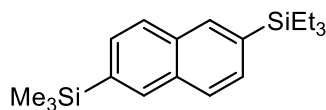
Scheme 3.29, Entry D: Following general procedure C, Ni(cod)₂ (4.1 mg, 0.015 mmol), IPr*OMe (14.2 mg, 0.015 mmol), NaOᵗBu (36.0 mg, 0.375 mmol), *tert*-butyldimethyl((6-(trimethylsilyl)naphthalen-2-yl)oxy)silane (49.3 mg, 0.149 mmol), and triethylsilane (144 μL, 0.9 mmol) gave a crude residue which was purified by flash chromatography (100% hexanes) to afford the desired product (37.1 mg, 0.118 mmol, 79% yield). The reaction was performed in multiple iterations in concert with Eric Wiensch. The optimal yield from these reactions has been reported.

¹H-NMR (500 MHz, CDCl₃): δ 7.99 (s, 1H), 7.97 (s, 1H), 7.82 (dd, J = 8.0, 4.5 Hz, 2H), 7.61 (d, J = 8.0 Hz, 1H), 7.58 (d, J = 8.5 Hz, 1H), 1.00 (t, J = 8.5 Hz, 9H), 0.88 (q, J = 8.0 Hz, 6H), 0.35 (s, 9H).

¹³C-NMR (125 MHz, CDCl₃): δ 138.3, 135.4, 134.6, 133.5, 133.1, 133.0, 130.7, 129.7, 127.0, 136.8, 7.4, 3.4, 1.1.

IR (film, cm⁻¹): 3039, 2952, 2874, 1577, 1456, 1312, 1246.

HRMS (EI) *m/z*: [M]⁺ predicted for $C_{19}H_{30}Si_2$, 314.1886; found, 314.1889.

4'-(triethylsilyl)-[1,1'-biphenyl]-4-ol.
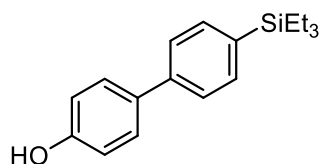
Scheme 3.29, Entry E: Following a modified general procedure C, Ni(cod)₂ (10.3 mg, 0.038 mmol), IPr*OMe (35.5 mg, 0.038 mmol), NaOᵗBu (36.0 mg, 0.375 mmol), 4'-((*tert*-butyldimethylsilyl)oxy)-[1,1'-biphenyl]-4-ol (44.3 mg, 0.147 mmol), and triethylsilane (144 μL, 0.9 mmol) gave a crude residue which was purified by flash chromatography (hexanes: ethyl acetate 95:5) to afford the desired product (30.4 mg, 0.107 mmol, 72% yield). The reaction was performed in multiple iterations in concert with Eric Wiensch. The optimal yield from these reactions has been reported.

¹H-NMR (500 MHz, CDCl₃): δ 7.55 - 7.49 (m, 6H), 6.90 (dt, *J* = 8.8, 2.2 Hz, 2H), 4.78 (s, 1H), 1.00 (t, *J* = 8.3 Hz, 9H), 0.83 (q, *J* = 7.8 Hz, 6H).

¹³C-NMR (125 MHz, CDCl₃): δ 155.1, 140.9, 135.5, 134.7, 134.0, 128.4, 125.9, 115.6, 7.4, 3.4.

IR (film, cm⁻¹): 3290, 2951, 2873, 1596, 1521, 1458, 1244.

HRMS (EI) *m/z*: [M]⁺ predicted for $C_{18}H_{24}OSi$, 284.1596; found, 284.1606.

***tert*-butyldimethyl((4'-(triethylsilyl)-[1,1'-biphenyl]-4-yl)methoxy)silane.**
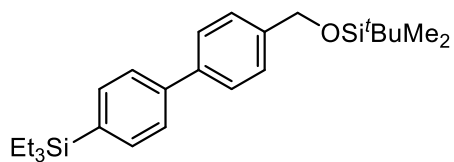
Scheme 3.29, Entry F: Following a modified general procedure C, Ni(cod)$_2$ (10.3 mg, 0.038 mmol), IPr*OMe (35.5 mg, 0.038 mmol), NaO^{t}Bu (36.0 mg, 0.375 mmol), *tert*-butyl((4'-((*tert*-butyldimethylsilyl)oxy)-[1,1'-biphenyl]-4-yl)methoxy)dimethylsilane (67.3 mg, 0.157 mmol), and triethylsilane (144 µL, 0.9 mmol) at 130 °C for 24 hours gave a crude residue which was purified by flash chromatography (100% hexanes) to afford the desired product (50.2 mg, 0.122 mmol, 78% yield). The reaction was performed in multiple iterations in concert with Eric Wiensch. The optimal yield from these reactions has been reported.

^{1}H-NMR (500 MHz, CDCl$_3$): δ 7.58 (m, 6H), 7.40 (d, *J* = 8.0 Hz, 2H), 1.00 (t, *J* = 8.0 Hz, 9H), 0.97 (s, 9H), 0.83 (q, *J* = 8.0 Hz, 6H), 0.13 (s, 6H).

^{13}C-NMR (125 MHz, CDCl$_3$): δ 141.3, 140.5, 139.8, 136.0, 134.7, 126.9, 126.5, 126.3, 64.8, 26.0, 18.5, 7.4, 3.4, -5.2.

IR (film, cm^{-1}): 2951, 2874, 1599, 1462, 1375, 1252.

HRMS (EI) *m/z*: [M]$^+$ predicted for C$_{25}$H$_{40}$OSi$_2$, 412.2618; found, 412.2628.
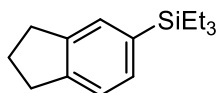
triethyl(4'-methoxy-[1,1'-biphenyl]-4-yl)silane.
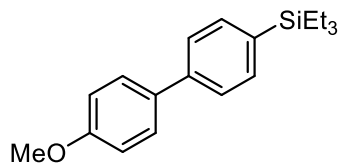
Scheme 3.29, Entry G: Following a modified general procedure C, Ni(cod)$_2$ (10.3 mg, 0.038 mmol), IPr*OMe (35.5 mg, 0.038 mmol), NaO^{t}Bu (36.0 mg, 0.375 mmol), *tert*-butyl((4'-methoxy-[1,1'-biphenyl]-4-yl)oxy)dimethylsilane (45.9 mg, 0.146 mmol), and triethylsilane (144 µL, 0.9 mmol) at 100 °C for 8 hours gave a crude residue which was purified by flash chromatography (hexanes: ethyl acetate 99:1) to afford the desired product (31.1 mg, 0.104 mmol, 71% yield). The reaction was performed in multiple iterations in concert with Eric Wiensch. The optimal yield from these reactions has been reported.

¹H-NMR (500 MHz, CDCl₃): δ 7.55 (m, 6H), 6.98 (dt, *J* = 8.8 Hz, 2H), 3.86 (s, 3H), 1.00 (t, *J* = 8.1 Hz, 9H), 0.81 (q, *J* = 7.8 Hz, 6H).

¹³C-NMR (125 MHz, CDCl₃): δ 159.2, 141.0, 135.4, 134.7, 133.7, 128.1, 125.9, 114.2, 55.3, 7.4, 3.4.

IR (film, cm⁻¹): 2952, 1602, 1492, 1462, 1248.

HRMS (EI) *m/z*: [M]⁺ predicted for $C_{19}H_{26}OSi$, 298.1753; found, 298.1763.

4,4'-bis(triethylsilyl)-1,1'-biphenyl.
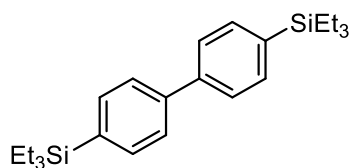
Scheme 3.29, Entry H: Following a modified general procedure C, Ni(cod)₂ (10.3 mg, 0.038 mmol), IPr*OMe (35.5 mg, 0.038 mmol), NaOʰBu (36.0 mg, 0.375 mmol), 4,4'-bis((*tert*-butyldimethylsilyl)oxy)-1,1'-biphenyl (63.9 mg, 0.154 mmol), and triethylsilane (144 μL, 0.9 mmol) gave a crude residue which was purified by flash chromatography (100% hexanes) to afford the desired product (43.1 mg, 0.113 mmol, 73% yield). The reaction was performed in multiple iterations in concert with Eric Wiensch. The optimal yield from these reactions has been reported.

¹H-NMR (500 MHz, CDCl₃): δ 7.58 (q, *J* = 7.5 Hz, 8 H, 1.0 (t, *J* = 8.0 Hz, 18H), 0.83 (q, *J* = 8.0 Hz, 12H).

¹³C-NMR (125 MHz, CDCl₃): δ 141.4, 136.2, 134.7, 126.3, 7.4, 3.4.

IR (film, cm⁻¹): 3068, 2950, 2872, 1594, 1455, 1380, 1236.

HRMS (EI) *m/z*: [M]⁺ predicted for $C_{19}H_{26}OSi$, 382.2512; found, 382.2510.

2-methyl-6-(triethylsilyl)quinolone.
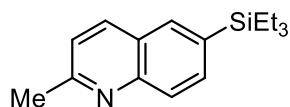
Scheme 3.29, Entry I: Following general procedure C, Ni(cod)$_2$ (3.9 mg, 0.015 mmol), IPr*OMe (14.2 mg, 0.015 mmol), NaO^{t}Bu (36.0 mg, 0.375 mmol), 6-((*tert*-butyldimethylsilyl)oxy)-2-methylquinoline (44.7 mg, 0.163 mmol), and triethylsilane (144 μL, 0.9 mmol) gave a crude residue which was purified by flash chromatography (hexanes: ethyl acetate 95:5) to afford the desired product (22.5 mg, 0.087 mmol, 53% yield). The reaction was performed in multiple iterations in concert with Eric Wiensch. The optimal yield from these reactions has been reported.

^{1}H-NMR (500 MHz, CDCl$_3$): δ 8.04 (d, J = 8.5Hz, 1H), 7.98 (d, J = 8.5 Hz, 1H), 7.89 (s, 1H), 7.77 (d, J = 8.0 Hz, 1H), 7.28 (d, J = 8.0 Hz, 1H), 2.75 (s, 3H), 0.94 (t, J = 8.0 Hz, 9H), 0.88 (q, J = 8.0 Hz, 6H).

^{13}C-NMR (125 MHz, CDCl$_3$): δ 159.2, 136.2, 135.1, 134.3, 134.3, 129.6, 127.5, 126.0, 121.9, 25.4, 7.4, 3.4.

IR (film, cm^{-1}): 2950, 2873, 1612, 1560, 1465, 1223.

HRMS (ESI+) *m/z*: [M+H]$^+$ predicted for C$_{16}$H$_{23}$NSi, 258.1673; found, 258.1671.

4-(3-(triethylsilyl)phenyl)morpholine.
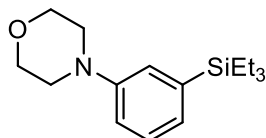
Scheme 3.29, Entry J: Following a modified general procedure C, Ni(cod)$_2$ (10.3 mg, 0.038 mmol), IPr*OMe (35.5 mg, 0.038 mmol), NaO^{t}Bu (36.0 mg, 0.375 mmol), 4-(3-((*tert*-butyldimethylsilyl)oxy)phenyl)morpholine (44.0 mg, 0.15 mmol), and triethylsilane (144 μL, 0.9 mmol) at 130 °C for 24 hours gave a crude residue which was purified by flash chromatography (100% hexanes) to afford the desired product (32.0 mg, 0.116 mmol, 77% yield). The reaction was performed in multiple iterations in concert with Eric Wiensch. The optimal yield from these reactions has been reported.

1H-NMR (500 MHz, CDCl₃): δ 7.28 (d, *J* = 7.6 Hz, 1H), 7.05 (d, *J* = 2.5 Hz, 1H), 7.02 (d, *J* = 7.1 Hz, 1H), 6.91 (dd, *J* = 8.1, 2.5 Hz, 1H), 3.88 (t, *J* = 4.9 Hz, 4H), 3.16 (t, *J* = 4.9 Hz, 4H), 0.96 (t, *J* = 7.8 Hz, 9H), 0.78 (q, *J* = 7.8 Hz, 6H).

13C-NMR (125 MHz, CDCl₃): δ 150.6, 138.4, 128.5, 126.1, 121.6, 116.2, 67.0, 49.6, 7.4, 3.4.

IR (film, cm⁻¹): 2953, 2873, 1586, 1449, 1229.

HRMS (EI) *m/z*: [M]⁺ predicted for C₁₆H₂₇NOSi, 277.1862; found, 277.1863.

9-methyl-2-(triethylsilyl)-9H-carbazole.
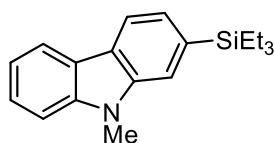
Scheme 3.29, Entry K: Following general procedure C, Ni(cod)₂ (4.1 mg, 0.015 mmol), IPr*OMe (14.2 mg, 0.015 mmol), NaO*t*Bu (36.0 mg, 0.375 mmol), 2-((*tert*-butyldimethylsilyl)oxy)-9-methyl-9H-carbazole (46.1 mg, 0.148 mmol), and triethylsilane (144 μL, 0.9 mmol)gave a crude residue which was purified by flash chromatography (hexanes: ethyl acetate 99:1) to afford the desired product (38.1 mg, 0.130 mmol, 87% yield). The reaction was performed in multiple iterations in concert with Eric Wiensch. The optimal yield from these reactions has been reported.

1H-NMR (500 MHz, CDCl₃): δ 8.10 (m, 2H), 7.53 (d, *J* = 2.5 Hz, 1H), 7.47 (t, *J* = 7.0 Hz, 1H), 7.41 (d, *J* = 8.0 Hz, 1H), 7.37 (dd, *J* = 7.5, 3.0 Hz, 1H), (7.23, dt, *J* = 8.0, 2.5 Hz, 1H), 3.89 (s, 3H), 1.03 (dt, *J* = 8.0, 3.5 Hz, 9H), 0.91 (dq, *J* = 8.0, 3.5 Hz, 6H).

13C-NMR (125 MHz, CDCl₃): δ 141.0, 140.6, 134.5, 125.8, 124.4, 123.3, 122.7, 120.4, 119.5, 118.7, 113.9, 108.4, 29.0, 7.54, 3.68.

IR (film, cm⁻¹): 2950, 2872, 1594, 1441, 1414, 1320, 1247.

HRMS (EI) *m/z*: [M]⁺ predicted for C₁₉H₂₅NSi, 295.1756; found, 295.1765.

2-(4-(triethylsilyl)phenyl)pyridine.
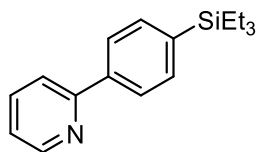
Scheme 3.29, Entry L: Following general procedure C, Ni(cod)$_2$ (4.1 mg, 0.015 mmol), IPr*OMe (14.2 mg, 0.015 mmol), NaO^{t}Bu (36.0 mg, 0.375 mmol), 2-(4-((*tert*-butyldimethylsilyl)oxy)phenyl)pyridine (40.0 mg, 0.139 mmol), and triethylsilane (144 µL, 0.9 mmol) gave a crude residue which was purified by flash chromatography (hexanes: ethyl acetate 90:10) to afford the desired product (26.4 mg, 0.098 mmol, 70% yield). The reaction was performed in multiple iterations in concert with Eric Wiensch. The optimal yield from these reactions has been reported.

^{1}H-NMR (500 MHz, CDCl$_3$): δ 8.70 (d, *J* = 5.0 Hz, 1H), 7.97 (d, *J* = 8.0 Hz, 2H), 7.76 (m, 2H), 7.61 (d, *J* = 8.0 Hz, 2H), 7.24 (m, 1H), 0.98 (t, *J* = 8.0 Hz, 9H), 0.83 (q, *J* = 8.0 Hz, 6H).

^{13}C-NMR (125 MHz, CDCl$_3$): δ 157.6, 149.7, 139.6, 138.4, 136.7, 134.7, 126.0, 122.1, 120.6, 7.4, 3.3.

IR (film, cm^{-1}): 2951, 2873, 1586, 1464, 1430, 1382, 1236.

HRMS (ESI+) *m/z*: [M+H]$^+$ predicted for C$_{17}$H$_{23}$NSi, 286.1622; found, 286.1623.

N-(4-(triethylsilyl)phenyl)acetamide.
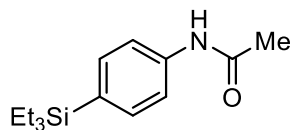
Scheme 3.29, Entry M: Following a modified general procedure C, Ni(cod)$_2$ (10.3 mg, 0.038 mmol), IPr*OMe (35.5 mg, 0.038 mmol), NaO^{t}Bu (36.0 mg, 0.375 mmol), N-(4-((*tert*-butyldimethylsilyl)oxy)phenyl)acetamide (39.8 mg, 0.15 mmol), and triethylsilane (144 µL, 0.9 mmol) at 130 °C for 24 hours gave a crude residue which was purified by flash chromatography (100% hexanes) to afford the desired product (27.7 mg, 0.111 mmol, 74% yield). The reaction was

performed in multiple iterations in concert with Eric Wiensch. The optimal yield from these reactions has been reported.

¹H-NMR (500 MHz, CDCl₃): δ 7.48 (d, *J* = 8.5 Hz, 2H), 7.3 (d, *J* = 8.0 Hz, 2H), 7.30 (b, 1H), 0.95 (t, *J* = 8.0 Hz, 9H), 0.77 (q, *J* = 8.0 Hz, 6H).

¹³C-NMR (125 MHz, CDCl₃): δ 168.3, 138.3, 135.0, 133.0, 128.4, 119.0, 24.6, 7.3, 3.6.

IR (film, cm⁻¹): 3307, 2952, 2874, 1669, 1590, 1526, 1388.

HRMS (EI) *m/z*: [M]⁺ predicted for $C_{14}H_{23}NOSi$, 249.1549; found, 249.1548.

(4-(*tert*-butyl)phenyl)triethylsilane.
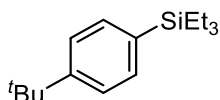
Scheme 3.29, Entry N: Following a modified general procedure C, Ni(cod)₂ (10.3 mg, 0.038 mmol), IPr*OMe (35.5 mg, 0.038 mmol), NaO*t*Bu (36.0 mg, 0.375 mmol), *tert*-butyl(4-(*tert*-butyl)phenoxy)dimethylsilane (39.6 mg, 0.15 mmol), and triethylsilane at 130 °C for 24 hours gave a crude residue which was purified by flash chromatography (100% hexanes) to afford the desired product (34.0 mg, 0.137 mmol, 91% yield). The spectral data matches that previously reported in the literature.[61] The reaction was performed in multiple iterations in concert with Eric Wiensch. The optimal yield from these reactions has been reported.

¹H-NMR (500 MHz, CDCl₃): δ 7.43 (m, 2H), 7.37 (m, 2H), 1.32 (s, 9H), 0.97 (t, *J* = 7.5 Hz, 9H), 0.78 (q, *J* = 7.5 Hz, 6H).

(2,3-dihydro-1H-inden-5-yl)triethylsilane.

Scheme 3.29, Entry O: Following a modified general procedure C, Ni(cod)₂ (10.3 mg, 0.038 mmol), IPr*OMe (35.5 mg, 0.038 mmol), NaO*t*Bu (36.0 mg, 0.375 mmol), *tert*-butyl((2,3-dihydro-

1H-inden-5-yl)oxy)dimethylsilane (37.2 mg, 0.15 mmol) and triethylsilane (144 μL, 0.9 mmol) at 130 °C for 24 hours gave a crude residue which was purified by flash chromatography (100% hexanes) to afford the desired product (29.7 mg, 0.128 mmol, 85% yield). The reaction was performed in multiple iterations in concert with Eric Wiensch. The optimal yield from these reactions has been reported.

¹H-NMR (500 MHz, CDCl₃): δ 7.37 (s, 1H), 7.25 (q, *J* = 7.5 Hz, 2H), 2.92 (dt, *J* = 7.5, 3.0 Hz, 4H), 2.06 (pentet, *J* = 7.5 Hz, 2H), 0.97 (t, *J* = 7.5 Hz, 9H), 0.78 (q, *J* = 7.5 Hz, 6H).

¹³C-NMR (125 MHz, CDCl₃): δ 145.0, 143.5, 134.5, 132.0, 130.1, 123.9, 32.9, 32.8, 25.1, 7.5, 3.5.

IR (film, cm⁻¹): 2950, 2873, 1458, 1415, 1236.

HRMS (EI) *m/z*: [M]⁺ predicted for C₁₅H₂₄Si, 232.1647; found, 232.1646.

triethyl(5,6,7,8-tetrahydronaphthalen-2-yl)silane.
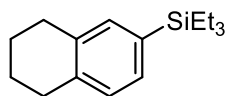
Scheme 3.29, Entry P: Following a modified general procedure C, Ni(cod)₂ (10.3 mg, 0.038 mmol), IPr*OMe (35.5 mg, 0.038 mmol), NaOᵗBu (36.0 mg, 0.375 mmol), *tert*-butyldimethyl((5,6,7,8-tetrahydronaphthalen-2-yl)oxy)silane (39.1 mg, 0.149 mmol), and triethylsilane (144 μL, 0.9 mmol) at 130 °C for 24 hours gave a crude residue which was purified by flash chromatography (100% hexanes) to afford the desired product (29.3 mg, 0.119 mmol, 82% yield). The reaction was performed in multiple iterations in concert with Eric Wiensch. The optimal yield from these reactions has been reported.

¹H-NMR (500 MHz, CDCl₃): δ 7.21 (d, *J* = 7.5 Hz, 1H), 7.18 (s, 1H), 7.05 (d, *J* = 7.5 Hz, 1H), 2.78 (m, 4H), 1.81 (m, 4H), 0.98 (t, *J* = 8.0 Hz, 9H), 0.78 (q, *J* = 8.0 Hz, 6H).

¹³C-NMR (125 MHz, CDCl₃): δ 137.8, 136.3, 135.2, 133.9, 131.2, 128.5, 29.42, 29.39, 23.3, 23.2, 7.5, 3.4.

IR (film, cm^{-1}): 2929, 2873, 1458, 1415, 1236.

HRMS (EI) *m/z*: [M]$^+$ predicted for C$_{16}$H$_{26}$Si, 246.1804; found, 246.1807.

***tert*-butyldimethyl(((8R,9S,13S,14S,17S)-13-methyl-3-(triethylsilyl)-7,8,9,11,12,13,14,15,16,17-decahydro-6H-cyclopenta[a]phenanthren-17-yl)oxy)silane.**
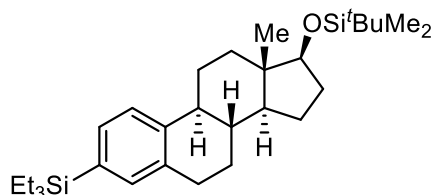
Scheme 3.29, Entry Q: Following a modified general procedure C, Ni(cod)$_2$ (10.3 mg, 0.038 mmol), IPr*OMe (35.5 mg, 0.038 mmol), NaO^{t}Bu (36.0 mg, 0.375 mmol), (((8R,9S,13S,14S,17S)-13-methyl-7,8,9,11,12,13,14,15,16,17-decahydro-6H-cyclopenta[a]phenanthrene-3,17-diyl)bis(oxy))bis(*tert*-butyldimethylsilane) (77.4 mg, 0.155 mmol), and triethylsilane (144 μL, 0.9 mmol) at 130 °C for 24 hours gave a crude residue which was purified by flash chromatography (100% hexanes) to afford the desired product (70.2 mg, 0.148 mmol, 94% yield). The reaction was performed in multiple iterations in concert with Eric Wiensch. The optimal yield from these reactions has been reported.

^{1}H-NMR (500 MHz, CDCl$_3$): δ 7.28 (m, 2H), 7.19 (s, 1H), 3.65 (t, J = 8.0 Hz, 1H), 2.86 (m, 2H), 2.31 (m, 1H), 2.24 (dt, *J* = 11.5, 4.0 Hz, 1H), 1.89 (m, 3H), 1.66 (m, 1H), 1.49 (m, 3H), 1.32 (m, 2H), 1.18 (m, 2H), 0.97 (t, *J* = 7.5 Hz, 9H), 0.90 (s, 9H), 0.77 (q, *J* = 8.0 Hz, 6H), 0.74 (s, 3H), 0.03 (d, *J* = 6.5 Hz, 6H).

^{13}C-NMR (125 MHz, CDCl$_3$): δ 153.2, 137.9, 133.3, 126.1, 119.9, 117.1. 81.8, 49.7, 44.1, 43.6, 38.9, 37.2, 31.0, 29.7, 27.3, 26.4, 25.9, 25.7, 23.3, 18.2, 18.1, 11.4, -4.4, -4.8.

IR (film, cm^{-1}): 2949, 2866, 1594, 1462, 1371, 1253.

HRMS (EI) *m/z*: [M]$^+$ predicted for C$_{30}$H$_{52}$OSi$_2$, 484.3557; found, 484.3558.

5.3.4 Scheme 3.30 Scope of the Silanes in the Silylation Reaction

[1,1'-biphenyl]-4-yl(ethyl)dimethylsilane.
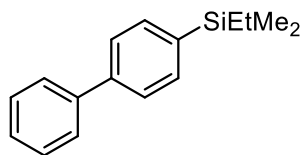
Scheme 3.30, Entry 1: Following general procedure C, Ni(cod)$_2$ (4.1 mg, 0.015 mmol), IPr*OMe (14.2 mg, 0.015 mmol), NaO^{t}Bu (36.0 mg, 0.375 mmol), ([1,1'-biphenyl]-4-yloxy)(*tert*-butyl)dimethylsilane (43.4 mg, 0.153 mmol), and dimethylethylsilane (119 µL, 0.9 mmol) gave a crude residue which was purified by flash chromatography (100% hexanes) to afford the desired product (26.6 mg, 0.111 mmol, 73% yield). The yield for biphenyl was determined by GC-FID analysis using tridecane as an internal standard due to sublimability of the product (tridecane integration: 318617645, biphenyl integration: 12130473, 0.007 mmol, 4%). The reaction was performed in multiple iterations in concert with Eric Wiensch. The optimal yield from these reactions has been reported.

^{1}H-NMR (500 MHz, CDCl$_3$): δ 7.61 (m, 6H), 7.45 (t, *J* = 7.5 Hz, 2H), 7.36 (t, *J* = 7.5 Hz, 1H), 1.00 (t, *J* = 7.5 Hz, 3H), 0.78 (q, *J* = 7.5 Hz, 2H), 0.30 (s, 6H).

^{13}C-NMR (125 MHz, CDCl$_3$): δ 141.5, 141.2, 138.2, 134.1, 128.7, 127.3, 127.1, 126.4, 7.4, 3.5.

IR (film, cm^{-1}): 3023, 2953, 2873, 1597, 1484, 1247.

HRMS (EI) *m/z*: [M]$^+$ predicted for C$_{16}$H$_{20}$Si, 240.1334; found, 240.1326.

[1,1'-biphenyl]-4-yldiethyl(methyl)silane.
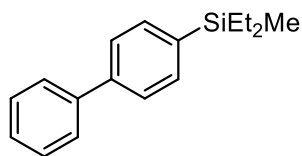
Scheme 3.30, Entry 2: Following general procedure C, Ni(cod)$_2$ (4.1 mg, 0.015 mmol), IPr*OMe (14.2 mg, 0.015 mmol), NaO^{t}Bu (36.0 mg, 0.375 mmol), ([1,1'-biphenyl]-4-yloxy)(*tert*-butyl)dimethylsilane (42.4 mg, 0.149 mmol), and diethylmethylsilane (131 µL, 0.9 mmol) gave a crude residue which was purified by flash chromatography (100% hexanes) to afford the desired product (28.3 mg, 0.111 mmol, 75% yield). The yield for biphenyl was determined by GC-FID analysis using tridecane as an internal standard due to sublimability of the product (tridecane integration: 231029643, biphenyl integration: 6144535, 0.005 mmol, 3%). The reaction was performed in multiple iterations in concert with Eric Wiensch. The optimal yield from these reactions has been reported.

^{1}H-NMR (500 MHz, CDCl$_3$): δ 7.62 (m, 6H), 7.45 (t, *J* = 7.5 Hz, 2H), 7.36 (t, *J* = 7.5 Hz, 1H), 1.00 (t, *J* = 7.5 Hz, 6H), 0.81 (q, *J* = 7.5 Hz, 4H), 0.29 (s, 6H).

^{13}C-NMR (125 MHz, CDCl$_3$): δ 141.5, 141.2, 137.2, 134.4, 128.7, 127.3, 127.1, 126.4, 7.4, 5.5, -6.0.

IR (film, cm^{-1}): 3022, 2952, 2873, 1597, 1484, 1251.

HRMS (EI) *m/z*: [M]$^+$ predicted for C$_{17}$H$_{22}$Si, 254.1491; found, 254.1491.

[1,1'-biphenyl]-4-yl(benzyl)dimethylsilane
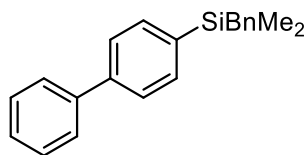
Scheme 3.30, Entry 8: Following general procedure C, Ni(cod)$_2$ (4.1 mg, 0.015 mmol), IPr*OMe (14.2 mg, 0.015 mmol), NaO^{t}Bu (36.0 mg, 0.375 mmol), ([1,1'-biphenyl]-4-yloxy)(*tert*-butyl)dimethylsilane (43.3 mg, 0.152 mmol), and benzyldimethylsilane (140 µL, 0.9 mmol) gave a crude residue which was purified by flash chromatography (100% hexanes) to afford the desired product (20.0 mg, 0.066 mmol, 43% yield). The yield for biphenyl was determined by GC-FID

analysis using tridecane as an internal standard due to sublimability of the product (tridecane integration: 244625734, biphenyl integration: 27662478, 0.020 mmol, 12%). The reaction was performed in multiple iterations in concert with Eric Wiensch. The optimal yield from these reactions has been reported.

^{1}H-NMR (500 MHz, CDCl[3]): δ 7.56 (m, 6H), 7.47 (t, J = 7.5 Hz, 2H), 7.37 (t, J = 7.5 Hz, 1H), 7.21 (t, J = 7.5 Hz, 2H), 7.09 (t, J = 7.5 Hz, 1H), 6.98 (d, J = 7.5 Hz, 2H), 2.36 (s, 2H), 0.30 (s, 6H).

^{13}C-NMR (125 MHz, CDCl[3]): δ 141.8, 141.0, 139.6, 137.2, 134.2, 128.8, 128.3, 128.1, 127.4, 127.1, 126.4, 124.1, 26.2, 3.4.

IR (film, cm[-1]): 3026, 2961, 2889, 1596, 1492, 1483, 1246.

HRMS (EI) m/z: [M]$^+$ predicted for $C_{21}H_{22}Si$, 302.1491; found, 302.1491.

5.3.5 Scheme 3.38 Amination Substrate Scope

***N*-octyl-4-(pyridin-2-yl)aniline.**
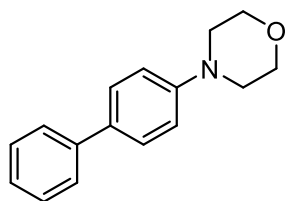
Scheme 3.38, Entry A: Following general procedure D, Ni(cod)$_2$ (4.1 mg, 0.015 mmol), IPr^{Me}·HCl (13.6 mg, 0.03 mmol), NaO^{t}Bu (72.0 mg, 0.750 mmol), ([1,1'-biphenyl]-4-yloxy)(*tert*-butyl)dimethylsilane (79.3 mg, 0.279 mmol), and morpholine (39 µL, 0.45 mmol) gave a crude residue which was purified by flash chromatography (hexanes: ethyl acetate 92.5:7.5) to afford the desired product (62.3 mg, 0.260 mmol, 93% yield). The spectral data matches that previously reported in the literature.[78] The reaction was performed in multiple iterations in concert with Eric Wiensch. The optimal yield from these reactions has been reported.

¹H-NMR (500 MHz, CDCl₃): δ 7.55 (m, 4H), 7.41 (t, *J* = 7.5 Hz, 2H), 7.29 (t, *J* = 7.5 Hz, 1H), 6.98 (d, *J* = 8.5 Hz, 2H), 3.89 (t, *J* = 5.0 Hz, 4H), 3.22 (t, *J* = 5.0 Hz, 4H).

Spectra for ITol·BF₄:

Spectra for Ni(ITol)(MMA)₂:

1H-Ni(ITol)(MMA)2_C6D6

13C-Ni(ITol)(MMA)2_C6D6
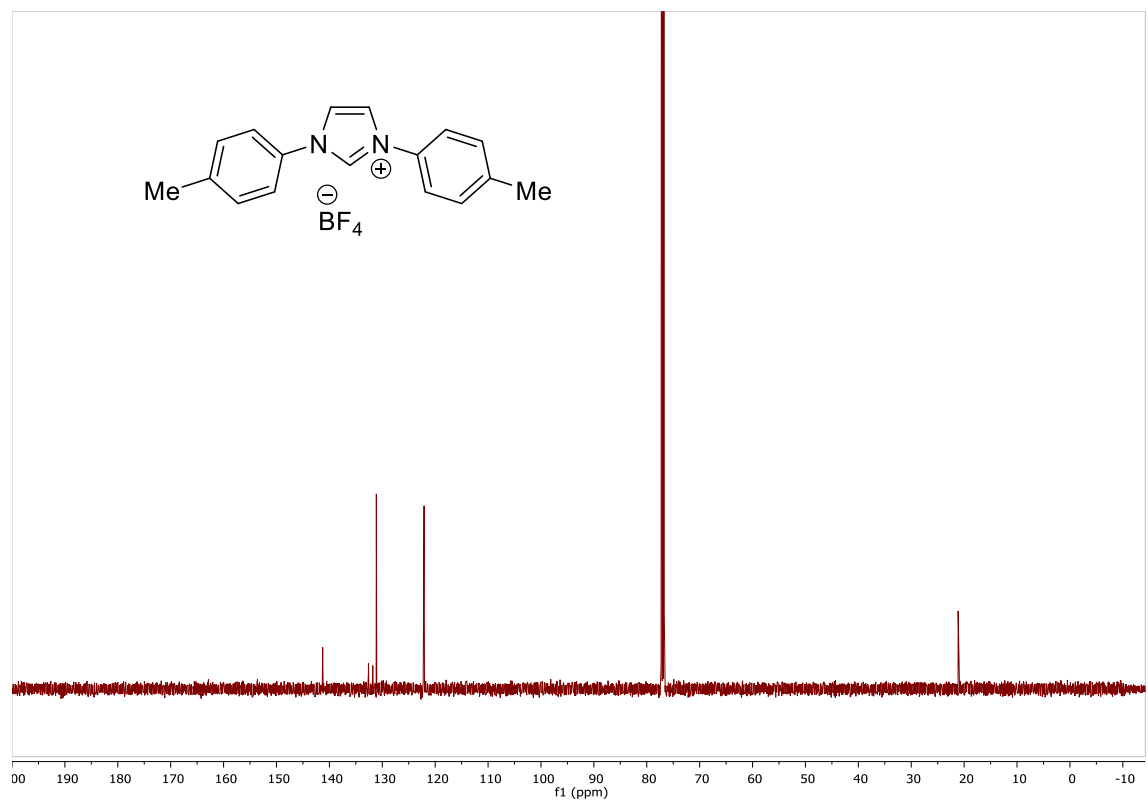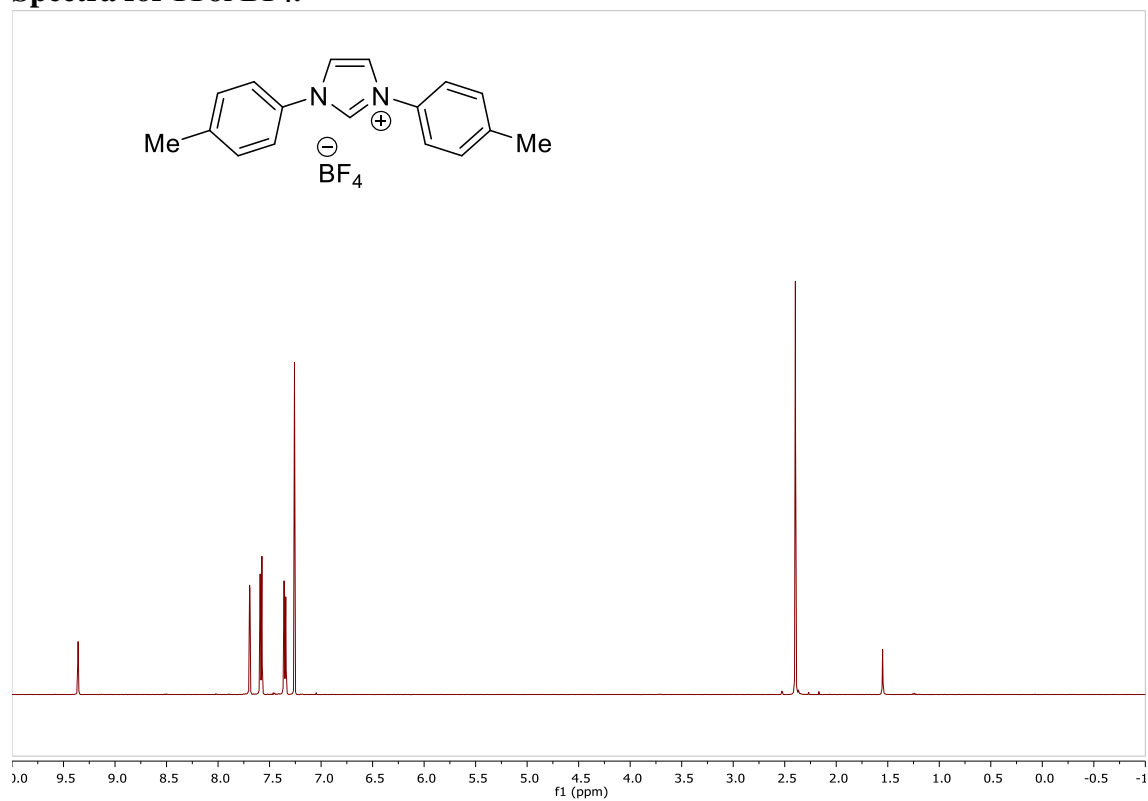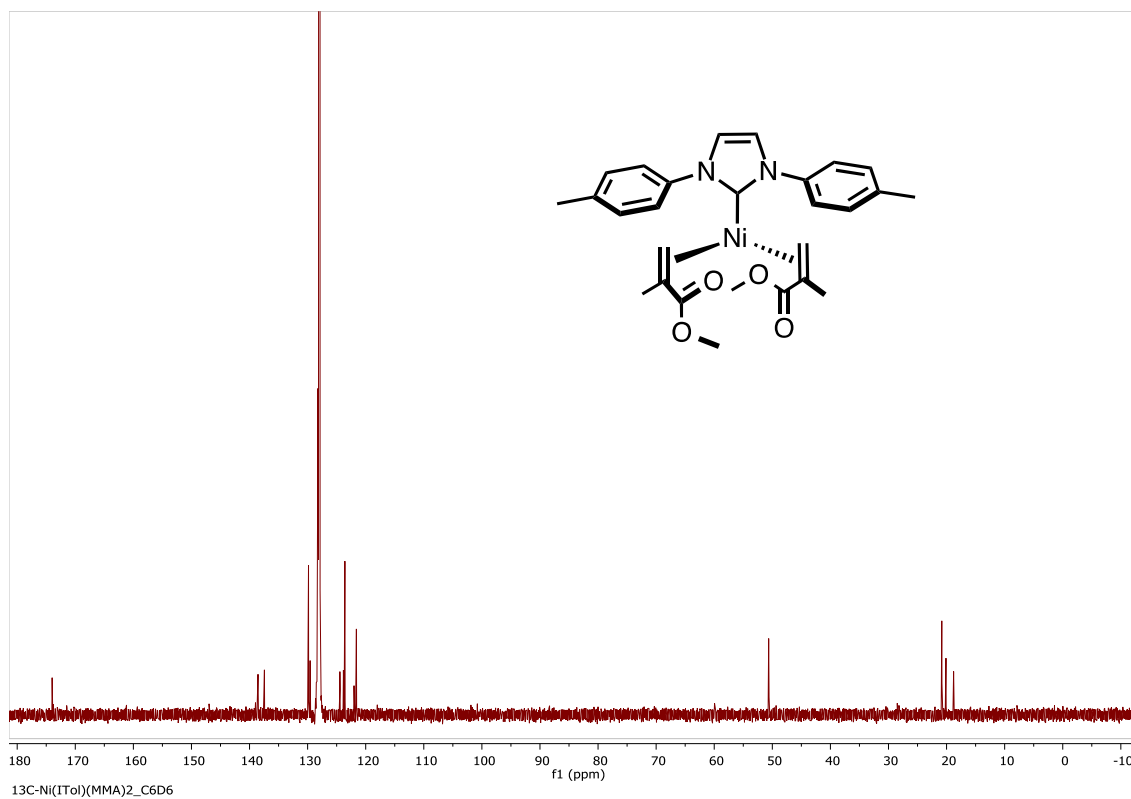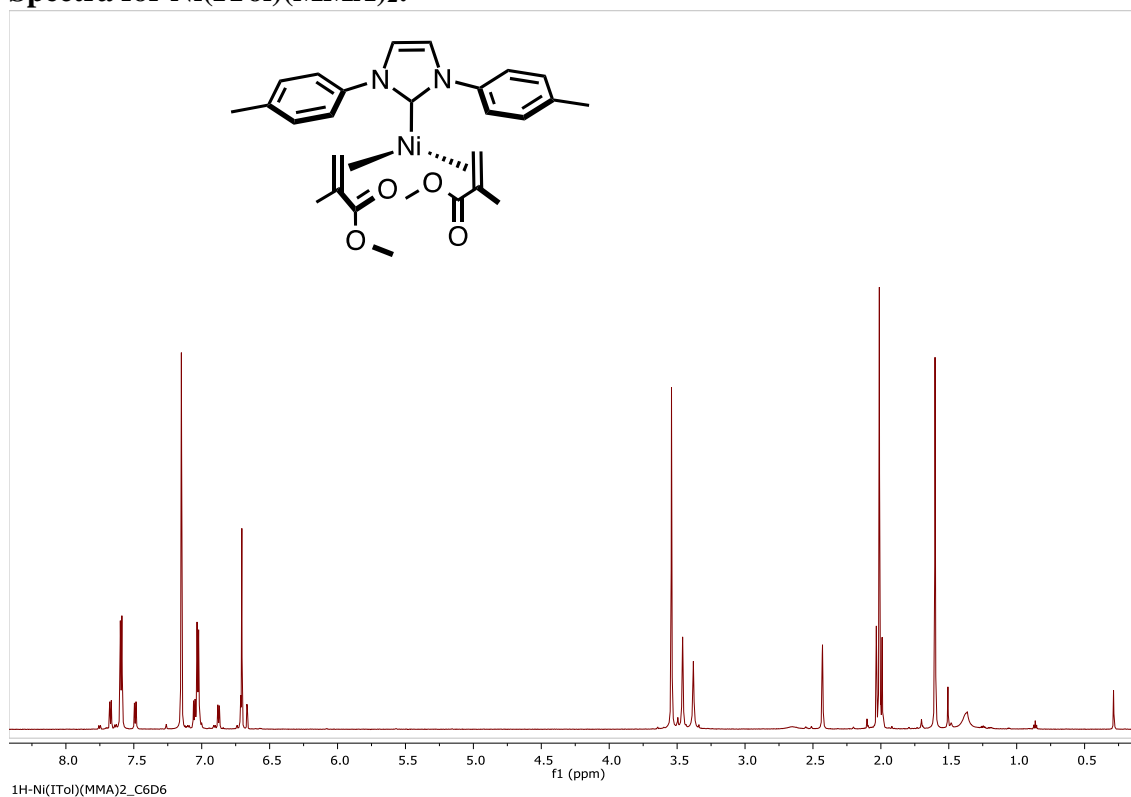
Scheme 2.12, Compound A:

Scheme 2.12, Compound B:

136
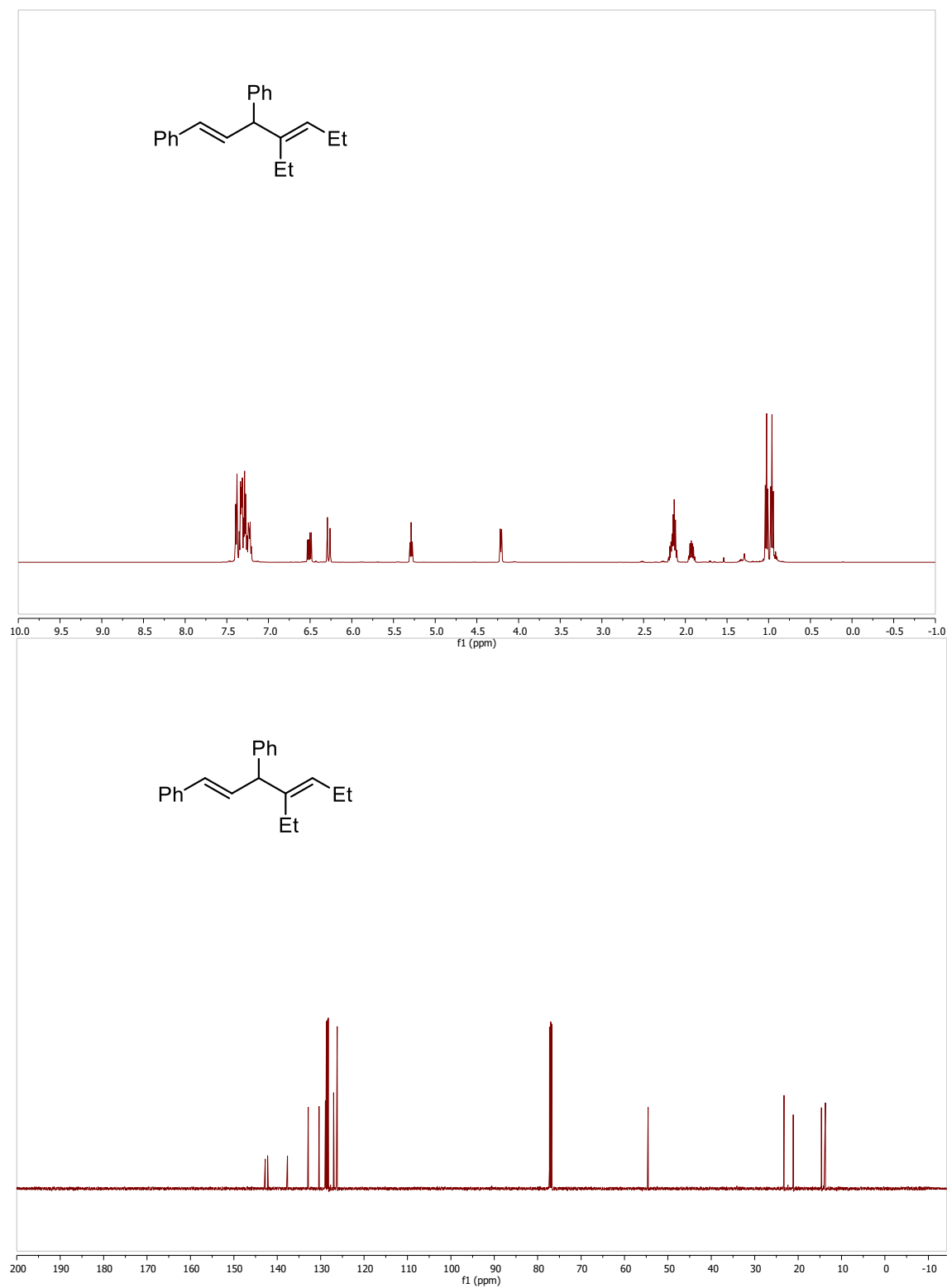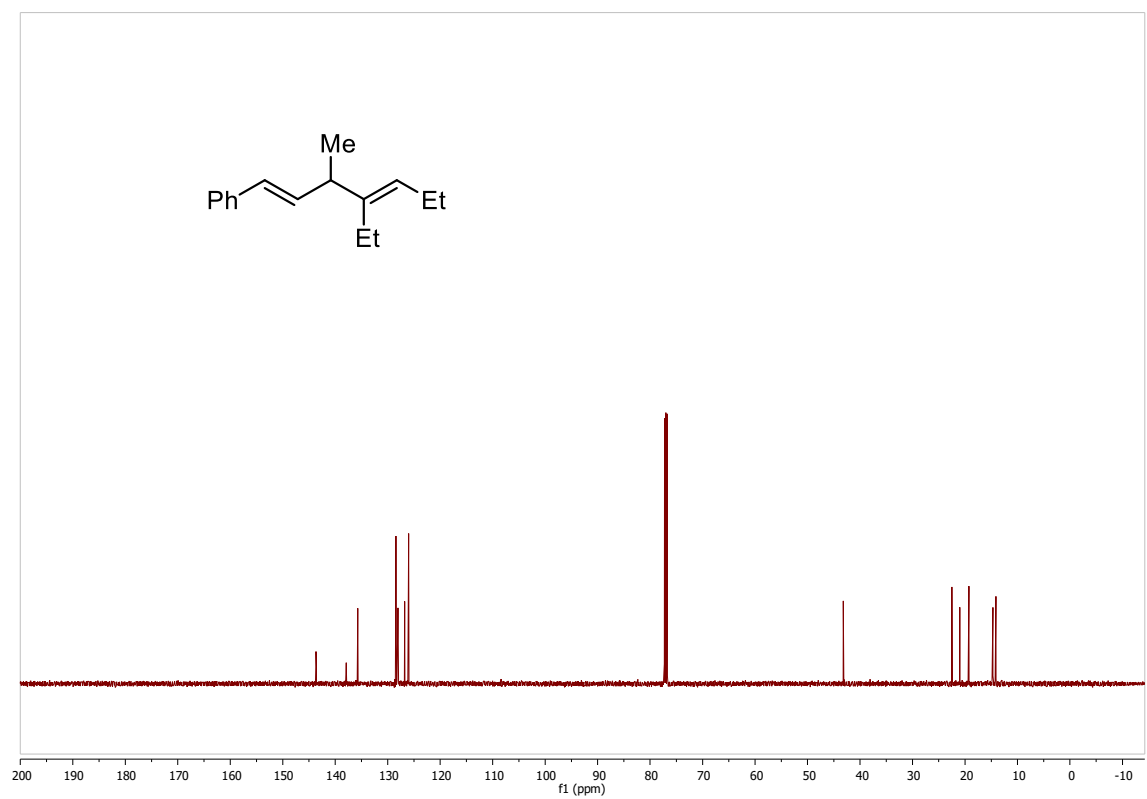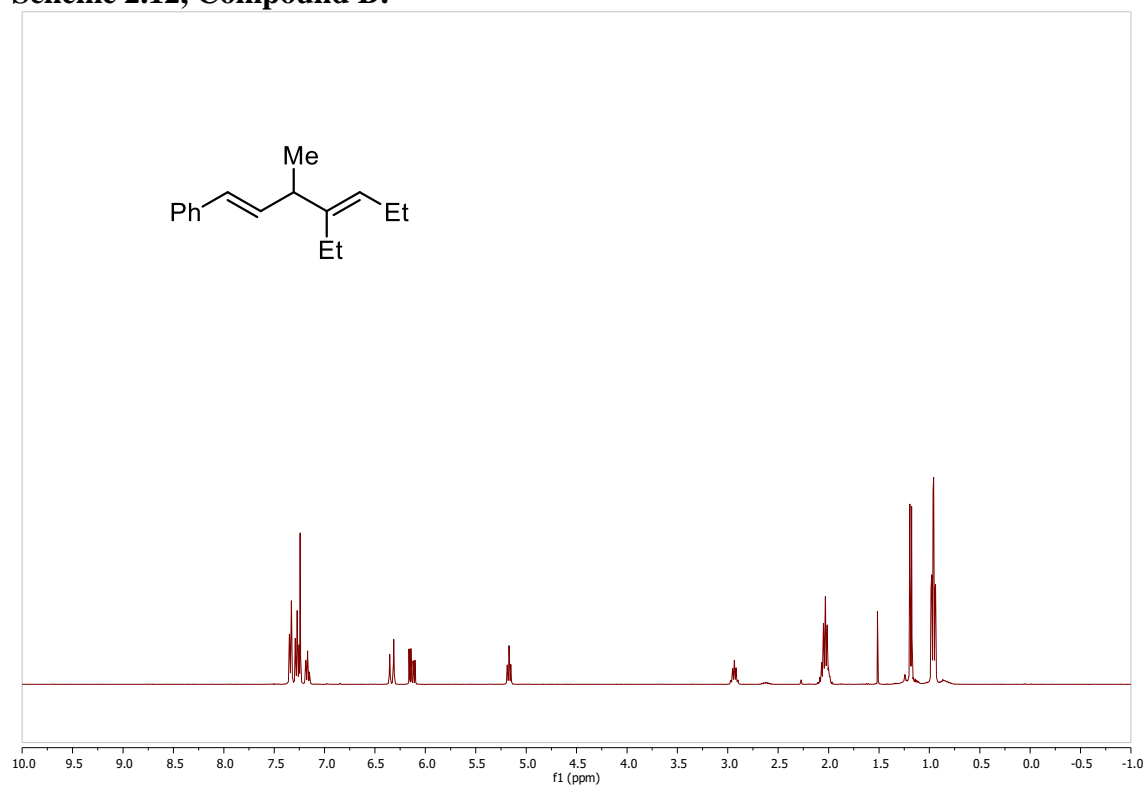
Scheme 2.12, Compound C:
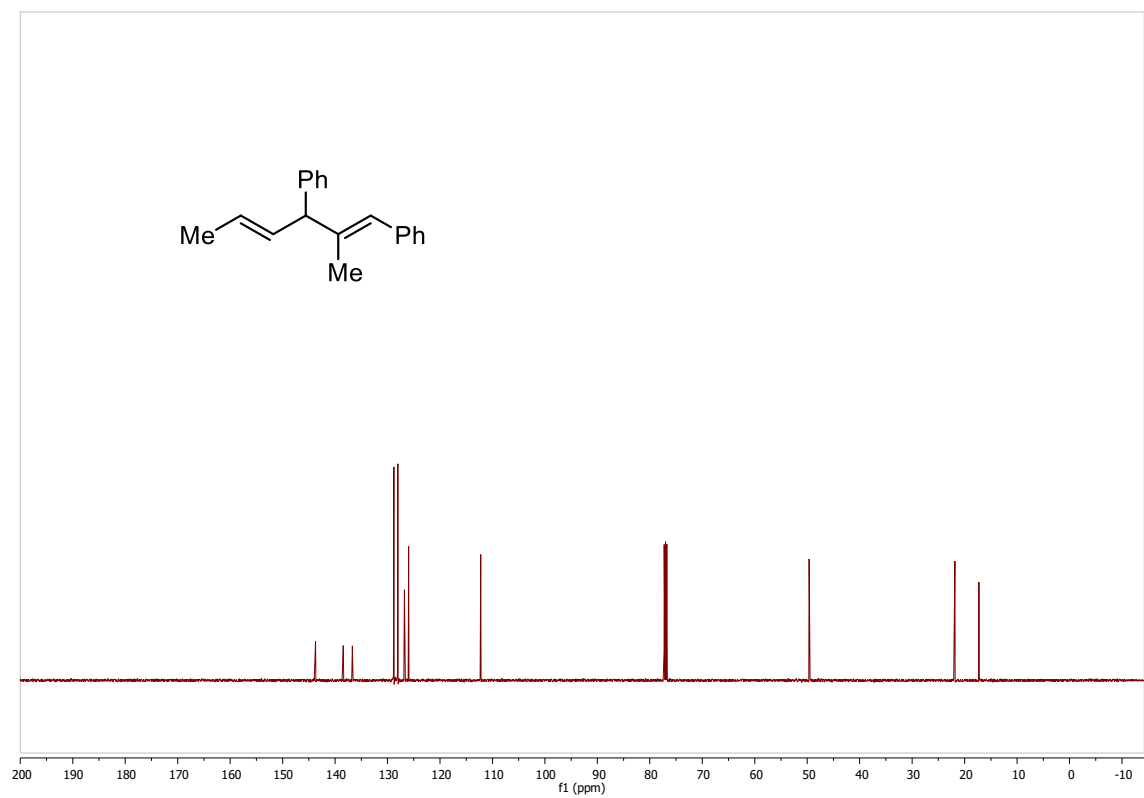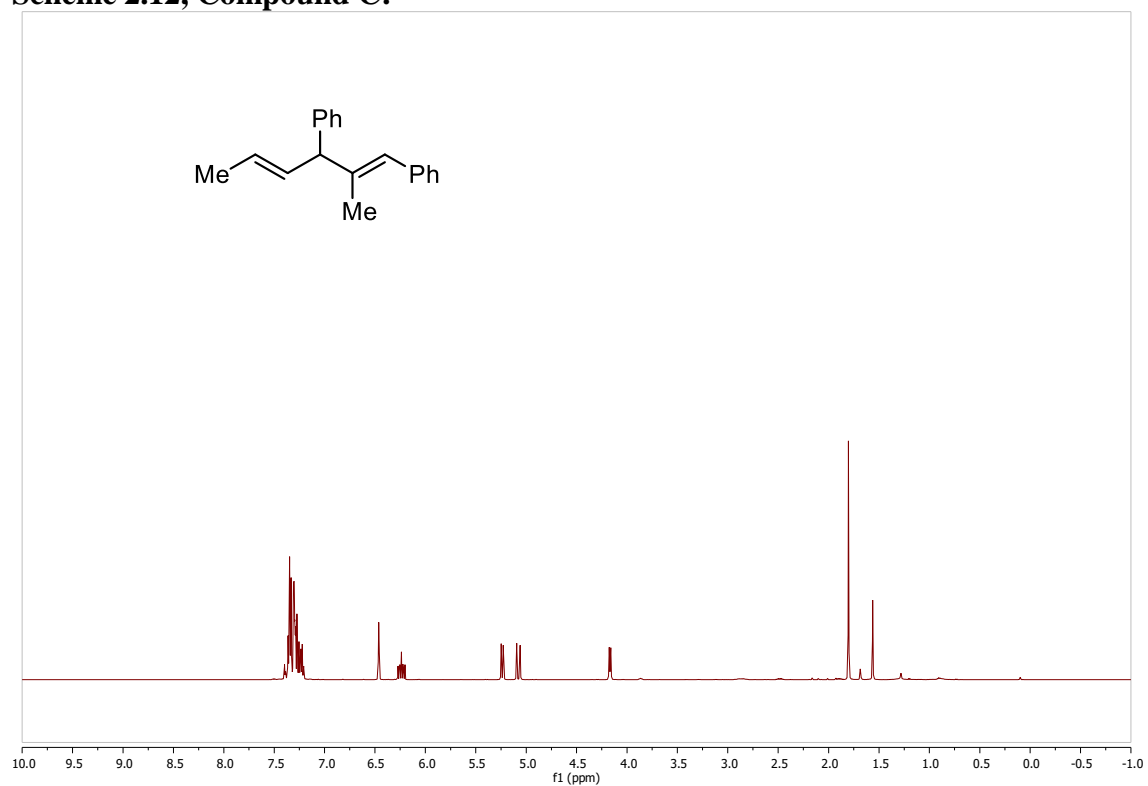
Scheme 2.12, Compound D:
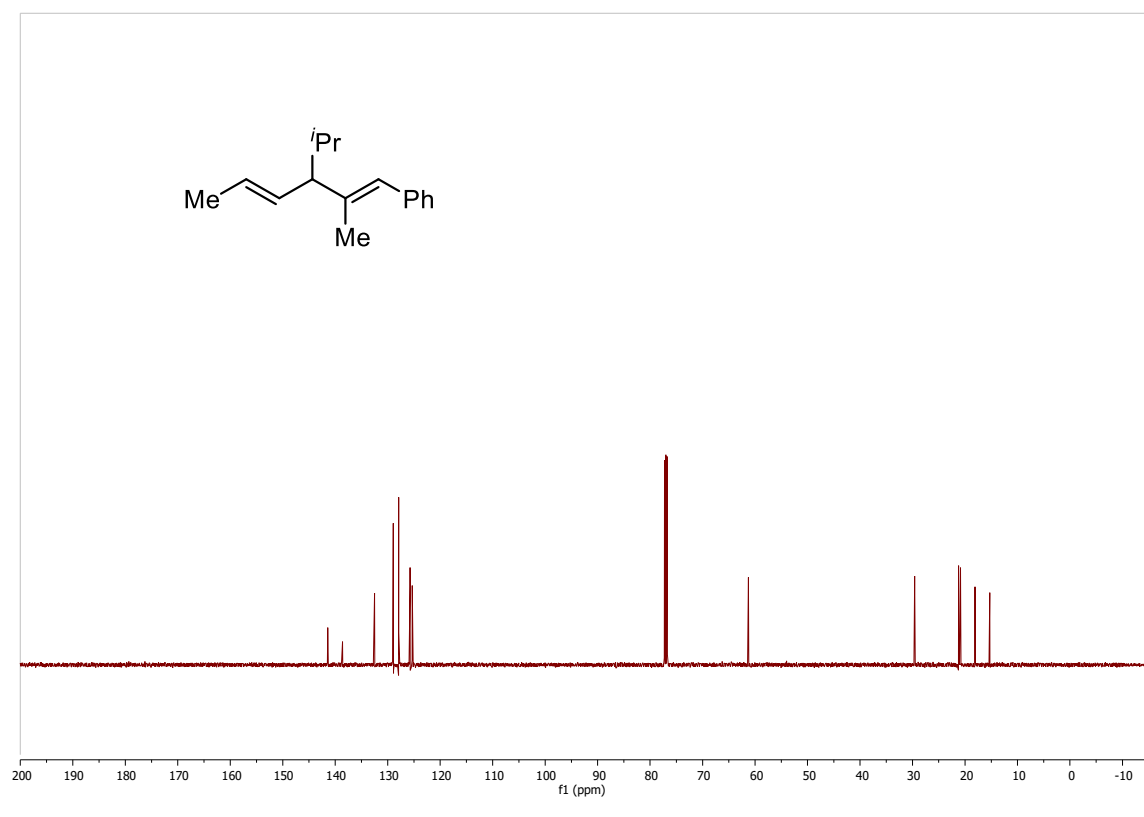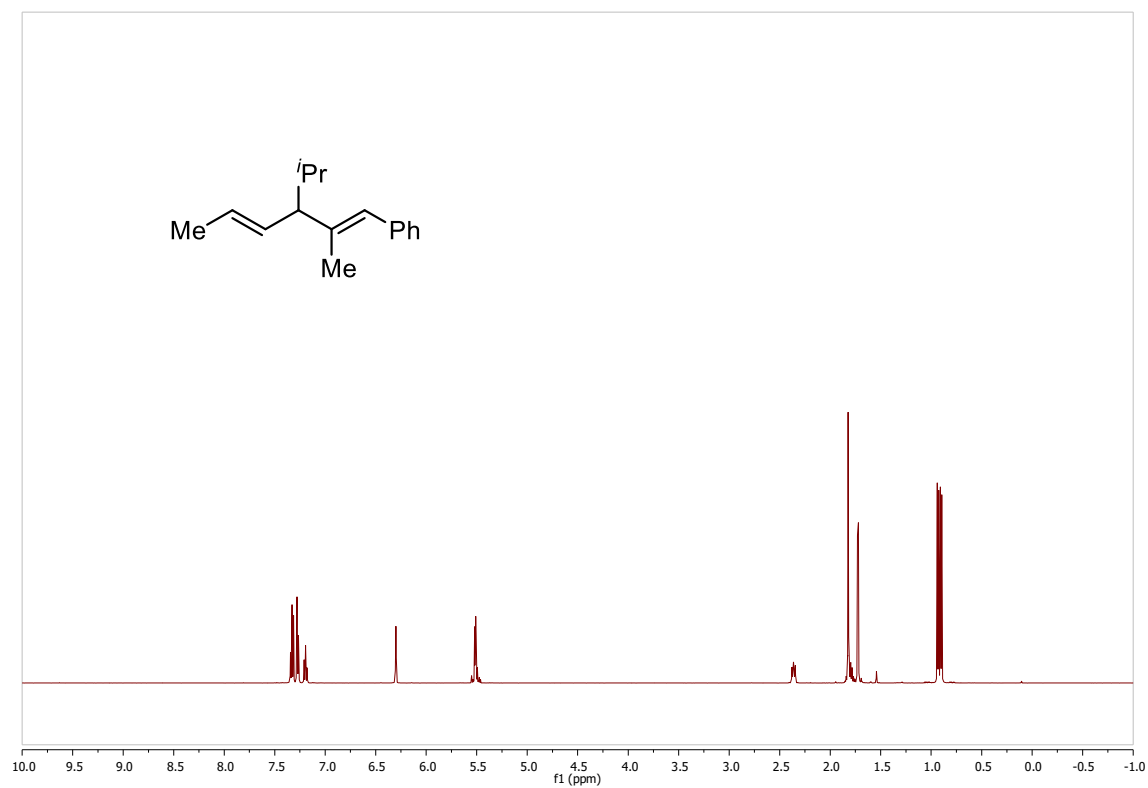
Scheme 2.12, Compound E:
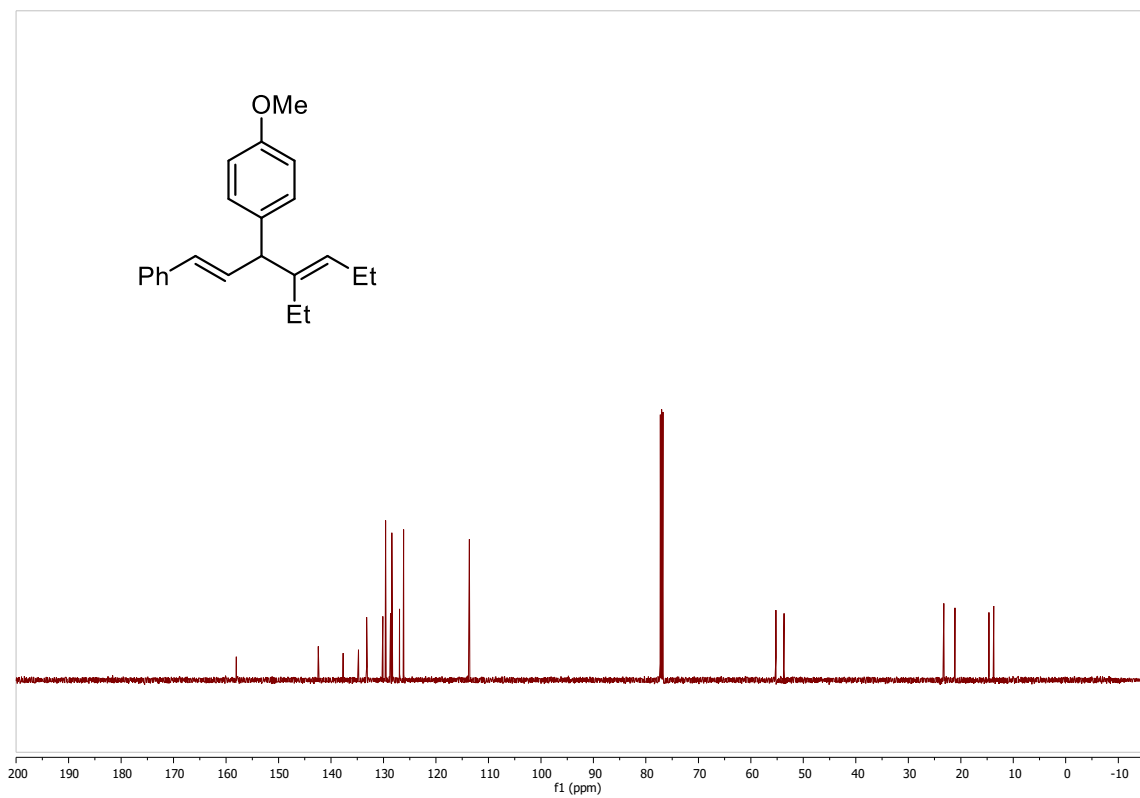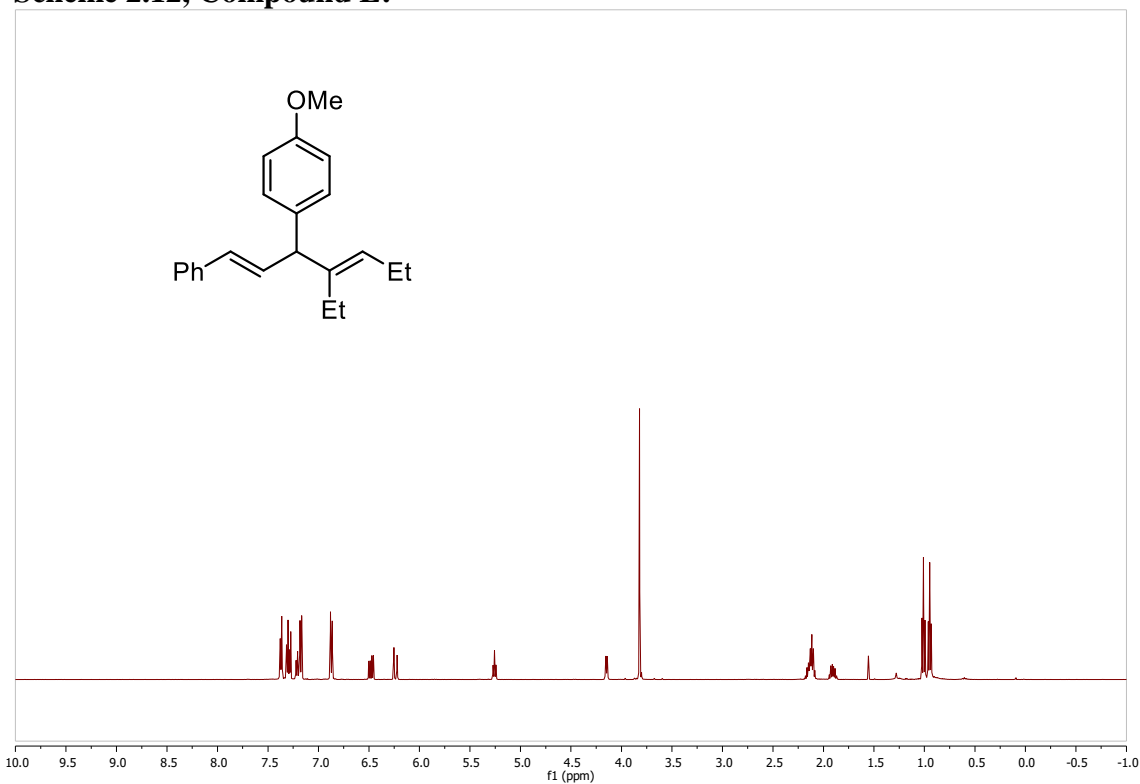
Scheme 2.12, Compound F:
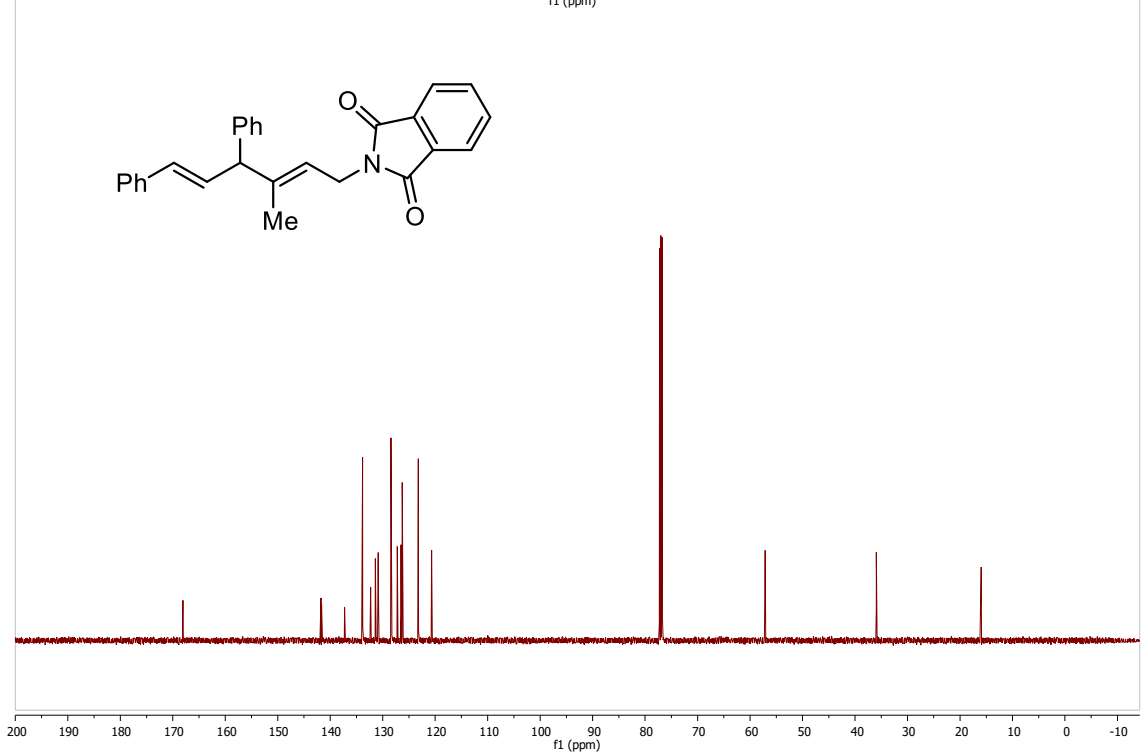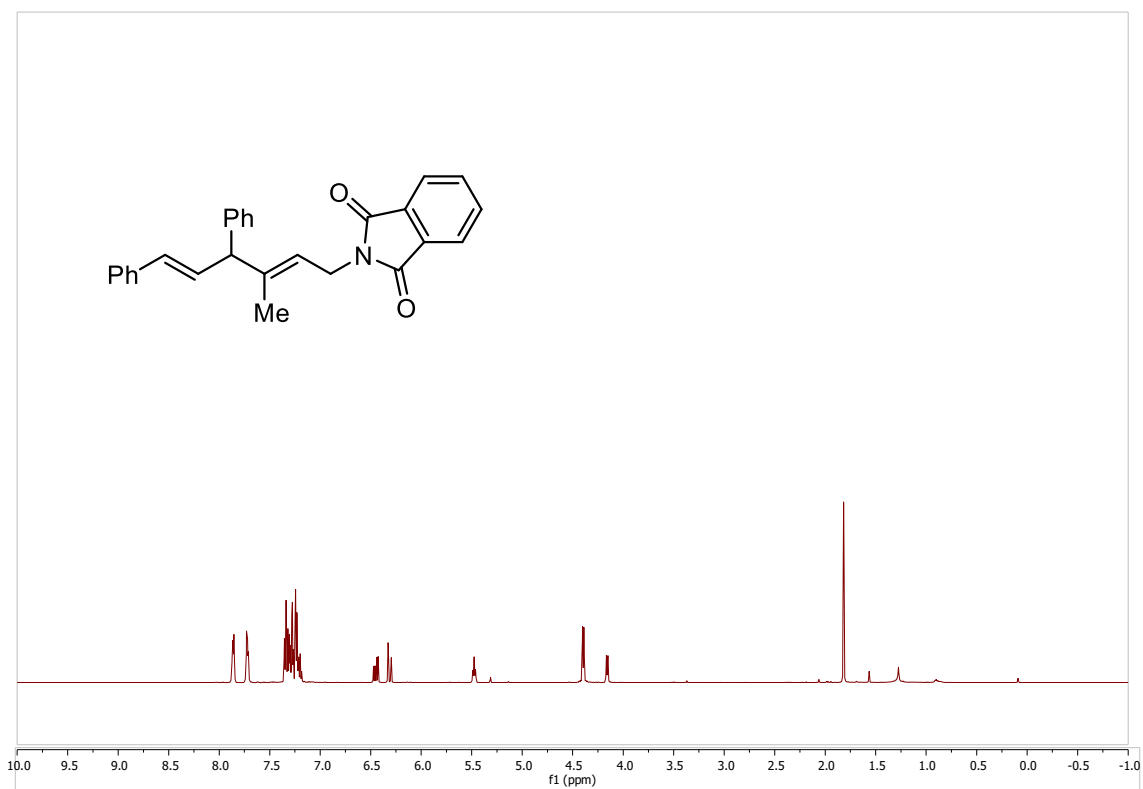
Scheme 2.12, Compound G:
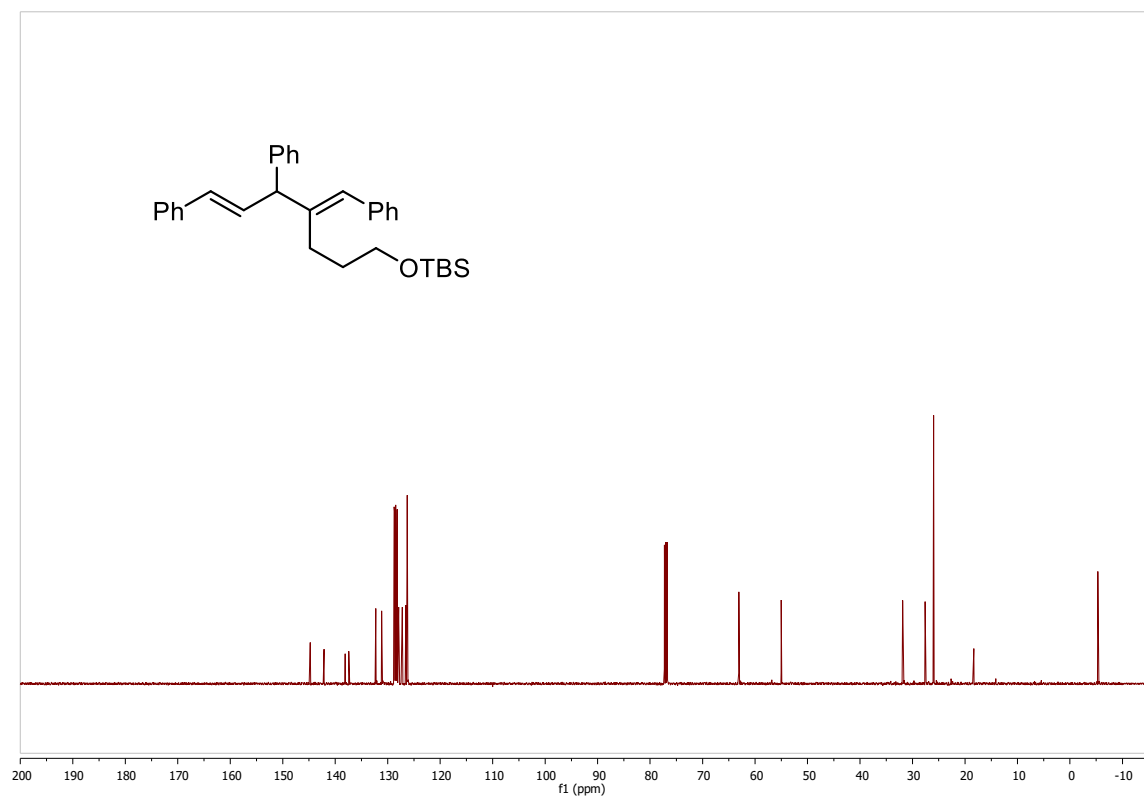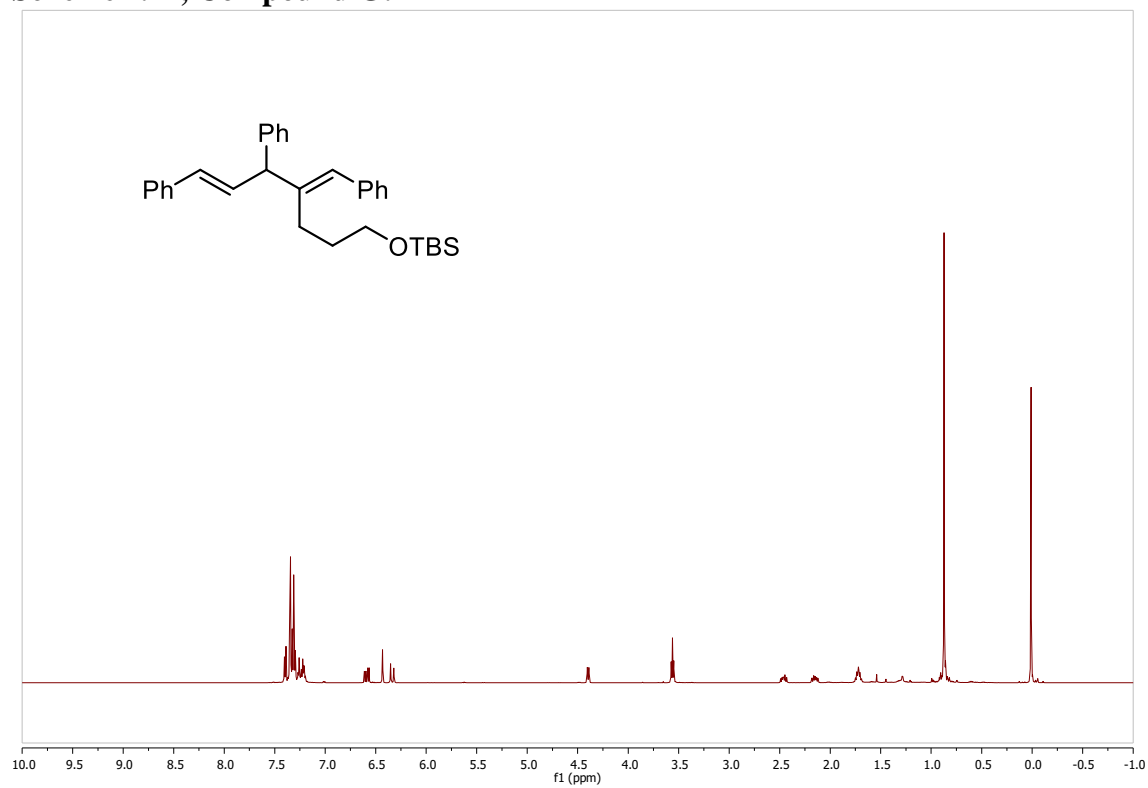
Scheme 2.12, Compound H:
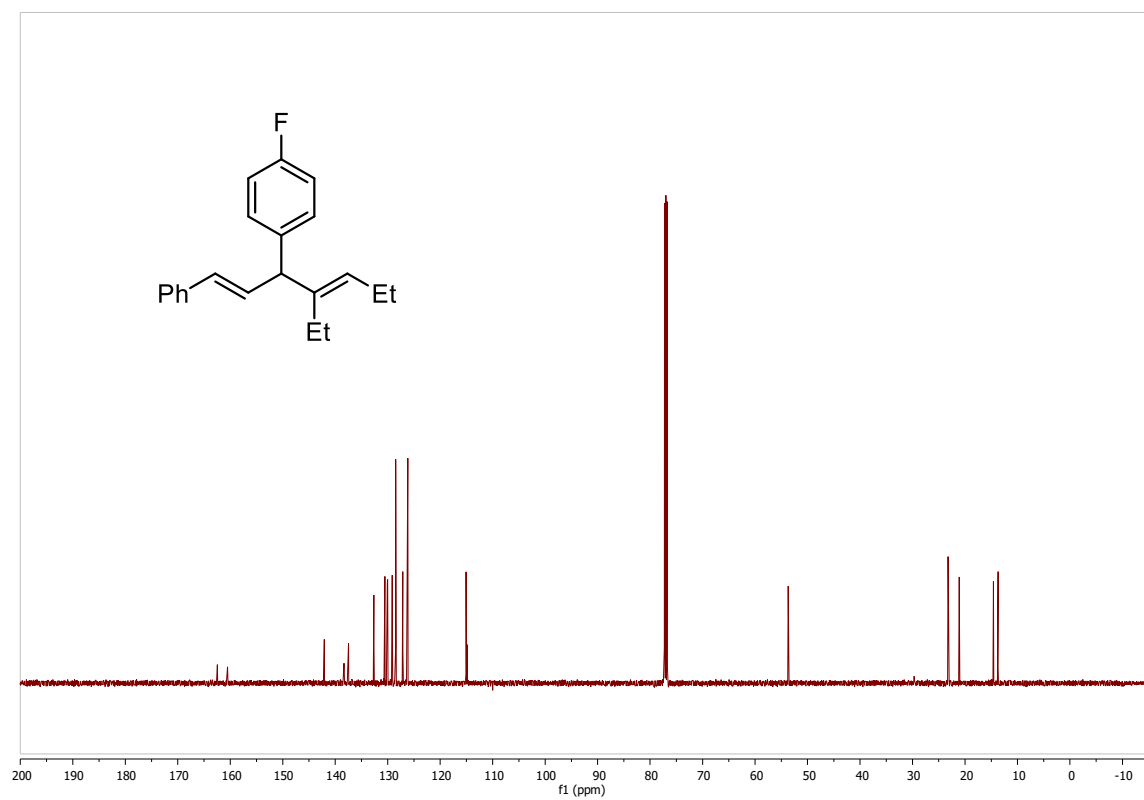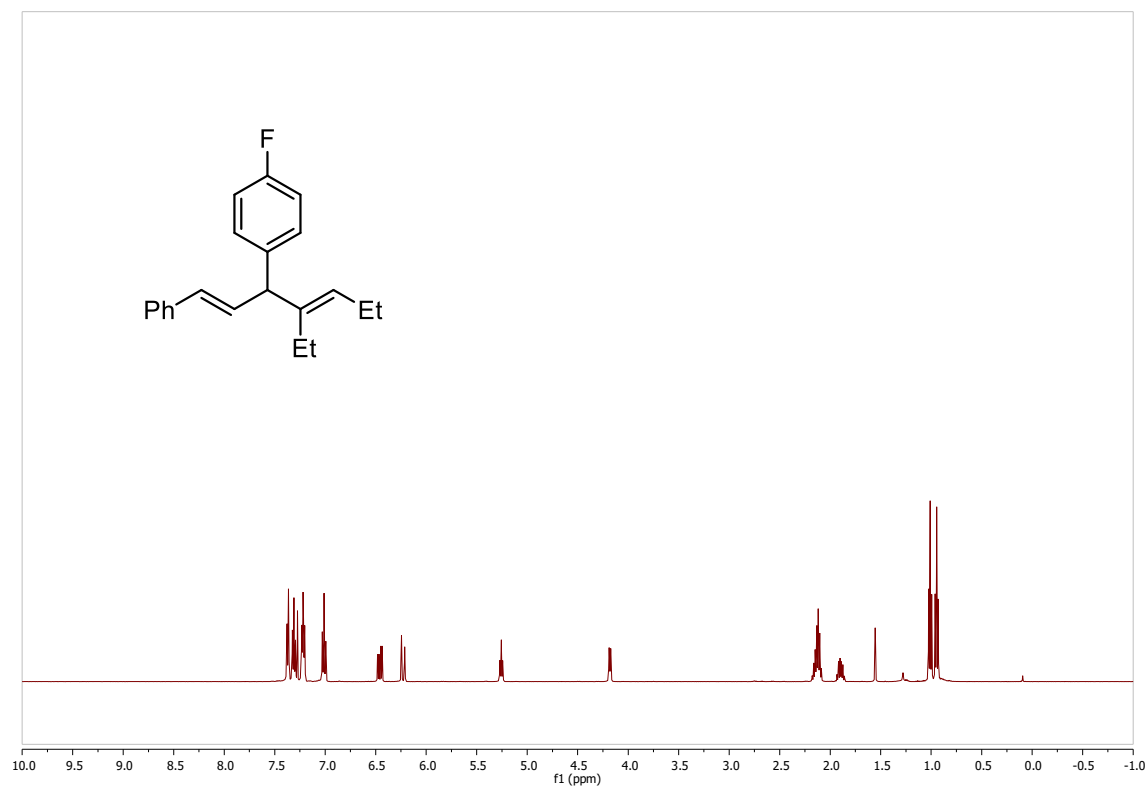
Scheme 2.12, Compound I:

Scheme 2.12, Compound J:

144
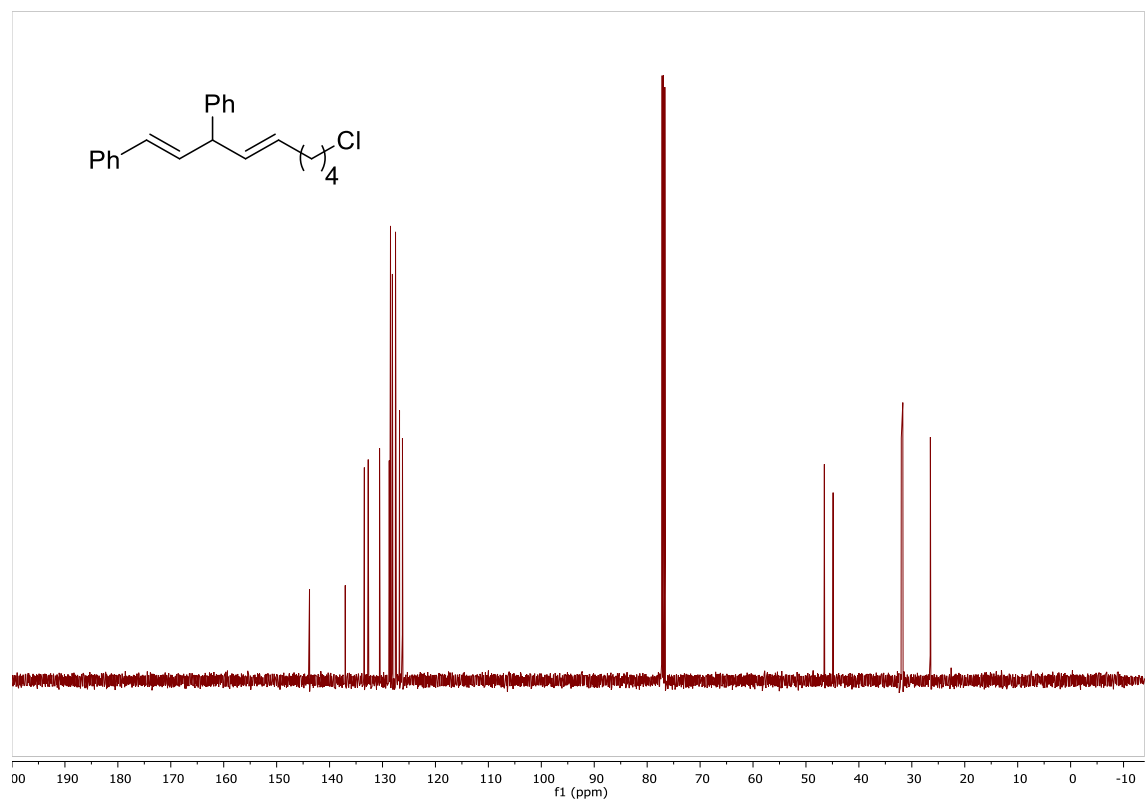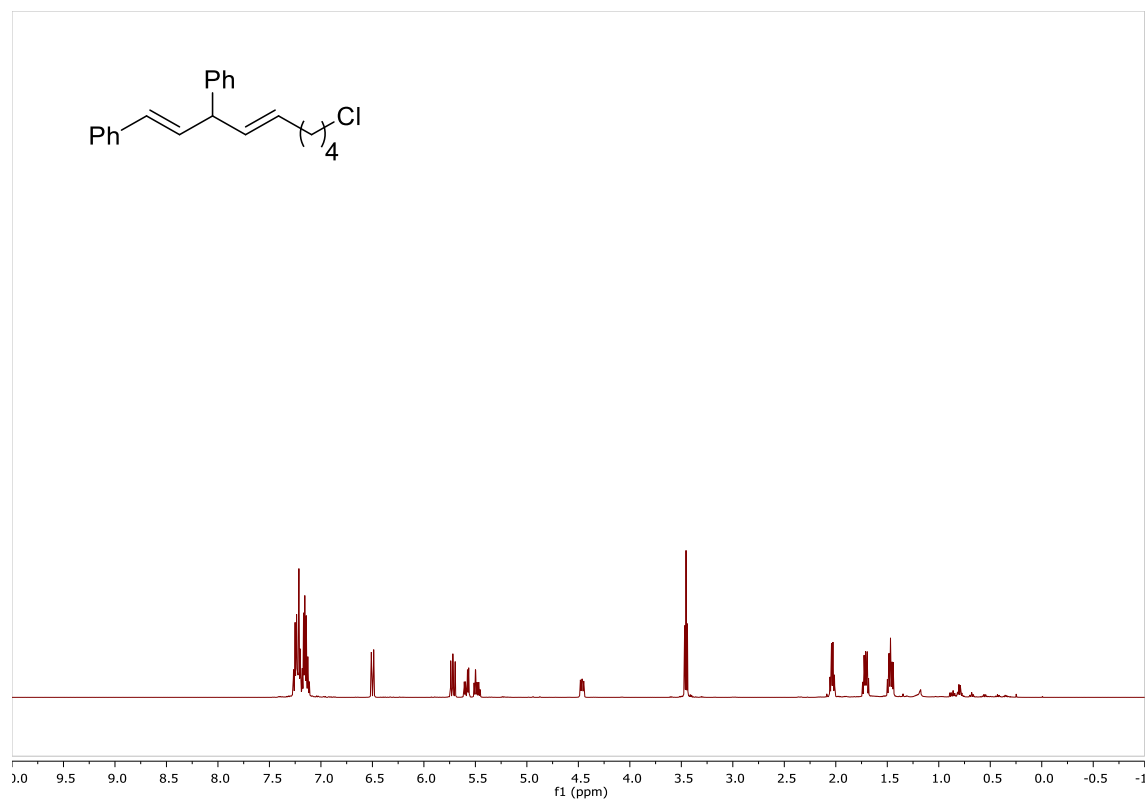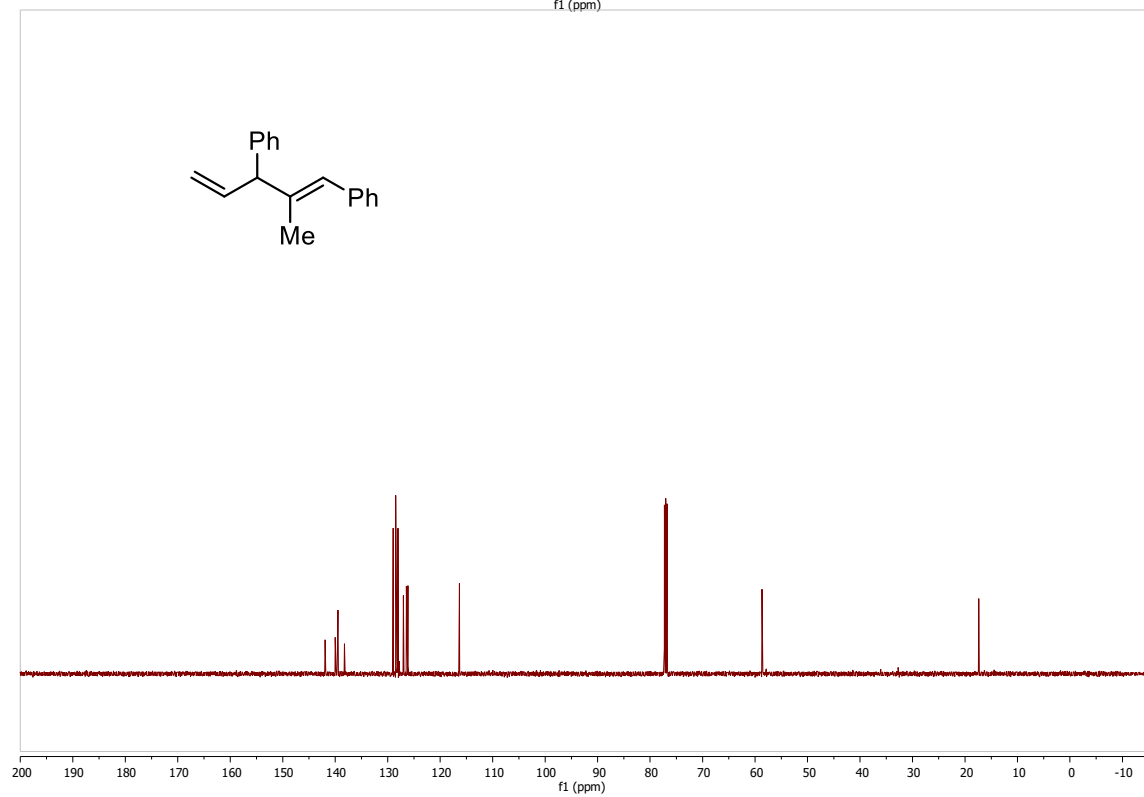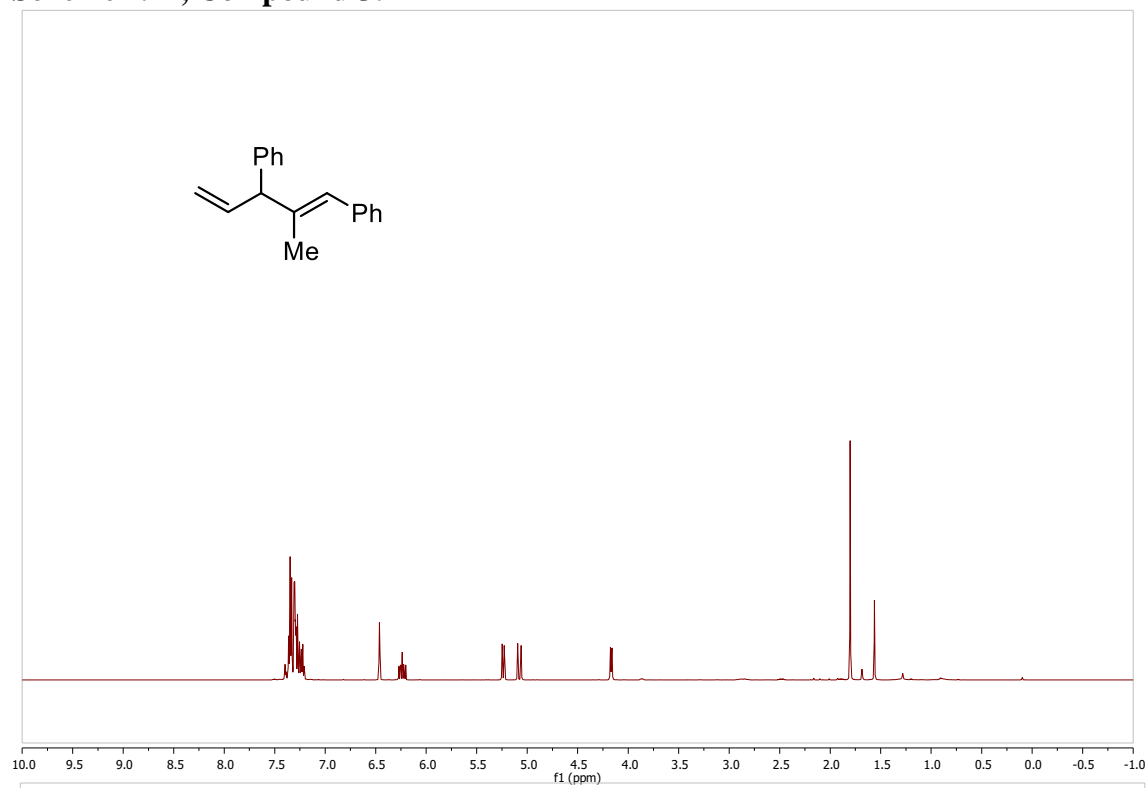
Scheme 2.12, Compound K:

Scheme 2.12, Compound L:

146
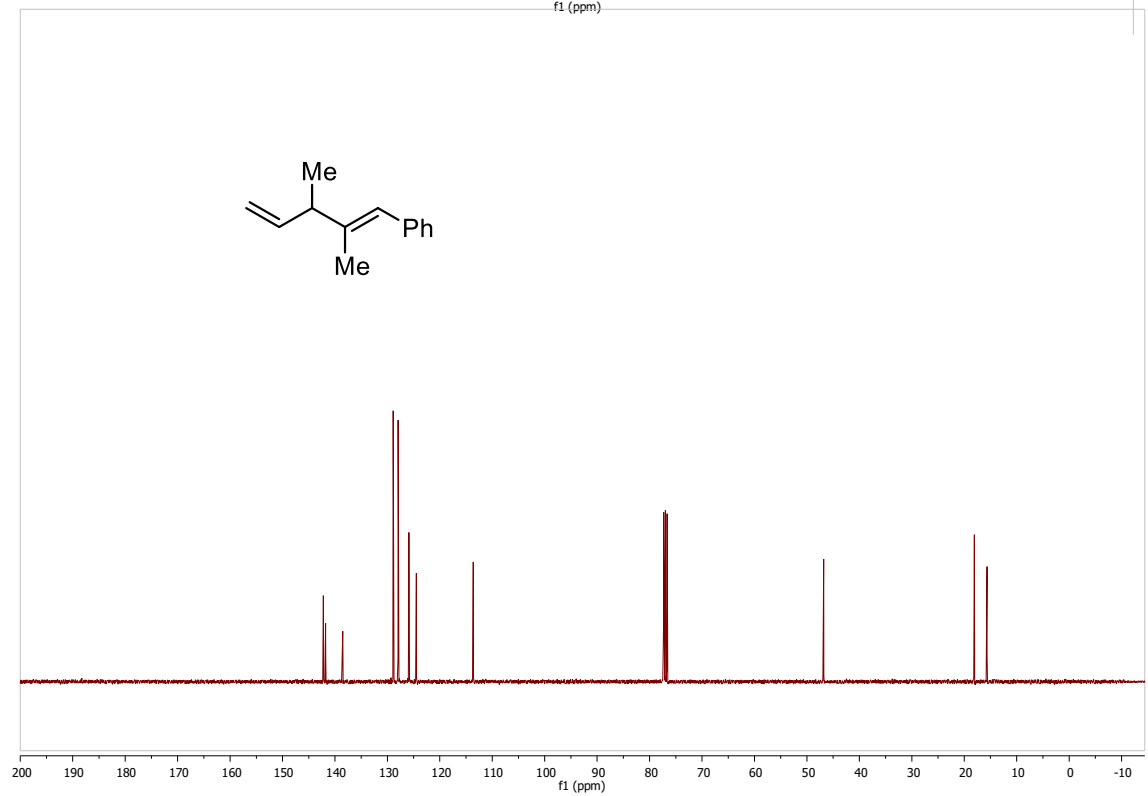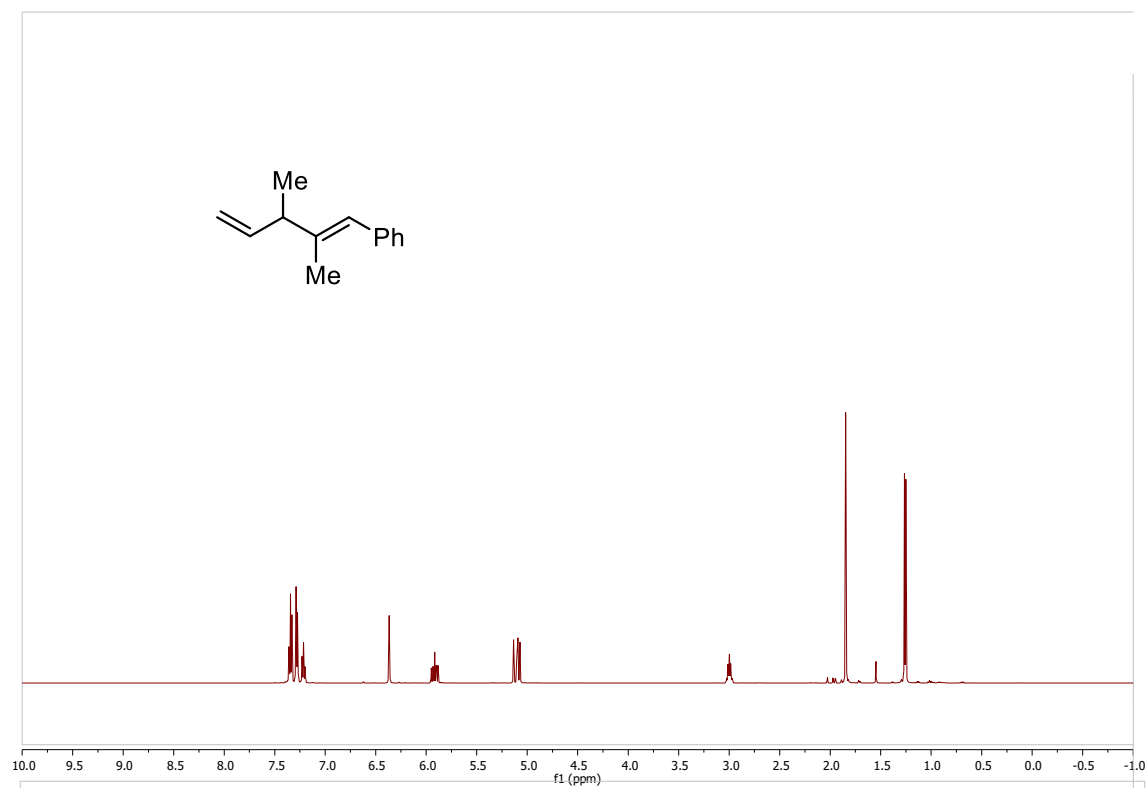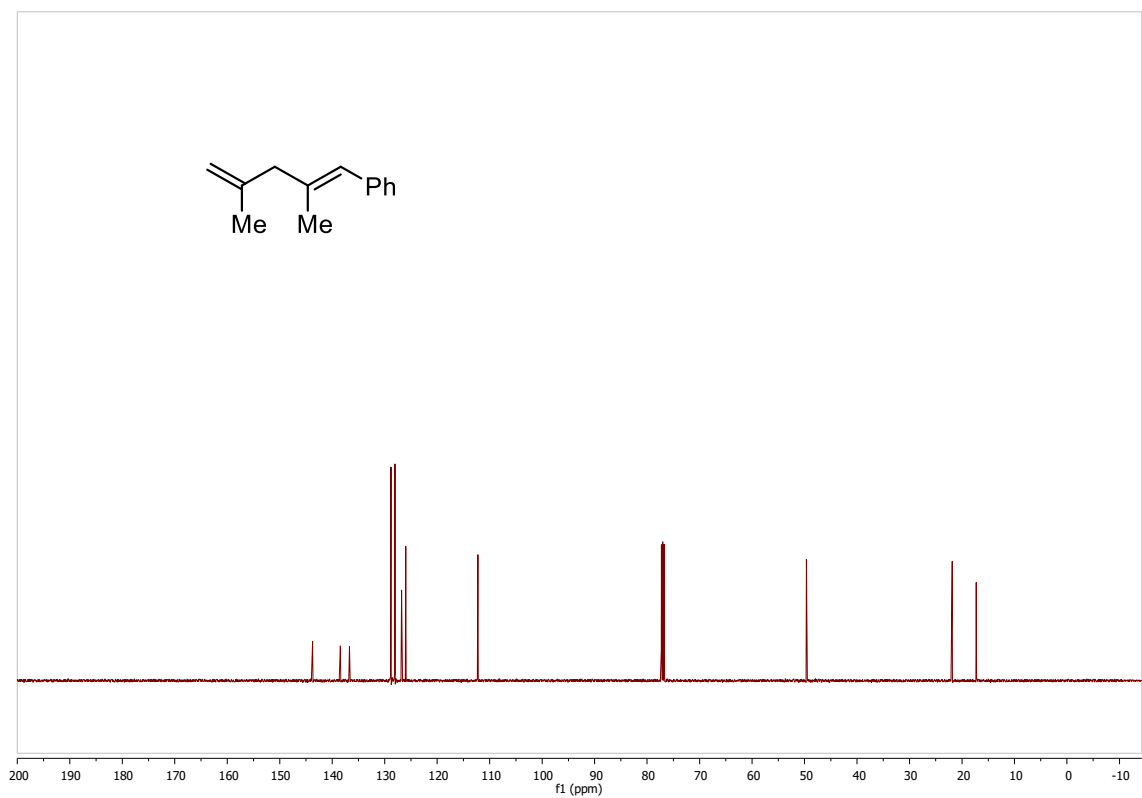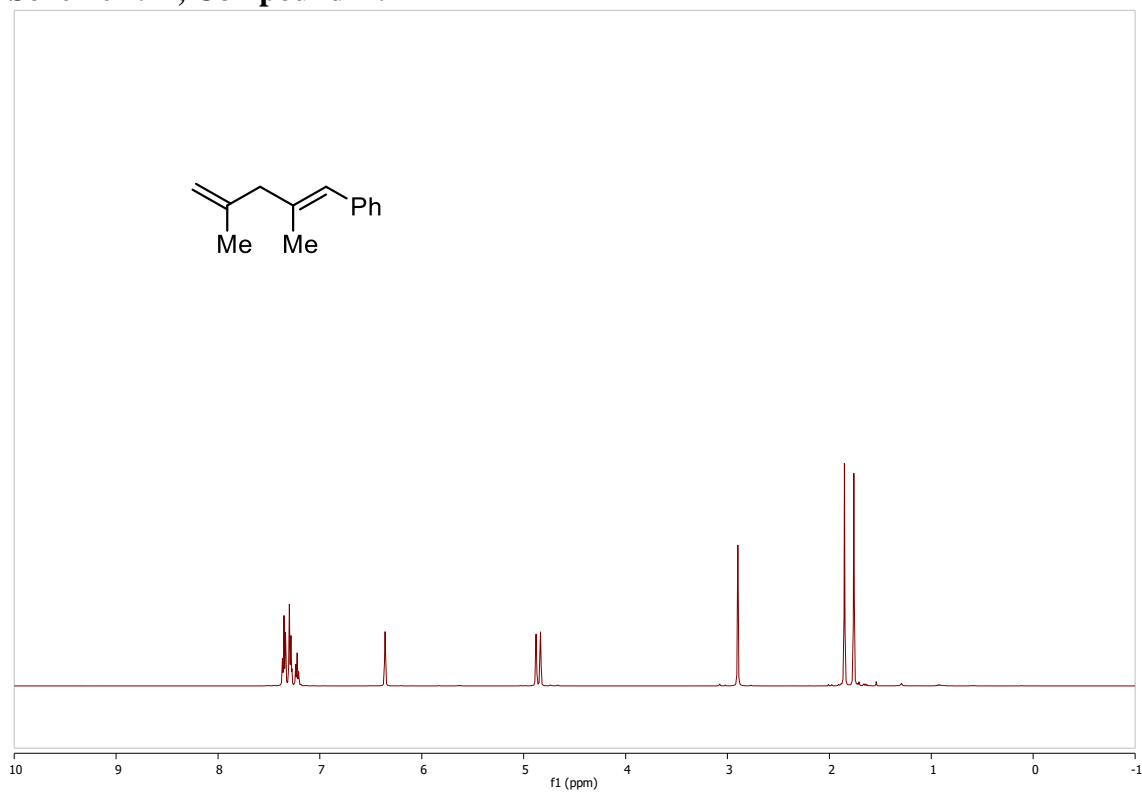
Scheme 2.12, Compound M:
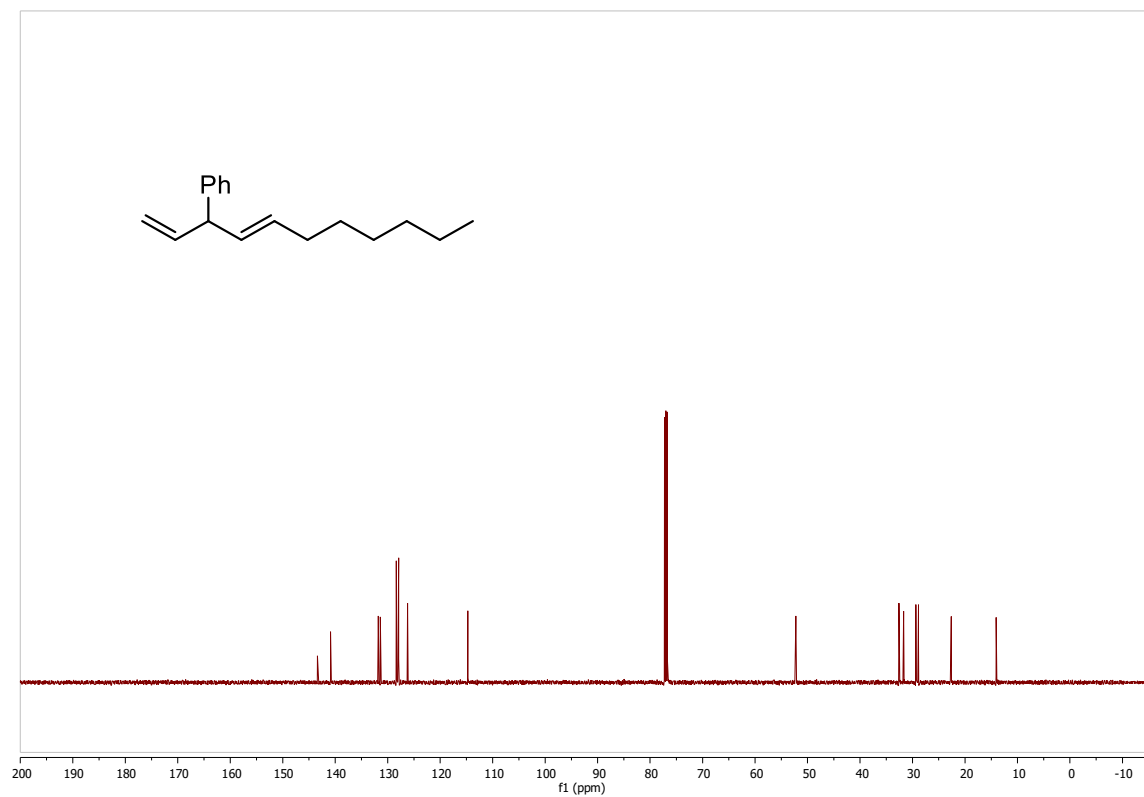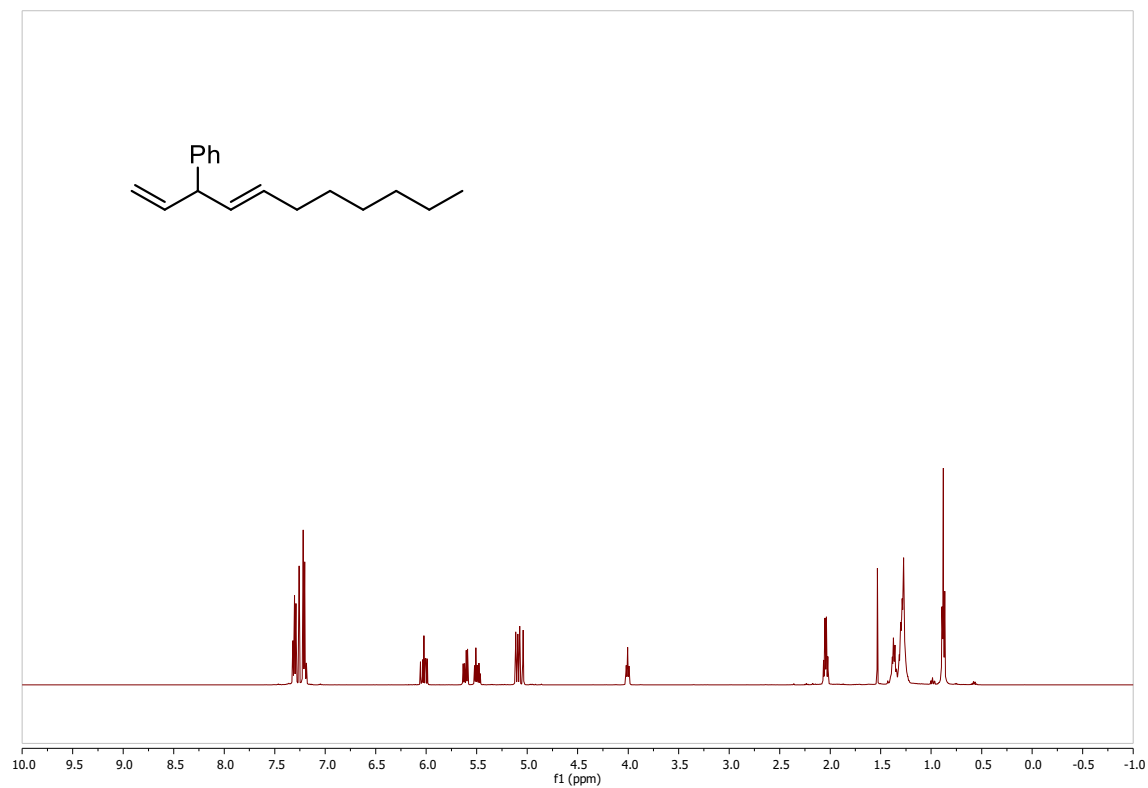
Scheme 2.12, Compound N:
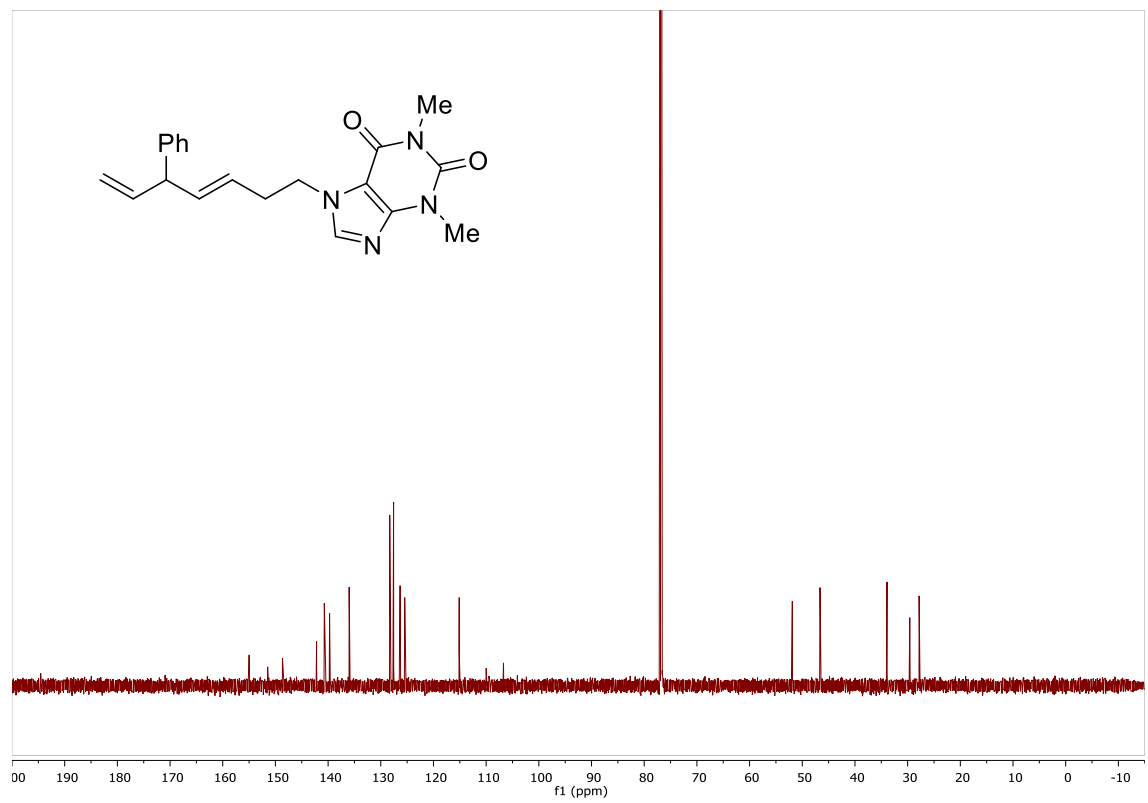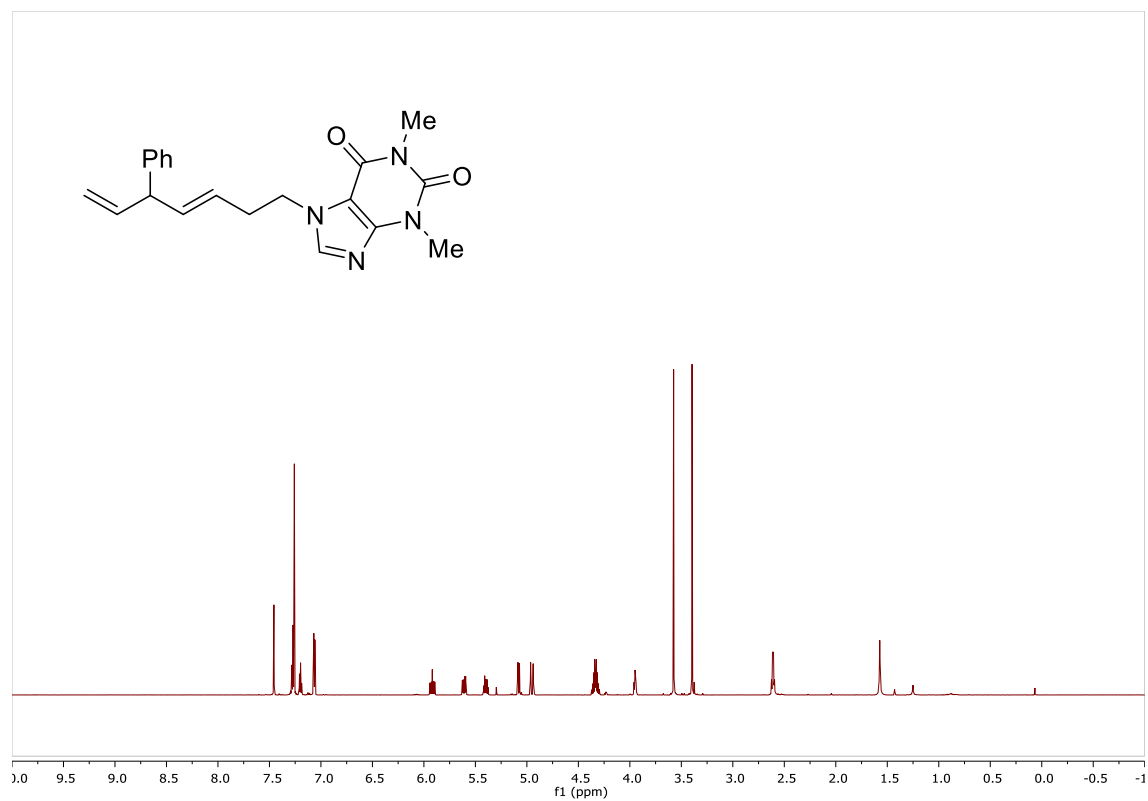
Scheme 2.18, Entry A:
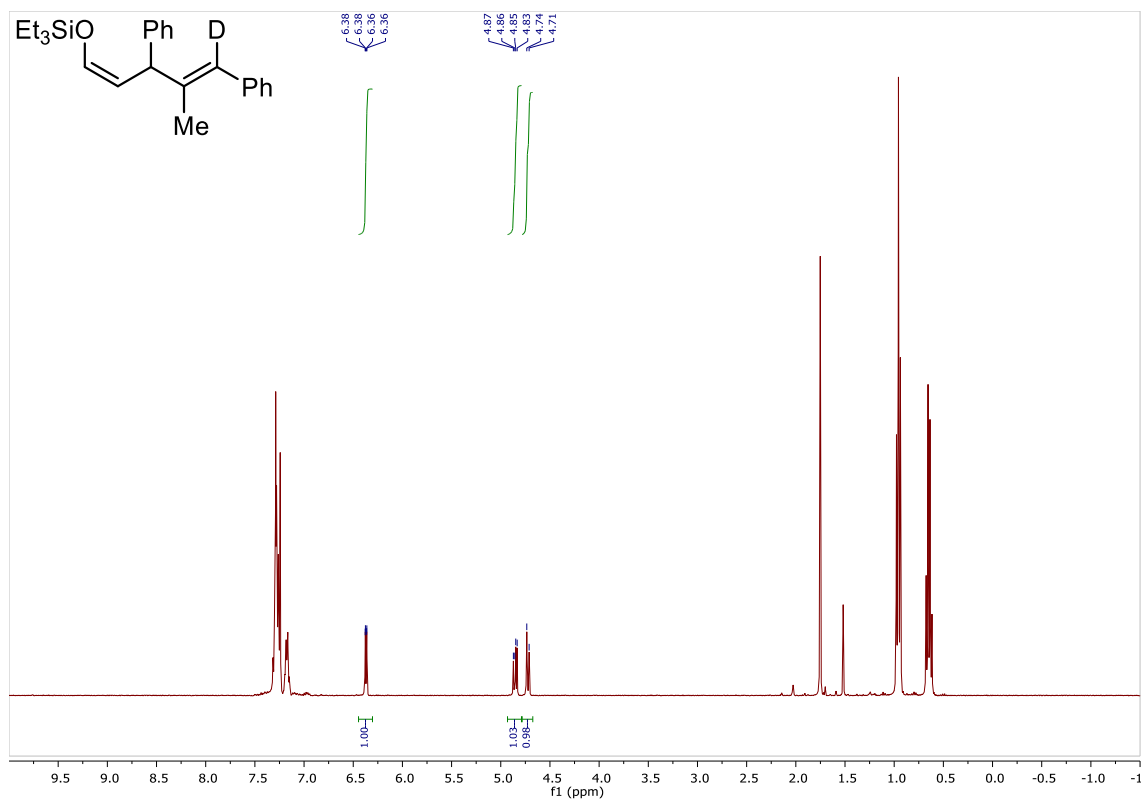
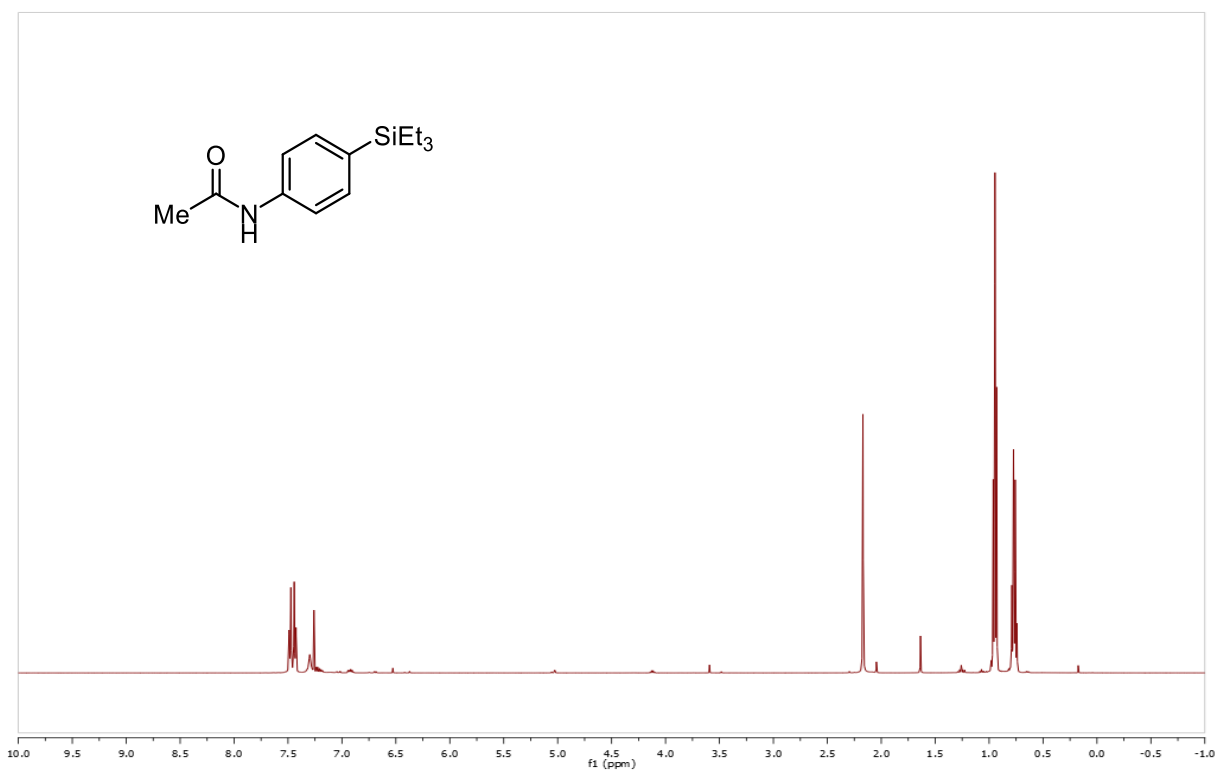**Scheme 2.18, Entry B:**
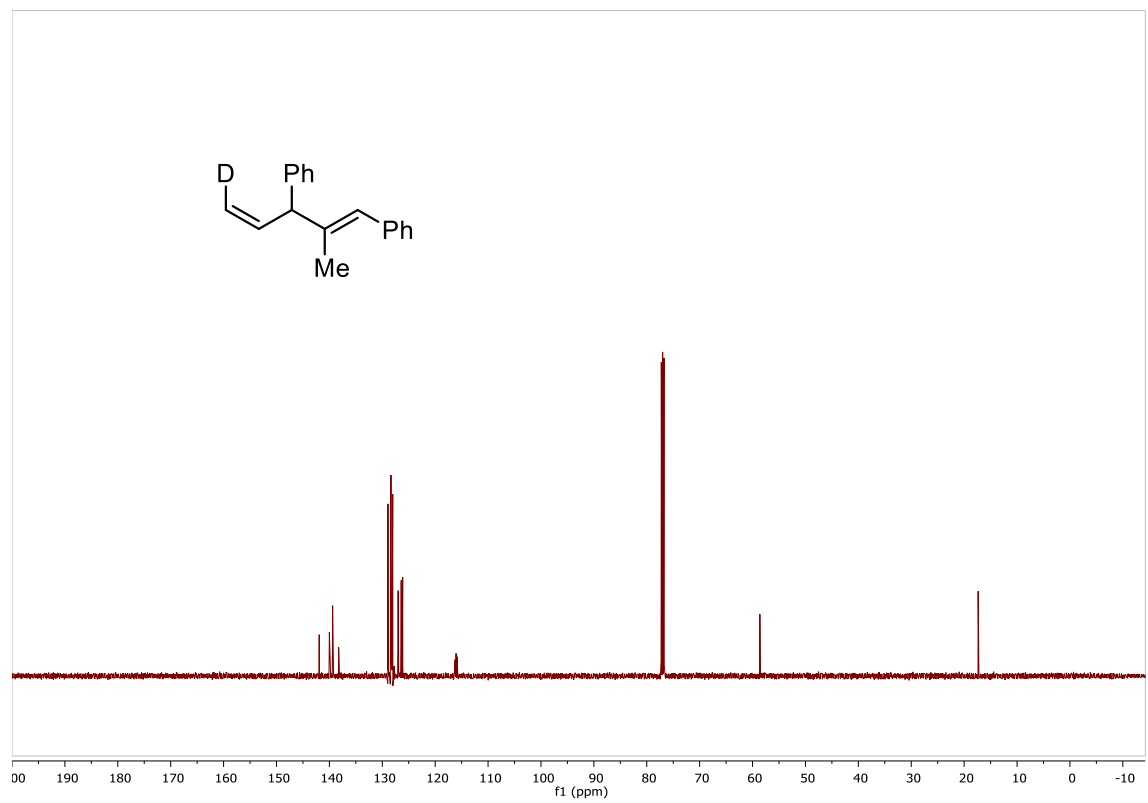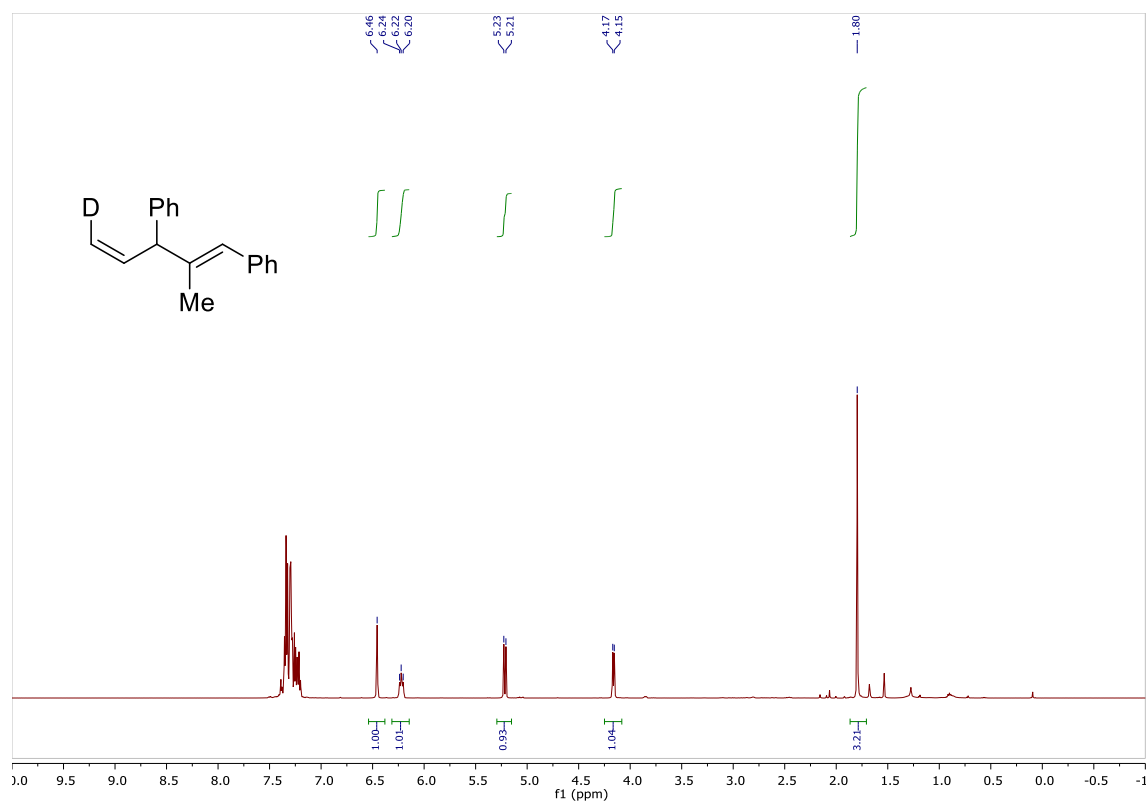
Scheme 2.18, Entry C:
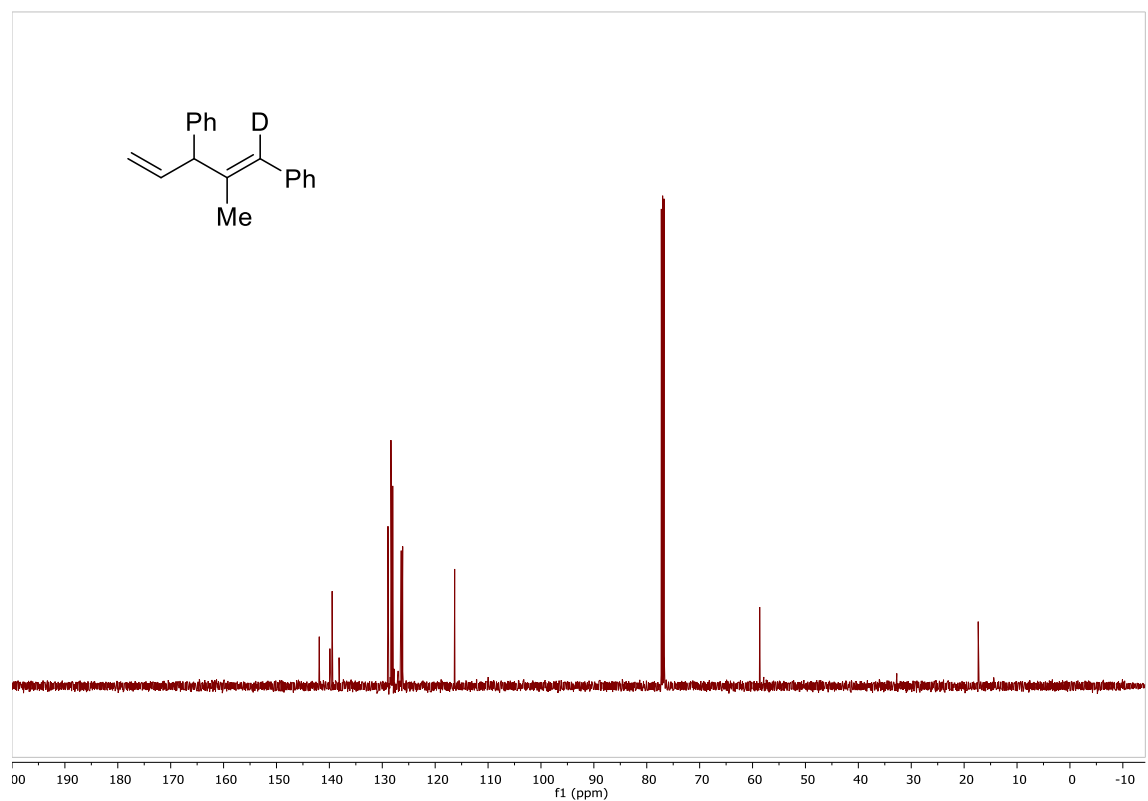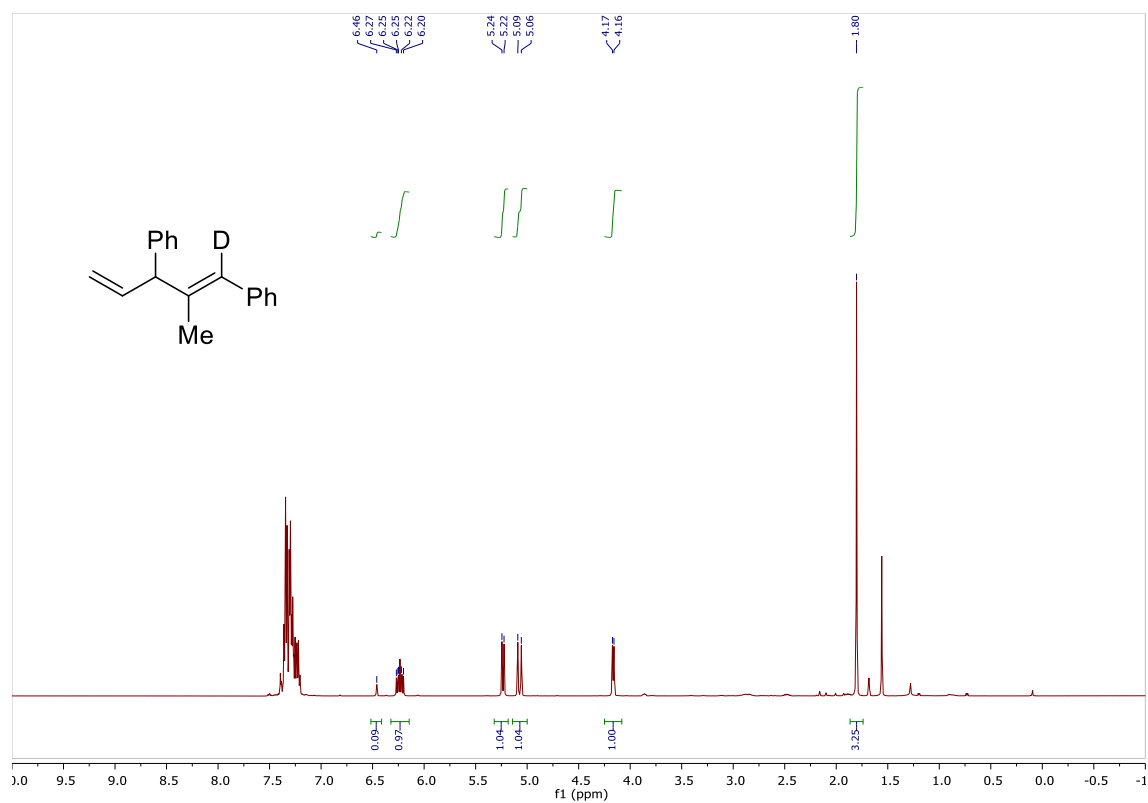
Scheme 3.17, Entry Q:
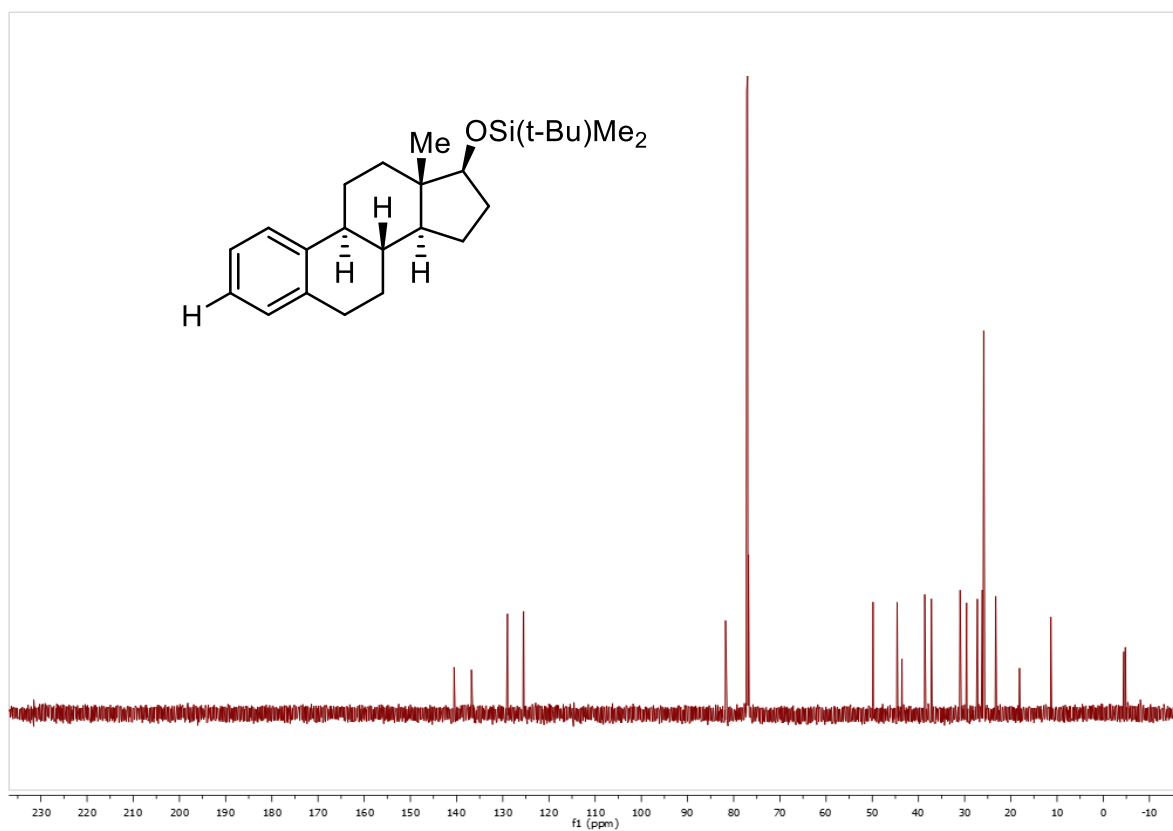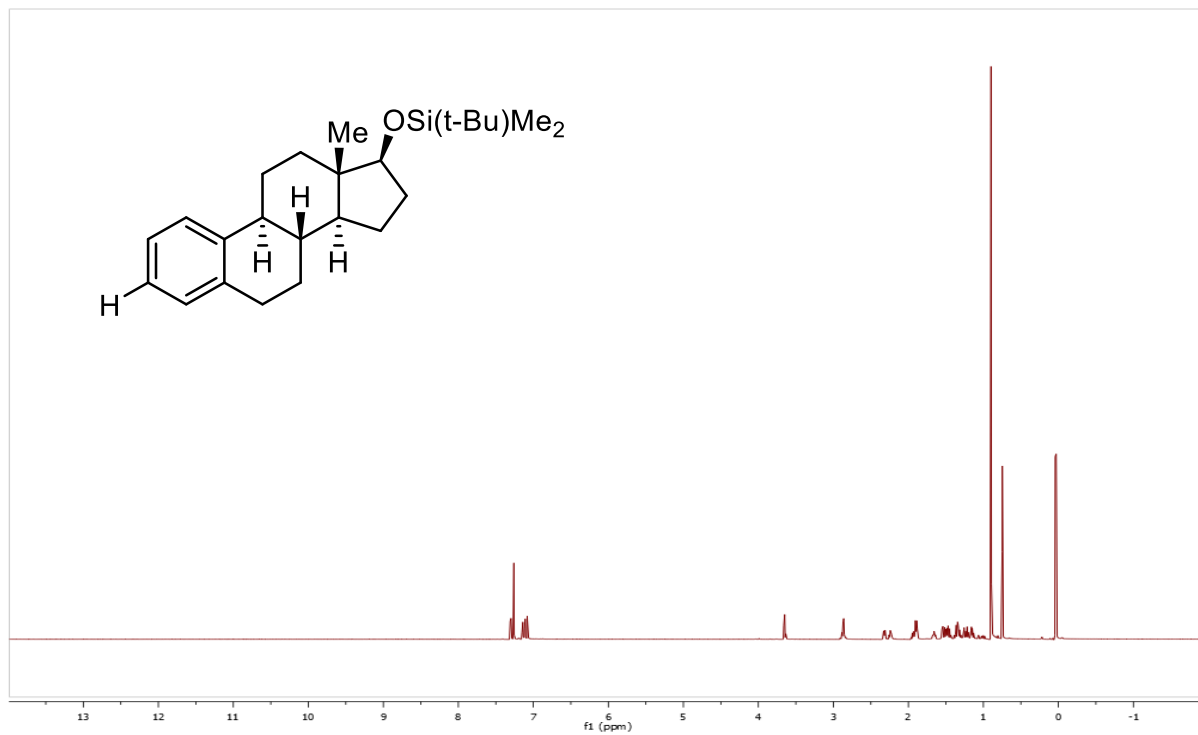
Scheme 3.29, Entry D:
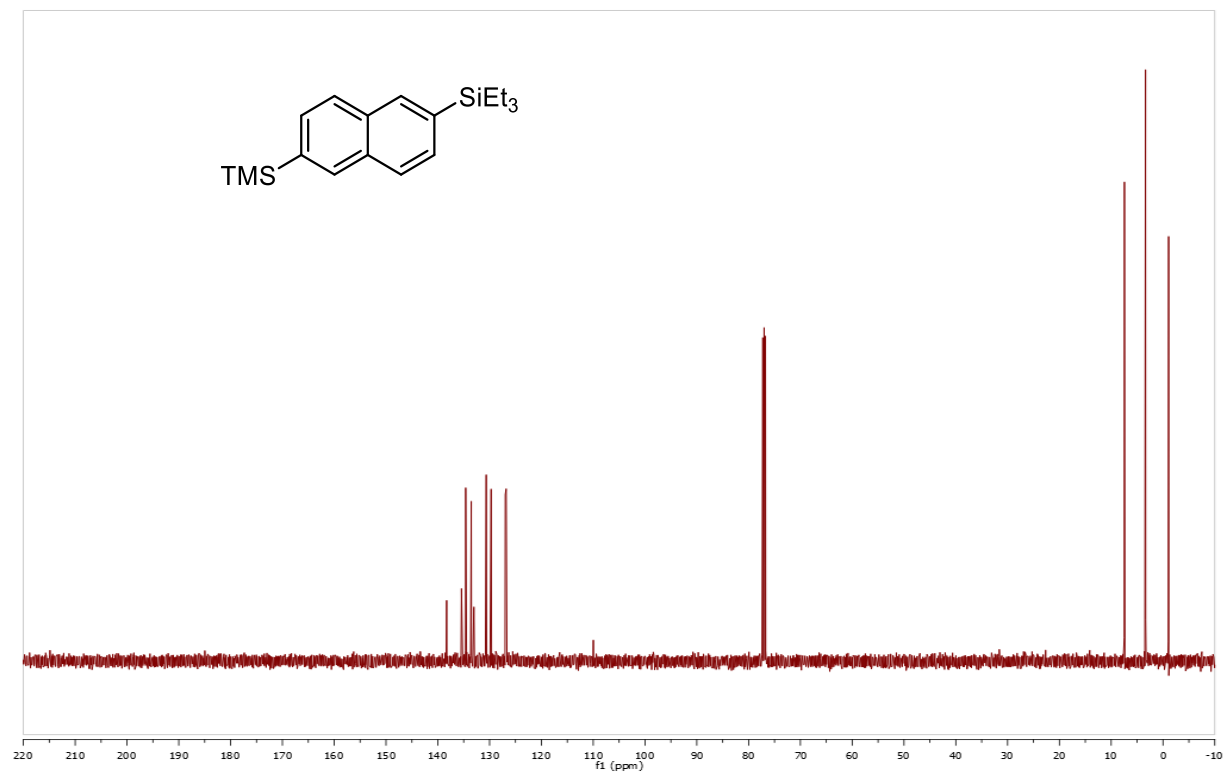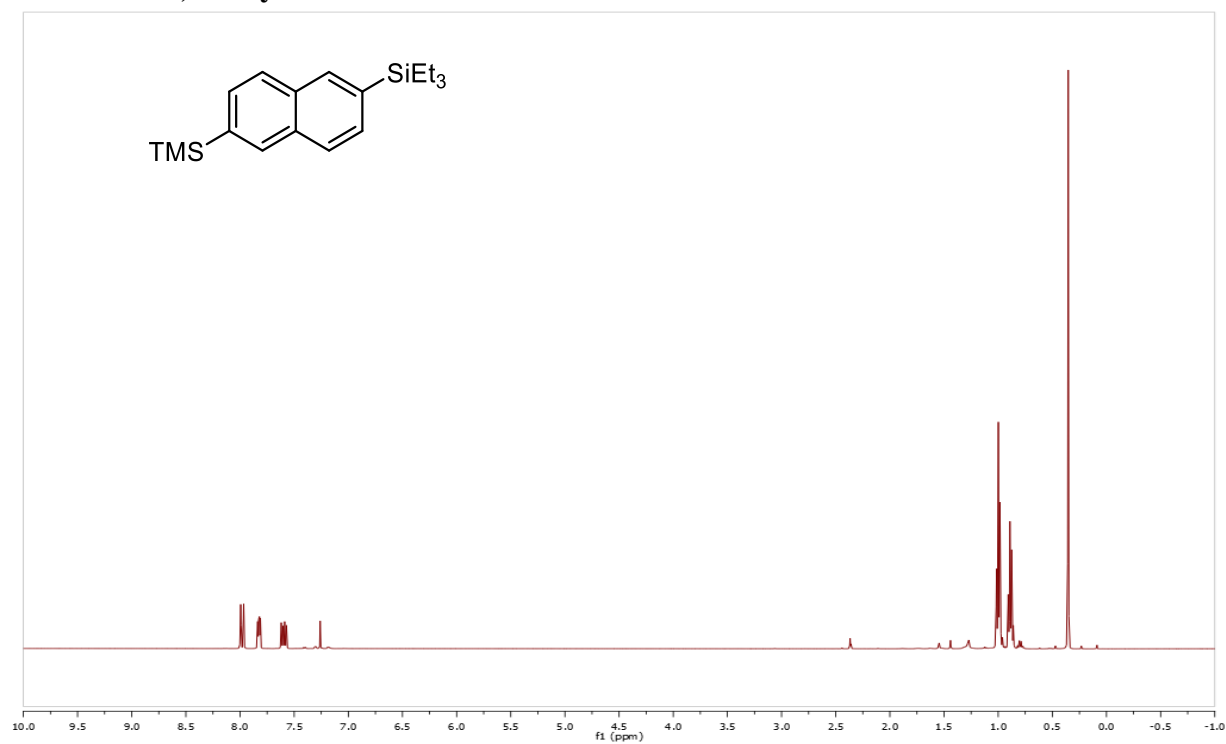
Scheme 3.29, Entry E:
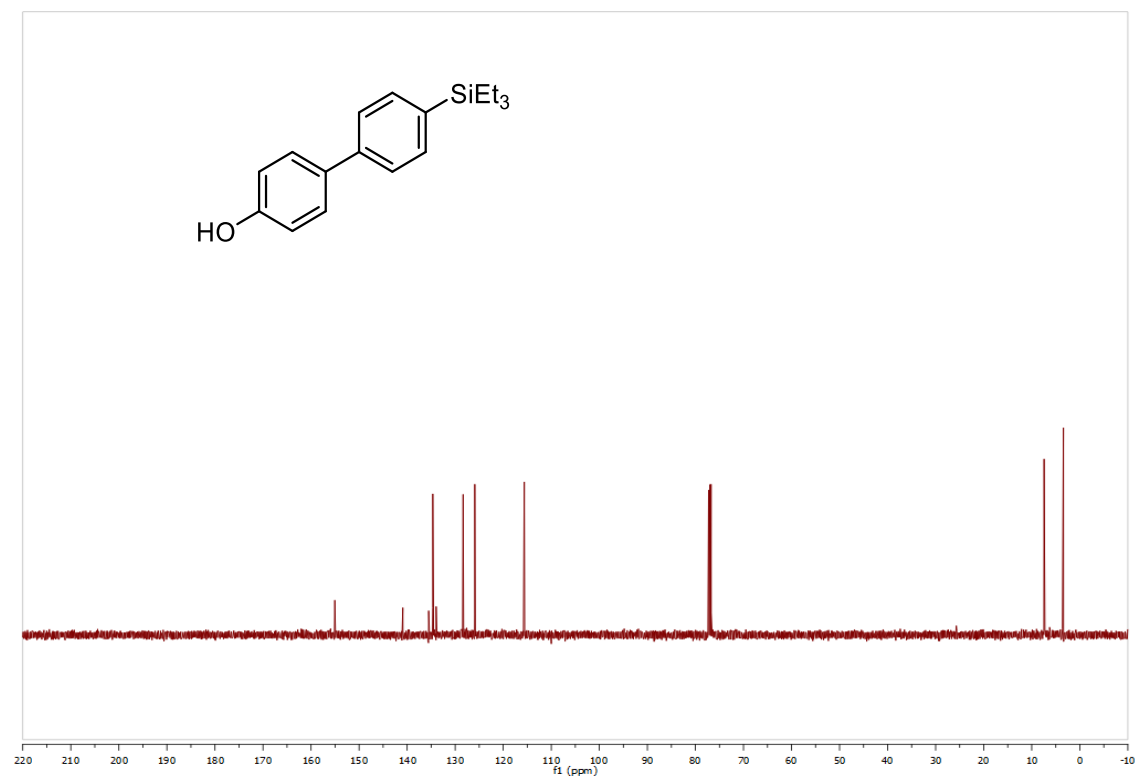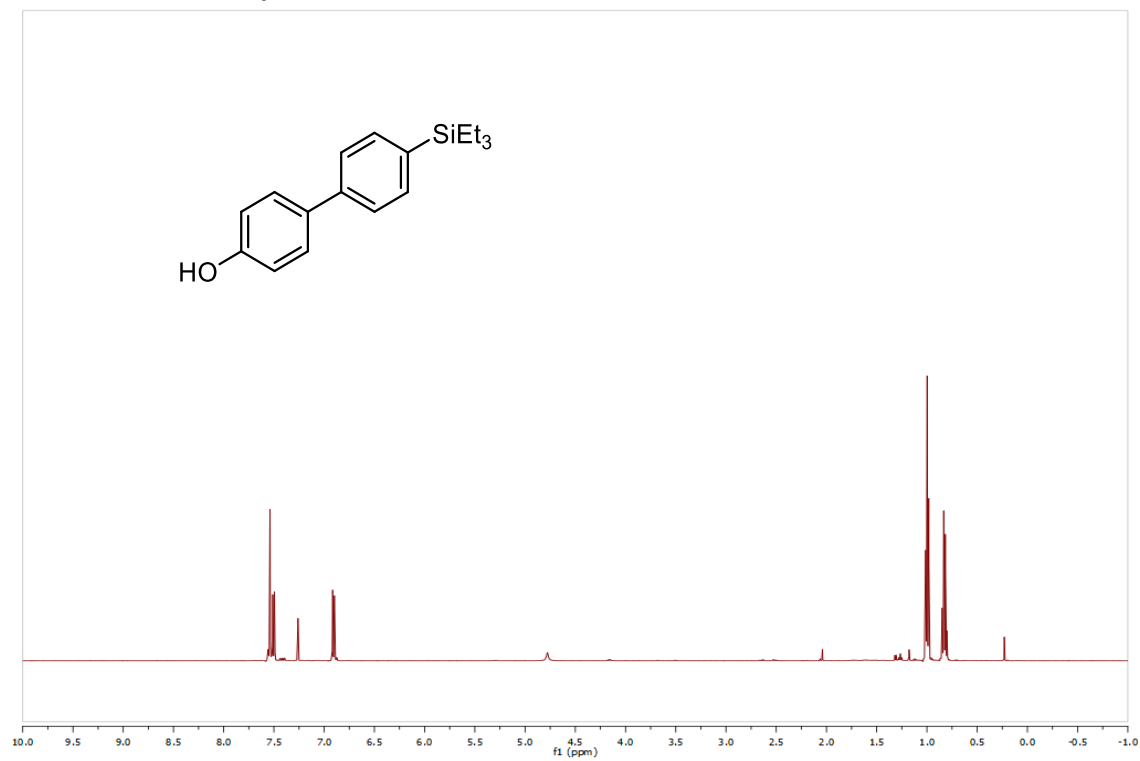
Scheme 3.29, Entry F:
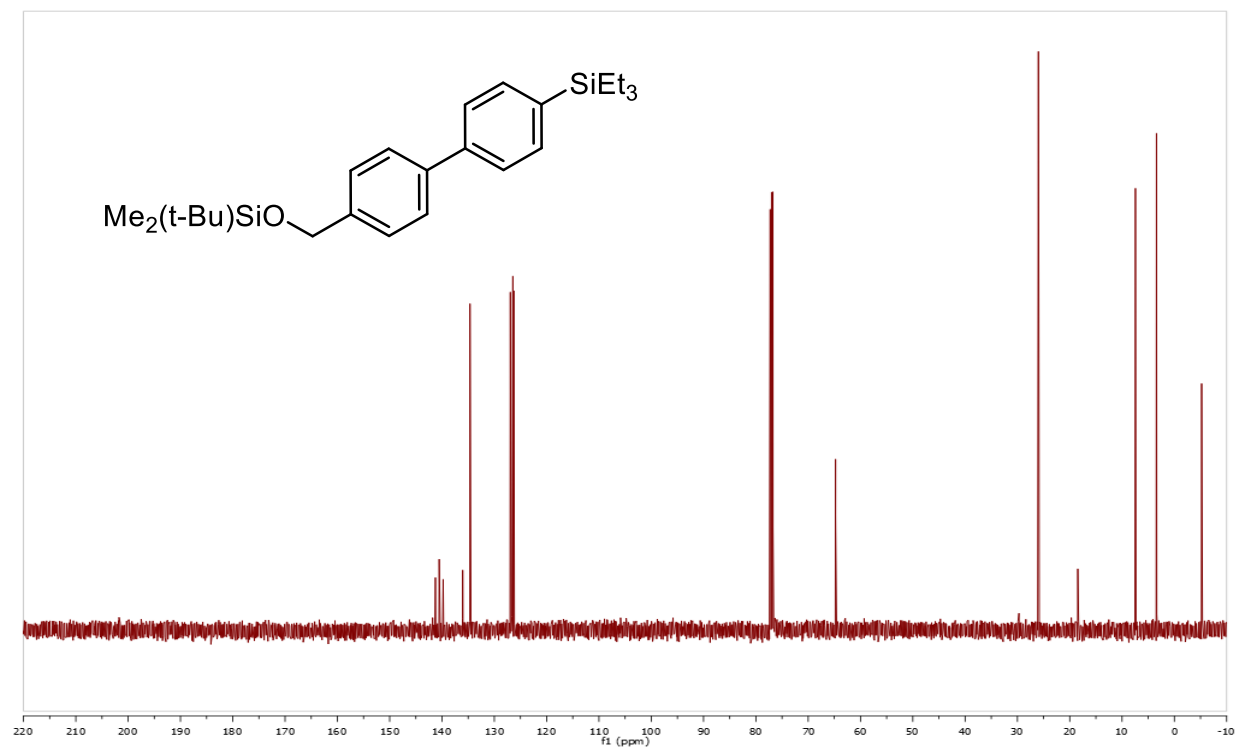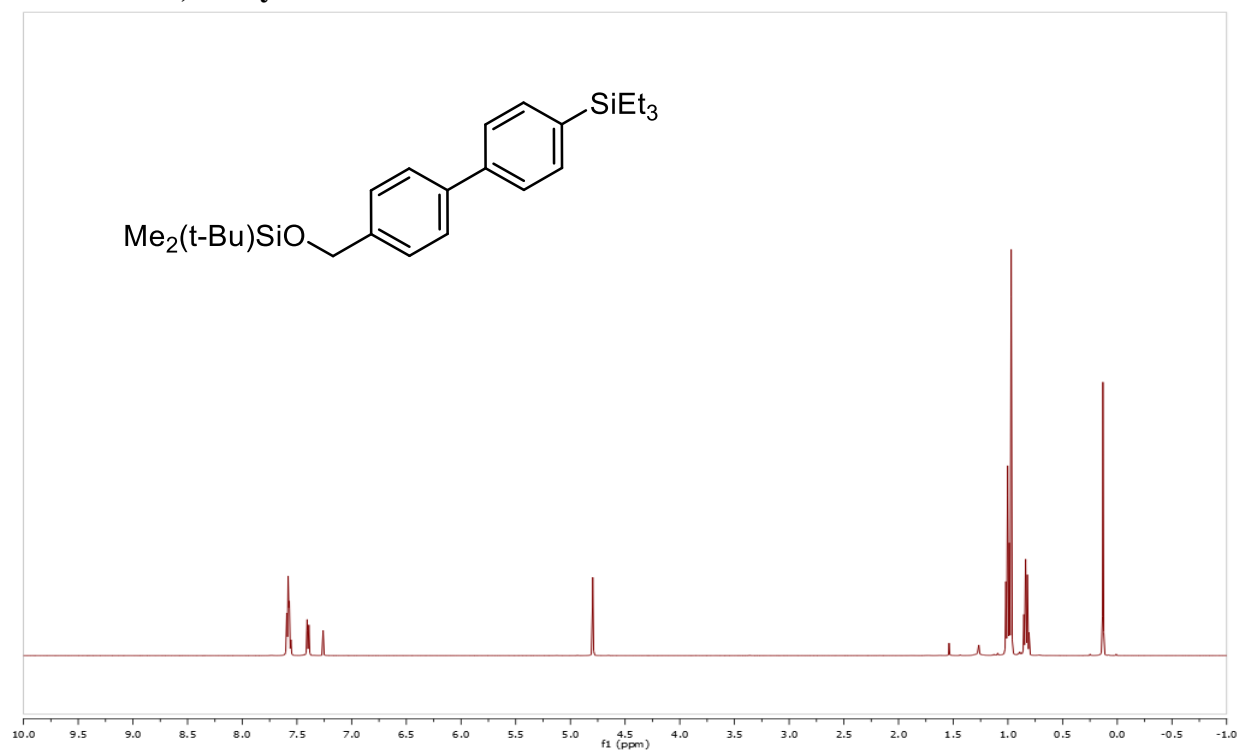
Scheme 3.29, Entry G:
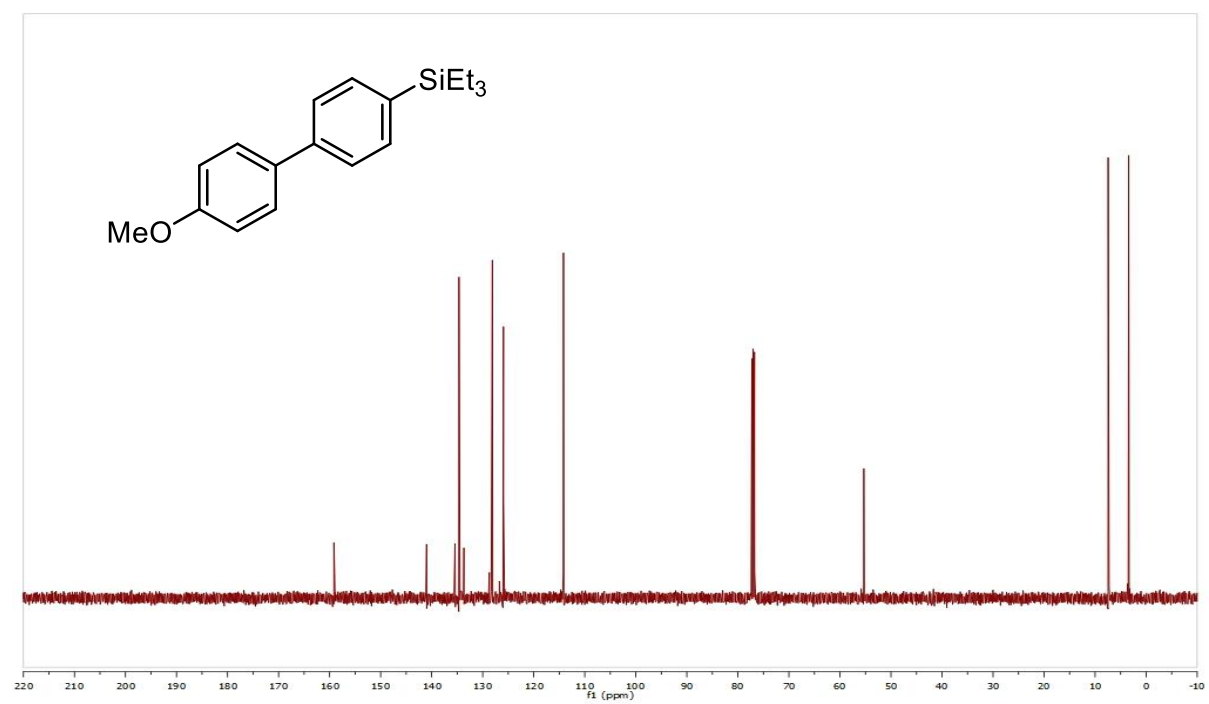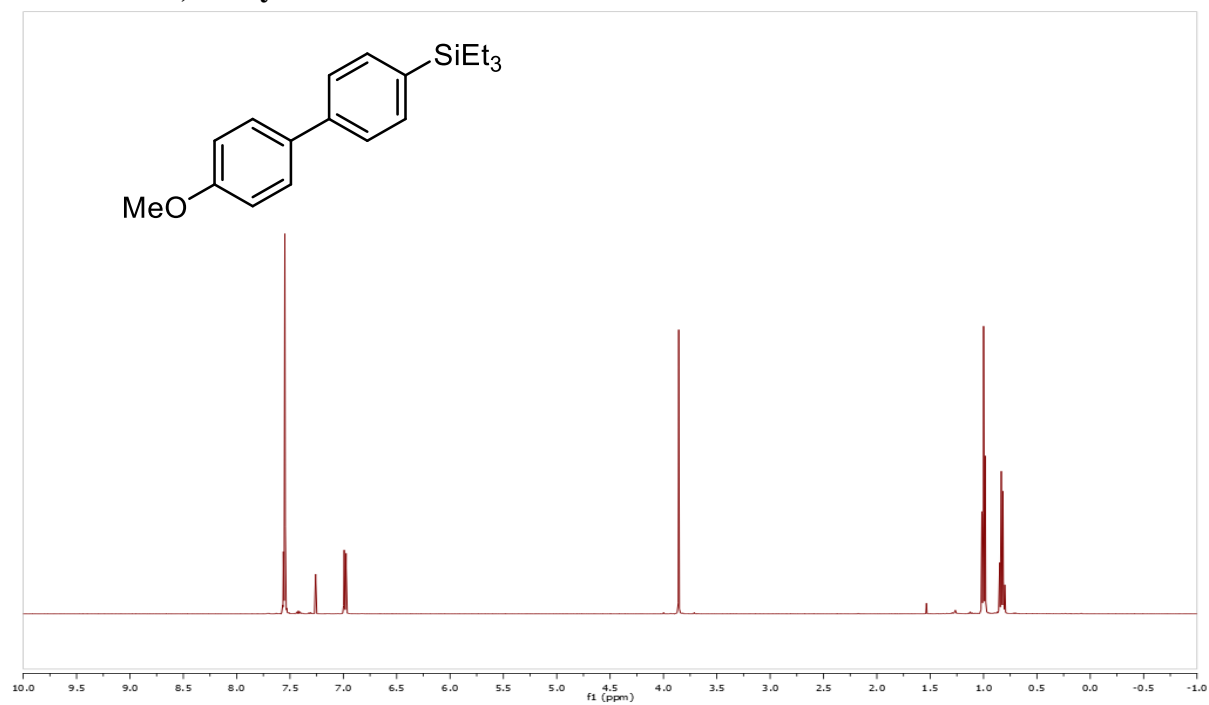
Scheme 3.29, Entry H:
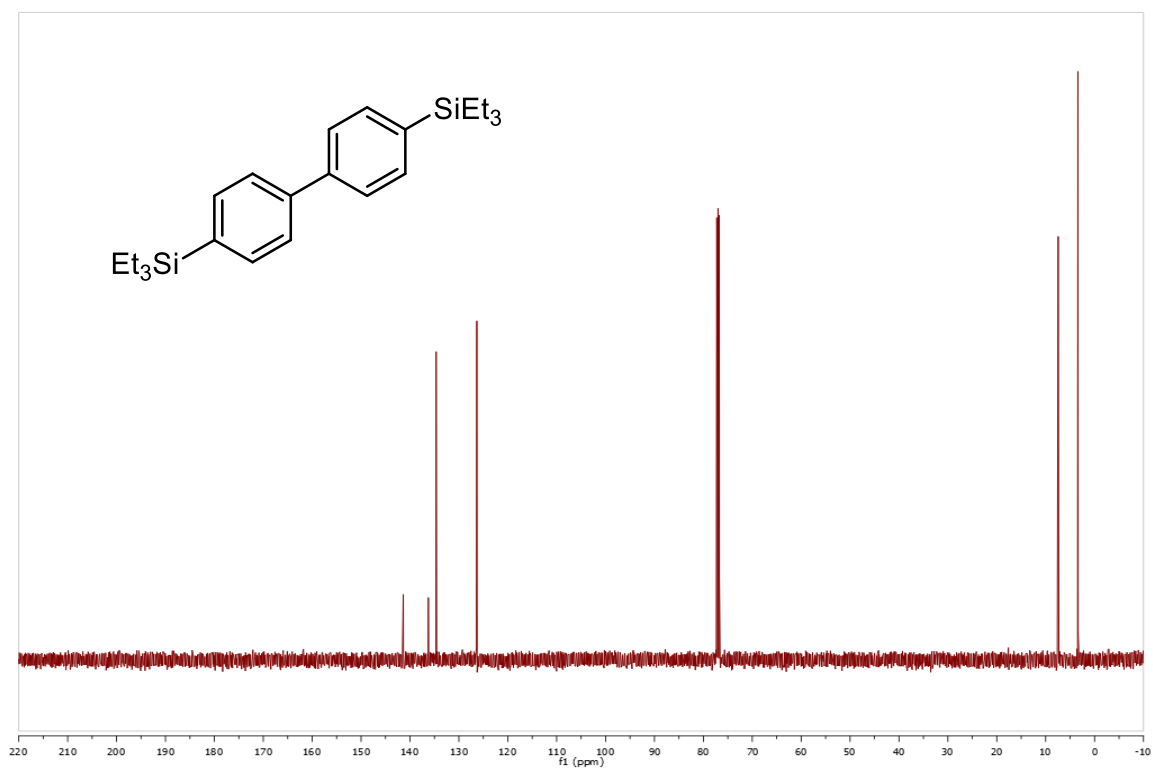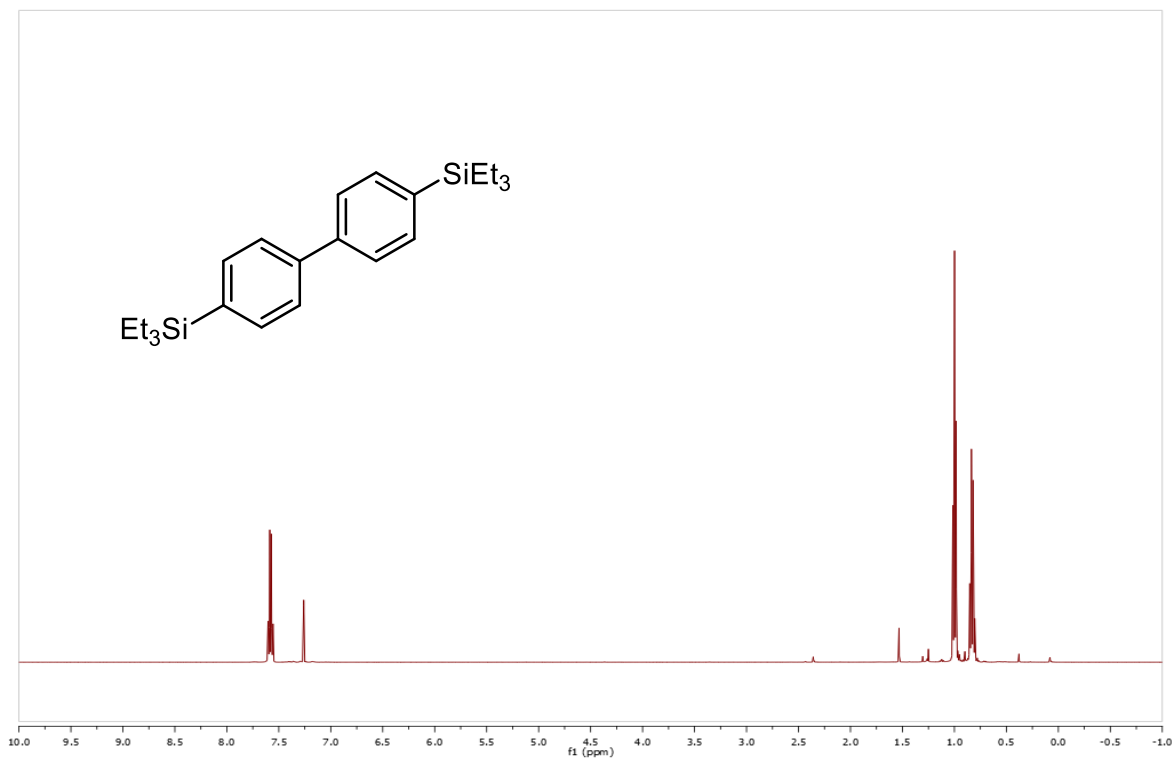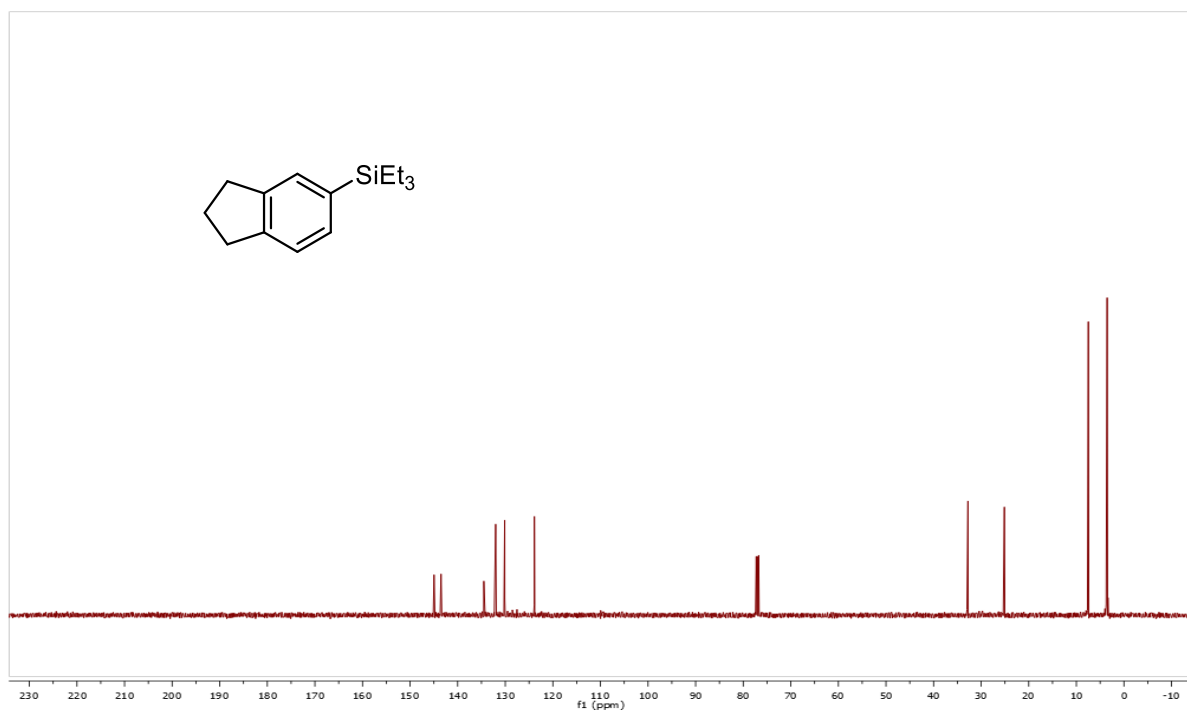
Scheme 3.29, Entry I:
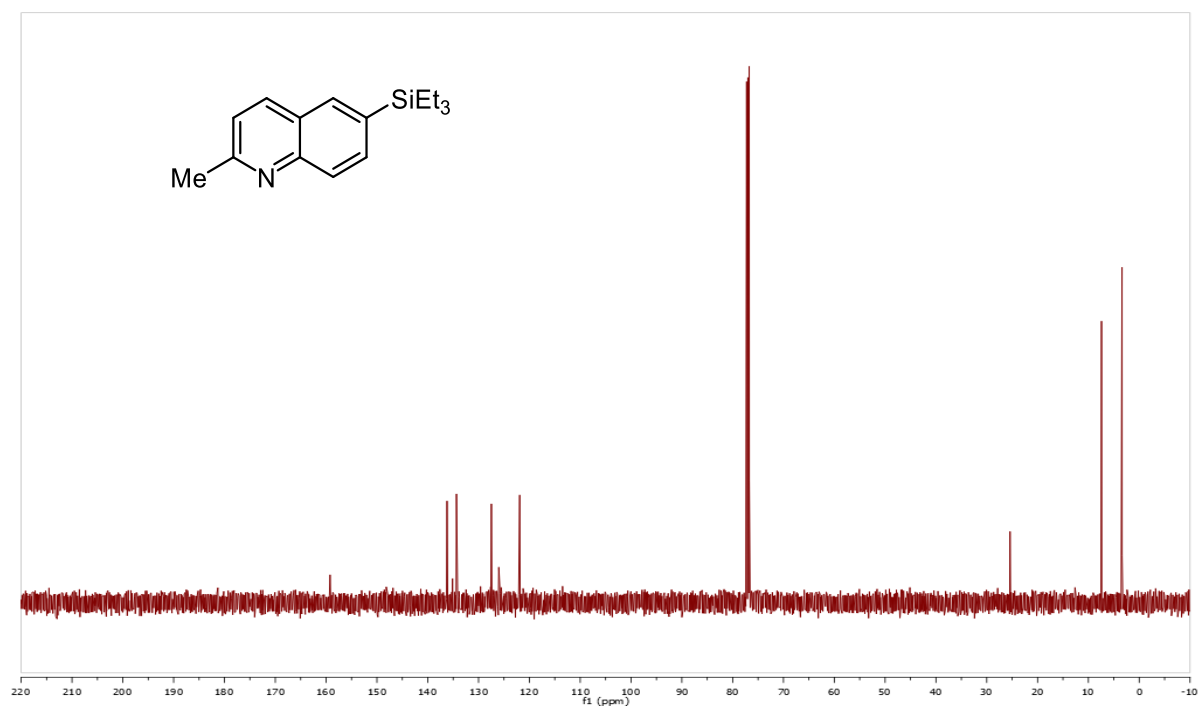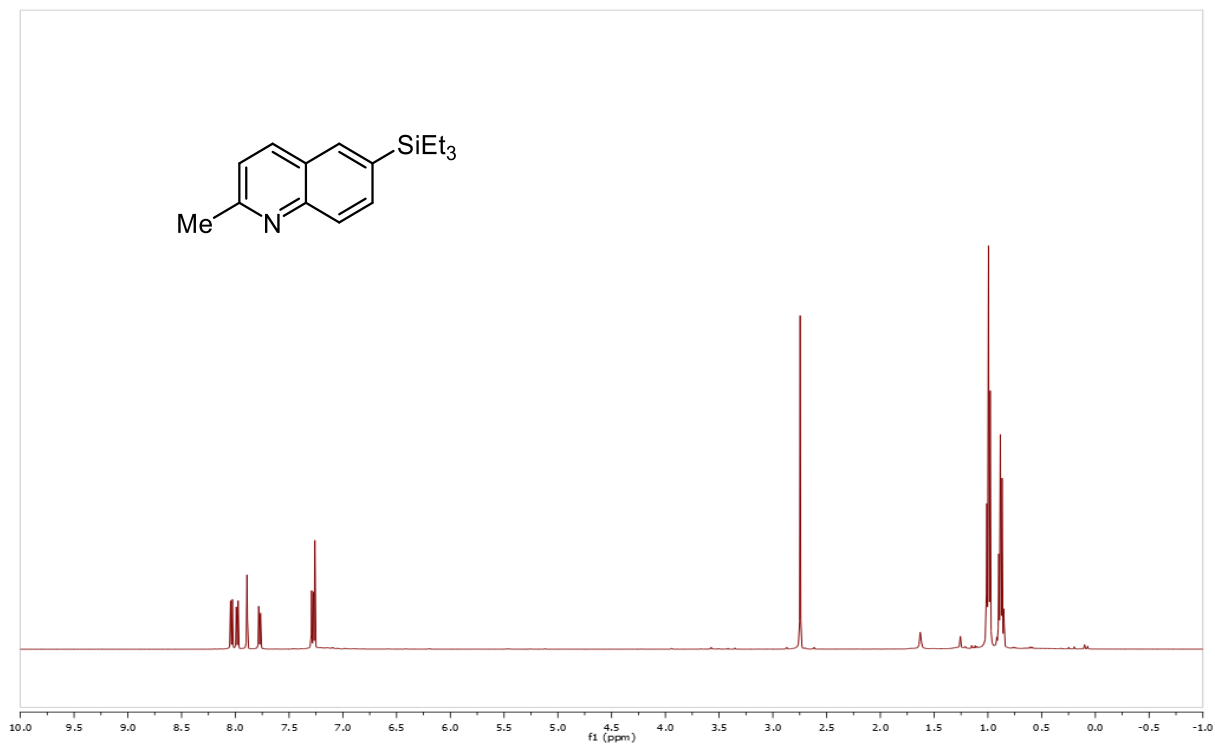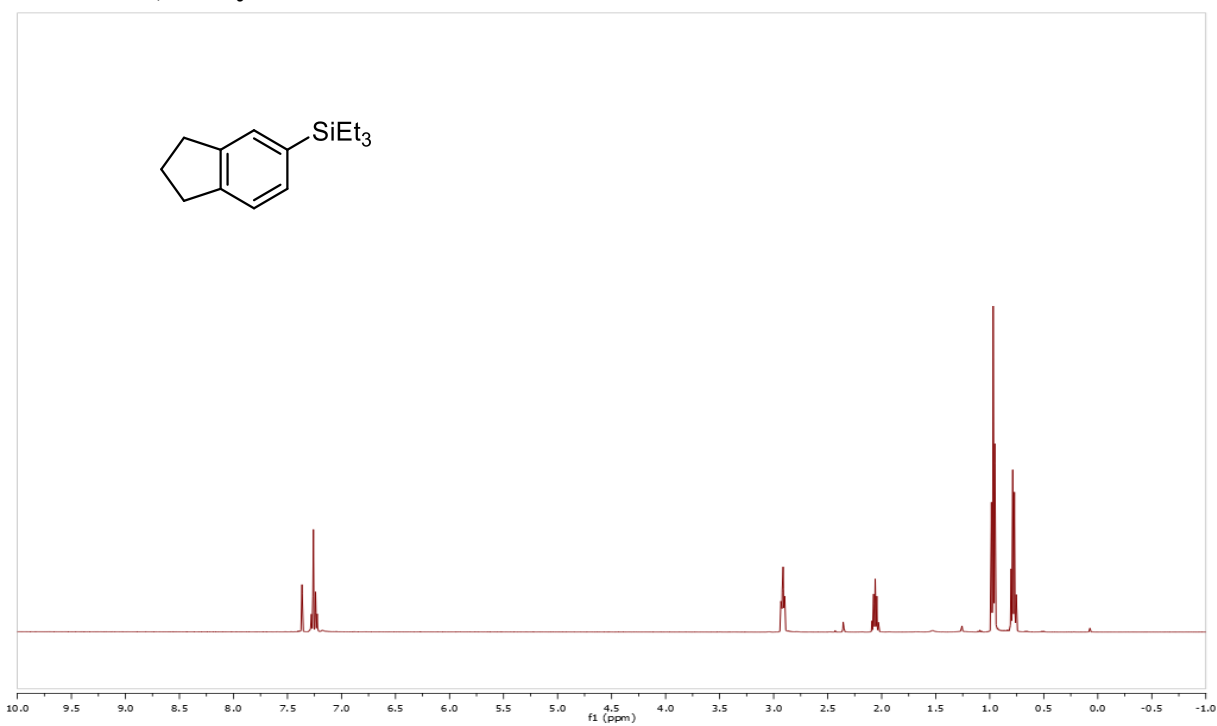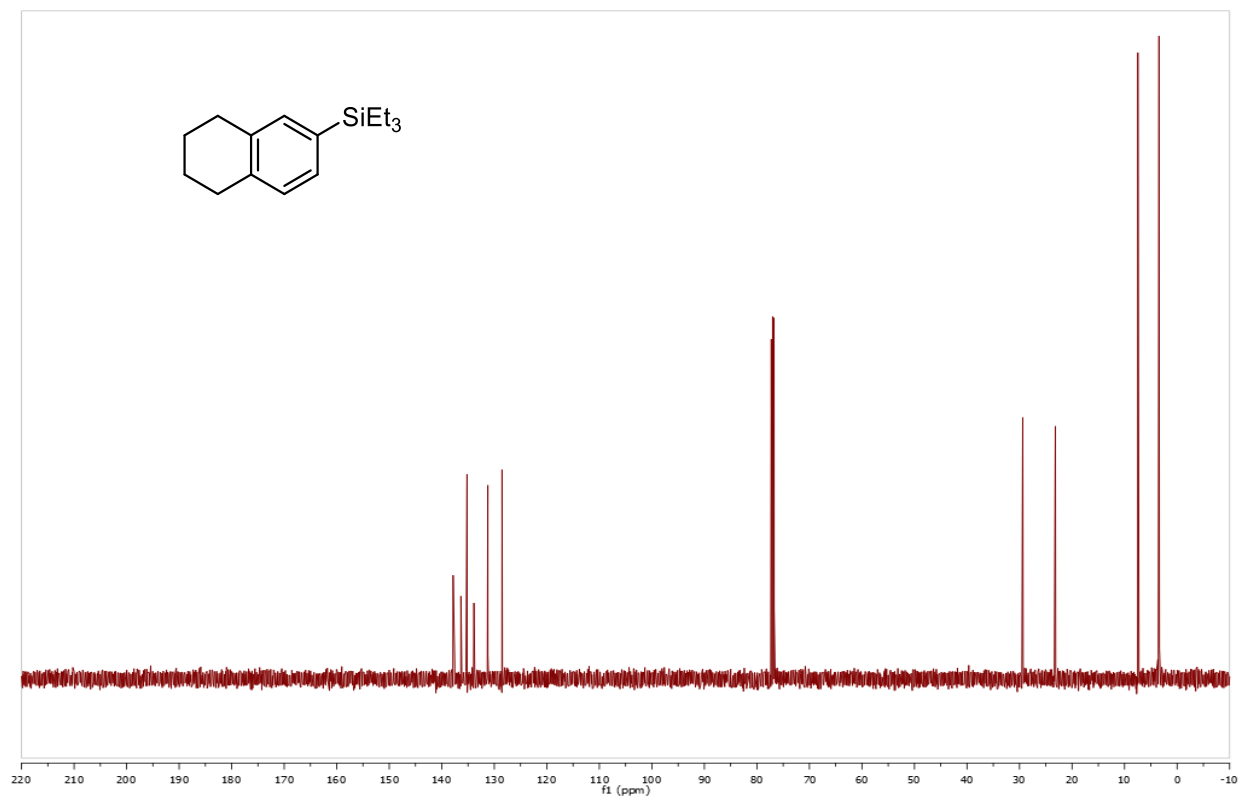
Scheme 3.29, Entry J:
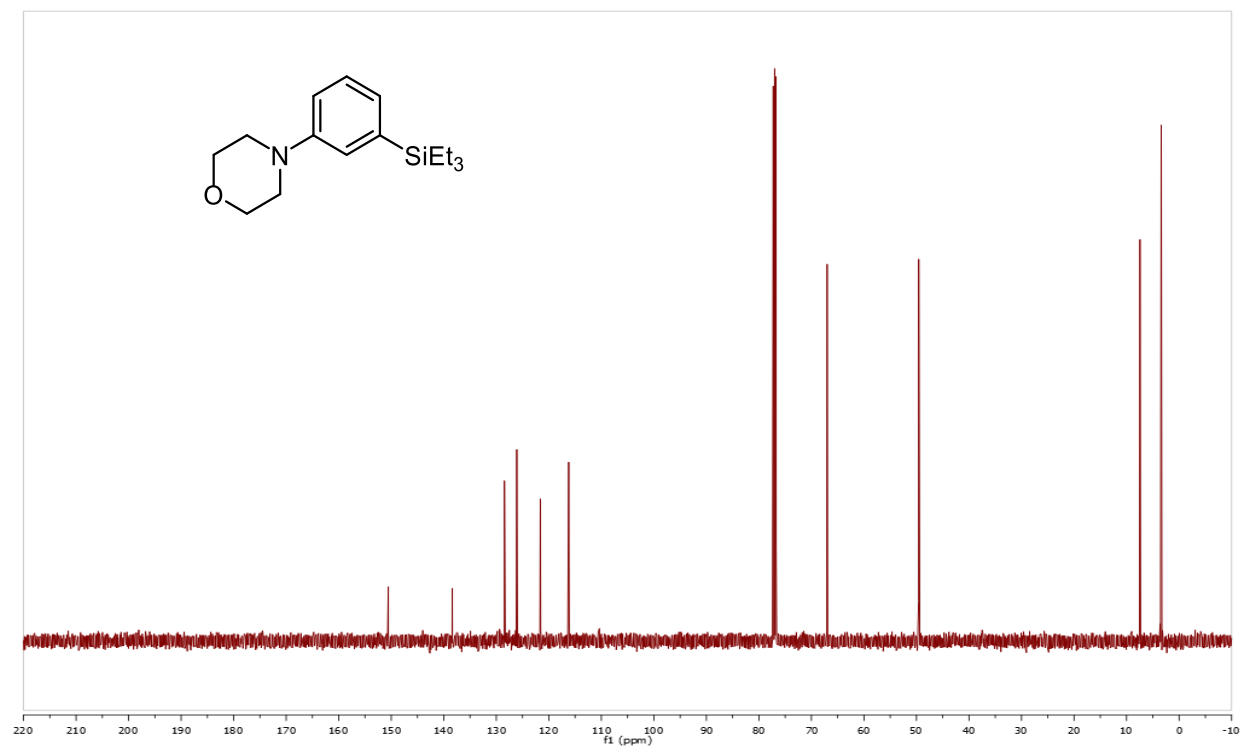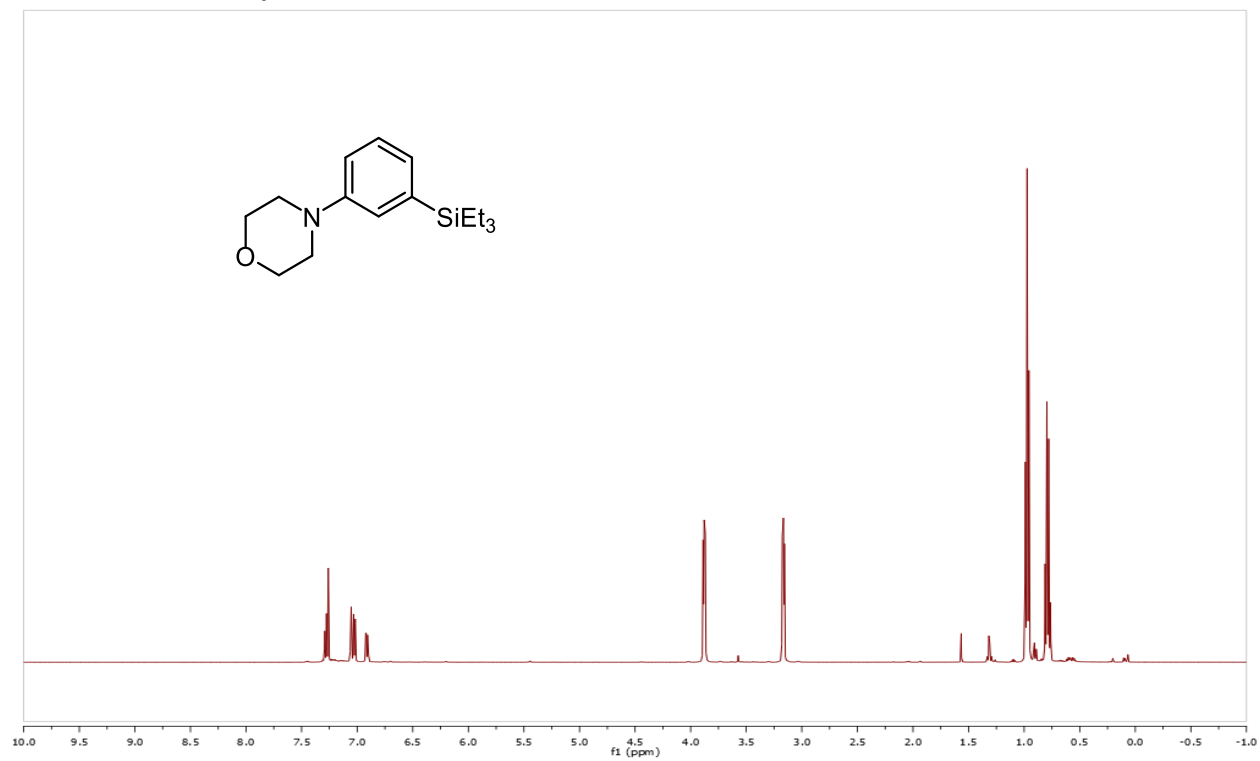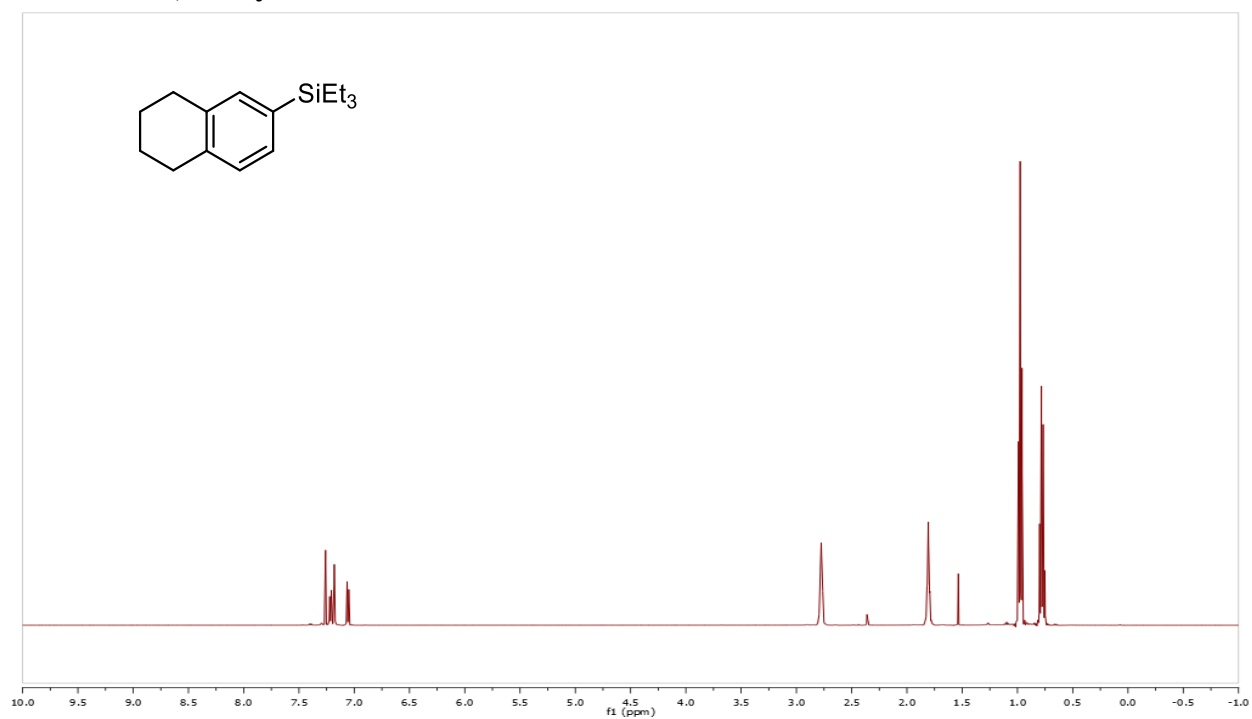
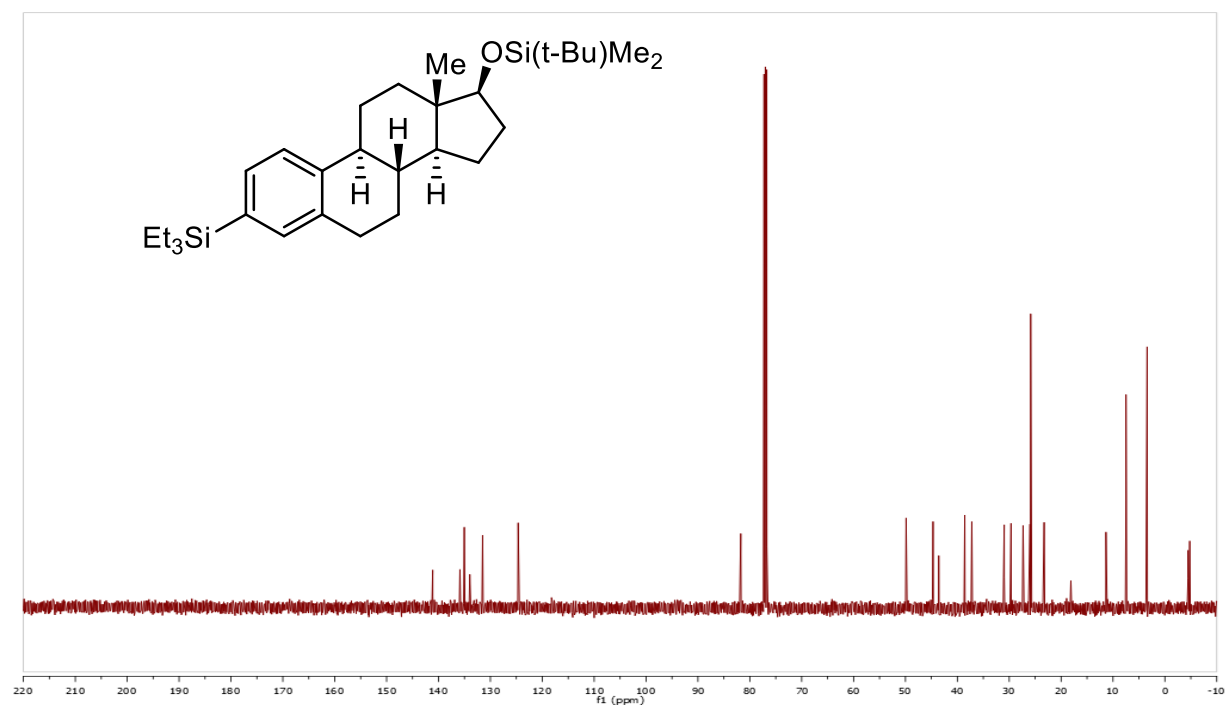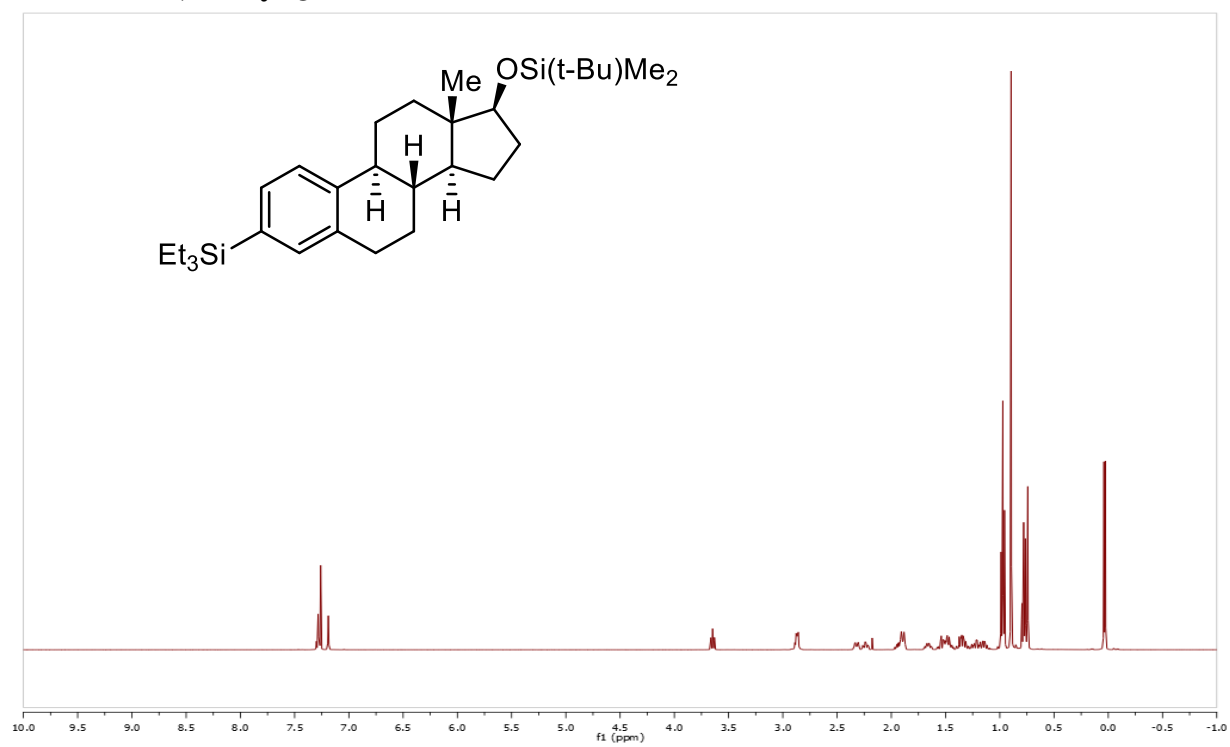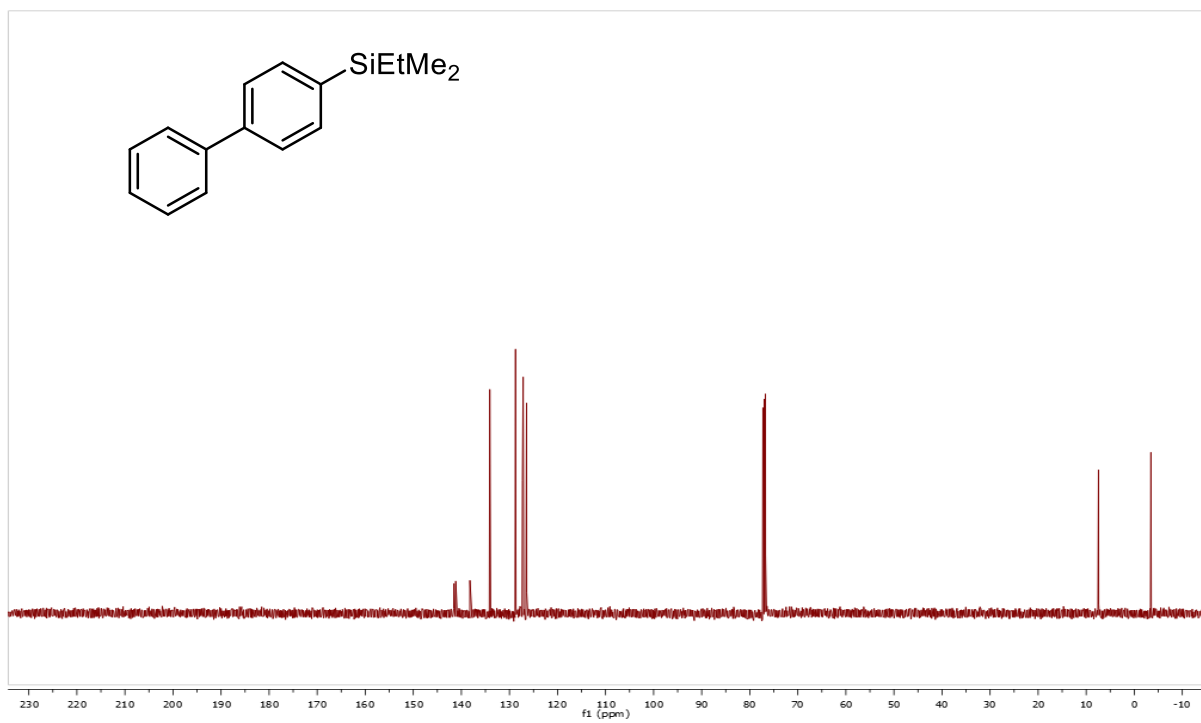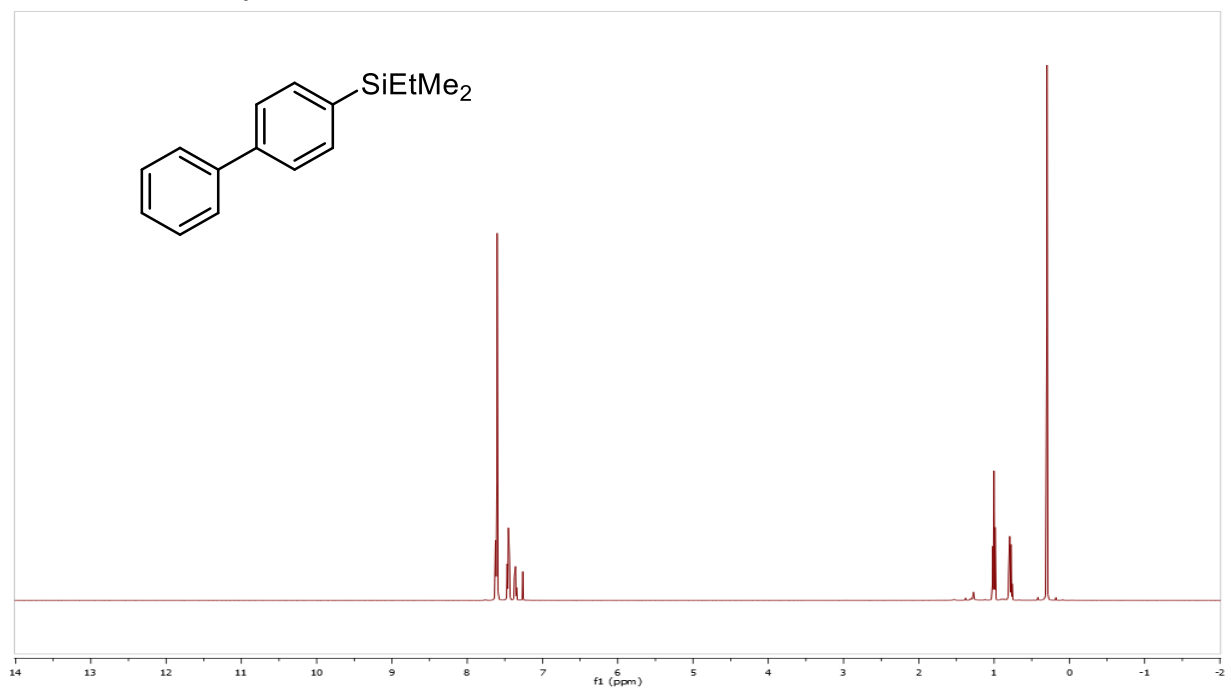**Scheme 3.29, Entry K:**
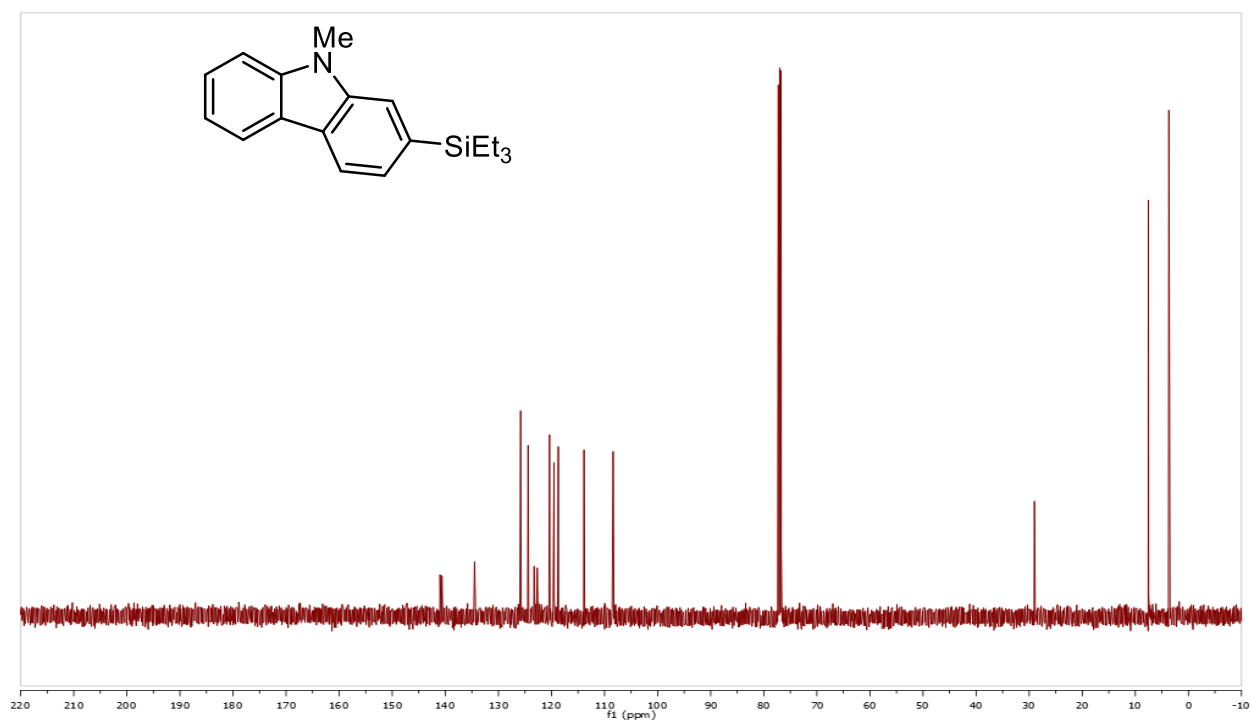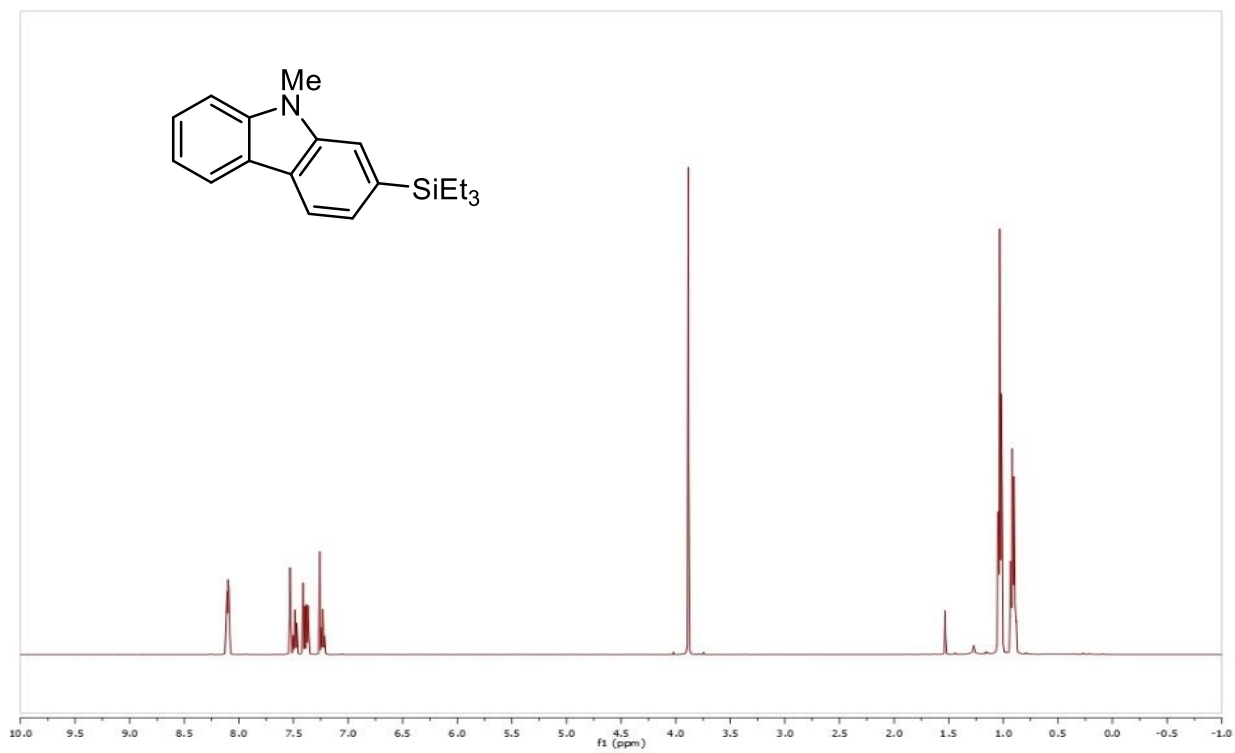
Scheme 3.29, Entry L
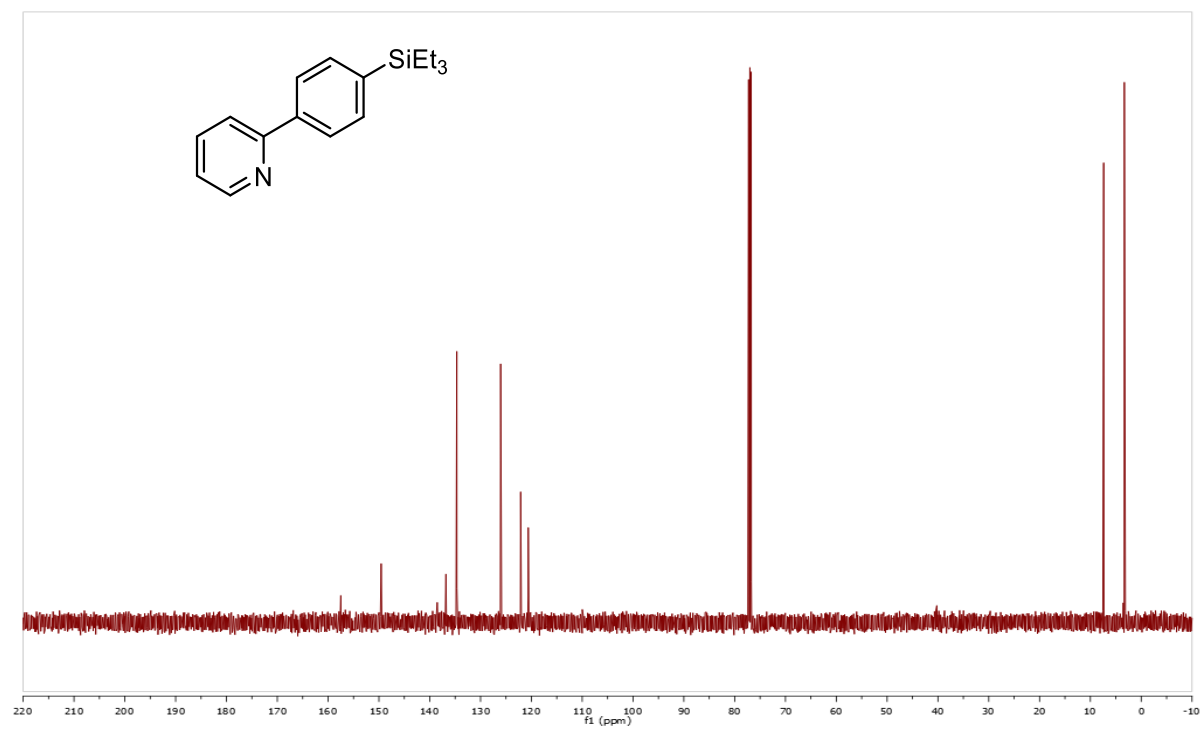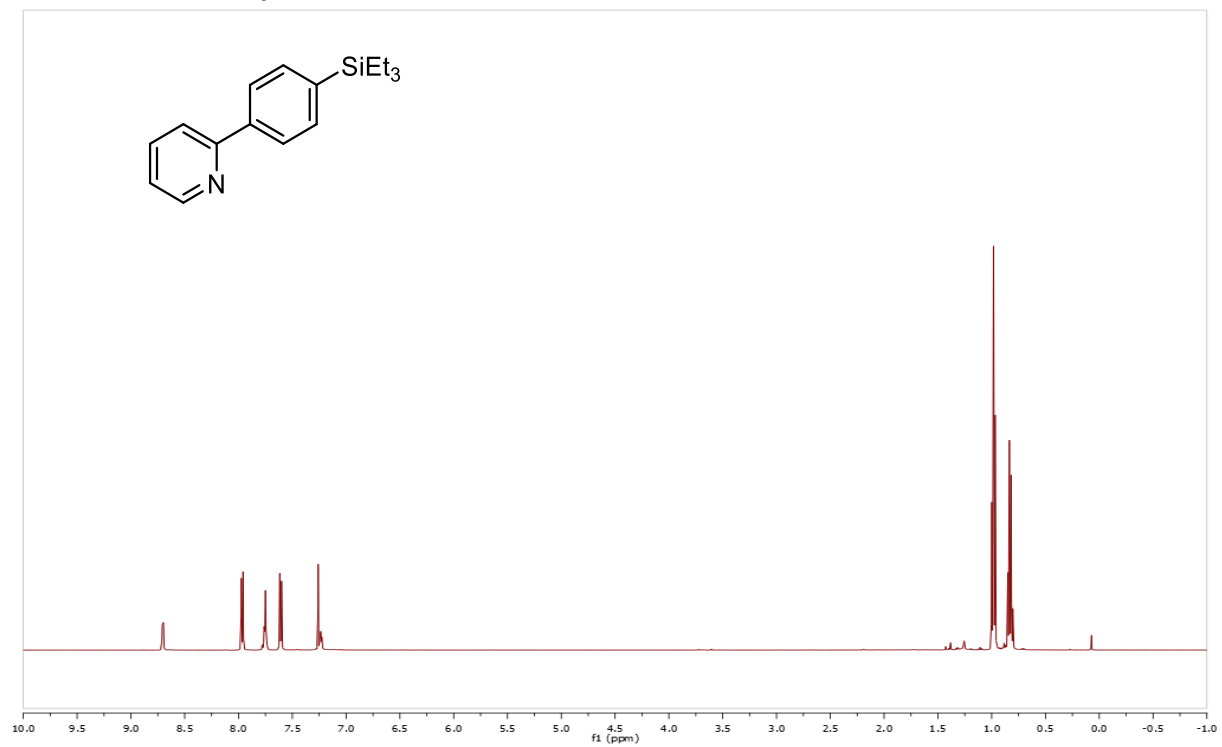
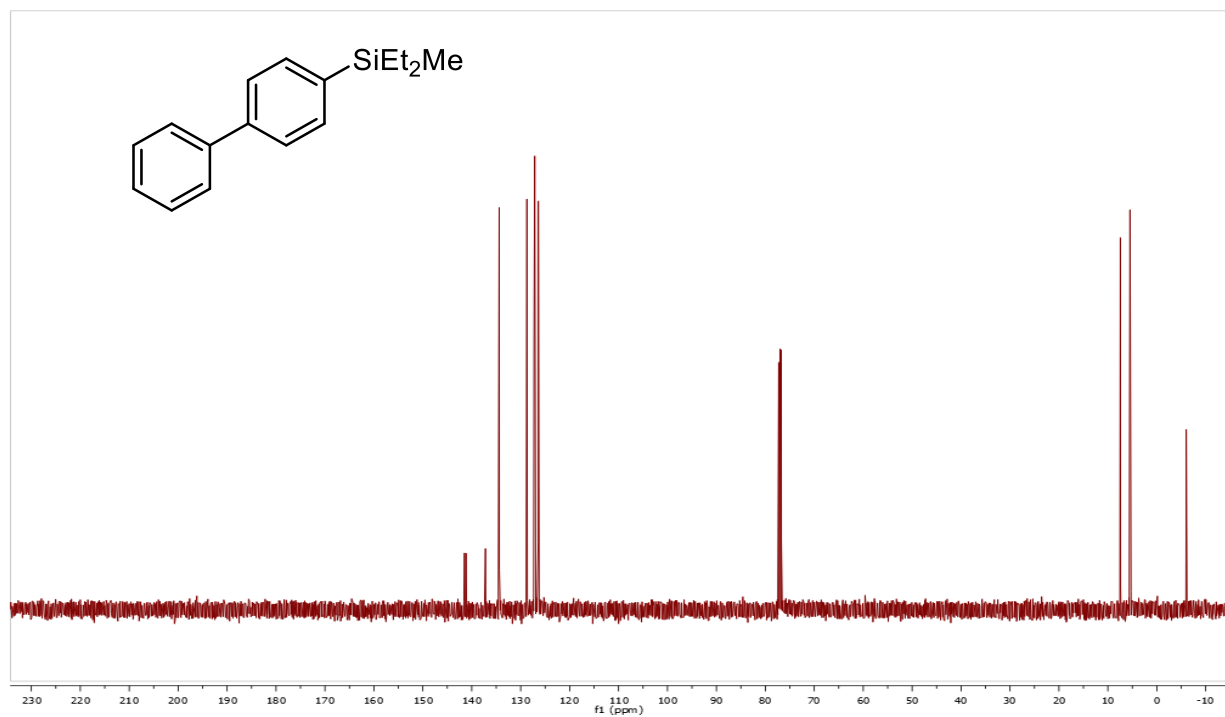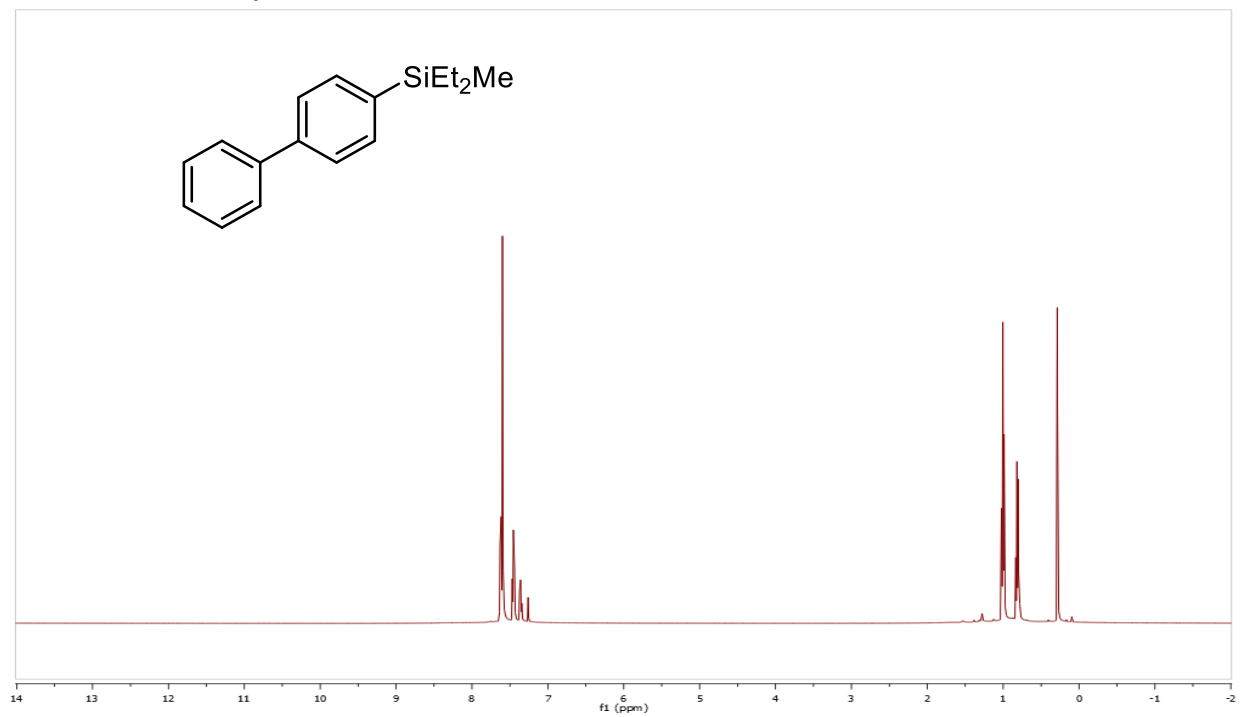**Scheme 3.29, Entry M:**
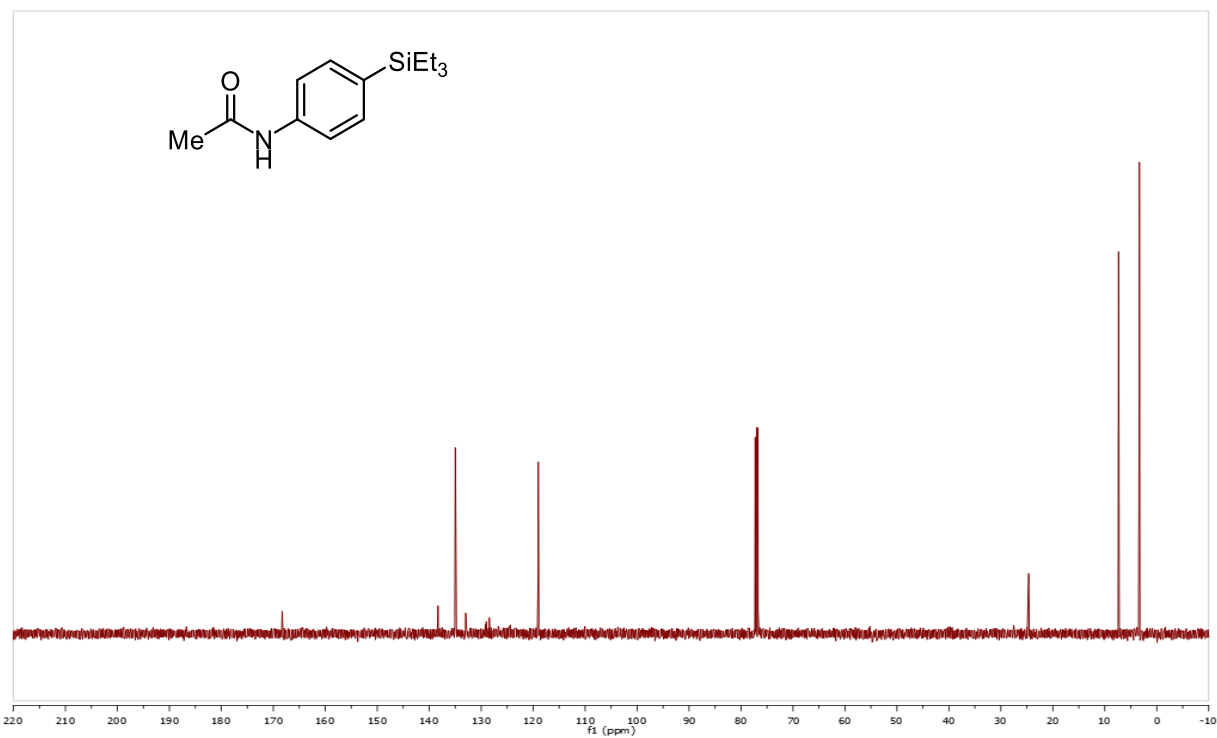
Scheme 3.29, Entry O:

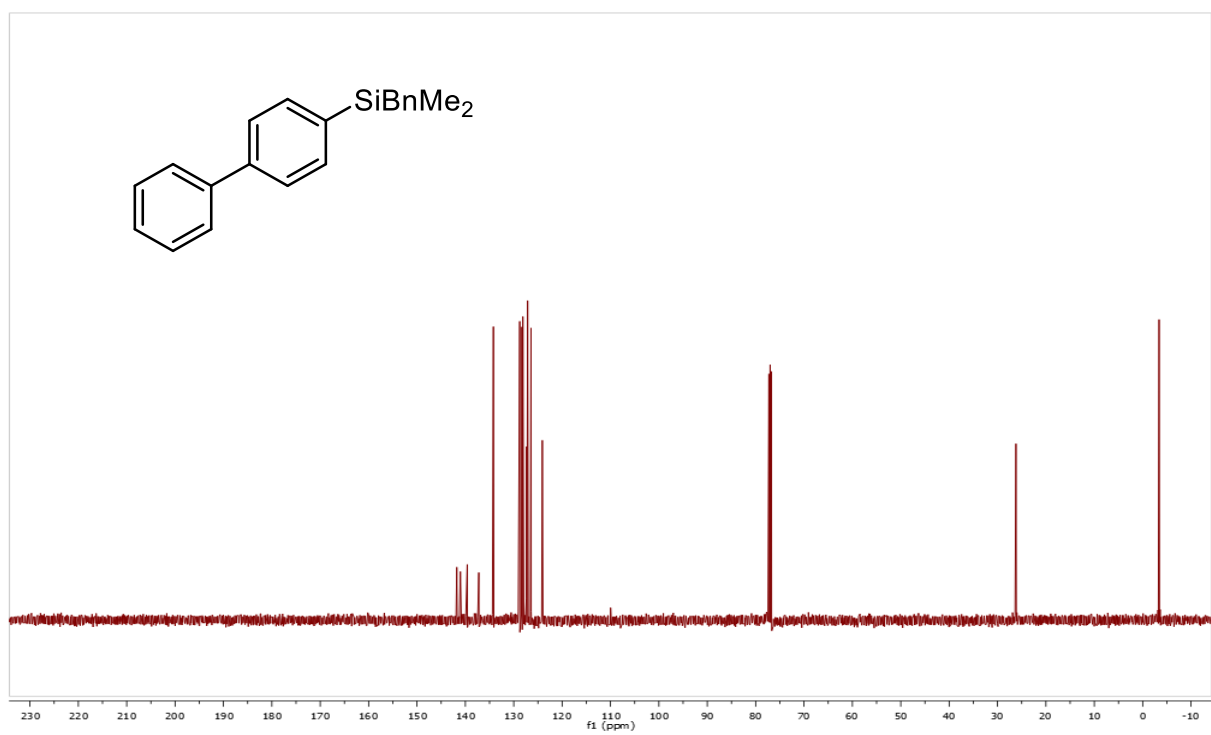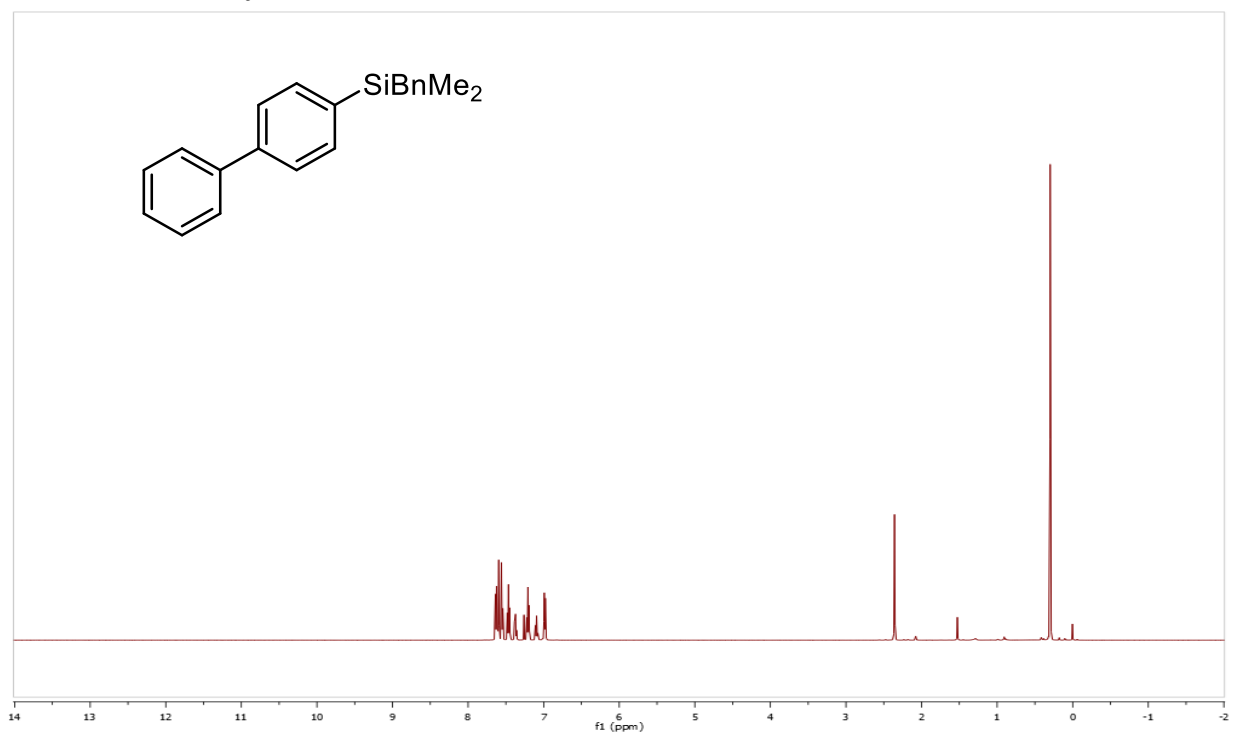**Scheme 3.29, Entry P:**

164

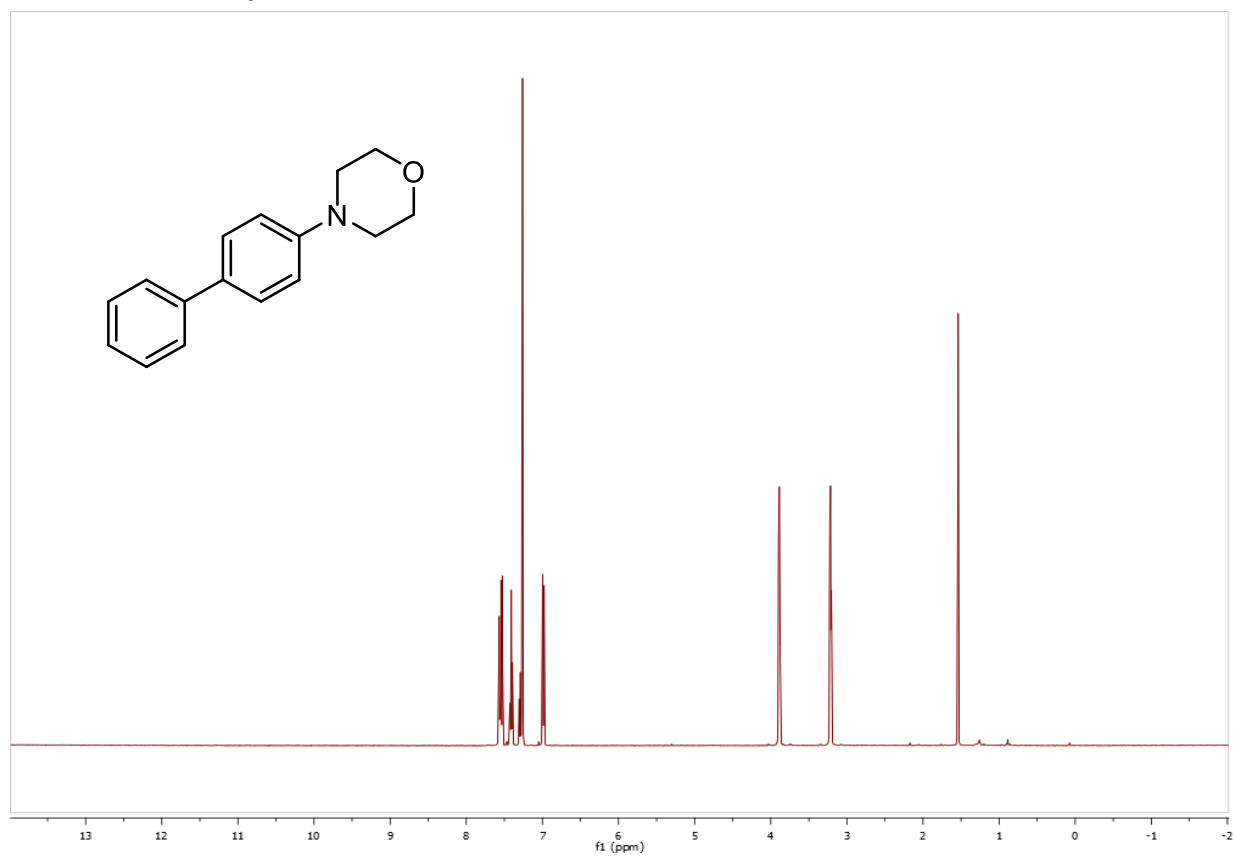**Scheme 3.29, Entry Q:**

Scheme 3.30, Entry 1:

Scheme 3.30, Entry 2:

Scheme 3.30, Entry 8:

Scheme 3.38, Entry A:

References

1. Mejeire A.; Diedrich F. Metal-Catalyzed Cross-Coupling Reactions. 2nd ed. Weinheim, Germany: Wiley-VCH; 2004.

2. Rappoport Z. The Chemistry of Phenols. Chichester, UK: John Wiley & Sons Ltd.; 2003.

3. Hill, C.M.; Senator, G.W.; Haynes, L.; Hill, M.E. *J. Am. Chem. Soc*. **1954**, *76*, 4538.

4. Meyers, A.I.; Gabel, R.; Mihelich, E.D. *J. Org. Chem*. **1978**, *43*, 1372.

5. Leowanawat, P.; Zhang, N.; Percec, V. *J. Org. Chem*. **2012**, *77*, 1018.

6. Cornella, J.; Zarate, C.; Martin, R. *Chem. Soc. Rev*. **2014**, *43*, 8081.

7. Miyaura, N.; Suzuki, A. *Chem. Rev*. **1995**, *95*, 2457.

8. Stille, W. *J. Am. Chem. Soc*. **1987**, *109*, 5478.

9. Wolfe, J. P.; Buchwald, S. *J. Org. Chem*. **1997**, *62*, 1264.

10. Li, Z.; Zhang, S.; Fu, Y.; Guo, Q.; Liu, L. *J. Am. Chem. Soc*. **2009**, *131*, 8815.

11. Nakamura, E.; Sato, K. *Nat. Mater*. **2011**, *10*, 158.

12. Wenkert, E.; Michelotti, E. L.; Swindell, C.S. *J. Am. Chem. Soc*. **1979**, *101*, 2246.

13. Dankwardt, J. W. *Angew, Chem. Int. Ed*. **2004**, *43*, 2428.

14. Tobisu, M.; Chatani, N. *Acc. Chem. Res*. **2015**, *48*, 1717.

15. Zarate, C.; Gemmeren, M.; Somerville, R. J.; Martin, R. *Advances in Organometallic Chemistry*, **2016**.

16. Rosen, B.; Quasdorf, K.; Wilson, D.; Zhang, N.; Resemerita, A.; Garg, N.; Percec, V. *Chem. Rev*. **2011**, *111*, 1346.

17. Macklin, T.K.; Micalizio, G.C. *Nature Chemistry* **2010**, *2*, 638.

18. Wilson, S.R.; Zucker, P. A. *J. Org. Chem*. **1988**, *53*, 4682.

19. Trost, B. M.; Probst, G. D.; Schoop, A. J. *J. Am. Chem. Soc*. **1998**, *120*, 9228.

20. Kolundzic, F.; Micalizio, G.C. *J. Am. Chem. Soc*. **2007**, *129*, 15112.

21. Moreau, B.; Wu, J.; Ritter, T. *Org. Lett*. **2009**, *11*, 337.

22. Trost, B. M.; Fredericksen, M. U.; Rudd, M. T. *Angew. Chem. Int. Ed.* **2005**, *44*, 6630.

23. RajanBabu, T. V. *Chem. Rev.* **2003**, *103*, 2845.

24. Hoshimoto, Y.; Ohashi, M.; Ogoshi, S. *Acc. Chem. Res.* **2015**, *48*, 1746.

25. Bower, J. F.; Kim, I. S.; Patman, R.; Krische, M. J. *Angew. Chem. Int. Ed.* **2009**, *48*, 34.

26. Lysenko, I. L.; Kim, K.; Lee, H.; Cha, J. K. *J. Am. Chem. Soc.* **2008**, *130*, 15997.

27. Montgomery, J. Oragnonickel Chemistry. In *Organometallics in Synthesis: Fourth Manual*; Lipshutz, B. H., Ed.; Wiley: Hoboken, NJ, 2013; 319.

28. Jackson, E. P.; Malik, H. A.; Sormunen, G. J.; Baxter, R. D.; Liu, P.; Wang, H.; Shareef, A.; Montgomery, J. *Acc. Chem. Res.* **2015**, *48*, 1736.

29. Herath, A.; Montgomery, J. *J. Am. Chem. Soc.* **2008**, *130*, 8132.

30. Li, W.; Herath, A.; Montgomery, *J. Am. Chem. Soc.* **2009**, *131*, 17024.

31. Tobisu, M.; Shimasaki, T.; Chatani, N. Chem. Lett. 2009, 38, 710.

32. Das, P.; Lysenko, I.; Cha, J. K. *Angew. Chem. Int. Ed.* **2011**, *50*, 9459.

33. Amarasinghe, K.; Chowdhury, S.; Heeg, M.; Montgomery, J. Organometallics 2001, 20, 370.

34. Mahandru, G.; Skauge, A.; Chowdhury, S.; Amarasinghe, K.; Heeg, M.; Montgomery, J. *J. Am. Chem. Soc.* **2003**, *125*, 13481.

35. Li, W.; Chen, N.; Montgomery, J. *Angew. Chem. Int. Ed.* **2010**, *49*, 8712.

36. Malik, H. A.; Baxter, R. D.; Montgomery, J. *J. Am. Chem. Soc.* **2010**, *132*, 6304.

37. Green, T.W.; Wuts, P.G. (**1999**). *Protective Groups in Organic Synthesis*. New York; John Wiley & Sons.

38. Corey, E. J.; Venkateswarlu, A. *J. Am. Chem. Soc.* **1972**, *94*, 6190.

39. Hayashi, T.; Katsuro, Y.; Kumada, M. *Tetrahedron Lett.* **1980**, *21*, 3915.

40. Zhao, F.; Yu, D.; Zhu, R.; Xi, Z.; Shi, Z. *J. Chem. Lett.* **2011**, *40*, 1001.

41. Clayden, J. *Organolithiums: Selectivity for Synthesis*, VCH: Weinheim, 2002.

42. Snieckus, V. *Chem. Rev*. **1990**, *90*, 879.

43. Zakzeski, P.; Bruijnincx, A.; Jongerius, L., Weckhuysen, B. *Chem. Rev*. **2010**, *110*, 3552.

44. Huber, G.; Iborra, S.; Corma, A. *Chem. Rev*. **2006**, *106*, 4044.

45. Marshall, A.; Alaimo, P. *Chem. Eur. J*. **2010**, *16*, 4970.

46. Alvarez-Bercedo, P.; Martin, R. *J. Am. Chem. Soc*. **2010**, *132*, 17532.

47. Cornella, J.; Gomez-Bengoa, E.; Martin, R. *J. Am. Chem. Soc*. **2013**, *135*, 1997.

48. Tobisu, M.; Yamawaka, K.; Shimasaki, T.; Chatani, N. *Chem. Commun*. **2011**, *47*, 2946.

49. Sergeev, Alexey.; Hartwig, J. *Science* **2011**, *332*, 439.

50. Tobisu, M.; Morioka, T.; Ohtsuki, A.; Chatani, N. *Chem. Sci*. **2015**, *6*, 3410.

51. Kelly, P.; Lin, S.; Edouard, G.; Day, M.; Agapie, T. *J. Am. Chem. Soc*. **2012**, *134*, 5480.

52. Todd, D. P.; Thompson, B. B.; Nett, A. J.; Montgomery, J. *J. Am. Chem. Soc*. **2015**, *137*, 12788.

53. Xu, L.; Chung, L.; Wu, Y. *ACS Catal*. **2016**, *6*, 483.

54. Hirano, K.; Urban, S.; Wang, C.; Glorius. *Org. Lett*. **2009**, *11*, 1019.

55. Blackwell, J.; Foster, K.; Beck, V.; Piers, W. *J. Org. Chem*. **1999**, *64*, 4887.

56. Bains, W.; Tacke, R. *Curr. Opin. Drug Discovery Dev*. **2003**, *6*, 526.

57. Liu, X.; He, C.; Haung, J.; Xu, J. *Chem. Mater*. **2005**, *17*, 434.

58. You, Y.; An, C.; Kim, J.; Park, S. Y. *J. Org. Chem*. **2007**, *72*, 6241.

59. Denmark, S.; Regens, C. *Acc. Chem. Res*. **2008**, *41*, 1486.

60. Nakao, Y.; Hiyama, T. *Chem. Soc. Rev*. **2011**, *40*, 4893.

61. Zarate, C.; Martin, R. *J. Am. Chem. Soc*. **2014**, *136*, 2236.

62. Shekhar, S.; Shen, Q.; Barrios-Landeros, F.; Hartwig, J. *The Chemistry of Anilines*, Rapoport, Z., Ed. Wiley Interspace: New York, **2007**, 455.

63. Hartwig, J. *Angew. Chem. Int. Ed*. **1998**, *37*, 2046.

64. Wolfe, J.P.; Tomori, H.; Sadighi, J.P.; Yin, J.; Buchwald, S. *J. Org. Chem.* **2000**, *65*, 1158.

65. Federsel, H.; Hedburg, H.; Qvarnstrom, F.; Tian, W. *Org. Process. Res. Dev.*, **2008**, *12*, 512.

66. Tobisu, M.; Shimasaki, T.; Chatani, N. *Chem. Lett*. **2009**, *38*, 710.

67. Tobisu, M.; Yasutome, A.; Yamawaka, K.; Shimasaki, T.; Chatani, N. *Tetrahedron*, **2012**, *68*, 5157.

68. Tobisu, M.; Shimasaki, T.; Chatani, N. *Angew. Chem. Int. Ed*. **2008**, *47*, 4866.

69. Tobisu, M.; Yasutome, A.; Kinuta, H.; Nakamura, K.; Chatani, N. *Org. Lett*. **2014**, *16*, 5572.

70. Yatagi, H. *J. Org. Chem*. **1980**, *45*, 1640.

71. Li, L.; Chen, Z.; Zhong, H.; Wang, R. *Chem. A Eur. J.* **2014**, *20*, 3050.

72. Inamoto, K.; Kuroda, J. I.; Sakamoto, T.; Hiroya, K. *Synthesis.* **2007**, No. 18, 2853.

73. Fors, B. P.; Davis, N. R.; Buchwald, S. L. *J. Am. Chem. Soc.* **2009**, *131*, 5766.

74. Barbero, N.; Martin, R. *Org. Lett.* **2012**, *14*, 796.

75. Stuart, D. R.; Bertrand-Laperle, M.; Burgess, K. M. N.; Fagnou, K. *J. Am. Chem. Soc.* **2008**, *130*, 16474.

76. Kalutharage, N.; Yi, C. S. *J. Am. Chem. Soc.* **2015**, *137*, 11105.

77. Venning, A. R. O.; Bohan, P. T.; Alexanian, E. J. *J. Am. Chem. Soc.* **2015**, *137*, 3731.

78. Ackermann, L.; Born, R.; Spatz, J. H.; Meyer, D. *Angew. Chemie. Int. Ed.* **2005**, *44*, 7216.